Pertanika Journal of

SCIENCE & TECHNOLOGY

JST

VOL. 21 (1) JAN. 2013

PERTANIKA JOURNALS

A scientific journal published by Universiti Putra Malaysia Press

Journal of Science & Technology
Journal of Science & Technology
Journal of Science & Technology

About the Journal

Pertanika is an international peer-reviewed journal devoted to the publication of original papers, and it serves as a forum for practical approaches to improving quality in issues pertaining to tropical agriculture and its related fields. *Pertanika* began publication in 1978 as the Journal of Tropical Agricultural Science. In 1992, a decision was made to streamline *Pertanika* into three journals to meet the need for specialised journals in areas of study aligned with the interdisciplinary strengths of the university. The revamped Journal of Science & Technology (JST) aims to develop as a pioneer journal focusing on research in science and engineering, and its related fields. Other *Pertanika* series include Journal of Tropical Agricultural Science (JTAS); and Journal of Social Sciences and Humanities (JSSH).

JST is published in **English** and it is open to authors around the world regardless of the nationality. It is currently published two times a year, i.e. in **January** and **July**.

Goal of Pertanika

Our goal is to bring the highest quality research to the widest possible audience.

Quality

We aim for excellence, sustained by a responsible and professional approach to journal publishing. Submissions are guaranteed to receive a decision within 12 weeks. The elapsed time from submission to publication for the articles averages 5-6 months.

Indexing of Pertanika

Pertanika is now over 33 years old; this accumulated knowledge has resulted in Pertanika journals being indexed in SCOPUS (Elsevier), EBSCO, DOAJ, AGRICOLA, and CABI etc. JST is indexed in SCOPUS, EBSCO, DOAJ, ISC and ERA.

Future vision

We are continuously improving access to our journal archives, content, and research services. We have the drive to realise exciting new horizons that will benefit not only the academic community, but society itself.

We also have views on the future of our journals. The emergence of the online medium as the predominant vehicle for the 'consumption' and distribution of much academic research will be the ultimate instrument in the dissemination of research news to our scientists and readers.

Aims and scope

Pertanika Journal of Science and Technology aims to provide a forum for high quality research related to science and engineering research. Areas relevant to the scope of the journal include: *bioinformatics, bioscience, biotechnology and biomolecular sciences, chemistry, computer science, ecology, engineering, engineering design, environmental control and management, mathematics and statistics, medicine and health sciences, nanotechnology, physics, safety and emergency management,* and related fields of study.

Editorial Statement

Pertanika is the official journal of Universiti Putra Malaysia. The abbreviation for Pertanika Journal of Science & Technology is *Pertanika J. Sci. Technol.*

Editorial Board

2013-2015

Editor-in-Chief

Mohd. Ali HASSAN, *Malaysia*
Bioprocess engineering, Environmental biotechnology

Chief Executive Editor

Nayan D.S. KANWAL, *Malaysia*
Environmental issues- landscape plant modelling applications

Editorial Board Members

Abdul Halim Shaari (Professor Dr), *Superconductivity and Magnetism,* Universiti Putra Malaysia, Malaysia.

Adem KILICMAN (Professor Dr), *Mathematical Sciences,* Universiti Putra Malaysia, Malaysia.

Ahmad Makmom Abdullah (Associate Professor Dr), *Ecophysiology and Air Pollution Modelling,* Universiti Putra Malaysia, Malaysia.

Ali A. MOOSAVI-MOVAHEDI (Professor Dr), *Biophysical Chemistry,* University of Tehran, Tehran, Iran.

Amu THERWATH (Professor Dr), *Oncology, Molecular Biology,* Université Paris, France.

Angelina CHIN (Professor Dr), *Mathematics, Group Theory and Generalisations, Ring Theory,* University of Malaya, Malaysia.

Bassim H. HAMEED (Professor Dr), *Chemical Engineering: Reaction Engineering, Environmental Catalysis & Adsorption,* Universiti Sains Malaysia, Malaysia.

Biswa Mohan BISWAL (Professor Dr), *Medical, Clinical Oncology, Radiotherapy,* Universiti Sains Malaysia, Malaysia.

Christopher G. JESUDASON (Professor Dr), *Mathematical Chemistry, Molecular Dynamics Simulations, Thermodynamics and General Physical Theory,* University of Malaya, Malaysia.

Ivan D. RUKHLENKO (Dr), *Nonliner Optics, Silicon Photonics, Plasmonics and Nanotechnology,* Monash University, Australia.

Kaniraj R. SHENBAGA (Professor Dr), *Geotechnical Engineering,* Universiti Malaysia Sarawak, Malaysia.

Kanury RAO (Professor Dr), *Senior Scientist & Head, Immunology Group, International Center for Genetic Engineering and Biotechnology, Immunology, Infectious Disease Biology and Systems Biology,* International Centre for Genetic Engineering & Biotechnology, New Delhi, India.

Karen Ann CROUSE (Professor Dr), *Chemistry, Material Chemistry, Metal Complexes – Synthesis, Reactivity, Bioactivity,* Universiti Putra Malaysia, Malaysia.

Ki-Hyung KIM (Professor Dr), *Computer and Wireless Sensor Networks,* AJOU University, Korea.

Kunnawee KANITPONG (Associate Professor Dr), *Transportation Engineering- Road traffic safety, Highway Materials and Construction,* Asian Institute of Technology, Thailand.

Megat Mohamad Hamdan MEGAT AHMAD (Professor Dr), *Mechanical and Manufacturing Engineering,* Universiti Pertahanan Nasional Malaysia, Malaysia.

Mirnalini KANDIAH (Professor Dr), *Public Health Nutrition, Nutritional Epidemiology,* Universiti Malaysia Perlis (UniMAP), Malaysia.

Mohamed Othman (Professor Dr), *Communication Technology and Network, Scientific Computing,* Universiti Putra Malaysia, Malaysia.

Mohd Adzir Mahdi (Professor Dr), *Physics, Optical Communications,* Universiti Putra Malaysia, Malaysia.

Mohd Sapuan Salit (Professor Dr), *Concurrent Engineering and Composite Materials,* Universiti Putra Malaysia, Malaysia.

Narongrit SOMBATSOMPOP (Professor Dr), *Engineering and Technology: Materials and Polymer Research,* King Mongkut's University of Technology Thonburi (KMUTT), Thailand.

Prakash C. SINHA (Professor Dr), *Physical Oceanography, Mathematical Modelling, Fluid Mechanics, Numerical Techniques,* Universiti Malaysia Terengganu, Malaysia.

Rajinder SINGH (Dr), *Biotechnology, Biomolecular Science, Molecular Markers/ Genetic Mapping,* Malaysian Palm Oil Board, Kajang, Malaysia.

Renuganth VARATHARAJOO (Professor Dr-Ing Ir), *Engineering, Space System,* Universiti Putra Malaysia, Malaysia.

Riyanto T. BAMBANG (Professor Dr), *Electrical Engineering, Control, Intelligent Systems & Robotics,* Bandung Institute of Technology, Indonesia.

Sabira KHATUN (Professor Dr), *Engineering, Computer Systems and Software Engineering, Applied Mathematics,* Universiti Malaysia Pahang, Malaysia.

Shiv Dutt GUPTA (Dr), Director, IIHMR, *Health Management, public health, Epidemiology, Chronic and Non-communicable Diseases,* Indian Institute of Health Management Research, India.

Shoba RANGANATHAN (Professor Dr), *UNESCO Chair of Biodiversity Informatics Bioinformatics and Computational Biology, Biodiversity Informatics, Protein Structure, DNA sequence,* Macquarie University, Australia.

Suan-Choo CHEAH (Dr), *Biotechnology, Plant Molecular Biology,* Asiatic Centre for Genome Technology (ACGT), Kuala Lumpur, Malaysia.

Waqar ASRAR (Professor Dr), *Engineering, Computational Fluid Dynamics, Experimental Aerodynamics,* International Islamic University, Malaysia.

Wing-Keong NG (Professor Dr), *Aquaculture, Aquatic Animal Nutrition, Aqua feed Technology,* Universiti Sains Malaysia, Malaysia.

Yudi SAMYUDIA (Professor Dr Ir), *Chemical Engineering, Advanced Process Engineering,* Curtin University of Technology, Malaysia.

International Advisory Board

Adarsh SANDHU (Professor Dr), *Editorial Consultant for Nature Nanotechnology and contributing writer for Nature Photonics, Physics, Magnetoresistive Semiconducting Magnetic Field Sensors, Nano-Bio-Magnetism, Magnetic Particle Colloids, Point of Care Diagnostics, Medical Physics, Scanning Hall Probe Microscopy, Synthesis and Application of Graphene, Electronics-Inspired Interdisciplinary Research Institute* (EIIRIS), Toyohashi University of Technology, Japan.

Graham MEGSON (Professor Dr), *Computer Science,* The University of Westminster, U.K.

Kuan-Chong TING (Professor Dr), *Agricultural and Biological Engineering,* University of Illinois at Urbana-Champaign, USA.

Malin PREMARATNE (Professor Dr), *Advanced Computing and Simulation,* Monash University, Australia.

Mohammed Ismail ELNAGGAR (Professor Dr), *Electrical Engineering,* Ohio State University, USA.

Peter G. ALDERSON (Associate Professor Dr), *Bioscience,* The University of Nottingham, Malaysia Campus.

Peter J. HEGGS (Emeritus Professor Dr), *Chemical Engineering,* University of Leeds, U.K.

Ravi PRAKASH (Professor Dr), *Vice Chancellor, JUIT, Mechanical Engineering, Machine Design, Biomedical and Materials Science,* Jaypee University of Information Technology, India.

Said S.E.H. ELNASHAIE (Professor Dr), *Environmental and Sustainable Engineering,* Penn. State University at Harrisburg, USA.

Suhash Chandra DUTTA ROY (Emeritus Professor Dr), *Electrical Engineering,* Indian Institute of Technology (IIT) Delhi, India.

Vijay ARORA (Professor), *Quantum and Nano-Engineering Processes,* Wilkes University, USA.

Yi LI (Professor Dr), *Chemistry, Photochemical Studies, Organic Compounds, Chemical Engineering,* Chinese Academy of Sciences, Beijing, China.

Pertanika Editorial Office

Office of the Deputy Vice Chancellor (R&I), 1st Floor, IDEA Tower II, UPM-MTDC Technology Centre
Universiti Putra Malaysia, 43400 Serdang, Selangor, Malaysia
Tel: +603 8947 1622
E-mail: executive_editor.pertanika@upm.my
URL: http://www.pertanika.upm.edu.my/editorial_board.htm

Publisher

The UPM Press
Universiti Putra Malaysia
43400 UPM, Serdang, Selangor, Malaysia
Tel: +603 8946 8855, 8946 8854 • Fax: +603 8941 6172
penerbit@putra.upm.edu.my
URL: http://penerbit.upm.edu.my

The publisher of Pertanika will not be responsible for the statements made by the authors in any articles published in the journal. Under no circumstances will the publisher of this publication be liable for any loss or damage caused by your reliance on the advice, opinion or information obtained either explicitly or implied through the contents of this publication.

All rights of reproduction are reserved in respect of all papers, articles, illustrations, etc., published in Pertanika. Pertanika provides free access to the full text of research articles for anyone, web-wide. It does not charge either its authors or author-institution for refereeing/ publishing outgoing articles or user-institution for accessing incoming articles.

No material published in Pertanika may be reproduced or stored on microfilm or in electronic, optical or magnetic form without the written authorization of the Publisher.

Copyright © 2013 Universiti Putra Malaysia Press. All Rights Reserved.

Editorial[i]

Milk and Its Bioactive Peptides: Phenomenal Nutraceutical Food of the Century

EXPRESSION OF THOUGHT:
Professor Ali A. Moosavi –Movahedi,
University of Tehran, Iran

We live in a century where everything is observed in nano size scale and there is a new vision and a new way of looking at everything that already exits. Scientists and researchers are very precise in observing everything and finding new functionalities from the existing materials. Different side effects have been reported to result from the uses of synthetic drugs and food additives, and thus, finding natural drugs and food additives from natural sources is at the top of research list in most developed countries. In fact, we have reached the time where the terms drug and additives have been replaced with nutraceuticals and where prevention is more important than treatment. Unfortunately more than 50% of the people are suffering from diseases such as cardiovascular disease, bone defects, rheumatoid arthritis, atherosclerosis, cancer, AIDS, Alzheimer, and diabetes. The first step in reducing the risk of suffering from different diseases is to have a double check at what we eat every day, i.e. to consider everyday food not only from its nutritional aspect but also from health and medicinal point of view and to eat food with high antioxidant agent. Among food that is consumed every day, milk has a high potential in this regard. Milk is a rich source of dietary protein, which is made of caseins and whey proteins. Its great nutritional value has made milk an important must-use everyday food for centuries. During the last two decades, an increasing number of data have shown that milk can play additional functions than merely energetic and nutritional ones. Milk proteins exert a wide range of biological, nutritional and functional activities such as chaperon activity and bioactivity of their peptides. It has been reported that multiple biologically active (bioactive) proteins and peptides can originate from milk. Bioactive peptides are a great source of natural drugs, which can both prevent and cure different diseases. These peptides can be produced in vivo during gastrointestinal digestion or in vitro through food processing using specific enzymes. Milk protein derived peptides have different functionalities including antioxidant activity, antimicrobial activity and blood pressure–lowering effect. These peptides have been used in the formulation of other food products for the production of functional food. Most food products are produced using bovine's milk proteins

but bovine milk allergy by far is the most prevalent food allergy, especially in children, and β-lactoglobulin (β-LG) is considered the dominant bovine milk allergen. Camel milk lacks β-LG and is enriched with α-Lactalbumin such as human milk. The milk of camel, a high-tech animal whose antibodies have successfully been used for the treatment of cancer, contains proteins that can cure hepatitis and diabetes. Thus, the health benefits of camel milk are attributed to the presence of high concentrations of insulin-like protein and other factors that have positive effects on immunity. Its composition is closer to human milk compared to bovine's milk. The functionality of the bioactive peptides produced from camel milk has been studied both in vitro and in vivo. The results are phenomenal. The bioactive peptides produced from camel milk open a new era for the production of healthy additives, nutraceutical components and new products, in which health and prevention is considered the most important factor in the food industry.

Ali A. Moosavi –Movahedi, PhD
Institute of Biochemistry and Biophysics
University of Tehran, Iran

Telephone: + (9821) 6640 3957.
Fax: + (9821) 6640 4680.
moosavi@ibb.ut.ac
www.ibb.ut.ac.ir/~moosavi

January, 2013

Dr. Ali A. Moosavi-Movahedi is currently a professor of Biophysics at the Institute of Biochemistry and Biophysics, University of Tehran. He graduated from the National University of Iran (NUI) with a BSc in Chemistry in 1975 from Eastern Michigan University (EMU) USA, followed by an MSc in Chemistry in 1979 and a PhD in Biophysical Chemistry in 1986 from University of Manchester, UK. In recognition of his outstanding research in the field of science, he was awarded the International Khawrazmi Prize (1990), National Distinguished Professor (1997), the first class medal for research at the University of Tehran (2003), National Eminent Character (2003), Razi Festival First Rank Award (2005), Elsevier-Scopus International Award for Top Researcher in the Field of Biochemistry & Molecular Biology (2007), Avicenna Festival First Rank Award for Top Researcher (2008), Eminent National Researcher (2009) and also selected as an Eminent Professor of the University of Tehran in 2010.

Professor Dr. Ali A. Moosavi-Movahedi is also the author of 13 books and 360 full research papers published in international research journals, mainly in the area of structural elucidation of protein, enzyme and DNA. To date, the avid researcher has supervised 33 PhD and 42 MSc students and also guided postdoctoral researchers in the cited area. Apart from being a member of various societies such as Biophysical Society (USA), Protein Society (USA), Iranian Chemical Society, Iranian Biochemical Society, Professor Ali A. Moosavi-Movahedi is also currently the President of Iran Society of Biophysical Chemistry.

[i] DISCLAIMER
The views expressed in this article are those of the author and do not necessarily represent the views of, and should not be attributed to, the Pertanika Journal or the Pertanika Editorial Board.

Pertanika Journal of Science & Technology
Vol. 21 (1) Jan. 2013

Contents

Selected Articles from UPM-Malaysian Nuclear Agency Symposium 2011
Guest Editor: Mohd Sapuan Salit
Guest Editorial Board: Mansor Ahmad, Syams Zainudin, Hawa Ze Jaafar, Fathinul Fikri Ahmad Saad, Kamarudin Hashim and Mohamad Azwar Hashim

Selected Articles from The International Conference on Information Retrieval and Knowledge Management, CAMP'12
Guest Editors: Shyamala Doraisamy and Ramlan Mahmod
Guest Editorial Board: Lili Nurliyana Abdullah, Rusli Abdullah, Masrah Azmi Murad, Rodziah Atan and Rabiah Abdul Kadir

Pertanika J. Sci. & Technol. 21 (1): 1 - 14 (2013)

SCIENCE & TECHNOLOGY

Journal homepage: http://www.pertanika.upm.edu.my/

Aspect of Fatigue Analysis of Composite Materials: A Review

Suriani, M. J.[1]*, Aidy Ali[1], S. M. Sapuan[1] and A. Khalina[2]

[1]*Department of Mechanical and Manufacturing Engineering, Faculty of Engineering, Universiti Putra Malysia, 43400 Serdang, Selangor, Malaysia*

[2]*Department of Biological and Agriculture Engineering, Faculty of Engineering, Universiti Putra Malysia, 43400 Serdang, Selangor, Malaysia*

ABSTRACT

This paper reviewed the aspect of fatigue approaches and analysis in a fibre reinforced composite materials which have been done by researchers worldwide. The aim of this review is to provide a better picture on analytical approaches that are presently available for predicting fatigue life in composite materials. This review also proposes a new interpretation of available theories and identifies area in fatigue of natural fibre reinforced composite materials. Thus, it was concluded there are still very limited studies on fatigue analysis of natural fibre reinforced composite materials, especially using non-destructive technique (NDT) methods and a new mathematical modelling on fatigue should be formulated.

Keywords: Fatigue life, composite materials, non-destructive technique

INTRODUCTION

Fatigue life of the classical engineering materials is difficult to predict, and not even surprisingly for composite materials. Predicting fatigue life for homogeneous materials was done in the past three decade but from a review of the limited research done and developed on natural fibre reinforced composite. Previously, a vast majority of the fatigue studies focused on synthetic fibre/resin system (Harris, 2003). Research on the fatigue properties of natural fibre composites is a new field and these have become a focus for many engineers and scientists. In composites, fatigue damage and failure mechanism commonly occurs is more complex compared to homogenous materials such as metal. There are four basic failure occurs in the composites under cyclic loading which are matrix cracking, interfacial debonding, delamination and fibre breakage (Wu & Yau, 2009).

Article history:
Received: 23 April 2010
Accepted: 5 August 2011

E-mail addresses:
surianimatjusoh@gmail.com (Suriani, M. J.),
aidy@eng.upm.edu.my (Aidy Ali),
sapuan@eng.upm.edu.my (S. M. Sapuan)
khalina@eng.upm.edu.my (A. Khalina)
*Corresponding Author

ISSN: 0128-7680 © 2013 Universiti Putra Malaysia Press.

A long time ago, a man produced materials used which were widely in building and in many structure but later the materials had changes in the composites. Nowadays, due to the increased interest in the potential of natural fibre composites for applications in primary structures such as automotive parts and buildings, a fundamental study of their fatigue properties is essential (Towo & Ansell, 2008). Recently, scientists and researchers have discussed and worked on natural fibre in composites such as Kenaf, sugar palm, coconut, coir, jute, sisal, bamboo, wood, pineapple and banana. There are many reasons for using natural fibre as a filler or reinforcement in composites compared to glass fibres, and these include low density, biodegradable and recyclable, high strength and stiffness good fibre adhesion and environmental consciousness (Sapuan *et al*., 2006). Thus, the following section will elaborate on the aspect of the composites analysis of fatigue to better understand the integrity of this new material under dynamic loading.

PREDICTING FATIGUE LIFE

Fatigue can be defined as a failure under a repeated or varying load. These failures have two domains of cyclic or stressing and straining in different mechanisms of low-cycle fatigue and high-cycle fatigue (Wu & Yau, 2009).

Fatigue failure process involves two distinct phases in the rubber. The first phase is a period during which cracks nucleate in regions that were initially invisible or free of observable cracks. The period during which nucleated cracks grow to the point of failure is the second phase of the fatigue failure process. It will be seen that in the second phase, nucleation, growth and final failure may be rationalized in terms of the fracture mechanical behaviour of rubber (Mars & Fatemi, 2002).

Normally, three methods are used to predict life including total life by plotting stress-life (S-N) curve, crack initiation strain-life (E-N) and crack growth. Meanwhile, there are two approaches used for predicting the models for rubber. The first approach focuses on predicting crack nucleation life, given the history of quantities that are defined at a material point, in the sense of continuum mechanics. Stress and strain are examples of such quantities. The second approach, based on the ideas from fracture mechanics, focuses on predicting the growth of a particular crack, given the initial geometry and energy release rate history of the crack (Mars & Fatemi, 2002).

Predicting fatigue life in composite materials is more complicated as compared to metal. This is because in the composite materials, failure does not occur by the propagation of a single macroscopic crack. The micro-structural mechanisms of damage accumulation, including fibre breakage and matrix cracking debonding, transverse-ply cracking, and delamination, occur independently sometimes and interactively at times, and the predominance of one or the other may strongly affect both materials variables and testing conditions. Fig.1 shows the degradation of composites strength until failure occurs (Harris, 2003).

Many experiments have been done by the researchers to predict fatigue analysis by using the derived empirical S–N curves between stress and fatigue life. Fig.2 shows a typical S-N graph, where straight lines indicate endurance limit region. These relationships have been suggested for use in design in numerous industries such as aerospace, automotive and construction. The

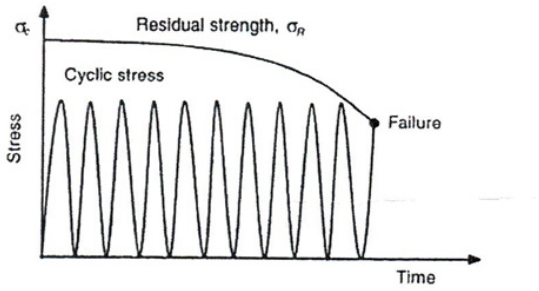

Fig.1: The degradation of composites strength until failure occurs (Harris, 2003)

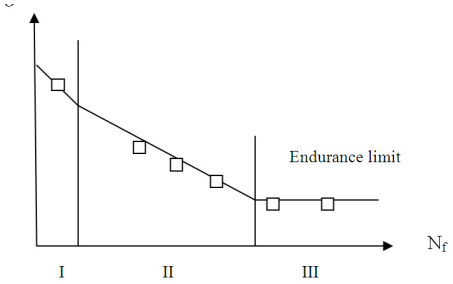

Fig.2: A typical S-N graph where straight lines indicate endurance limit region (Harris, 2003)

linear and non-linear S–N curves have been proposed (Yang, 1978; Nicholas, 2000). It also uses a non-linear curve between strains to predict the fatigue life of the composite materials (Reifsnider *et al*., 2000). It also discusses on a linear relationship between the maximum stress *S* and the logarithm of *N*, while the number of load cycles to fatigue failure is widely used to fit the experimental data, as follows:

$$S = m \log N = b \tag{1}$$

where *m* and *b* are parameters dependent on material properties. By predicting fatigue life under constant cyclic loading, fatigue damage can be evaluated after a given number of cycles. Composite is assumed to fail in the phase when accumulated damage exceeds the critical level of damage (Clark *et al*., 1999).

In a study on the flexural behaviour of sandwich composite materials under cycling loading, El Mahi *et al.* (2004) utilized Wohler Curve (S-N Curve) to obtain the comparison between the experimental result and analytical results. It was reported that a good agreement had been found between these two analyses. The approach was based on the interpolation by empirical function, in which the parameters were obtained from the experimental results using the stiffness concept. It was also reported that this approach is able to predict the fatigue life and the evolution of damage according to the loading level, which will reduce the number of experiments. In their work on the derivation of the model for fatigue life criteria, the failure

occurs to residual strength degradation method. The failures were caused by the degradation of residual strength to the applied stress.

Another approach that has been used by several authors is strain failure criterion which considers the final failure of the composite materials that occurs at the stage of resultant strain that reaches the ultimate static strain (D'amore *et al*., 1999; Clark *et al*., 1999). The other method used to predict fatigue life, done by Salvia *et al*. (1997), is stiffness reduction or degradation which needs another failure condition rather than the total failure of the specimen such as predefined critical number of cycles representing certain damage state. The critical number of the cycles was obtained when a given stiffness loss (predefined) was reached, and then the critical cycle numbers and stiffness reduction were associated.

MODELLING FATIGUE IN COMPOSITES

Damage Accumulation

Damage evolution mechanism is one of the important focuses and also a foundation to predict fatigue life. The mechanical properties of the composite materials show progressive degradation with the increasing of the number of cyclic loading. Two quantitative relations, obtained from a study on a fatigue damage model of composite, are defined by the stiffness degradation rule in the loading direction. The proposed model is as follows:

$$D(n) = \frac{E_0 - E(n)}{E_0 - E_f} = 1 - \left(1 - (\frac{n}{N})^B\right)^A \quad (2)$$

Where E_0 is the initial Young's modulus, E_f is the failure Young's modulus, $E(n)$ is Young's modulus of the material subjected to *n*th cycling loading, *n* is the cycle, *N* is the fatigue life, A and B are model parameters, *D(n)* is the fatigue damage which equals 0 when n=0 and equals 1 when n=N (Wu & Yau, 2009).

Shen *et al*. (1993), in predicting of fatigue life of Boron/Aluminium composite, worked on a technique involving the iteration of damage accumulation and internal stress redistribution. As pointed by Shen *et al*. (1993), damage accumulation can be determined by applying the fatigue damage evolution law and the redistribution of stress. The characteristics of damage growth in the composite materials have been studied and compared with those of the damage growth in homogeneous materials.

The study on the fatigue damage of composite materials of characteristic of damage accumulation in composites materials was done in 2002 by Mao and Mahadevan, who reported that the concept of damage accumulation might be used as a more suitable approach to predict the fatigue life of the structures of composite materials. However, fatigue damage cannot be measured directly. Therefore, for quantitative evaluation of fatigue damage, Young's modulus or the stiffness of composite materials is often used to evaluate the fatigue damage due to cyclic loading. Fig.3 shows a schematic comparison of damage accumulation in the composite materials and homogeneous materials as a function of fatigue cycle ratio. Fig.3 is plotted in terms of damage index versus cycle ratio, where the damage index is defined as Eq. (3):

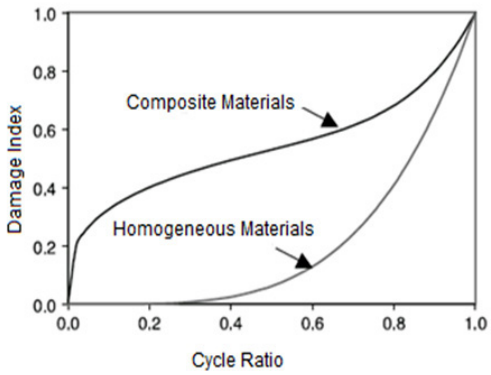

Fig.3: Sketched fatigue damage accumulation (Mao & Mahadevan, 2002)

$$D_1 = 1 - \frac{E}{E_0} \tag{3}$$

where D_1 is accumulated fatigue damage, E is the Young's modulus of the damaged material and E_0 is Young's modulus of undamaged material. The cycle ratio is the number of cycles at a given instant divided by the fatigue life.

Mao and Mahadevan (2002) presented a new damage accumulation model to describe the degradations of composite materials. This model accurately explains the rapid damage growth during both the early and final stages of life. The proposed function is of the following form:

$$D = q\left(\frac{n}{N}\right)^{m_1} + (1-q)\left(\frac{n}{N}\right)^{m_2} \tag{4}$$

where D is the normalized accumulated damage; q, m_1 *and* m_2 are material dependent parameters; n is the number of applied loading cycles, and N is the fatigue life at the corresponding applied load level. The parameters for Eq. (4) are defined as:

$$q = \frac{A\left(\frac{N_0}{N}\right)^{\alpha}}{1-(1-A)\left(\frac{N_0}{N}\right)^{\alpha}} \tag{5}$$

$$m_1 = \left(\frac{N_o}{N}\right)^{\beta} \tag{6}$$

$$m_2 = \left(\frac{N}{N_0}\right)^{\gamma} \tag{7}$$

where N_0 is the reference fatigue life. The parameters α, β and γ are material dependent constants. These parameters can be obtained with fatigue experimental data. Once the damage indices are obtained during the fatigue tests, regression analysis can be carried out to obtain the parameters q, m_1 and m_2. Then, the parameters α, β and γ can be calculated using Eqs. (5) – (7).

Crack Nucleation Approaches

Fatemi *et al*. (2002) stated that there are two approaches used in the models for predicting fatigue life in rubber. The first one focuses on predicting crack nucleation life, given the history of quantities that are defined at a material point, in the sense of continuum mechanics. Stress and strain are examples of such quantities. The other approach, based on the ideas from fracture mechanics, focuses on predicting the growth of a particular crack, given the initial geometry and energy release rate history of the crack.

Crack Growth Approaches

Fatigue crack growth approach has been used to analyze fatigue in composites (see Salvia *et al*., 1997; Fatemi *et al*., 2002; Dawis & Bradstreet, 1970; Savastano Jr., 2009; Woo *et al*., 2008). It was started to be used and applied widely since 1960s and the cracks were claimed to be related to damage. In the experimental study of resistance-curve behaviour and fatigue crack, the crack growth was observed to have occurred in three stages, namely, an initial decelerated growth, a steady-state growth and the final catastropic crack growth (Savastano Jr., 2009). Nowadays, this concept was applied with sophisticated tool and a technique available that can measure a very small crack up to 1μm (Fatemi & Yang, 1998). Southen and Thomas (1978) applied fracture mechanic approach based on fatigue crack growth to develop a model for abrasive wear of rubber. Stevenson, (1987) also stated that compressive loading must be considered carefully in any analysis of fatigue growth.

Savastano Jr. (2009) presented the results of an experimental study on resistance-curve behaviour and fatigue crack growth in cementitious matrices reinforced with eco-friendly natural fibre obtained from agricultural by-products. He used blast furnace slag cement (BFS) reinforced with pulped fibres of sisal, banana and bleached eucalyptus pulp and ordinary Portland cement (OPC), which was reinforced with bleached eucalyptus pulp. Meanwhile, single-edge notched specimen was used to analyze fatigue crack growth and fracture resistance (R-curve). Then, the analysis of crack/microstructure interaction was done by using the NDT method via scanning electron microscopy (SEM) and X-ray spectroscopy (EDS). As pointed in this study, fatigue crack growth occurs in three stages, which are initial decelerated growth, a steady-state growth, and a final catastrophic crack growth. The crack growth diagram was plotted and the results of Sisal BFS, Banana BFS, Eucalyptus BFS and Eucalyptus OPC are shown in Fig.4a to Fig.4d, respectively.

The fatigue life of banana and sisal fibre reinforced composite mostly occurred in the second stage of steady state crack growth (Fig.4a and Fig.4b). The fatigue crack growth rates of Eucalyptus reinforced composites are faster as compared to the sisal and banana reinforced composites (Fig.4c and Fig.4d). The results of the crack/microstructure interactions revealed

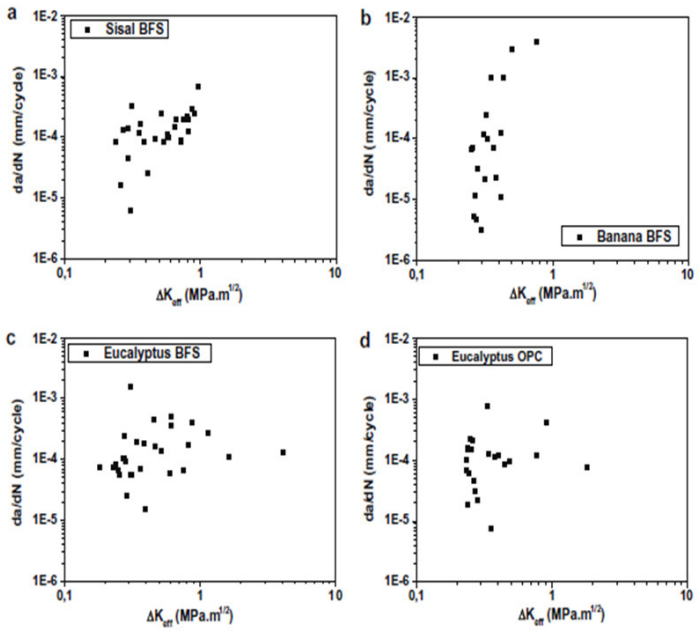

Fig.4: Fatigue crack growth rate of diagram (a) Sisal BFS, (b) Banana BFS, (c) Eucalyptus BFS, and (d) Eucalyptus OPC (Savastano Jr *et al*., 2009)

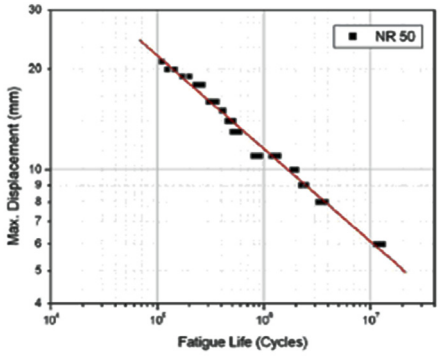

Fig.5: Fatigue life of rubber materials at maximum displacement (Woo *et al*., 2008).

that fatigue crack growth in composites occurred by matrix cracking, crack deflection around fibres and crack-bridging by uncracked fibres and ligaments (Savastano Jr., 2009).

Woo *et al.* (2008) studied on the material properties and fatigue life of natural rubber component. The fatigue lifetime prediction methodology by using the incorporating of finite element (using Green-Lagrange strain) analysis and fatigue damage parameters has been proposed. Meanwhile, fatigue damage parameters were obtained from the fatigue test and Green-Lagrange (G-L) strain determined at the critical location. A single function of G-L strain was then used to represent the equation for predicting fatigue life. Fatigue test was performed using a 3D dumbbell specimen and roll front component in ambient temperature under the stroke controlled condition with a sine waveform of 5 Hz and the mean displacement is 0-10mm at a displacement range is -11 to 21mm. Fig.5 shows the relationship between the maximum

displacement with fatigue life. This shows that fatigue life decreases as the maximum tension displacement increases. In this study, the fatigue lives of the 3D specimens are represented by the maximum G-L strain parameter, $N_{f,}$ as performed in Eq. (8):

$$N_f = 495,450\left[\varepsilon_{\mathrm{G-L}}\right]^{-1.324} \tag{8}$$

Toubal *et al.* (2006) worked on woven laminates composite of fabric (HR 285/G803), with high strength carbon fibre and the matrix is epoxy resin. This composite has been used in manufacturing aeronautical structures. The fatigue test was carried out under tension-tension load and analysis of temperature on external surface involving thermal concept or thermal imaging technique using infra-red camera applied in this research. This study intended to relate the damage evolution and heat dissipation in composites. An analytical model based on the cumulative damage has also been proposed to predict damage evolution. Roylance (2001) stated that a cumulative damage model is often hypothesized when the cyclic load level varies during the fatigue process. They are considered to be two main approaches for cumulative damage such as Miner's rule and the other is that of residual strength. Miner's rule can be written as Eq. (9):

$$\sum \frac{n_i}{N_i} = 1 \tag{9}$$

where n_i is the number of cycles applied at a load corresponding to a lifetime of *Ni*, and for residual strength $\sigma_{R,}$ Broutman and Sahu (1972) stated Eq. (10) as follows:

$$\sigma_R = \sigma_S - \sum_i \left(\sigma_S - \sigma_i\right)\frac{n_i}{N_i} \tag{10}$$

where σ_S is the instantaneous tensile static strength as measured on the virgin material before any fatigue damage is induced as $\sigma_S = \sigma_i$ (with σ_i being the maximum stress in the cycle). In another example, Granda *et al*. (2008) reported from their prediction of fatigue damage of an automotive axle, which was subjected to variable loading observations that there was a localized damage process which resulted from a cumulative damage. Marin (1962) proposed a cumulative damage based on the consideration of the relations between damage as a function of cycle ratio and changes in the S-N curve due to damage accumulation.

Cumulative damage, as a function of loading cycles, is described in Fig.6. It was determined that *D* is cumulative damage, *N* is the three numbers of loading cycles and N_f is the number of cycles to failure. Cumulative damage was determined by using Equation (11):

$$D = 1 - \frac{E}{E_0} \tag{11}$$

where *E* is the residual modulus and E_0 is the initial modulus (Toubal *et al*., 2006).

Toubal *et al.* (2006) used Eq. (4) proposed by Mao and Mahadevan (2002) to determine the analytical model of accumulation damage and the values of *q, m_1 and m_2* are given in Table 1 and plotted in Fig.7 to Fig.8, respectively.

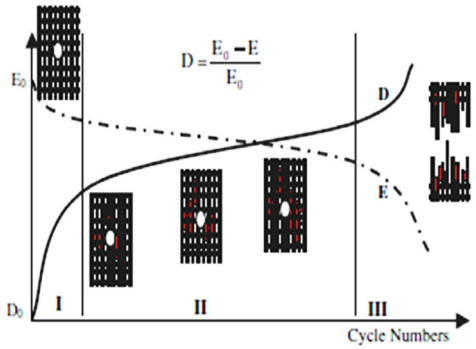

Fig.6: Evolution of the modulus of elasticity E and damage D according to the number of cycle (Toubal *et al*., 2006)

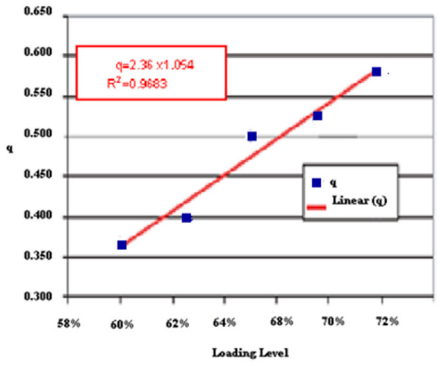

Fig.7: Evolution of *q* according to load (Toubal *et al*., 2006).

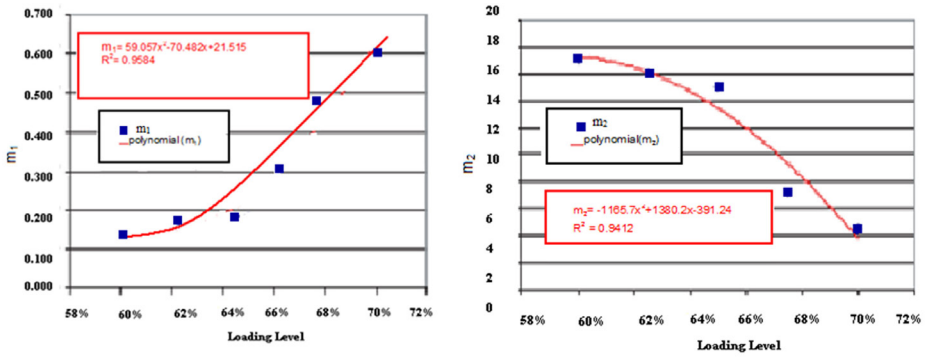

Fig.8: Evolution of m_1 and m_2 according to load (Toubal *et al*., 2006).

Table 1: The values of *q*, m_1 and m_2, Toubal *et al.* (2006)

Loading of load (%)	*q*	m_1	m_2
70	0.585	0.600	4.50
67.5	0.520	0.460	7.20
65	0.500	0.180	10
62.5	0.400	0.142	14
60	0.365	0.135	15

Fig.9 shows a comparison of the evolution of the damage for different loads by analytical means using Eq. (4), as proposed by Mao and Mahadevan (2002) and the experimental approaches. Fig.10 shows an image of the thermal distribution on the surface of the examined specimens provided by an infrared camera. It shows that the hot zone is localized at the centre of the specimens. The correlation between the increase of temperature and the damage evolution in the composites was done by using this thermography and experimental data. Fig.11a, Fig.11b, and Fig.11c show a comparison between the change of temperature and the damage at different loadings.

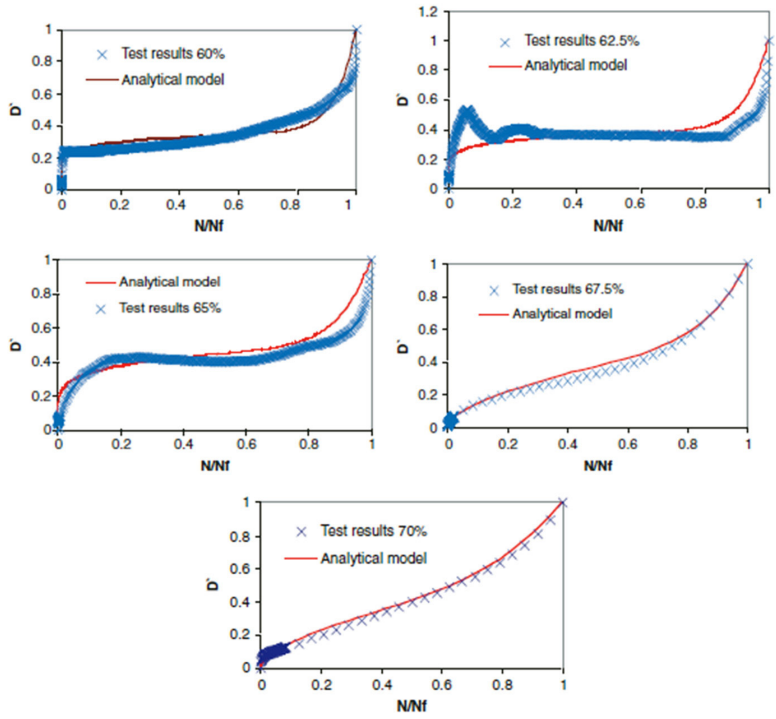

Fig.9: A comparison of the evolution of the damage by experimental and analytical (Toubal *et al*., 2006).

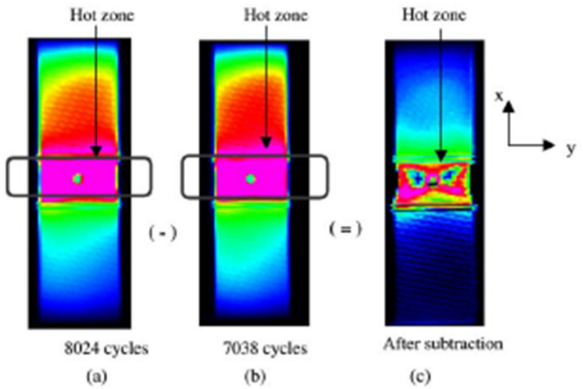

Fig.10: Various cartographics of temperature for various cycles (Toubal *et al*., 2006)

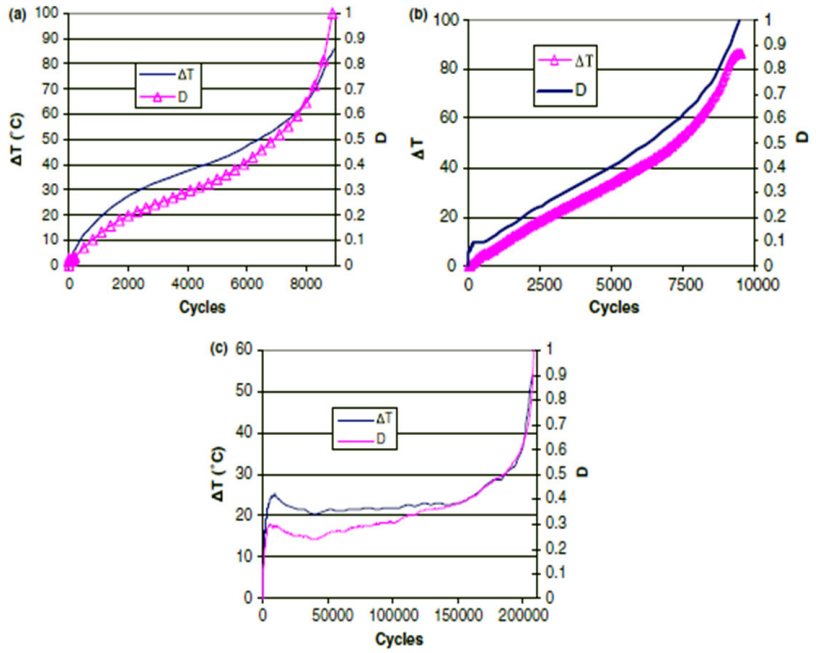

Fig.11: A comparison between the change of the temperature and the damage; (a) 70%loading, (b) 67.5% loading, and (c) 60% loading (Toubal *et al*., 2006).

Non-destructive Technique (NDT)

Non-destructive technique (NDT) is used for a group or a single part of an instrumental which does not damage or disturb (permanently) the object. NDT for testing and evaluating are the concepts and terms that have been used by the scientists or researchers for only the past 50-60 years (Boogard, 1994). The terms 'technique' and 'method' have been cautiously applied as follows*: method* will be used for the description of a discipline such as ultrasonic inspection, while pulse-echo or through-transmission is qualified as a *technique*. The principal objective of a non-destructive examination (NDE) is to provide the inspector with quantitative as well as qualitative information (Coffey, 1983). Non-destructive testing (NDT) is particularly relevant to the inspection of large and expensive components. The aerospace, food, nuclear and offshore industries are only a few examples of industries which employ a wide range of the NDT techniques. The most commonly used NDT methods in industry include visual inspection, liquid penetrant inspection, magnetic particle inspection, eddy current testing, alternating current potential drop, alternating current field measurement, ultrasonic testing, radiography and thermography. These NDT techniques can be used for the detection of unwanted discontinuities and separations in a material (flaws), structural assessment of a component (microstructure and matrix structure), metrology and dimensional purposes (thickness measurement, checking of displacement and alignment), determination of the physical properties of a material (electrical, magnetic or mechanical properties, as well as the detection of foreign bodies in food (Gros, 1996). In addition, NDT also provides information about product's properties such as composition and chemical analysis, stress and dynamics response, signature analysis and abnormal sources of heat (Giorleo & Meola, 2002).

CONCLUSION

Most of the presented studies conducted on predicting fatigue life of the composites materials or the proposed models have used synthetic fibre. There are still limited works done on predicting the fatigue life of natural fibre reinforced composites materials. Based on the review, the following are concluded:

1. Generally, it was found that many fatigue analyses had been done in composites materials but studies carried out on composites materials reinforced by natural fibres are rather limited.
2. As observed in the present results, most of the researchers obviously intended to use a non-destructive technique (NDT) in their work.

ACKNOWLEDGEMENTS

The authors wish to thank the Department of Mechanical Engineering and the technical staff at UPM for their support.

REFERENCES

Boogard, J. (1994). Non Destructive Technique. In X. P. V. Maldague (Ed.), *Need and Necessity of NDT* (pp. 3-7). Boston MA: Cahners Publishing.

Broutman, L. J., & Sahu, S. (1972). A new theory to predict cumulative damage in glass reinforced composites. *Composite Materials Testing and Design, ASTM STP*, *497*, 170-188.

Chrysochoos, A. (2002). Infrared thermography, a potential tool for analysing the material behaviour. *Meca Indus*., 135-141.

Clark, S. D., Shenoi, R. A., & Allen, H. G. (1999). Modelling the fatigue behaviour of sandwish beams under monotonics, 2 step and block loading regimes. *Composites Science Technology, 59*, *471-486.*

Coffey, J. M. (1983). Advances in non-destructive examination for structural integrity: Applied Science. In Nicholas, R. W. (Ed), *NDT International, 16*(6), 360-361.

D'amore, A., Caprino, G., Stupak, R., Zhou, J., & Nicholas, L. (1999). Effect of stress ratio on the flexural fatigue behaviour of continuous stand mat reinforced palstics. *Science Engineering Composite Materials*, *5*, 1-8.

Dawis, L. W., & Bradstreet, W. S. (1970). *Metal and Ceramic Matrix Composites* (pp. 193-194). Boston MA: Cahners Publishing.

El Mahi, A., Khawar Farooq, M., Sahraoui, S., & Bezazi, A. (2004). Modeling the flexural behaviour of sandwish composites materials under cyclic fatigue. *Materials and Design*, *25*, 199-208.

Fatemi, A., & Yang, L. (1998). Cumulative fatigue damage and life prediction theories: a survey of the state of the art for homogeneous materials. *Int. J. Fatigue*, *20*(1), 9-34.

Fatemi, A., & Mars, W. V. (2002). A literature survey on fatigue analysis approach for rubber. *International Journal of Fatigue, 24*, 949-961.

Giorleo, G., & Meola, C. (2002). Comparison between pulsed and modulated thermography in glass-epoxy laminates, *NDT & E International, 35*(5), 287-292.

Granda, M., Hernandez, G., Urriolagoitia, C., Urriolagoitia, S., & Merchan, C. (2008). Cumulative Damage Evaluation under Fatigue Loading. *Applied Mechanics and Materials, 13*(14), 141-150.

Gros, X. E. (1996). *NDT Data Fusion*. London: Arnold Publisher.

Harris, B. (2003). Fatigue in Composites. In B. Harris, B. (Ed). *Fatigue in composites science and technology of the fatigue response of fibre-reinforced plastics* (pp.145-156).Cambridge: Woodhead Publishing.

Harris, B. (2003). Fatigue in Composites. In Harris (Ed.), *A historical review of the fatigue behavior of fibre-reinforced plastics* (pp. 3-31). Cambridge: Woodhead Publishing.

Kim, W. D., Lee, H. J., Kim J. Y., & Koh, S. K. (2004). Fatigue life estimation of an engine rubber mount. Fatigue life estimation of an engine rubber mount. *International Journal of Fatigue*, *26*, 553-560.

Lawson, R. N. (1956). Implications of surface temperatures in the diagnosis of breast cancer. *Canadian Medical Association Journal, 75*, 309-310.

Li, Y., Mai, Y. W., & Ye, L. (2000). Sisal fibre and its composites: a review of recent developments. *Composite Science Technology*, *60*(11), 2037-55.

Lindley, P. B., & Stevenson, A. (1982). Fatigue resistance of natural rubber in compression. *Rubber Chemistry and Technology, 55*, 337-351.

Mao, H., & Mahadevan, S. (2002). Fatigue damage modelling of composites materials. *Composite Structures, 58*, 405-410.

Marin, J. (1962). *Mechanical Behaviour of Engineering Materials*. Prentice-Hall.

Mars, W. V., & Fatemi, A. (2002). A literature survey on fatigue analysis approaches for rubber. *International Journal of Fatigue, 24*, 949-961.

Mathur, V. K. (2006). Composite materials from local resources. *Construction and Building Materials*, *20*, 470-477.

Nicholas, T. (2000). An approach to fatigue life modelling in titanium-matrix composites. *Materials Science Engineering A*., 29-37.

Reifsnider, K., Case, S., & Duthoit, J. (2000). The mechanics of composite strength evolution. *Composites Science Technology, 60*, 2539-2546.

Royo, J. (1992). Fatigue Testing of Rubber Materials and Articles. *Polymer Testing*, *II*, 325-344.

Roylance, D. (2001). *Fatigue by Department of Materials Science and Engineering, Massachusetts Institute of Technology, Cambridge*. Retrieved from http://ocw.mit.edu/courses/materials_science_and_engineering/3_11_mechanics-of-materials_fall_1999/modules/fatigue.pdf.

Salvia, M., Fournier P., & Vincent, L. (1997). Flexural fatigue behaviour of UDGFRP experimental approach. *International Journal of Fatigue*, *19*(3), 253-262.

Sapuan, S. M., Leenie, M., Harimi, & Beng, Y. K. (2006). Mechanical properties of woven banana fibre reinforced epoxy composites. *Materials and Design*, *27*, 689-693.

Savastano Jr, H., Santos, S. F., Randojic, M., & Soboyejo, W. O. (2009). Fracture and fatigue fiber-reinforced cementitious composites. *Cement and Concrete Composites, 31*, 232-243.

Shen, G., Glinka, G., & Plumtree. (1993). A Fatigue life prediction of a B/Al Composite. *Engineering Fracture Mechanics*, *44*(3), 449-457.

Southern, E., & Thomas, A. G. (1978). Studies of rubber abrasion. *Plastic and Rubber Materials and Applications*, *3*, 133-138.

Stevenson, A. (1987). Crack at fatigue resistance. *Europe Rubber Journal*, *169*(11), 24-29.

Woo C. S., Kim, W. D. & Kwon, J. D. (2008). A study on material properties and fatigue life prediction of natural rubber component. *Materials & Science A*., *483-484*, 376-381

Yuanjian, T., & Isaac, D. H. (2007). Impact and fatigue behavior of hemp fibre composites. *Composites Science & Technology, 67*, 3300-3307.

Wu, F., & Yao, W. (2009). A fatigue damage model of composite materials. *International Journal of Fatigue*. Article in Press.

Pertanika J. Sci. & Technol. 21 (1): 15 - 28 (2013)

SCIENCE & TECHNOLOGY

Journal homepage: http://www.pertanika.upm.edu.my/

Application of Anthropometric Dimensions for Estimating Stove Height, Stove Depth and Cooking Task Envelope for Malaysian Elderly Population

Ruhaizin Sulaiman[1]*, Zahari Taha[2] and Siti Zawiah Md. Dawal[3]

[1]Department of Industrial Design, Faculty of Design & Architecture, Universiti Putra Malaysia, 43400 Serdang, Selangor, Malaysia

[2]Department of Manufacturing Engineering, Universiti Malaysia Pahang, Lebuhraya Tun Razak, 26300 Gambang, Kuantan, Pahang, Malaysia

[3]Centre for Product Design and Manufacturing (CPDM), Department of Engineering Design and Manufacturing, Faculty of Engineering, University of Malaya, Lembah Pantai, 50603 Kuala Lumpur, Malaysia

ABSTRACT

Elderly are exposed to physical impairment. This has a strong impact on their daily activities including frying, which is one of the most popular cuisine preparations. The stove height and work envelope are two major ergonomic issues in performing cooking task. There has been little research focusing on Malaysian elderly task performing in addressing these issues. The objectives of this study were to identify the acceptable stove height and depth and to determine the working envelope among Malaysian elderly using anthropometric data. A total of 55 Malaysian elderly (25 male and 30 female) aged between 60 to 85 years participated in this study. Five body measurements were taken from each subject using an anthropometer. The measurements are stature height, shoulder height, arm span, arm reach forward and waist height. Apart from these anthropometric measurements, their present stove height was also measured. The acquisition of stove height dimensions was performed through a series of door to door visit of the elderly homes in Kg. Sg. Merab. These variables were used to estimate the elderly working envelope and determine the stove height, width and depth. Data were analysed using SPSS software. The waist height dimension was to estimate the stove height, the arm reach forward for the depth and the arm span for the length of the table-top where the stove was placed. Meanwhile the stature and shoulder height were used for estimating the position of the overhead compartment or placement of cooking utensils. The 5th percentile was chosen since it is appropriate to accommodate 90% of the studied population. The 5th percentile was also applied for the setting of the working envelope so as to provide better reaching tolerances. Meanwhile, standard was used to compare the present state of the studied kitchen setting. The results show that 56.4% of the elderly waist height is lower than the standard table-top height which is 36 inches (91.4cm) and 36.4% of

Article history:
Received: 4 November 2010
Accepted: 4 April 2011

E-mail addresses:
ruhaizin@putra.upm.edu.my (Ruhaizin Sulaiman),
ztr.motion@googlemail.com (Zahari Taha),
sitizawiahmd@um.edu.my (Siti Zawiah Md. Dawal)
*Corresponding Author

ISSN: 0128-7680 © 2013 Universiti Putra Malaysia Press.

the stove height was found higher than that of the standard. This could apparently cause fatigue and discomfort to shoulders, the neck, the arm and the back of the user. Anthropometrics measurements can be used for estimating the stove height, length and depth. These could also calculate a space taken for certain physical activities, such as frying task envelope. Providing a good combination of stove height, length, depth and ergonomic working envelope could hopefully improve the elderly cooking task and increase their quality of life.

Keywords: Elderly, fatigue, discomfort, ergonomic working envelope, quality of life

INTRODUCTION

Physical dimensions and human movement are significant to a space they occupy in any performance of task. This human anthropometrics is also very useful as a guideline in designing products, equipment, furniture, transport or even buildings.

Anthropometry means the study of human body measurement for use in anthropological classification and comparison (Answer.com, 2010). Work envelope, on the other hand, means a space which can cater part or the whole human body movement when performing certain tasks. In this paper, the investigation was carried out based on standing work posture and the work envelope derived from the anthropometrics measurements of the elderly. There are other methods of assessing working posture, such as Rapid Entire Body Assessment (REBA) by Hignett (1998), McAtamney and Hignett (1995), or Rapid Upper Limb Assessment (RULA) by McAtamney and Corlett (1993); nonetheless, these will not be discussed further in this paper.

Working in a kitchen could be an issue for some elderly, especially when preparing their meal. This is due to shrunk cartilage throughout the spine that begs their standing strength ability and endurance. The posture among the aged also has a slumped character that could limit the movement (Tilley, 2008). According to Opila *et al*. (1988), line of gravity is forward of the spine (L4-5), i.e. the body has a forward bending moment which is counterbalanced by ligament forces and back muscle forces. If the body centre gravity is moved forward, it causes a variety of biomechanical stresses while standing or walking (Lee *et al*., 2001). Another factor is the 50% reduction of leg strength (Tilley, 2008) which decreases the elderly standing endurance and this may require them to use supportive instrument, such as canes, tripod aids, walkers, or even chair when performing cooking task.

Ecologically, elderly are exposed to breakdown of functional impairments. These include changes in anthropometry, musculoskeletal attributes, respiration and circulation, nervous functions, capacity for physical work, brain and memory, visual functions, hearing, taste and smell, as well as sensitivity and also sensory and psychomotor performance (Taha & Ruhaizin, 2010). These factors have negative impacts on their performance in instrumental activities of daily living (IADL) or even the basic activities of daily living (BADL). In a household setting, a task such as opening a can of red beans is considered far more complex than cellular or molecular mechanisms of aging due to complex body and environmental systems involved. Some surveys conducted show that older populations (65+) have greater difficulty in performing one or more common self-care activities, such as eating, using the toilet, dress, bathing, or

preparing meals in the kitchen (Dawson *et al*., 1987; AARP, 2000; Taha & Ruhaizin, 2008).

Cooking task is normally performed in a standing posture. This is because ordinary meal preparation requires high physical mobility between a work-triangle. The performers in this case, who are the elderly, will have to stand and use both their hands while performing the task regardless of whether they are right-, or left-handed. The dominant hand normally performs the main task and is supported by the other hand. For example, a right-handed user holds the ladle with his right hand while the left hand will hold and stabilise the frying pan caused by forces of stirring.

Besides physical frailty, the other factors effecting cooking performance are the height of the stove and work-top. For example, the incorrect height of the table-top could contribute to shoulder fatigue, neck pain, back pain and elbow pain after completing the task. The actual frying task normally requires higher hand rising due to additional stove height and the height of the frying pan. Furthermore, the ladle set used for mixing the cuisine could also add-up the height of hand rising and make the situation worst. Although providing stepping stool for

Fig.1: The height of the stove is higher than the subject's waist height.

Fig.2: Subject's arm could easily rise-up close to his shoulder height while stirring.

Fig.3: The stove is too low than the subject's waist height. Bending the neck exceeding 20 degree could cause neck fatigue.

Fig.4: The arm is lifted above the shoulder height. This contributes to shoulder pain and arm fatigue.

shorter persons may overcome this problem, this is merely a short-term solution and can still contribute to accident in the kitchen.

Fig.1, Fig.2, Fig.3 and Fig.4 illustrate the subjects performing frying task in their kitchen settings. Each figure shows a different ratio between the subject's waist height and the height of the stove. In particular, both Fig.1 and Fig.4 show that the table-top is too high. It is clear that the pan is higher than the subject's elbow height. This position may cause shoulder discomfort or fatigue. Meanwhile, Fig.3 illustrates that the tabletop level is far below the waist height, and this position forces the subject to tilt her neck down. As shown in Fig.5, the neck flexion angle should not exceed the range between 0-20 degrees to prevent neck fatigue.

Some of the examples above show that incorrect stove height could contribute to musculoskeletal disorder, primarily on the shoulder and the neck. Pain on the elbow is also reported at times. Konz and Johnson (2004) stated that musculoskeletal disorder is also known as occupational cerviobrachial disorder (OCD) and upper limb disorder (ULD). If an elderly is diagnosed of having this disorder, the chances to come back to a normal healthy state are very slim or there is no chance for it at all. He or she will definitely depend on others for the rest of his or her life.

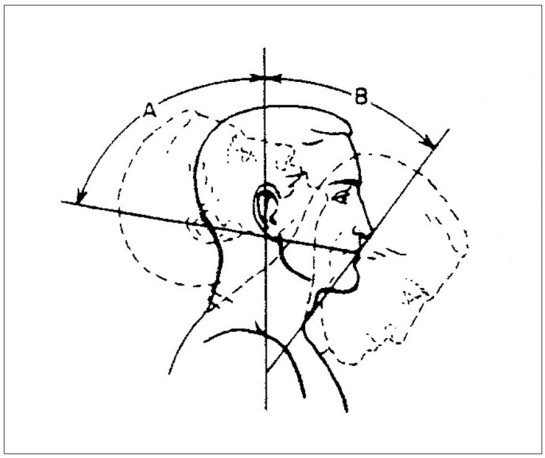

Fig.5: The Neck Extension (A) and Flexion (B) (Source: FAA William J. Hughes Technical Centre) (Exhibit 14.3.3.2.1 Joint movement ranges)

Therefore, greater focus on elderly anthropometrics measurement, their working envelopes, and the kitchens stove height should be investigated. This paper presents the result of a study on the elderly stoves height and their nature of working envelopes in everyday cooking task.

The most common height for a kitchen counter top is 36 inches (or 91.4cm). Premade based cabinets are designed for this finished height. Thus, the height of 36 inches (91.4cm) is typically the optimal and most ergonomic height for a kitchen counter. It may not be the best for a specific task, but it is apparently the best overall compromise for the majority of tasks done in the kitchen. For most people, a kitchen counter top height of 36 inches (91.4cm) provides a comfortable work station. Extremely short or tall people, or those with special needs, may want to modify that height to better suit their needs (About.com, 2008).

According to the National Kitchen and Bath Association (NKBA), the minimum height of the first level, which is 28 inches (71cm), shows that it is fully complied for the elderly requirement. On the other hand, the maximum height of the second level, which is 45 inches (114cm), is too high for Malaysian elderly.

According to Peterson (1998) and Tilley (2002), the standard kitchen cabinet height is 36 inches (91.4cm) and 24 inches (61cm) deep. NKBA has proposed two level ranges of work-counter heights. One is 28 inches (71cm) to 36 inches (91.4cm) above the finished floor and the second is 36 inches (91cm) to 45 inches (114cm), (Krengel, 1997).

METHOD AND INSTRUMENT

Anthropometrics measurement

A total of 55 Malaysian elderly (25 males and 30 females) aged between 60 to 85 years, with the mean age of 66.98 years, participated in the anthropometrics measurement of this study. The subjects were pooled in a community hall for a briefing on the objectives of the research and the procedures of the data acquisition. Basic subjects' background information, such as name, age, health status, gender and address, was also recorded for demographic purposes.

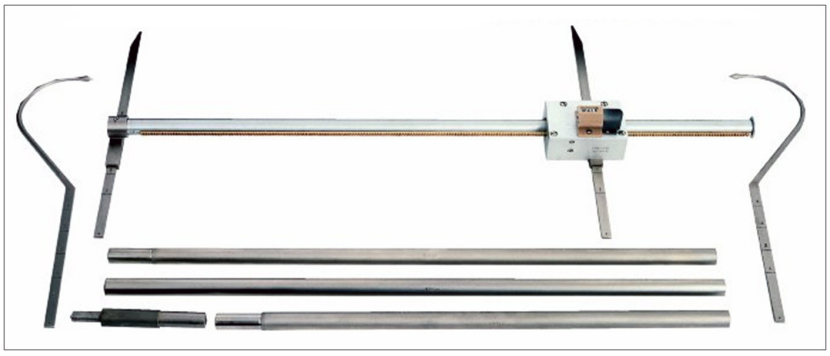

Fig.6: Instrument used to acquire anthropometric data

Five body dimensions were measured on each individual elderly during the session. These include stature (standing height), shoulder height, arm span, arm reach forward and waist height. The *"anthropometer"* is the main instrumental set used in the data acquisition (see Fig.6). Each measurement was taken 3 times and the average was recorded for statistical analysis.

Measuring the Table-top, Stove and Frying Pan Height

The acquisition of these measurements was performed through a series of door-to-door visit of 55 elderly homes in Kg. Sg. Merab. These data are important to evaluate the existing kitchen settings and to compare those with the present guidelines or standard, as well as the relation with the elderly anthropometrics. Each of the table-top, stove and pan heights, as well as the depth of their kitchen worktops, was measured using an ordinary measuring tape. The data were analysed using SPSS software.

Fig.7, Fig.8, Fig.9, Fig.10 and Fig.11 show the acquired anthropometrics measurements in this study.

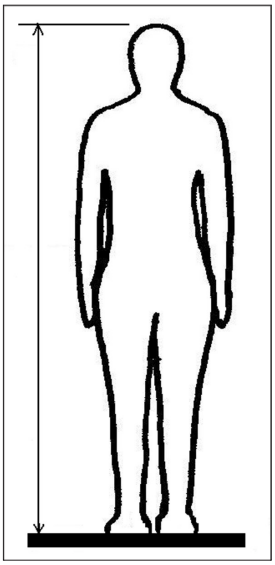

Fig.7: Stature height

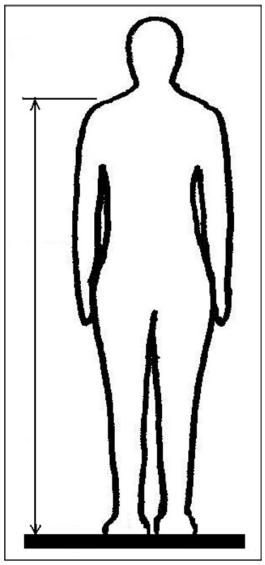

Fig.8: Shoulder height

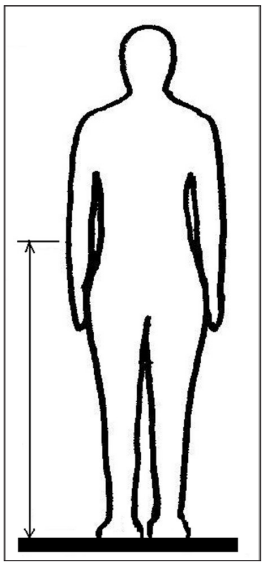

Fig.9: Waist height

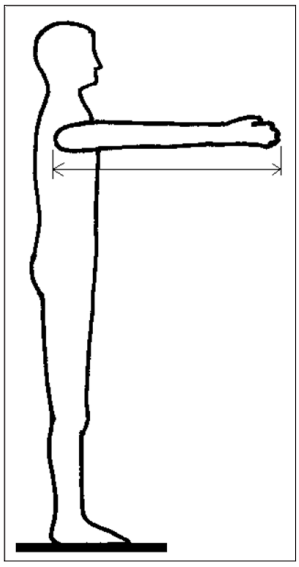

Fig .10: Arm reach forward

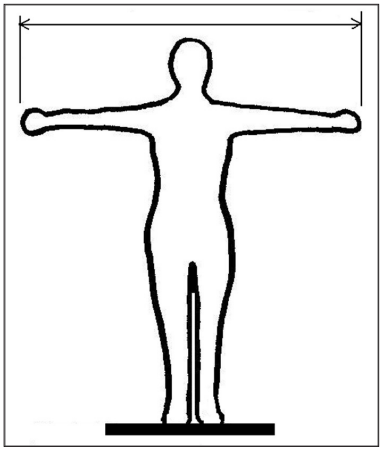

Fig.11: Arm span

RESULTS AND DISCUSSION

The anthropometrics data acquisition involved 5 measurements, and these included stature height, shoulder height, arm span, arm reach forward and waist height. The other variable is stove height. The statistical results are shown in Table 1 to Table 8 as well as Fig.7 to Fig.12. Table 9, on the other hand, shows the comparison with the previous findings.

The Stove Height

The 'stove height' is a dimension measured from the floor to the top of the stove. This includes table or cabinet where the stove is placed on. The results are in Tables 1, and 2, as well as in Fig.12. Table 2 shows that 36.4% of the stove height is higher than 36 inches (91.4cm) which is as suggested by NKBA.

TABLE 1: Statistics of the stove height

Stove Height

N	Valid	55
	Missing	0
Mean		87.5709
Std. Deviation		7.10870
Minimum		73.60
Maximum		99.00
Percentiles	5	74.6400
	50	86.3000
	95	99.0000

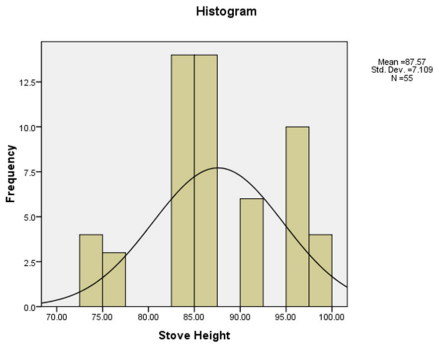

Fig.12: Frequency of the height of stoves

TABLE 2: Frequency of the height of stoves

		Frequency	Percentage	Valid Percentage	Cumulative Percentage
Valid	73.6	2	3.6	3.6	3.6
	74.9	2	3.6	3.6	7.3
	76.2	3	5.5	5.5	12.7
	83.8	14	25.5	25.5	38.2
	86.3	14	25.5	25.5	63.6
	91.4	6	10.9	10.9	74.5
	96.5	10	18.2	18.2	92.7
	99	4	7.3	7.3	100.0
	Total	55	100.0	100.0	

TABLE 3: Statistics of waist height

Waist Height

N	Valid	55.0000
	Missing	.0000
Mean		90.0491
Std. Deviation		4.3723
Minimum		81.0000
Maximum		101.0000
Percentiles	5	82.6000
	50	90.0000
	95	96.6000

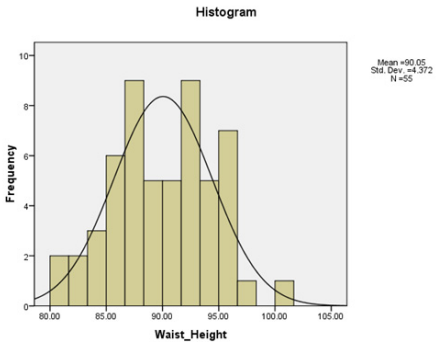

Fig.13: Frequency of waist height

TABLE 4: Frequency of waist height

		Frequency	Percentage	Valid Percentage	Cumulative Percentage
Valid	81	2	3.6	3.6	3.6
	83	1	1.8	1.8	5.5
	83.2	1	1.8	1.8	7.3
	84	1	1.8	1.8	9.1
	84.2	1	1.8	1.8	10.9
	84.5	1	1.8	1.8	12.7
	85	1	1.8	1.8	14.5
	85.1	1	1.8	1.8	16.4
	85.8	1	1.8	1.8	18.2
	86.4	1	1.8	1.8	20.0
	86.5	2	3.6	3.6	23.6
	87	1	1.8	1.8	25.5
	87.2	1	1.8	1.8	27.3
	87.5	2	3.6	3.6	30.9
	87.8	1	1.8	1.8	32.7
	88	4	7.3	7.3	40.0
	88.8	1	1.8	1.8	41.8
	89	2	3.6	3.6	45.5
	89.5	1	1.8	1.8	47.3
	89.6	1	1.8	1.8	49.1
	90	1	1.8	1.8	50.9
	91	3	5.5	5.5	56.4
	91.4	1	1.8	1.8	58.2
	92	3	5.5	5.5	63.6
	92.1	1	1.8	1.8	65.5
	92.2	1	1.8	1.8	67.3
	92.5	2	3.6	3.6	70.9
	92.7	1	1.8	1.8	72.7
	93	1	1.8	1.8	74.5
	93.5	1	1.8	1.8	76.4
	93.8	2	3.6	3.6	80.0
	93.9	1	1.8	1.8	81.8
	94.5	1	1.8	1.8	83.6
	95	1	1.8	1.8	85.5
	95.1	1	1.8	1.8	87.3
	95.2	1	1.8	1.8	89.1
	95.5	2	3.6	3.6	92.7
	95.9	1	1.8	1.8	94.5
	96.5	1	1.8	1.8	96.4
	97	1	1.8	1.8	98.2
	101	1	1.8	1.8	100.0
	Total	55	100.0	100.0	

Tables 3 and 4, as well as Fig.13, show the results of the waist height of the elderly. It was found that 56.4% of the waist height of the elderly is lower than 36 inches (91.4cm).

Referring to the heights of both the stoves and the waist, it was found that Malaysian elderly are working on a higher work-top, and therefore, they are exposed to discomfort and fatigue.

The recommended stove height for Malaysian elderly is 82.6cm (32.5 inches). This is a little bit higher than the height of countertop for seated user which is between 28 – 32 inches (71cm – 81.3cm), as suggested by Peterson (1998). In order to fulfil the majority of the elderly stove height requirement, a range of stove height is more significant and it should be established. The 5th percentile of both the stove height (74.6cm) and waist height (82.6cm) could accommodate 90% of the studied population. Therefore, the recommended range of stove height should be from 74.6 - 82.6cm (or 29.4 - 32.5 inches).

The Working Envelope

All the variables (namely, stature height, shoulder height, arm span, arm reach forward and waist height) were measured and analysed to identify the elderly working envelopes. The *stature* and *shoulder height* were meant for setting the overhead compartment height. Meanwhile, the *arm span* dimension is to set the width of kitchen cabinet and considering the left and right reaching. The *arm reach forward* is to set the work-top depth and the frontal reaching. Meanwhile, the *waist height* is to set the height of the work-top. In this study, the working envelope was calculated based on the 5th percentile of the above variables so as to ensure that the space fit most subjects. Table 5 shows that the arm reach forward is 67.28cm (26.7 inches), while Fig.14 reveals the frequency of arm reach forward. Table 6 shows that the height envelope is 138.14cm (or 54.4 inches). Meanwhile, the arm span (see Table 7) is 142.6cm (or 56.1 inches). Table 8 shows the results of the shoulder height at 114.2cm (or 45.0 inches).

The results of the arm span presented in Table 7 and Fig.16 are to identify the minimum length of the work-top. All the visited kitchens have a longer table top and this comply with the anthropometric of the studied population.

TABLE 5: Statistics of arm reach forward

ArmReach_Forward

N	Valid	55.0000
	Missing	.0000
Mean		76.1964
Std. Deviation		4.8223
Minimum		66.8000
Maximum		89.5000
Percentiles	5	67.2800
	50	76.0000
	95	85.5200

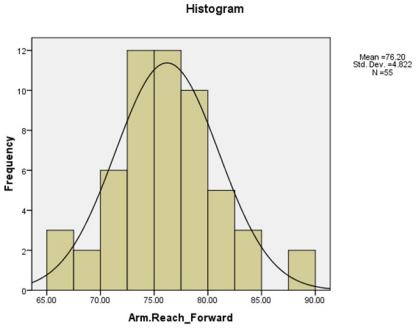

Fig.14: Frequency of arm reach forward

TABLE 6: Statistics of stature height

Height

N	Valid	55.0000
	Missing	.0000
Mean		149.8055
Std. Deviation		7.4186
Minimum		135.0000
Maximum		167.4000
Percentiles	5	138.1400
	50	150.0000
	95	163.7600

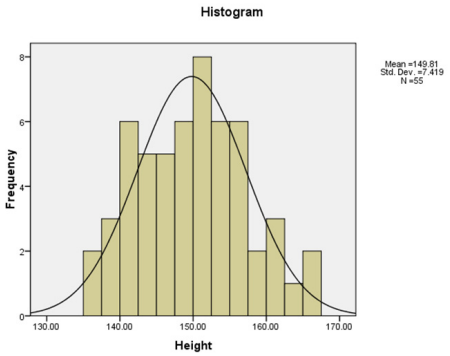

Fig.15: Frequency of the stature height

TABLE 7: Statistics of arm span

Arm Span

N	Valid	55.0000
	Missing	.0000
Mean		155.8782
Std. Deviation		8.1482
Minimum		134.8000
Maximum		172.8000
Percentiles	5	142.6000
	50	155.6000
	95	170.2600

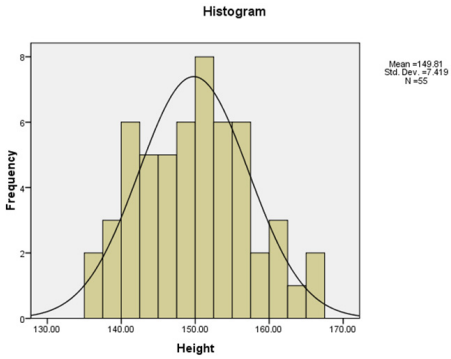

Fig.16: Frequency of arm span

TABLE 8: Statistics of Shoulder Height

Shoulder Height

N	Valid	55.0000
	Missing	.0000
Mean		125.0109
Std. Deviation		6.5600
Minimum		111.5000
Maximum		141.6000
Percentiles	5	114.2000
	50	124.5000
	95	136.3200

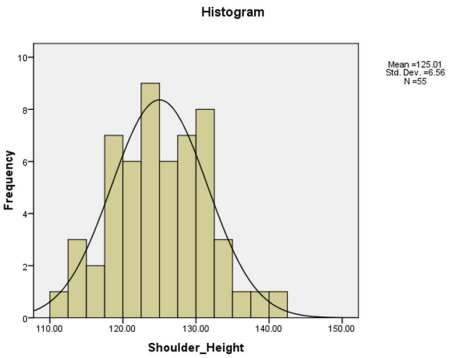

Fig.17: Frequency of shoulder height

According to Hignett and McAtamney (2000), the good work envelope should consider the limitations of body movements and measurements. Trunk flexion is within 0-20 degree and extension may reach 60 degree. Meanwhile, the neck movement is within 0-20 degree in flexion and extension. The knees flexion is within 30-60 degrees. The upper arm extension is within 20 degree, while the flexion may be up to 90 degree and over. The lower arms flex is between 60-100 degrees and over. As for the wrist movement, it is 0-15 degree, either in flexion or extension. Following these setting could avoid illness or syndrome from bad working envelope.

According to Grey (1997), there are two worktop heights. One is for the use of small appliances which is 17-25cm (7-10inches) lower than the elbow height. The other is 5-10cm (3-4inches) below the users' flexed elbow height while work on food preparation.

On the other hand, Sharifah Norazizan *et al*. (2006) also measured the elderly elbow height and found that the mean of Malaysian elderly elbow height is 89.20cm for the females and this is 97.10 cm for the males. The average for both the means is 93.15cm. Therefore, the stove height for both genders is 68.15-76.15cm and the worktop height is 83.15-88.15cm based on Grey's tolerances.

Table 9 shows the estimating dimension of stove deep. In contrast with the high reach and easy reach dimensions, the 5th percentile was used. This was done to ensure the optimum reach for majority of the studied population. Meanwhile, Woodson *et al*. (1992) stated that the counter width or deep dimensions should be between 16-24 inches (or 40.64 - 60.96cm). It was found that the proposed width or depth dimension (60.00-70.00cm) was above that of Woodson's findings.

Both the variables in this study are important in the sense of user friendly task performing and the recommended values should met requirement for most of the user populations, i.e. the 'design for the tall accommodates the small (Konz & Johnson, 2004).

CONCLUSION

Anthropometric measurements can be used to estimate the work envelope as well as to suggest the stove height, depth and length dimensions. It is also crucial for Malaysian elderly to have the right working envelope setting to avoid fatigue which could further contribute to musculoskeletal disorder (MSD) problem in the long-term. Besides, this could also improve safety, especially to avoid kitchen accident during meal preparations. It is suggested to further investigate other ADL or IADL tasks envelope and compare it with the anthropometrics of Malaysian elderly in order to improve their task performance and quality of life.

Moreover, the future kitchen furniture design should incorporate ergonomics consideration, specifically the height and reaching distance of the users. The recommendations are stated in the last column of Table 9. In more specific, providing an ideal or custom stove length, width and height will hopefully reduce ergonomics issues of cooking and ensure user's comfort. In order to accommodate 90% of the elderly population, the 5th percentile of their waist height, arm span and arm reach forward data were used as the reference point for designing the stove height, length and depth. On the other hand, the elderly should also be exposed to a good meal preparation practice and basic understanding on ergonomics. According to Saxon and Etten (2002), the gerogogy approach of teaching should be adapted to the elderly so as to increase their

ergonomics awareness towards performing any BADL, ADL and IADL. A good understanding and realization of self physical and physiological limitations may also help the elderly reduces exhaustion, muscle pain, eliminate fatigue and so forth upon completing certain tasks. It is hoped this doing this will further increase their independency and improve their well being.

TABLE 9: A Comparison of the Standing Work Envelope

	SAE (1977)	Grey (1997) tolerance	NKBA & Krengel (1997)	Peterson (1998) & Tilley (2002)	Sharifah Norazizan et. al. (2006)	Finding 5thtile (2010)	Proposed dimensions
Elbow Height (cm)	104.00	-	-	-	93.15	-	-
Table -top Height (cm)	91.50	5-10cm Below Elbow height	91.00 – 114.00	91.00	83.15 – 88.15*	-	-
Stove Height (cm)	-	17-25cm Below Elbow height	71.00 – 91.00	-	68.15 – 76.15*	74.64	74.60 - 82.60
Stove Depth (cm)	76.00	60.00cm (based on shelf depth)	-	61.00	-	67.28	60.00 – 70.00
Stove Length (cm)	-	-	-	-	-	-	Minimum 142.60

* Estimating using Grey's tolerances.

REFERENCES

Dawson, D., Hendershot, G., & Fulton, J. (1987). *Functional Limitations of Individuals Age 65 Years and Over*, Advanced Data, Vital and Health Statistics No. 133. US Public Health Service, Hyattsville, MD, June 10.

Grey, J. (1997). *Home Design Workbooks: Kitchen*. London: Dorling Kindersley Limited.

Hignett, S., & McAtamney, L. (2000). Rapid Entire Body Assessment (REBA). *Applied Ergonomics, 31*, 201-205.

Konz, S., & Johnson, S. (2004). *Work Design: Occupational Ergonomics* (6th ed). Arizona: Holcomb Hathaway Publishers.

Krengel, J. W., & Baczynski, B. (1997). *Kitchens, Lifestyle and design.* Glen Cove, N.Y.: PBC International Inc.

Lee, C-M, Jeong, E-H, & Freivalds, A. (2001). Biomechanical effects of wearing high-heeled shoes. *Int. J. Of Ind. Ergonomics*, *28*, 321-326.

McAtamney, L., & Corlett, N. (1993). RULA: a survey method for the investigation of work-related upper limb disorders. *Applied Ergonomics*, *24*(2), 91-99.

Opila, K., Wagner, S., Schiowitz, S., & Chen, J. (1988). Postural alignment in barefoot and high-heeled stance. *Spine*, *13*(5), 542-547.

Peterson, M. J. (1998). *Universal kitchen and bathroom planning*. New York: McGraw-Hill.

Saxon, S. V., & Etten, M. J. (2002). *Physical Change and Aging: A Guide for the Helping Professions* (4th ed). New York: Springer Publishing Company, Inc.

Sharifah Norazizan, S. A. R., Rosnah, M. Y., Tengku Aizan, H., Ahmad Hariza, H., Aini, M. S., Mohd Rizal, H., Hirfarizan Mardianah, M. T., & Lina, G. S. C. (2006). Anthropometric data of older Malaysians. *Asia Pacific Journal of Public Health*. *18*.

Taha, Z., & Ruhaizin, S. (2008). *Ergonomics Consideration in the Design of Products for the Elderly Population.* Proceedings of the 9th Asia Pacific Industrial Engineering & Management Systems Conference (APIEMS2008) (p. 309), Bali, Indonesia, December 3rd – 5th.

Taha, Z., & Ruhaizin, S. (2010). Perceived Kitchen Environment among Malaysian Elderly. *American Journal of Engineering and Applied Sciences 3*(2), 270-276.

Tilley, A. R. (2002). *The Measure of Man and Woman: Human Factors in Design*. New York: John Wiley & Sons, Inc.

Wagner, D., Birt, J. A., Snyder, M., & Duncanson, J. P. (1996). *Human Factors Design Guide: for acquisition of Commercial-Off-The-Shelf Subsystems, Non-developmental Items, and Developmental Systems*. *Final Report and Guide*. FAA William J. Hughes Technical Center, USA. DOT/FAA/CT-96/1

Woodson, W. E., Tillman, B., & Tillman, P. (19920. Human Factors Design Handbook (2nd ed.) New York: McGraw-Hill, Inc.

Pertanika J. Sci. & Technol. 21 (1): 29 - 36 (2013)

SCIENCE & TECHNOLOGY

Journal homepage: http://www.pertanika.upm.edu.my/

Different Media Formulation on Biocellulose Production by *Acetobacter xylinum* (0416)

Suryani Kamarudin[1,2]*, Mohd Sahaid, K.[1], Mohd Sobri, T.[1], Wan Mohtar, W. Y.[3], Dayang Radiah, A. B.[2] and Norhasliza, H.[2]

[1]Department of Chemical and Process Engineering, Faculty of Engineering and Build Environment, University Kebangsaan Malaysia, 43600 Bangi, Selangor, Malaysia

[2]Department of Chemical and Environmental Engineering, Faculty of Engineering, University Putra Malaysia, 43400 Serdang, Selangor, Malaysia

[3]Department of Bioscience and Biotechnology, Faculty of Science, University Kebangsaan Malaysia, 43600 Bangi, Selangor, Malaysia

ABSTRACT

Biocellulose (BC), produced by *Acetobacter xylinum* (0416), was carried out using three types of medium composition under static surface culture. The media used in this experiment included CWHSM (Coconut water in Hestrin-Schramm medium), CM (Complex medium) and HSM (Hestrin-Schramm medium). CWHSM and CM used coconut water from agro-waste as the main source of sugar. The fermentation was conducted for 12 days and the results of BC dry weight, cell entrapped, pH medium and productivity were evaluated and compared. The results show that CWHSM is the most suitable medium for BC production with a productivity of up to 0.044 g l^{-1} day^{-1}.

Keywords: Acetobacter xylinum, agro-waste, biocellulose, coconut water, production medium

INTRODUCTION

It is known that some *Acetobacte*r strains produce cellulose. This cellulose is called bacterial cellulose (BC) (Ross *et al*., 1991). BC is a chemically pure form of cellulose and it is free from hemicellulose, pectin, and lignin, which are associated with plant cellulose and are difficult to eliminate (Bielecki *et al*., 2002; Jung *et al*., 2005). In addition, BC is extremely pure and it exhibits a high degree of polymerisation and crystallinity. BC has many applications

Article history:
Received: 1 February 2011
Accepted: 4 October 2011

E-mail addresses:
suryani@eng.upm.edu.my (Suryani Kamarudin),
sahaid@eng.ukm.my (Mohd Sahaid, K.),
sobri@vlsi.eng.ukm.my (Mohd Sobri, T.),
wantar@pkrisc.cc.ukm.my (Wan Mohtar, W. Y.),
dayang@eng.upm.edu.my (Dayang Radiah, A. B.),
snowiequeen809@yahoo.com (Norhasliza, H.)
*Corresponding Author

ISSN: 0128-7680 © 2013 Universiti Putra Malaysia Press.

which include temporary artificial skin for the therapy of burns, ulcers and dental implants; it is also used as non-woven paper or fabric to improve latex or other binders and repair old documents, as sensitive diaphragms for stereo headphones, cellulose for immobilisation of proteins and chromatographic techniques, stabiliser for emulsions in cosmetics, food and coating compositions and edible cellulose for addition to food (Jonas & Farah, 1998).

BC production has been demonstrated from glucose, sucrose, fructose, glycerol, mannitol and arabitol, among which mannitol and fructose are better carbon sources (Masaoka *et al*., 1993; Oikawa *et al*., 1995a; Oikawa *et al*., 1995b; Ross *et al*., 1991; Shoda & Sugano, 2005). The high economic cost of mannitol and fructose, as well as the relatively low-yield production with these carbon sources, limits industrial production and extended commercial applications of BC. Therefore, it is challenging and meaningful for us to look for a new approach to prepare a carbon source for high-yield BC production (Hong *et al*., 2007). There are many sources of carbon that have been experimentally verified as substrates but the elimination is in the method of preparation, which involves highly toxic chemicals and time consuming steps such as hydrolysis and detoxification. It is necessary for the substrate to be detoxified before being utilised.

In this research, a relatively low-cost carbon source of culture media was successfully developed from agro-waste. The results indicate that coconut water, waste from copra and coconut milk industries with additional nutrient formulation could serve as a feedstock or potential media for bacterial cellulose production. Meanwhile, direct application of coconut water without involving any hydrolysis and detoxification steps makes it very economical as a main carbon source of media for BC production. The usage of coconut water as a medium substrate has also been suggested by Budhiono *et al*. (1999), but the formulation is totally different from the proposed medium in this study. Other than the nutrient, the significant difference was in the initial pH value of 4.5 for them and 6.0 for this study. With the aim to manipulate the waste into a valuable material, the waste from coconut water is turned into a valuable polymeric material for commercial application. The productivity and BC production rate are the important parameters in this study.

MATERIALS AND METHODS

The strain *Acetobacter xylinum* (0416) was supplied by the Malaysian Agricultural Research and Development Institute (MARDI) in Serdang, Selangor, Malaysia. Three types of media formulation for the new proposed medium are: (1) CWHSM (Coconut water in Hestrin-Schramm medium), (2) CM (Complex medium) as suggested by MARDI, and, (3) HSM (Hestrin-Schramm medium) as suggested by Hestrin and Schramm (1954). The composition of each medium is stated in Table 1. The fermentation was carried out in 250 ml conical flasks containing 100 ml of the medium for 12 days. Each flask was inoculated with a 3-day old preculture grown statically at 30°C. The dry weight of BC, cell entrapped within the pellicle, pH of the medium and productivity for each medium were evaluated and compared.

TABLE 1: Composition of media used

MEDIUM COMPOSITION					
(1) CWHSM: Coconut water in HS medium		(2) CM: Complex medium		(3) HSM: HS medium	
Sodium hydrogen phosphate (Na_2HPO_4)	2.7 g l^{-1}	Sucrose	80 g l^{-1}	Glucose	20 g l^{-1}
Bacto peptone	5 g l^{-1}	Ammonium sulphate $(NH_4)_2SO_4$	5 g l^{-1}	Sodium hydrogen phosphate (Na_2HPO_4)	2.7 g l^{-1}
Yeast extract	5 g l^{-1}	Coconut water	Up to 1 l	Bacto peptone	5 g l^{-1}
Citric acid	1.15 g l^{-1}	pH	4.5	Yeast extract	5 g l^{-1}
Coconut water	Up to 1 l	Strain *A. xylinum*	100 ml	Citric acid	1.15 g l^{-1}
pH	6.0			Distilled water	Up to 1 l
Strain *A. xylinum*	100 ml			pH	6.0
				Strain *A. xylinum*	100 ml

Harvesting method

After removing the BC sample from the flask, the BC was washed twice with distilled water. Then, the gel was boiled in 0.5 M sodium hydroxide solution (NaOH) for 20 minutes to dissolve the cell entrapped within the pellicle. After that, it was drained and rewashed with distilled water several times. The gel was soaked in distilled water overnight to remove alkaline solution in the BC gel. The purpose of this step is to ensure that the alkaline used in this treatment is totally removed from the gel. This step was also performed to ensure that the degradation of BC would not occur as it could disturb the consistency of the BC dry weight measurement and the quality of the BC produced. Then, the gel was slowly dried in an oven at 40°C for about 5 hours. The dried gel sheets were weighed and the data were claimed as a dry weight of the BC production. The samples were stored in airtight cases.

RESULTS AND DISCUSSION

Fig.1 shows that M1-CWHSM (Coconut water in HS medium) gave the maximum BC production in the dry weight of product, followed by M2-CM (Complex medium) and the lowest was M3-HSM (HS medium). In order to get uniform results and for the purpose of comparison, the pre-culture used throughout the experiments was obtained from the same batch. The trend of the BC production in M1 and M3 is almost the same, while M2 remains constant throughout the experiment. A major difference observed between M1 and M3 formulation is only by substituting coconut water for the distilled water and glucose. The high production rate in M1 was probably because of the monosaccharide and disaccharides present in the medium, as suggested by Unagul *et al*. (2007), and which would have affected the metabolic pathway of the BC production. The highest production rate was obtained at day-8 of M1 by 0.343 g l^{-1}, which is approximately 4.0 fold higher than M3.

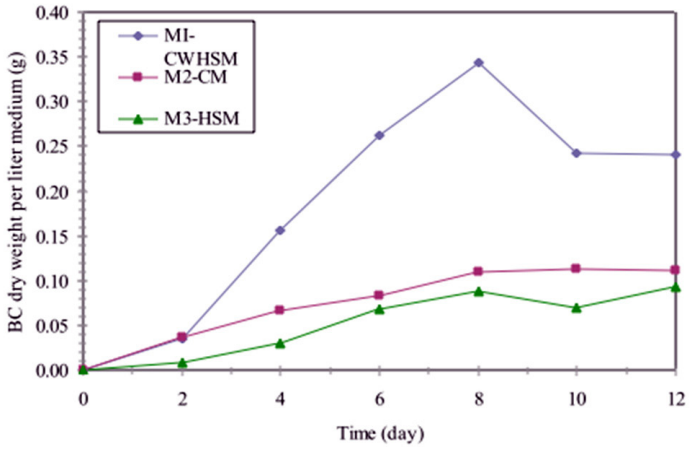

Fig.1: The dry weight of BC in different fermentation media

The metabolic pathway suggested by Serafica (1997) clearly states that glucose will directly convert to glucose-6-phosphate and phosphogluconic acid as a by-product. The precursors in cellulose synthesis are UDP-glucose and glucose, while sucrose and fructose are used as substrates for growth and BC formation. This is in a good agreement with the finding by Vandamme *et al*. (1998). When *A. Xylinum* is grown on a dextrose substrate (or a carbohydrate substrate of which it is a component), it was observed to have converted 26% of glucose into gluconic and 2-keto-gluconic acid (European Patent No. 86308092.5).

Medium M3, which only contains glucose as a substrate, was consumed by about one-third into by-product and this limited the conversion to BC as a major product. This result was verified and shown in Fig.2 for pH profile for each medium. A comparison between M1 and M3 clearly showed that a significant drop in pH was observed on day-4 of M3, which is strongly believed to be due to the accumulation of gluconic acid or acidic by-products in the medium. In more specific, the accumulation of acidic by-products is inversely proportional to the BC formation. Glucose for BC production was applied for the formation of other by-products. The first reading at day-2 showed that the pH value had dropped significantly for all the media. After that, the increase in the pH of the medium was observed up to day-6 for M1; however, M2 remained constant throughout the fermentation time. Medium M1 was too flexible as compared to the others, which is strongly believed to be due to various types of carbohydrate (monosaccharide and disaccharide) that is present in the medium. This condition provides a chance for microorganisms to adapt with the mild environment and promotes growth and conversion of polysaccharide. The accumulation of one type of substrate, with high concentration results in the medium to fast conversion reduces the chances for microbes to convert glucose into BC. The profile pH for M3 almost fluctuated because of the conversion of BC and acidic by-products by the glucose substrate.

Fig.3 shows the amount of cells entrapped within the BC pellicles plus water (wet state) in different medium formulations. The assumption was made that the amount of water that could be retained in the BC pellicle was almost the same. It is strongly believed that the amount of cells entrapped plus water is reflected in the amount of cells producing BC in the sample. It

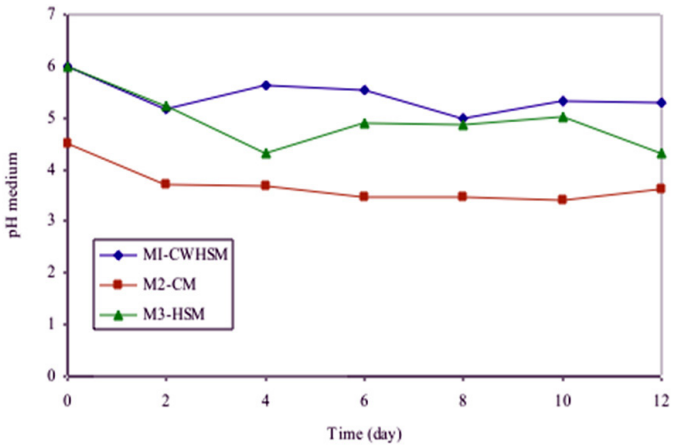

Fig.2: The pH of BC fermentation media

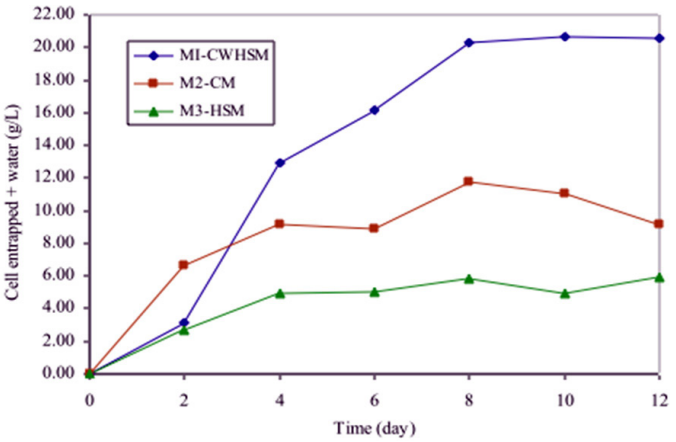

Fig.3: The amount of cells entrapped plus water in different fermentation media (wet state)

also represents active and viable cells that could synthesize BC. The BC pellicle formation mechanisms by *A. xylinum* cells is in a backward and forward motions of the *Acetobacter* cells known as reversal movements caused by synthesis of the cellulose (Shah & Malcolm, 2004). Recent research suggests that the build up of strain during the crystallisation of cellulose may be responsible for these reversals. The amount of cells entrapped within the pellicle is proportional to the BC production rate, as shown by media M1, M2 and M3. These results are in close agreement with those reported by Marx-Figini and Pion (1974); cellulose synthesis only occurs in growing bacterial populations and the yield of cellulose and the growth of bacterial populations obey the same reaction law, which is a first-order one. The fact that the cellulose synthesis only occurs when the bacteria is able to divide indicates that the production of BC must be combined with cell division itself or with some other events in the cell related to it (Marx-Figini & Pion, 1974).

Fig.4 shows the productivity of BC in different fermentation media, which is proportional to the dry weight of BC. The highest productivity was obtained by M1 at day-6 of incubation at 0.044 g l^{-1} day^{-1}. This means the M1 medium formulation shows excellent productivity compared to the other media. Hestrin and Schramm (1954) and Forng *et al*. (1989) reported that although various undefined and synthetic media have been developed for *A. xylinum*, more cellulose has been produced by the undefined medium compared to the synthetic medium. M1 medium formulation serves the most complex composition compared to the others, which covers the requirements for BC production.

CONCLUSION

Based on the results obtained in this experiment, it can be concluded that medium formulation M1 CWHSM can be a potential medium for production of BC. The advantage of CWHSM is that the medium substrate is easy to procure, as it can be locally sourced and is inexpensive as well. The use of coconut water, without any pre-treatment or hydrolysis, makes it very effective from the economic point of view. In addition, it does not involve toxic and hazardous materials in producing BC, which is excellent and suitable for safe environments such as medical and cosmetic applications. Moreover, the static surface culture fermentation also requires a low cost operation and is easy to perform.

ACKNOWLEDGEMENTS

The study was supported by an E-Science Fund Grant from the Ministry of Science Technology and Innovation (MOSTI).

REFERENCES

Bielecki, S., Krystynowicz, A., Turkiewicz, M., & Kalinowska, H. (2002) In E. J. Vandamme, S. De Baets, & A. Steinbuechel. *Biopolymers.* Weinheim: Wiley-VCH.

Ben-Bassat, A., Bruner, R., Shoemaker, S. P., Aloni, Y., Wong, H., Johnson, D. C., & Naogi, A. N. (1987). *European Patent No. 86308092.5*.

Budhiono, A., Rosidia B., Tahera, H., & Iguchib, M. (1999). Kinetic aspects of bacterial cellulose formation in *nata-de-coco* culture system. *Carbohydrate Polymers*, *40*, 137 - 143.

Forng, E. R, Anderson, S. M., & Cannon, R. E. (1989). Synthetic medium for *Acetobacter xylinum* that can be used for isolation of auxotrophic mutants and study of cellulose biosynthesis. *Applied Environment Microbiology*, *55*(5), 1317 - 1319.

Hestrin, S., & Schramm, M. (1954). Synthesis of cellulose by *Acetobacter xylinum*: preparation of freeze dried cells capable of polymerizing glucose to cellulose, *Biochemical Journal*, *58*, 345.

Hong, F., & Qiu, K. (2007). An alternative carbon source from konjac powder for enhancing production of bacterial cellulose in static cultures by a model strain *Acetobacteraceti* subsp. *xylinus* ATCC 23770, *Carbohydrate Polymers, 72*(3), 545 - 549.

Jonas, R., & Farah, L. F. (1998). Production and application of microbial cellulose. *Polymer Degradation and Stability, 59*, 101 - 106.

Jung, J. Y., Park, J. K., & Chang, H. N. (2005). Bacterial cellulose production by *Gluconacetobacter hansenii*in an agitated culture without living non-cellulose producing cells. *Enzyme and Microbial Technology*, *37*, 347 - 354.

Marx-Figini, M., & Pion, B. G. (1974). Kinetic investigations on biosynthesis of cellulose by *Acetobacter xylinum. Biochimicaet Biophysica Acta, 338*, 382 - 393.

Masaoka, S., Ohe, T., & Sakota, N. (1993). Production of cellulose from glucose by *Acetobacter xylinum*. *Journal of Fermentation and Bioengineering, 75*, 18 - 22.

Oikawa, T., Morino, T., & Ameyama, M. (1995a). Production of cellulose from D-arabitol by *Acetobacter xylinum KU-1. Bioscience Biotechnology and Biochemistry*, *59*, 1564 - 1565.

Oikawa, T., Ohtori, T., & Ameyama, M. (1995b). Production of cellulose from D-mannitol by *Acetobacter xylinum KU-1. Bioscience Biotechnology and Biochemistry*, *59*, 331 - 332.

Ross, P., Mayer, R., & Benziman, M. (1991). Cellulose biosynthesis and function in bacteria. *Microbiology and Molecular Biology Reviews*, *55*, 35 - 58.

Serafica, G. C. (1997). Production of bacterial cellulose using a rotating disk film bioreactor by *Acetobacter xylinum* (PhD Thesis dissertation). Renselaer Polytechnic Institute.

Shah, J., & Malcolm, B. R. Jr. (2004). *US patent 60/507,961*.

Shoda, M., & Sugano, Y. (2005). Recent advances in bacterial cellulose production. *Biotechnology and Bioprocess Engineering, 10*, 1-8.

Unagul, P., Assantachai C., Phadungruengluij S., Suphantharika, M., Tanticharoen, M., & Verduyn, C. (2007). Coconut water as a medium additive for the production of docosahexaenoic acid (C22:6n3) by *Schizochytrium mangrovei* Sk-02. *Bioresource Technology, 98*, 281 - 287.

Vandamme, E. J, de Baets, S., Vanbaelen, A., Joris, K., & de Wulf, P. (1998). Improved production of bacterial cellulose and its application potential. *Polymer Degradation Stability*, *59*, 93 - 99.

Pertanika J. Sci. & Technol. 21 (1): 37 - 44 (2013)

SCIENCE & TECHNOLOGY

Journal homepage: http://www.pertanika.upm.edu.my/

Solving Delay Differential Equations by Using Implicit 2-Point Block Backward Differentiation Formula

Heng, S. C.*, Ibrahim, Z. B., Suleiman, M. and Ismail, F.

Mathematics Department, Faculty of Science, Universiti Putra Malaysia, 43400 Serdang, Selangor, Malaysia

ABSTRACT

In this paper, an implicit 2-point Block Backward Differentiation formula (BBDF) method was considered for solving Delay Differential Equations (DDEs). The method was implemented by using a constant stepsize via Newton Iteration. This implicit block method was expected to produce two points simultaneously. The efficiency of the method was compared with the existing classical 1-point Backward Differentiation Formula (BDF) in terms of execution time and accuracy.

Keywords: Block Backward Differentiation formula, Delay Differential Equations, Interpolations

INTRODUCTION

In the recent years, the Mathematics society is gradually shifting their interest into numerical treatment of DDEs due to its ability in Mathematical modelling of processes in various applications as it provides the best, if not the only realistic simulation of the observed phenomena (Ismail *et al*., 2002). This is because many physical systems possess the feature of having a delayed respond in input conditions so that the rate at which processes occur depends not only on the current state of the systems but also the past states (Ismail 1999).

Some of the known application areas of DDEs include the fields of Engineering, Biology and Economy, such as in mixing of liquid, population growth, prey-predator population model and electrodynamics (Driver 1976). The general form of the first order DDE is as follows:

$$y'(t) = f(t, y, y(t-\tau_1), \ldots y(t-\tau_n)), \quad t \geq t_0 \qquad (1)$$

$$y(t) = \phi(t), \quad t \leq t_0 \qquad (2)$$

where $\phi(t)$ is the initial function, and τ_i is the delay function with $i = 1, 2, \ldots, n$. According to Bellen and Zennaro (2003), the delays τ_i or

Article history:
Received: 18 March 2011
Accepted: 13 September 2011

E-mail addresses:
cerylyn@yahoo.com (Heng, S. C.),
zarina@math.upm.edu.my (Ibrahim, Z. B.),
msuleiman@science.upm.edu.my (Suleiman, M.)
fudziah@science.upm.edu.my (Ismail, F.)
*Corresponding Author

ISSN: 0128-7680 © 2013 Universiti Putra Malaysia Press.

lags as known to some, and which are always non-negative, can be divided into three different situations according to the complexity of the phenomenon. The delays may be just constant, which is referred to as the constant delay case, or the function of t, where $\tau_i = \tau_i(t)$ which is referred to as the variable or time dependant delay case, or even the function of t and y itself, where $\tau_i = \tau_i\left(t, y\left(t\right)\right)$, which is referred to as the state dependant delay case.

Currently, most of the numerical methods for solving ordinary differential equations (ODEs) can be adapted to give corresponding techniques in solving DDEs. For example, stiff DDEs are recognized through the behaviour of ODEs. This is because of the solutions in the systems of DDEs, which may contain strongly damped components that rapidly approach equilibrium states (Roth, 1980). In general, the largest source of stiff DDEs is the stiffness in the ODEs components that are without the delay term. The stiffness of a linear system of ODEs $\tilde{y}' = A\tilde{y}$ is expressed as ratio $\left(\max_i |\operatorname{Re}\lambda_i| / \min i |\operatorname{Re}\lambda_i|\right)$ where λ_i are eigenvalues of A. For this reason, there are actually many numerical methods proposed for solving DDEs. The range of the methods comprises of one-step methods, as in Euler method and Runge-Kutta methods, as well as multistep methods and block implicit methods (Ismail, 1999). Among the proposed methods, the family of Runge-Kutta is the most famous numerical method used to solve DDEs.

Research has shown various families of Runge-Kutta methods and interpolation techniques which are used to solve DDEs. Among other, Oberle and Pesch (1981) developed two numerical methods known as the Runge-Kutta-Fehlberg methods of orders 4 and 7 to solve DDEs. Hermite interpolation is used to approximate the delay term. Ismail *et al*. (2002) solved delay differential equations by using embedded Singly Diagonally Implicit Runge–Kutta method and the delay term was obtained by using Hermite interpolation.

While most numerical methods to determine the solution for DDEs are based on the Runge-Kutta formulas, some opted for Adams and backward differentiation formula (BDF) methods to solve them. For instance, Bocharov *et al*. (1996) considered the application of the linear multistep methods for the numerical solution of initial value problem for stiff delay differential equations with several constant delays. As for the approximation of delayed variables, Bocharov *et al*. (1996) used Nordsieck's interpolation technique.

BLOCK BACKWARD DIFFERENTIATION FORMULA

The purpose of this paper is to solve stiff DDEs using 2-point block backward differentiation formula (BBDF) method derived by Ibrahim *et al*. (2007). The corrector formulas are formulated as follows:

$$y_{n+1} = -\frac{1}{3}y_{n-1} + 2y_n - \frac{2}{3}y_{n+2} + 2hf_{n+1} \tag{3}$$

$$y_{n+2} = \frac{2}{11}y_{n-1} - \frac{9}{11}y_n + \frac{18}{11}y_{n+1} + \frac{6}{11}hf_{n+2} \tag{4}$$

The numerical results were then compared to the classical 1-point backward differentiation formula (BDF). The corrector formula (Lambert, 1993) is given as:

$$y_{n+1} = \frac{2}{11}y_{n-2} - \frac{9}{11}y_{n-1} + \frac{18}{11}y_n + \frac{6}{11}hf_{n+1} \tag{5}$$

In general, most numerical methods for solving differential equations produce only one new approximation value. However, the implicit block method can produce two new values simultaneously at each step. Thus, it is logically safe to presume that this particular method can reduce the timing of the calculation and its computational cost as well.

IMPLEMENTATION OF THE METHOD

Newton iteration is implemented in the method to evaluate the values of y_{n+1} and y_{n+2} for solving equation [1]. The values for both y_{n+1} and y_{n+2} at $(i+1)$ th iterative are given as $y_{n+1}^{(i+1)}$ and $y_{n+2}^{(i+1)}$. According to Ibrahim *et al*. (2007), the Newton iteration takes the form of

$$y_{n+1}^{(i+1)} = y_{n+1}^{(i)} - \frac{F_1(y_{n+1}^{(i)})}{F_1^{'}(y_{n+1}^{(i)})} \tag{6}$$

and

$$y_{n+2}^{(i+1)} = y_{n+2}^{(i)} - \frac{F_2(y_{n+2}^{(i)})}{F_2^{'}(y_{n+2}^{(i)})} \tag{7}$$

Hence,

$$\left(1 - 2h\frac{\partial f_{n+1}}{\partial y_{n+1}}\right)\left(y_{n+1}^{(i+1)} - y_{n+1}^{(i)}\right) = -y_{n+1}^{(i)} - \frac{2}{3}y_{n+2}^{(i)} + 2hf_{n+1}^{(i)} + \varsigma_1 \tag{8}$$

$$\left(1 - \frac{6}{11}h\frac{\partial f_{n+2}}{\partial y_{n+2}}\right)\left(y_{n+2}^{(i+1)} - y_{n+2}^{(i)}\right) = \frac{18}{11}y_{n+1}^{(i)} - y_{n+2}^{(i)} + \frac{6}{11}hf_{n+2}^{(i)} + \varsigma_2 \tag{9}$$

where $\frac{\partial f}{\partial y}$ is a Jacobian and ς_1, ς_2 are the back values.

Let

$$e_{n+1}^{(i+1)} = y_{n+1}^{(i+1)} - y_{n+1}^{(i)} \tag{10}$$

$$e_{n+2}^{(i+1)} = y_{n+2}^{(i+1)} - y_{n+2}^{(i)} \tag{11}$$

Then, equations [8] and [9] can be rewritten in the matrix form, as follows:

$$\begin{bmatrix} 1-2h(\frac{\partial f_{n+1}}{\partial y_{n+1}}) & \frac{2}{3} \\ -\frac{18}{11} & 1-\frac{6}{11}h(\frac{\partial f_{n+2}}{\partial y_{n+2}}) \end{bmatrix} \begin{bmatrix} e_{n+1}^{(i+1)} \\ e_{n+2}^{(i+1)} \end{bmatrix} = \begin{bmatrix} -1 & -\frac{2}{3} \\ \frac{18}{11} & -1 \end{bmatrix} \begin{bmatrix} y_{n+1}^{(i)} \\ y_{n+2}^{(i)} \end{bmatrix} + h \begin{bmatrix} 2 & 0 \\ 0 & \frac{6}{11} \end{bmatrix} \begin{bmatrix} f_{n+1}^{(i)} \\ f_{n+2}^{(i)} \end{bmatrix} + \begin{bmatrix} \varsigma_1 \\ \varsigma_2 \end{bmatrix} \quad (12)$$

In order to solve the above matrix equation, LU decomposition, which is a matrix decomposition that rewrites the matrix in the upper triangular matrix and lower triangular matrix was used (William *et al*., 2007).

Let

$$A = \begin{bmatrix} 1-2h\left(\frac{\partial f_{n+1}}{\partial y_{n+1}}\right) & \frac{2}{3} \\ -\frac{18}{11} & 1-\frac{6}{11}h\left(\frac{\partial f_{n+2}}{\partial y_{n+2}}\right) \end{bmatrix} \quad (13)$$

$$B = \begin{bmatrix} -1 & -\frac{2}{3} \\ \frac{18}{11} & -1 \end{bmatrix} \begin{bmatrix} y_{n+1}^{(i)} \\ y_{n+2}^{(i)} \end{bmatrix} + h \begin{bmatrix} 2 & 0 \\ 0 & \frac{6}{11} \end{bmatrix} \begin{bmatrix} f_{n+1}^{(i)} \\ f_{n+2}^{(i)} \end{bmatrix} + \begin{bmatrix} \varsigma_1 \\ \varsigma_2 \end{bmatrix} \quad (14)$$

$$E = \begin{bmatrix} e_{n+1}^{(i+1)} \\ e_{n+2}^{(i+1)} \end{bmatrix} \quad (15)$$

$$A \cdot E = B \quad (16)$$

Suppose that matrix A is a product of the two matrices,

$$L \cdot U = A \quad (17)$$

where L is the lower triangular and U is the upper triangular. Thus,

$$(L \cdot U) \cdot E = B. \quad (18)$$

Let

$$X = U \cdot E. \quad (19)$$

Hence,

$$L \cdot X = B. \quad (20)$$

and then solving,

$$U \cdot E = X \tag{21}$$

to get the matrix value of E. Finally, the approximation values of y_{n+1} and y_{n+2} can be obtained. Furthermore, the existence of the delay term is the main difference between ODEs and DDEs. Thus, in order to get the numerical solutions for DDEs, the delay term needs to be solved in advance. For a situation where $\alpha \le t_0$, the initial function $\phi(t)$ is used to calculate the delay term, $y(\alpha)$. Otherwise, the delay term is calculated by using Newton Divided Difference interpolation.

Meanwhile, the formula to calculate the delay term (Richard *et al*., 1993) can be written as:

$$P_n(x) = z[x_0] + \sum_{k=1}^{n} z[x_0, x_1, \ldots, x_k](x - x_o)\ldots(x - x_{k-1}) \tag{22}$$

where $z[x_0] = z(x_0)$.

Equation [22] is known as the Newton's interpolatory divided-difference formula. Normally, the delay terms are obtained by interpolation on the values of the chosen support points. In order to obtain these support points, the delay argument should be close to the centre of the points. However, if the delay argument under consideration is outside the points, it will be treated as a special case and it can only be obtained through extrapolation.

PROBLEM TESTED

The followings are some of the tested problems to get the numerical results. All the tested problems are stiff DDEs. The numerical results are obtained by using C language with constant stepsize, H.

Problem 1:

$$y'(t) = -1000y(t) + y\left(t - (\ln(1000 - 1))\right), \quad 0 \le t \le 3,$$

$$y(t) = e^{-t}, \qquad t \le 0.$$

Exact solution is $y(t) = e^{-t}$.

Problem 2:

$$y'(t) = -1000y(t) + 997e^{-3}y(t-1) + \left(1000 - 997e^{-3}\right), \qquad 0 \le t \le 3,$$

$$y(t) = 1 + \exp(-3t), t \le 0.$$

Exact solution is $y(t) = 1 + \exp(-3t)$.

Problem 3:

$$y'(t) = -24y(t) - e^{(-25)}y(t-1), \qquad 0 \le t \le 3,$$

$$y(t) = e^{(-25)t}, t \le 0.$$

Exact solution is $y(t) = e^{-t}$.

NUMERICAL RESULTS AND DISCUSSION

In this section, the numerical results showed the performance of block method in solving the first order stiff DDEs. All the results were obtained using the Microsoft Visual Studio 2010 software on a personal computer with Intel Core2 Duo CPU. The abbreviations used are stated in Table 1.

TABLE 1: List of Abbreviations

Notation	Description
H	Stepsize
1BDF	1-point BDF method
2BBDF	2-point BBDF method
TS	total number of steps
MAXE	Maximum error
TIME	CPU time in seconds

The errors are calculated by using the following formulas:

$$err_t^i = \left| y_{exact}^i - y_{approximate}^i \right| \tag{23}$$

The maximum error, MAXE, is defined as:

$$\text{MAXE} = \max_{1 \le i \le TS} \left(err_t^i \right). \tag{24}$$

The numerical results are given in Table 2 to Table 4. In the results, the notation 9.75159e-004 represents the value of 9.75159 X 10^{-4}. From the numerical results, it is clear that the total number of steps in solving 2-point BBDF is half of the steps needed to solve the 1-point BDF. The execution time for the 2-point BBDF is reduced up to 77% as compared to the 1-point BDF. Meanwhile, the maximum errors for 2-point BBDF method are better than the 1-point BDF for all the tested problems.

TABLE 2: Numerical results for Problem 1[1]

H	METHOD	TS	MAXE	TIME(seconds)
10^{-2}	1BDF	300	9.75159e-004	0.00836748
	2BBDF	150	3.80236e-004	0.00190863
10^{-3}	1BDF	3000	3.22629e-007	0.01103256
	2BBDF	1500	2.61239e-007	0.00451134
10^{-4}	1BDF	30000	1.45149e-008	0.03742193
	2BBDF	15000	1.33568e-008	0.03079985
10^{-5}	1BDF	300000	1.73433e-010	0.29473164
	2BBDF	150000	1.57914e-010	0.27820763

[1]The time of the execution of the 2-point BBDF for Problem 1 is about 77%, 59%, 17%, and 5% faster for the step-sizes of 10^{-2}, 10^{-3}, 10^{-4}, and 10^{-5}, respectively. The smaller step-size obtained a small difference in the execution time. This is due to the total calculation of LU decomposition that requires matrix in 2BBDF.

TABLE 3: Numerical results for Problem 2[2]

H	METHOD	TS	MAXE	TIME(seconds)
10^{-2}	1BDF	300	8.73499e-003	0.00843524
	2BBDF	150	3.40594e-003	0.00295110
10^{-3}	1BDF	3000	2.88750e-006	0.01167929
	2BBDF	1500	2.33921e-006	0.00715678
10^{-4}	1BDF	30000	1.30592e-007	0.04287257
	2BBDF	15000	1.20176e-007	0.03564649
10^{-5}	1BDF	300000	1.56085e-009	0.32652507
	2BBDF	150000	1.42118e-009	0.30610835

[2]The time of the execution of the 2 point BBDF for Problem 2 is about 65%, 38%, 16%, and 6% faster for the respective step-sizes of 10^{-2}, 10^{-3}, 10^{-4}, and 10^{-5}

TABLE 4: Numerical results for Problem 3[3]

H	METHOD	TS	MAXE	TIME(seconds)
10^{-2}	1BDF	300	4.63438e-002	0.00857305
	2BBDF	150	4.41121e-002	0.00296303
10^{-3}	1BDF	2000	1.00359e-003	0.01145794
	2BBDF	1500	9.28409e-004	0.00553071
10^{-4}	1BDF	20000	1.10170e-005	0.03680099
	2BBDF	15000	9.97473e-006	0.02976354
10^{-5}	1BDF	200000	1.11197e-007	0.26814825
	2BBDF	150000	1.00464e-007	0.26649446

[3]The time of the execution of the 2-point BBDF for Problem 3 is about 65%, 51%, 19%, and 1% faster for the stepsizes of 10^{-2}, 10^{-3}, 10^{-4}, and 10^{-5}, respectively

CONCLUSION

In this paper, it was observed that the 2-point BBDF achieved better results in terms of the accuracy of the method as well as the execution time. Therefore, it can be concluded that the 2-point BBDF is suitable for solving stiff DDEs.

ACKNOWLEDGEMENTS

This work was fully supported by the Institute of Mathematical Research, Universiti Putra Malaysia, under the Fundamental Scheme Research Grant (Project code: 01-09-09-681FR).

REFERENCES

Bellen, A., & Zennaro, M. (2003). *Numerical Methods for Delay Differential Equations*. New York: Oxford University Press.

Bocharov, G. A., Marchuk, G. I., & Romanyukha, A. A. (1996). Numerical solution by LMMs of Stiff Delay Differential systems modelling an Immnune Response. *Numer. Math., 73*, 131-148.

Driver, R. D. (1976). *Ordinary and Delay Differential Equations*. New Year: Springer-Verlag.

Ibrahim, Z. B., Othman, K. I., & Suleiman, M. (2007). Implicit r-point Block Backward Differentiation Formula for Solving First Order Stiff ODEs. *Applied Mathematics and Computation, 186*, 558-565.

Ismail, F. (1999). Numerical Solution of Ordinary and Delay Differential Equations by Runge-Kutta Type Methods (Ph.D Thesis dissertation). Universiti Putra Malaysia, Malaysia.

Ismail, F., Al-Khasawneh, R. A., Lwin, A. S., & Suleiman, M. (2002). Numerical Treatment of Delay Differential Equations by Runge-Kutta Method Using Hermite Interpolation. *Matematika, 18*(2), 79-90.

Lambert, J. D. (1993). *Numerical Methods for Ordinary Differential Systems: The Initial Value Problem*. Chichester, England: John Wiley and Sons.

Oberle, H. J., & Pesch, H. J. (1981). Numerical Treatment of Delay Differential Equations by Hermite Interpolation. *Numer. Math., 37*, 235-255.

Richard, L., Burden, J., & Douglas, F. (1993). *Numerical Analysis*. Boston: PWS-Kent Pub. Co.

Roth, M. G. (1980). Difference Methods for Stiff Delay Differential Equations (Master Thesis dissertation). University of Illinois, Illinois.

William, H. P., Saul, A. T., William, T. V., & Brian, P. F. (2007). *Numerical Recipes: The Art of Scientific Computing*. New York: Cambridge University Press.

Pertanika J. Sci. & Technol. 21 (1): 45 - 58 (2013)

SCIENCE & TECHNOLOGY

Journal homepage: http://www.pertanika.upm.edu.my/

Effects of Process Temperature and Time on the Properties of Microwave Plasma Nitrided Ti-6Al-4V Alloy

Y. Yusuf*, J. M. Juoi, Z. M. Rosli, W. L. Kwan and Z. Mahamud

Faculty of Manufacturing Engineering, Universiti Teknikal Malaysia Melaka, Durian Tunggal, 76109 Melaka, Malaysia

ABSTRACT

Titanium alloy (e.g. Ti-6Al-4V) has an excellent combination of properties. However in many cases, the application is limited because of the poor wear property. In this work, a surface modification (plasma nitriding) is carried out to improve the surface properties of Ti-6Al-4V, as a treatment prior to a hardcoating deposition, leading to a duplex coating system. This is an effort to improve the surface and near surface property of Ti-6Al-4V. Plasma nitriding is performed utilizing microwave plasma method in 25% Ar- 75% N_2 atmosphere at temperatures of 600°C and 700°C for different processing times (1, 3 and 5 hours). The phase and microstructure of plasma nitrided substrate were characterized by using X-ray diffraction (XRD) and Scanning electron microscopy (SEM). The plasma nitrided Ti-6Al-4V properties (surface roughness, surface hardness and case depth) were determined using profilometer and microhardness, respectively. Results obtained showed a significant increase on the surface hardness of Ti-6Al-4V. This is due to the formation of TiN and Ti_2N phases in the form of compound layer. Besides, it shows that the diffusion of nitrogen into the Ti-6Al-4V substrate produces case depth up to 130 μm and this contributes to the improvement of the near surface hardness due to the changes in the microstructures. It was also found that the surface hardness and surface roughness increased with the increases in the process temperature and times.

Keywords: Ti-6Al-4V, surface modification, plasma nitriding, microwave plasma

INTRODUCTION

Titanium and its alloys have received extensive interest due to their excellent combination of properties, such as excellent corrosion resistance, high strength to weight ratio, high strength at elevated temperatures, low modulus elasticity and biological compatibility. Besides, titanium and its alloys

Article history:
Received: 26 April 2011
Accepted: 22 November 2011

E-mail addresses:
yusliza.yusuf@yahoo.com (Y. Yusuf),
jariah@utem.edu.my (J. M. Juoi),
zmr@utem.edu.my (Z. M. Rosli),
Kwailoon86@gmail.com (W. L. Kwan),
zainab.mahamud86@gmail.com (Z. Mahamud)
*Corresponding Author

ISSN: 0128-7680 © 2013 Universiti Putra Malaysia Press.

are widely used for a range of applications in the aerospace, automotive, marine, chemical and biomedical industries.

The most common titanium alloy used is Ti-6Al-4V. The reasons for the success of this particular type of alloy are its beneficial properties (e.g. high strength to weight ratio and corrosion resistance), making it remarkable for technical application varying from construction materials to medical implant materials. However, Ti-6Al-4V is found to be inconsiderably utilized in mechanical engineering applications, as in sliding systems (Ma *et al*., 2004). This is because of its poor tribological properties such as poor abrasive wear resistance, poor fretting behaviour and high coefficient of friction (Zhecheva *et al*., 2005). When the untreated titanium alloy surface is in rubbing contact with another material, even though being lubricated, there is a strong tendency for galling to take place leading to severe wear (Bell 1993).

Therefore, surface modifications become a fundamental requirement when Ti-6Al-4V is subjected to wear problem. Some examples of surface modifications of Ti-6Al-4V that are usually carried out are the deposition of hardcoating by chemical vapour deposition (CVD) or physical vapour deposition (PVD) techniques and thermochemical treatment such as diffusion techniques. However, the restriction on common use of hardcoating on Ti-6Al-4V substrate is the load carrying the capacity of the coating-substrate system with correlated to the soft substrate beneath the coating (Ma *et al*., 2004). As a consequence, delamination and premature failure of the hardcoating on the surface of Ti-6Al-4V components under wear conditions have been observed (Yetim *et al*., 2008). In order to prevent the failure, a surface modification (e.g. thermochemical treatment) is required intended as a pre-treatment to Ti-6Al-4V substrate before the hardcoating deposition with reference to the duplex coating concept.

Thus, the thermochemical treatment involving diffusion of the substrate material with different elements is an option for improvement in Ti-6Al-4V surface and near surface property. Diffusion treatment like plasma nitriding can increase the wear resistance, decrease the coefficient of friction and certainly harden the surface of materials (Yetim *et al*., 2009). The high reactivity of titanium with respect to nitrogen, oxygen and carbon is an advantage to produce high hardness of surface layer, making the diffusion treatment particularly interesting to improve the wear property of Ti-6Al-4V. Processes such as oxidation, carburizing and nitriding are among popular thermochemical treatments used to improve the surface properties of titanium alloy, especially Ti-6Al-4V (Holmberg & Matthews, 2009).

In conducting thermochemical treatment on the substrate, the utilization of plasma advantageously reduces the duration of process. This is due to the diffusion of high energy ions and intensification of the elements (nitrogen, oxygen, carbon) transportation from the surface to the substrate core. Besides, the process parameters such as temperature and time are available for the modification to improve the surface properties such as phase composition, microstructure and surface morphology (Zhecheva *et al*., 2005).

A common method used for thermochemical process of Ti-6Al-4V is plasma nitriding. The nitrogen used has high solubility in α-Ti phase, and it therefore strengthens the surface layer significantly. Modification on the surface layer of plasma nitride Ti-6Al-4V consists of a compound layer on top of the surface with TiN and Ti_2N phases. The presence of TiN and Ti_2N phases has significant effect on the surface hardness of Ti-6Al-4V (Yildiz *et al*., 2008; Lakshmi, 2002). Underneath the compound layer is the diffusion layer which consists of an

interstitial solution of nitrogen in the α-Ti phase (Yildiz *et al*., 2008). The diffusion layer is also known to improve the hardness properties of Ti-6Al-4V with the formation of case depth profile (Yildiz *et al*., 2008).

Various methods have been used by other researchers to ensure the success of the plasma nitriding process including Direct Current (DC) and Radio Frequency (RF) methods. DC plasma nitriding method is the most widely used. In this method, plasma is created by an electrical discharge between the two electrodes. According to Yildiz *et al*. (2008), the DC technique formed dense TiN phase as process temperature and time were increased, while the Ti_2N phase disappeared when the process temperature and time were increased. Besides, Yilbas *et al*., (1996) utilised the DC plasma nitriding method and also found that the diffusion of nitrogen increased with the increase in the surface temperature.

Another method used by researchers for the plasma nitriding process is RF plasma nitriding method. In this method, plasma is produced when the electrons absorb power from the RF field, and then transmit it through collisions of electrons with the gaseous atoms. The installation of RF is per the industrial band standard (13.56 MHz) in order to avoid interference with communication network (Chattopadhyay, 2004). The RF plasma nitriding also produces TiN and Ti_2N phases with significant improvement on the surface hardness of Ti-6Al-4V. These also lead to the improvements of wear resistance (Fouquet *et al*., 2004; El-Hossary *et al*., 2006).

Another method that can generate plasma for the nitriding process is microwave plasma nitriding method. The advantages of this method are due to its efficiency in generating the plasma and it is also readily available at low cost of 2.45 GHz microwave generators (Chattopadhyay, 2004). Besides, it requires low pressure as compared to the DC and RF methods. In addition, it applies magnetic field to encourage the formation of plasma. This study aimed to understand the effects of process parameters (e.g. temperature and time) on the microstructure and mechanical properties of microwave plasma nitride Ti-6Al-4V substrate.

EXPERIMENTAL

The samples used for this study is Ti-6Al-4V, with the following chemical compositions (wt %): Al (6), V (4) and Ti (balance). The samples were cut from a long rod, with 10mm × 25mm (thickness × diameter) and mechanically polished for surface roughness, Ra< 0.5. After polishing, the sample was cleaned using ultrasonic cleaning in ethanol bath for 15 minutes and then dried using hot air dryer.

The sample was put inside the chamber and evacuated by a rotary pump until the pressure reached 10^{-2} mTorr (Fig.1), and subsequently cleaned by hydrogen plasma with an overall pressure of 15 mTorr for 5 minutes. The samples were then heated to the required temperature (600°C, 700°C) and nitrogen along with argon gas was introduced into the microwave source (1kW, 2.45GHz) to produce plasma. The operating pressure in the chamber was fixed at 30 mTorr, and the flow rates of the N_2 and Ar gas mixtures were set at 25% (Ar): 75% (N_2). The nitriding temperatures were monitored and performed for 1hr, 3hr and 5 hr.

X-ray diffraction (XRD) for phase identification was carried out with X'Pert PRO system with monochromatic Cu Kα radiation in θ - 2θ geometry. All the XRD patterns were obtained with scan steps of 0.01° and a counting time of 40s. The surface roughness of the samples was

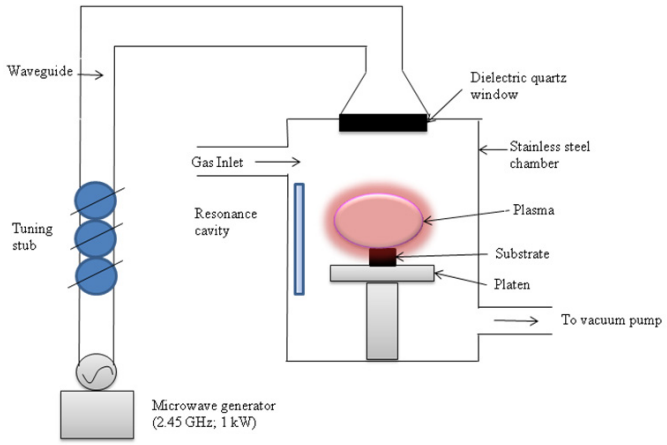

Fig.1: A schematic diagram of the Microwave plasma reactor

measured using Mitutoyo SJ 301 surface profilometer with SR10 tip type. Cross sectional metallographic examination was carried out using a scanning electron microscope (Zeiss). Prior to that, the cross sectioned area was ground and polished to produce mirror-like finish surface and the surface was etched using Kroll's reagent to reveal the microstructures. For the purpose of mechanical property study, Mitutoyo microhardness tester with Vickers indenter was employed with 100g load to measure the surface hardness and 25g for the case depth profile for the cross sectioned samples. The choice of load was based on the measurable indentation size produced during the experimental work. The lower load used for the case depth profiling was to avoid overlapping of indentation.

RESULTS

As received

The XRD patterns of as received Ti-6Al-4V revealed that the sample consisted of α-Ti (ICDD: 00-001-1198) and β-Ti (ICDD: 00-044-1288), as shown in Fig.2 and the SEM cross-sectioned micrograph is shown in Fig.3. It is shows that the microstructures consist of equiaxed α phases and fine acicular shape for the β transform phases. As for the surface roughness, the average Ra value obtained was 0.23 ± 0.03 μm and the surface hardness value was 349.04 ± 4.77 $HV_{0.1}$.

The Effects of Process Temperature and Time

Phase Composition

The XRD pattern of plasma nitride surface of the substrate revealed the formation of TiN phases with cubic structures (ICDD: 01-087-0633) and Ti_2N phases with tetragonal structure (ICDD: 01-0076-0198) (Fig.4). In addition, the diffraction peaks show that the TiN phases has a dominant (highest intensity) at [111] plane, while Ti_2N phases have a dominant at [111] plane. It was also observed that the diffraction pattern at both process temperatures (600°C and 700°C), the α-Ti of [100], [002] and [101] peaks were shifted to lower 2θ side. Whereas, the β-Ti

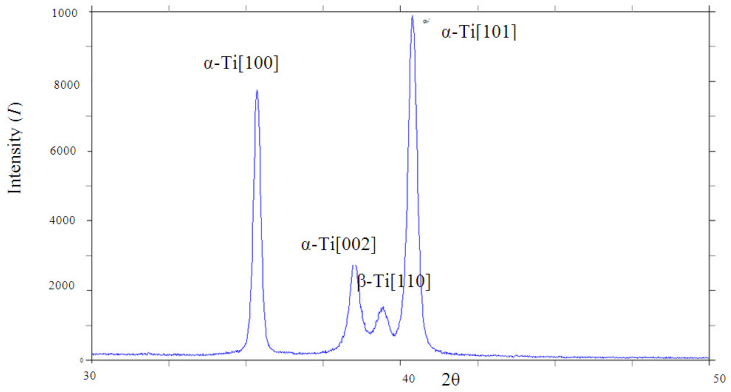

Fig.2: The XRD patterns of as received Ti-6Al-4V substrate

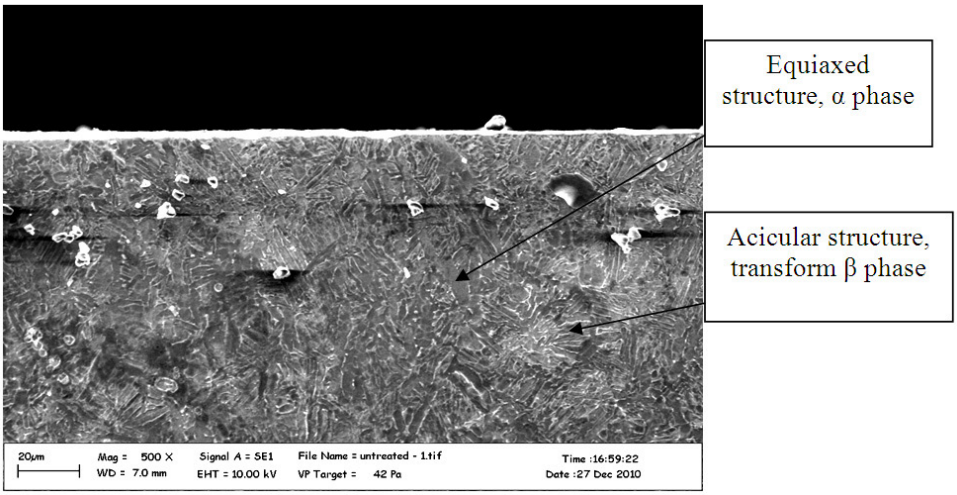

Fig.3: The SEM micrograph of the cross-sectioned of as-received Ti-6A1-4V substrate

peak (Observed in the as received Ti-6Al-4V) was not detected in the plasma nitrided samples.

In general, as the temperature increased, changes on the peak intensities of TiN [111] and [200] and Ti_2N [210] peaks were observed. The intensity of TiN [111] peak of the sample 600°C 3 hours was double the intensity of α-Ti [002], but for the 700°C 3 hours sample, the intensity was almost the same. The intensity of TiN [200] was almost the same with that of Ti_2N [210] peak for 600°C 5 hours sample, but for the 700°C 5 hours sample, the intensity of TiN [200] was more than 2 times higher than Ti_2N [210]. However, these changes did not affect conclusion made on the type of phase present in the samples. While the intensity of Ti_2N [111] peak showed increases with the decrease of the process temperature. This is evident in the samples nitrided for 5 hours at 600°C and 700°C. In contrast, as the process time increased, the intensities of TiN [111] and [200] and Ti_2N [210] peaks showed irregular changes in the intensities. Meanwhile, the Ti_2N [111] peak intensities increased as the process time increased.

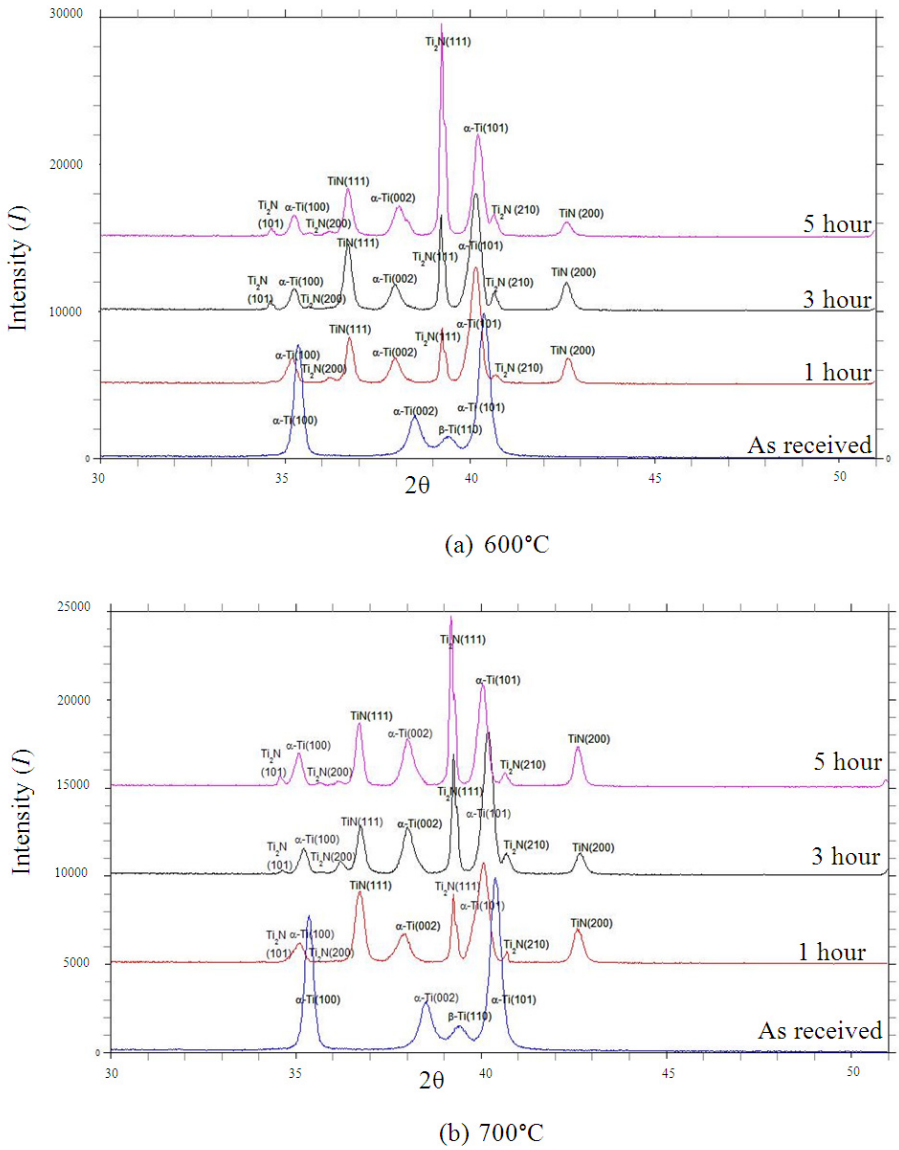

Fig.4: The XRD pattern of microwave plasma nitrided at various process temperatures and times

Microstructures

The SEM micrographs on the cross-sectioned plasma nitride samples revealed that the variation in the microstructure is visible at the depth of 120 μm (Fig.5). Throughout this depth, 3 distinct regions with different microstructures were observed. As the process temperature and time increased, the outermost layer was apparently observed. Underneath this continuous outermost layer, a distinct layer with lamellar and acicular structures was found to exist. These lamellar and acicular structures grew bigger with the increase of process temperature. Besides, the distinct layer was observed broadening with the increase of process time.

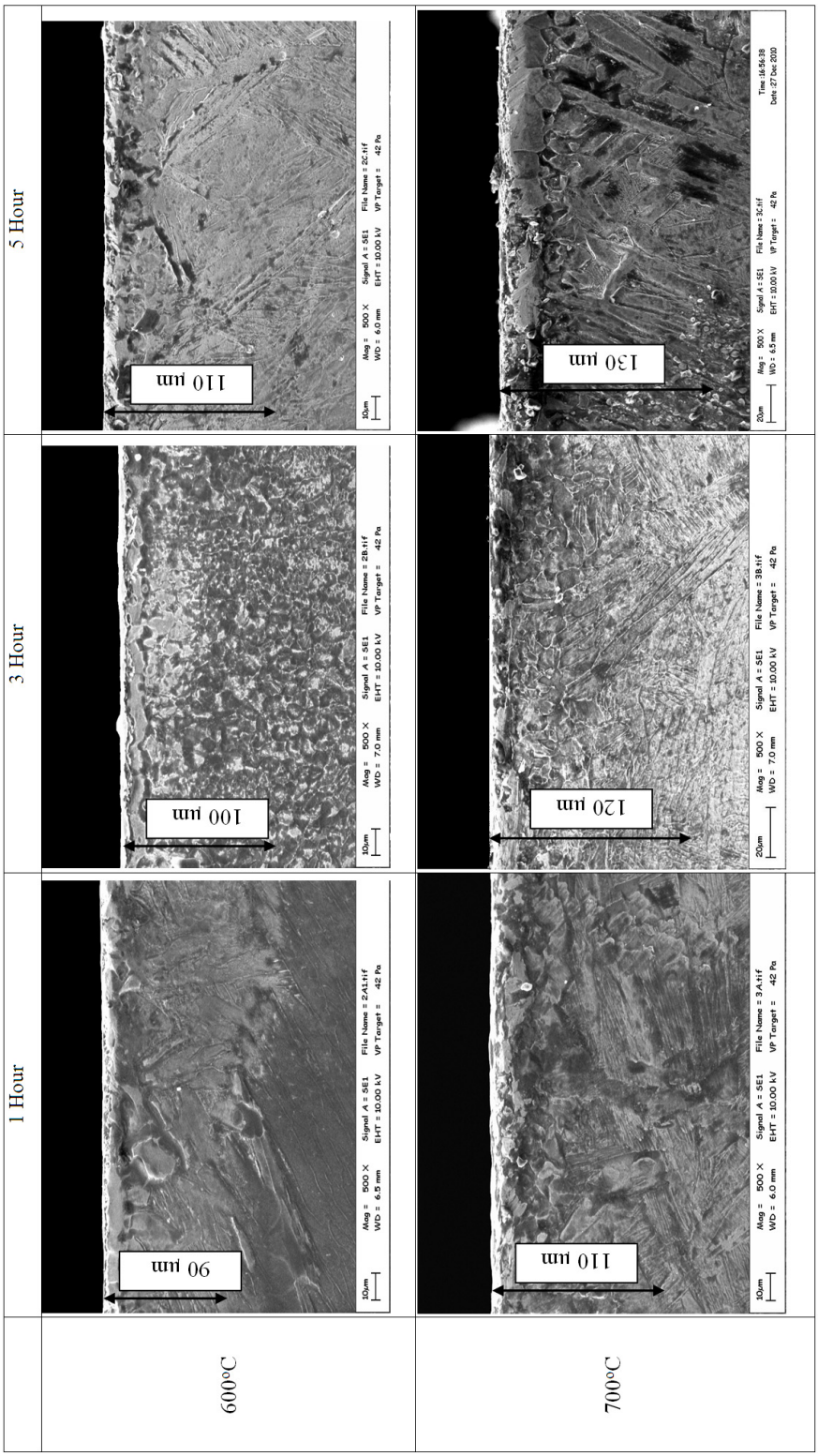

Fig.5: The SEM micrograph of the cross-sectioned microwave plasma nitrided Ti-6Al-4V at various of process temperatures and times, indicating the case depth obtained for each sample

Surface Roughness

The surface roughness, Ra of the as received and microwave plasma nitrided Ti-6Al-4V alloy at various temperatures and time is shown in Fig 6. It shows that the plasma nitriding process increased the Ra value of the nitrided samples as compared to the as received alloy. In general, the Ra value increased as of the process temperature and time increased. However, the increase of Ra value was less obvious for the samples nitrided at 700°C for 3 hours and 5 hours.

Surface Hardness

The surface hardness of plasma nitrided Ti-6Al-4V samples was found to be higher as compared to the as received sample (Fig.7). This means that the surface hardness for the plasma nitrided samples increased as the process temperature and time increased. The highest value was observed for the sample nitrided at 700°C for 5 hours and the lowest value was observed at

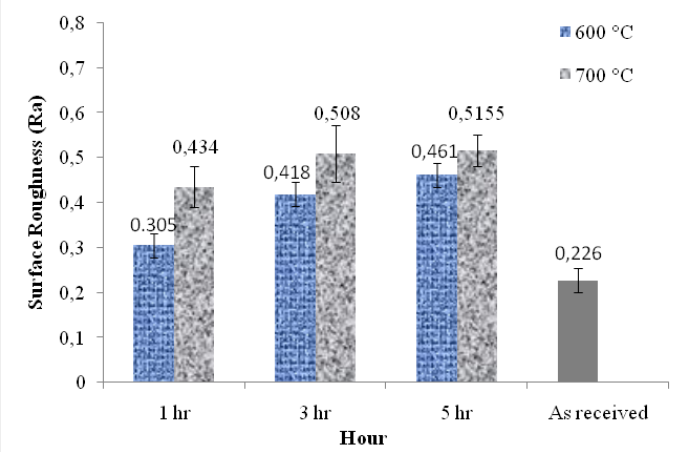

Fig.6: The surface roughness of the as received and microwave plasma nitrided Ti-6Al4V at various temperatures and times.

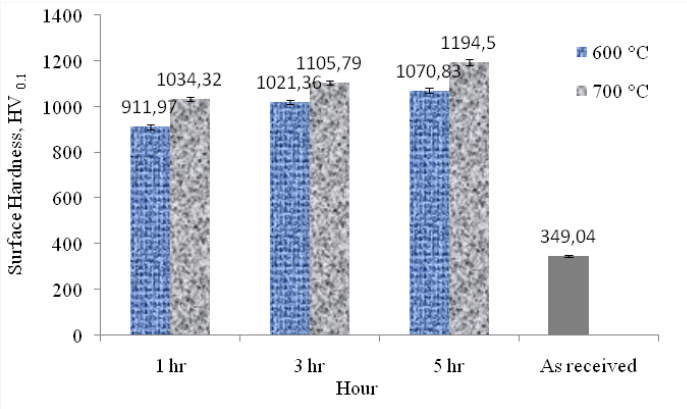

Fig.7: The surface hardness results of the as received and microwave plasma nitrided Ti-6Al-4V at various temperatures and times

the sample nitrided at 600°C for 1 hour. It should be noted that major increment on the surface hardness is due to the increase of temperature. This is evident for the sample nitrided for 1 hour at 600°C and 700°C, whereby the surface hardness of the sample was 911.97 ± 9.45 $HV_{0.1}$ at 600°C and 1034.32 ± 7.98 $HV_{0.1}$ at 700°C, respectively. In contrast, less significant increment of the surface hardness was observed for the sample nitrided at the same temperature, namely, the sample nitrided at 700°C for 3 hours the surface hardness was 1105.79 ± 9.84 $HV_{0.1}$ and with 5 hours, the surface hardness was 1194.5 ± 11.8 $HV_{0.1}$.

Case Depth Profile

Fig.8 shows the case depth profile of the microwave plasma nitrided samples in varying process temperatures and times. The hardness of as received Ti-6Al-5V is 350 ± 4.26 $HV_{0.025}$. Thus, it is considered as the hardness limit (core hardness). It was found that the highest hardness obtained was at the near surface area region. The hardness gradually decreased with the depth of the sample and finally reached the hardness limit (core hardness). This represents the case depth profile for each sample. It was also observed that the case depth profile increased with the increases of process temperatures and times. In particular, the highest case depth was obtained (130µm) in the sample nitrided at 700°C 5 hours.

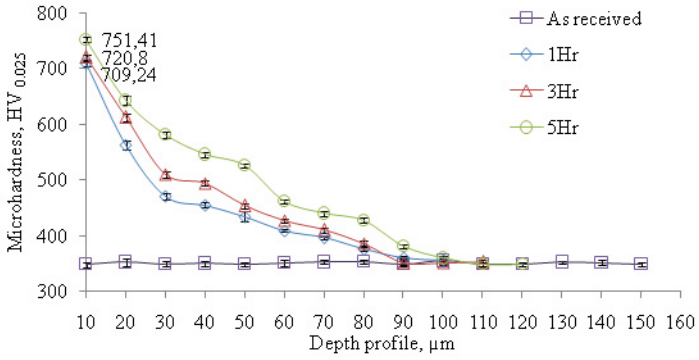

(a) 600°C

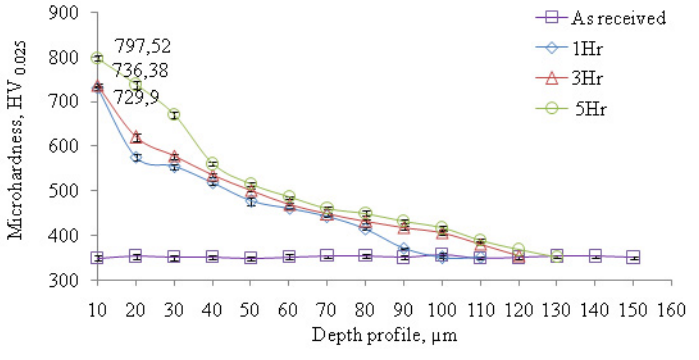

(b) 700°C

Fig.8: The case depth profile of microwave plasma nitrided Ti-6Al-4V at various of process temperatures and times

DISCUSSION

During microwave plasma nitriding, process parameter (temperature and time) plays a significant role on the microstructures and mechanical properties of the plasma nitrided Ti-6Al-4V substrate. The new phases, such as TiN and Ti_2N, were observed at 600°C for 1 hour. This parameter (600°C 1 hour) was lower processing parameter compared to other study (utilizing RF plasma) where a moderate parameter, 700°C 4 hours was required to form the TiN phase (Fouquet *et al*., 2004). This finding is in agreement with suggestion made by Yildiz *et al*. (2008), whereby it was mentioned that the Ti_2N phase is formed at the temperature < 700°C. However, there is an increase in the Ti_2N peak intensities with the process time increases, and this is in contrast with the result by Yildiz *et al*. (2008) which indicated that the intensity of Ti_2N decreased as the process time increased using the DC plasma method.

The determination of TiN and Ti_2N phases indicates that the compound layer is formed on the plasma nitrided Ti-6Al-4V surface at the process parameter of 600°C 1 hour. The formation of this particular compound layer during nitriding of titanium is as per in the schematic presentations of the kinetics of formation and the growth of surface layers during nitriding of titanium suggested by Zhecheva *et al*. (2005) (see Fig.9). This is also supported with the SEM micrograph cross section of the samples (Fig.5), where the existence of compound layer was observed on the outermost layer. The compound layer thickness increased as the process temperature and time increased.

The XRD pattern of the nitrided samples at 600°C and 700°C shows that the TiN phase has a dominant peak at [111] and [200] planes. This is in agreement with the findings by Yildiz *et al*. (2008) and Fouquet *et al*. (2004). Besides, Ti_2N phase has dominant planes at [111] and

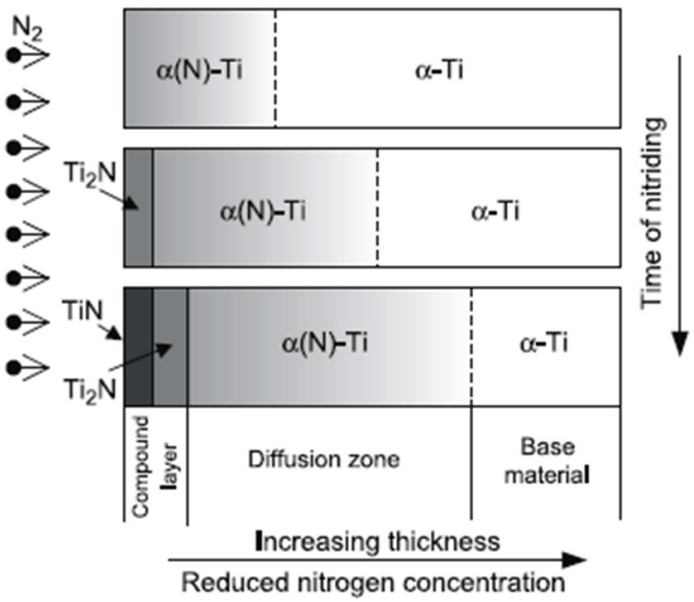

Fig.9: A schematic presentation of the kinetics of formation and growth of surface layers during nitriding of titanium (Zhecheva *et al*., 2005)

[210], but these findings contradict with the results obtained by Raaif *et al*. (2007) and Fouquet *et al*. (2004), where the Ti_2N dominant planes at [210] and [111]. This variation seems to be due to the different types of nitriding gases used, such as Raaif *et al*. (2007) who utilized pure nitrogen plasma and Fouquet *et al*. (2004) who utilized hydrogen. It was also observed that the Ti_2N phase is highly oriented and depending on the composition of gas (Raveh *et al*., 1989). Besides, the diffraction pattern of α-Ti phases with [100], [002] and [101] planes shifted to lower θ side and the peaks were broadened as the process time increased. This is due to the enlargement of α-Ti cell caused by the nitrogen atoms, where the compressive residual stresses occur (Yildiz *et al*., 2008). This also explains the undetected β-Ti peak as suggested by Yildiz *et al*. (2008).

In term of surface roughness, it was observed that it increased with the increases of the process temperature and time. This is consistent with findings by Yildiz *et al*. (2008) using the DC method and Fouquet *et al*. (2004) who used the RF method. The increase of the surface roughness of plasma nitrided Ti-6Al-4V alloy was probably due to the cones formed by the effect of ions bombardment during the nitriding process (Yildiz *et al*., 2008). This increment might also be caused by the enlargement of the α-Ti structures, as shown in the SEM micrograph of cross-sectioned microwave plasma nitrided samples (Fig.5). The α-Ti structures were observed to have enlarged during the plasma nitiriding process and grown as the process temperature increased. Consequently, this contributed to the roughness of the outer layer. In addition, it was also observed that when the process time increased, the growth α-Ti structure was more prominent leading to the agglomeration of the TiN grain forming a compound layer. As a result, a less significant increase in the surface roughness was observed. For example, at 700°C for 3 hours, Ra is 0.508 ± 0.063, while for 5 hours Ra is 0.515 ± 0.035.

The improvement of microwave plasma nitrided surface hardness samples is suggested by the existence of Ti_2N and TiN phases in the form of compound layer, the finding which has also been observed by El-Hossary *et al*. (2006). Besides, the increase in the surface hardness is also parallel with the increase of Ti_2N and TiN peak intensities. It was observed that the highest surface hardness of 1194.5 ± 11.81 $HV_{0.1}$ was obtained in this study when the microwave plasma method at 700°C for 5 hours was used. As a comparison, another study conducted by El-Hossary *et al*. (2006) utilizing the RF plasma method produced the hardness of nearly 600 $HV_{0.1}$ at 725°C. Meanwhile, Yildiz *et al*. (2008) utilized the DC plasma method to produce a hardness of 1180 $HV_{0.1}$ at 700°C for 4 hours. Thus, it can be seen that the microwave plasma method is able to produce a high surface hardness of plasma nitrided Ti-6Al-4V at a comparable of process parameter. Also, it was observed that the increase in the surface hardness is in conjunction with the increase of the compound layer thickness. This is evident when looking at the SEM micrographs of the cross-sectioned samples (Fig.5) where the thickest compound layer observed for the sample nitrided at 700°C for 5 hour yielded the highest surface hardness of 1194.5 ± 11.81 $HV_{0.1}$.

Generally, the case depth hardness is high at near surface area ($<700HV_{0.025}$) and gradually decreases until it reaches the core hardness; more than $550HV_{0.025}$ at the diffusion zone beneath the compound layer and 350 ± 4.26 $HV_{0.025}$ at the core hardness. This is explained by the diffusion of nitrogen into the Ti-6Al-4V surface to form solid solution or precipitation hardening which results in the increase of the diffusion layer strength (Zhecheva *et al*., 2005).

In addition, the case depth profile is in agreement with the cross-sectioned plasma nitrided samples observed in the SEM micrograph (Fig.5). To make a comparison with the other method, Yildiz *et al*. (2008) who had utilized DC reported the case depth of 50 μm for the sample nitrided at 700°C for 1 hour. In this study, the case depth was found to be 100 μm for the sample nitrided at 700°C for 1 hour.

CONCLUSION

In the current work, the plasma nitriding process of Ti-6Al-4V alloy was conducted utilizing the microwave plasma technique. The following conclusions are made based on the findings of this study:

1. The TiN and Ti_2N phases in the form of compound layer were observed for the sample nitrided at the temperature as low as 600°C for 1 hour. The thickness of this compound layer increased with the increases in the nitriding temperature and time.
2. The surface hardness increased with process temperature and time and is related to the formation of the compound layer.
3. The diffusion of nitrogen into the Ti-6Al-4V substrate produced a case depth up to 130 μm. This contributes to the improvement of hardness value of near surface area and causes changes in the microstructure.
4. The surface roughness of the plasma nitrided Ti-6Al-4V samples increases with the increases in process temperature and time.

ACKNOWLEDGEMENTS

This work was supported by PJP/2009/FKP (24A) S629 research grant from the Centre of Research and Innovation Management (CRIM), Universiti Teknikal Malaysia Melaka (UTeM).

REFERENCES

Bell, T. (1993). Engineering the surface to combat wear. *Thin Films in Tribology, 25*, 27-37.

Chattopadhyay, R. (2004). *Advanced thermally Assisted Surface Engineering process* (pp. 149-155). Mumbai: Kluwer Academic Publishers.

El-Hossary, F. M., Negm, N. Z., Khalil, S. M., & Raaif, M. (2006). Surface modification of titanium by radio frequency plasma nitriding. *Thin Solid Films, 497*, 196-202.

Fouquet, V., Pichon, L., Drouet, M., & Straboni, A. (2004). Plasma assisted nitridation of Ti-6Al-4V. *Applied Surface Science, 221*, 248-258.

Holmberg, K., & Matthews, A. (2009). *Coating Tribology properties, Mechanisms, Techniques and Applications in Surface Engineering*, pp. 29-31 (2nd Edition), Amsterdam, Elseivier.

Lakshmi, S. G. (2002). Surface modification and characterisation of Ti-Al-V alloys. *Materials Chemistry and Physics, 76*, 187-190.

Ma, S., Xu, K., & Jie, W. (2004). Wear behaviour of the surface of Ti-6Al-4V alloy modified with pulsed D.C. plasma–duplex process. *Surface and Coatings Technology, 185*, 205-209.

Raveh, A., Hansen, P. L., Avni, R., & Grill, A. (1989). Microstructure and composition of plasma nitride Ti-6Al-4V layers. *Surface and Coatings Technology, 38*, 339-351.

Raaif, M., El-Hossary, F. M., Negm, N. Z., Khalil, S. M., & Schaaf, P. (2007). Surface treatment of Ti-6AL-4V alloy by rf plasma nitriding. *Journal of Physics: Condensed Matter 19,* 1-12.

Yetim, A. F., Alsaran, A., Efeoglu, I., & Celik, A. (2008). A comparative study: The effect of surface treatments on the tribological properties of Ti-6Al-4V alloy. *Surface and Coatings Technology, 202*, 2428-2432.

Yetim, A. F., Yildiz, F., Vangolu, Y., Alsaran, A., & Celik, A. (2009). Several plasma diffusion processes for improving wear properties of Ti-6Al-4V alloy. *Wear, 276*, 2179-2185.

Yilbas, B. S., Sahin, A. Z., Al-Garni, A. Z., M.Said, S. A., Ahmed, Z., & Abdulaleem, B. J. (1996). Plasma nitriding of Ti-6Al-4V alloy to improve some tribological properties. *Surface and Coatings Technology, 80*, 287-292.

Yildiz, F., Yetim, A. F., Alsaran, A., & Celik, A. (2008). Plasma nitriding behaviour of Ti-6Al-4V orthopeadic alloy. *Surface and Coatings Technology, 202*, 2471-2476.

Zhecheva, A., Sha, W., Malinov, S., & Long, A. (2005). Enhancing the microstructure and properties of titanium alloys through nitriding and other surface engineering methods. *Surface and Coatings Technology, 200*, 2192-2207.

Pertanika J. Sci. & Technol. 21 (1): 59 - 74 (2013)

SCIENCE & TECHNOLOGY

Journal homepage: http://www.pertanika.upm.edu.my/

Modelling of Motion Resistance Ratios of Pneumatic and Rigid Bicycle Wheels

Ahmad, D.[1], Jamarei, O.[1], Sulaiman, S.[1], Fashina, A. B.[2] and Akande, F. B.[2]*

[1]*Faculty of Engineering, Universiti Putra Malaysia, 43400 Serdang, Selangor, Malaysia*

[2]*Department of Agricultural Engineering, Ladoke Akintola University of Technology, Ogbomoso, Nigeria*

ABSTRACT

The motion resistances of 660 mm pneumatic and rigid bicycle wheels of the same rim diameter were measured experimentally using the developed tractor-towed single non-lug narrow wheel motion resistance test rig for traction studies. The motion resistances measured were taken to be the towing forces determined in real time using Mecmesin Basic Force Gauge (BFG 2500). The test variables included two test surfaces [tilled and wet (mud) surfaces], the dynamic load and the towing velocity. The tyre inflation pressure of 414 kPa was chosen to make the surface synonymous with that of the rigid wheel. Motion resistance ratios of the two wheels were determined empirically and through semi-empirical approach. The motion resistances of the rigid wheel were found to be greater than those of the pneumatic wheel for both surfaces. Consequently, the motion resistance ratios of the rigid wheel were greater than those obtained from the pneumatic wheel. Analysis of variance showed that there were significant differences between the means of the motion resistance measured on the test surfaces, as well as between the two wheels and their interactions with the test surfaces. The motion resistance ratio exhibited a linear relationship with the towing velocity, while the relationship with the dynamic load was quadratic. However, such a relationship is either direct or inverse with the respective variables. The motion resistance ratio models for the pneumatic and rigid wheels showed that on different test conditions of the dynamic loads and the towing velocities, the relationships between the motion resistance ratio and the dynamic load, and motion resistance with dynamic load were also different.

Keywords: Motion resistance, motion resistance ratio, pneumatic and rigid wheels, dynamic load, towing velocity, test surface, regression models

Article history:
Received: 26 April 2011
Accepted: 24 June 2011

E-mail addresses:
desa@eng.upm.edu.my (Ahmad, D.),
jamarei@eng.upm.edu.my (Jamarei, O.),
suddin@eng.upm.edu.my (Sulaiman, S.),
bola_fashina@yahoo.com (Fashina, A. B.),
fbukkyakande@yahoo.com (Akande, F. B.)
*Corresponding Author

INTRODUCTION

Motion resistance is defined as the force required to overcome the frictional force between the surface of the tyre and the terrain upon which it rolls in the direction of travel. It is also known as the towing force (Code

ISSN: 0128-7680 © 2013 Universiti Putra Malaysia Press.

2003, R2009; Arregoces, 1985; Elwaleed, 1999). The other pertinent measures of the tractive performance are net traction ratio, gross traction ratio and tractive efficiency (Elwaleed, 1999; Gheissari & Loghavi, 2010). Plackett (1985) presented the work of Bernstein (1913) and stated the relationship between tyre inflation pressure (p) and sinkage level (z) in the process of rut formation and with soil factor (n-an exponent of soil deformation) and the coefficient or the modulus of soil deformability (k), as stated in Equation 1. This relationship forms the basis of most research in mobility studies.

$$p = kz^n \quad [1]$$

Single wheel testers have been developed for both indoor and field mobility tests by a number of researchers, and each researcher has defined performance measure (Yahya *et al*., 2007; Pope, 1971; Gotteland & Benoit, 2006; Kawase, Nakashima, & Oida, 2006; Gheissari & Loghavi, 2010). All these devices measure at least the input parameter torque T, and rotational speed ω, as well as the output parameters, pulling force F_p and the driven velocity v of the wheel (Schreiber & Kutzbach, 2007).

Mathematical models were derived for predicting the mobility number, wheel numeric for cohesive soil and for sandy soils, motion resistance ratios, net traction ratio, and tractive efficiencies, with respect to a particular tyre and test surface or terrain. Table 1 summarises some of the existing models and the respective researchers. However, a singular model cannot be used to represent all types of agricultural tyres and test surfaces because of the variation in the tyre design parameters and the soil and the system parameters.

TABLE 1: Existing wheel numeric, mobility number, and motion resistance ratio models

S/N	Measurement Parameters	Models	Source
1	Mobility Number, M	$Nc = \frac{CIbd}{W}(\frac{\delta}{h})^{\frac{1}{2}}[\frac{1}{1+\frac{b}{2d}}]$	Turnage (1972)
2	Wheel Numeric /Refined Mobility No (rigid wheel), Cn	$Cn = \frac{CIbd}{W}$	Wismer and Luth (1974)
3	Brixius Mobility Number, Bn	$Bn = \frac{CIbd}{W}[\frac{1+5\frac{\delta}{h}}{1+3\frac{b}{d}}]$	Brixius (1987)
4	Motion Resistance Ratio	$M_{RR} = 0.04 + \frac{1}{B_n} + \frac{0.5}{\sqrt{B_n}}$	Brixius (1987)
5	Coefficient of Rolling Resistance	$C_{RR} = 0.04 + \frac{0.287}{M}$	Gee-Clough *et al*. (1978)

Researchers are interested in reducing motion resistance force so as to generate higher drawbar pull from the traction device of any agricultural vehicle (Plackett, 1985). The relationship between drawbar pull (*P*), net traction (*H*) and motion resistance (*R*) is stated in Equation 2 (Macmillan, 2002).

$$P = H - R \quad [2]$$

Motion resistance ratio is preferred to motion resistance in the tractive performance of agricultural wheel or off-road traction and transport devices (Arregoces, 1985; Code, 2003, R2009) , and it is defined mathematically as the ratio of the motion resistance to the dynamic load acting on the wheel (see Equation 3). This relationship is found applicable in the empirical determination of the motion resistance ratio. With the measured motion resistance and the dynamic load on the wheel, the motion resistance ratio can be calculated using Equation 3, as follows:

$$MRR(\tau) = \frac{MR}{W} \quad [3]$$

where MR is the motion resistance force suffered by the wheel and W is the normal load on the wheel. Saarilahti (2003) classified motion resistance ratios into good, fair and poor, as shown in Table 2.

TABLE 2: Mobility classes based on motion resistance ratio

Mobility and Trafficability Class	Motion Resistance Ratio
Good	<0.20
Fair	0.20 to 0.30
Poor	>0.30

(Source: Saarilahti, 2003)

The semi-empirical or the analytical prediction of motion resistance ratios involves the measurements of tyre design parameters such as tyre overall wheel diameter (d), tyre deflection (δ), tyre sectional width (b), and tyre sectional height (h). Dynamic load (W) is also measured as the system parameter and the main soil parameter is the soil resistance to penetration (cone index) (Wismer & Luth, 1974; Wong, 1984; Pandey & Tiwari, 2006). All these parameters are substituted into the existing models so as to get mobility numbers or wheel numeric. This mobility number or wheel numeric is further substituted into the existing motion resistance ratio models.

Elwaleed (1999) developed motion resistance ratio, net traction ratio, and tractive efficiency for upland rice tyre. He found that the same model could not be used to generalise the tractive performance characteristics of all tyres. Other researchers also investigated the tractive performance of different agricultural tyre types. Each of these motion resistance models developed by Wismer and Luth (1974), and Brixius (1987), was derived for typical agricultural tyres.

Pneumatic wheel (tyre) is a structural vessel which holds a volume of air under pressure in order to support the vertical load imposed by a vehicle (Plackett, 1985). Unlike pneumatic wheels, rigid wheels do not have rubberised carcass materials and do not work under air pressure. Earlier research conducted has shown that the rigid wheels behave similarly to pneumatic wheels at high inflation pressures (Wang & Reece, 1984).

The use of narrow bicycle wheels as traction members in the development of simple agricultural machines for low income farmers and rural dwellers is paramount. The motion resistance ratios predictions for the bicycle wheel will be useful in the design of such simple machines to boost their agricultural productivity. The objectives of this study were to compare the motion resistance and motion resistance ratios of both the pneumatic and rigid bicycle wheels on deformable surfaces using empirical and semi-empirical approaches. In addition, models for predicting the motion resistance ratios of towed pneumatic and rigid bicycle wheels on both the tilled and wet surfaces using the two methods were also derived. The effect of the towing velocity was also modelled on both wheels and test surfaces.

MATERIALS AND METHOD

The empirical and analytical prediction methods were used to obtain the motion resistance ratio data used for model development. The motion resistance ratios obtained from the experimental measurements of the towing force and the dynamic load were compared with those obtained from the analytical prediction. The coefficients of variation obtained between the two sets of data were used as multiplying factors to the Brixius's (1987) motion resistance ration model to obtain a model for the pneumatic and rigid bicycle wheels.

Tilled and wet surfaces were considered for this study and the models were developed with respect to the two test surfaces. The soil physico-mechanical properties of the test surfaces are presented in Table 3 according to ASTM (2005).

TABLE 3: Some soil physico-mechanical properties of the tilled and wet Surfaces

Soil Properties	Values (Range of values) in Designated Unit
Soil Textural Classification	Sandy-clay-loam (60% sand, 32% clay, 8% silt).
Soil Bulk Density	1.48 kg/m^3 – 1.72 kg/m^3 (mean = 1.55 kg/m^3 db)
Liquid Limit	28.06% db
Plastic Limit	11.14% - 24.26% db (mean = 17.09%db)
Soil Moisture Contents range	10.75% - 15.63% wb (Tilled Surface) 35.7% - 45% wb (Wet Surface)
Cone Index (CI) range of the Tilled Surface	0.6 MPa -1.8 MPa (mean CI = 1.15 Mpa)
Cone Index (CI) range of the Wet Surface	0.7 MPa – 1.4MPa (mean CI = 1.15 MPa)
Soil Strength	Tilled Surface: 63.5 kPa-65 kPa (mean= 64.42 kPa) Wet – surface: 20 kPa-30 kPa (mean = 24.75kPa)

The Empirical Method

Fig.1 shows a complete test rig developed for motion resistance measurement as a subset of the traction studies on non-lug narrow wheel. The data acquisition system part of the test rig comprising of the Mecmesin Basic Force Gauge 2500 (BFG 2500) RS interfaced with the notebook PC is capable for real time data acquisition of the towing force (motion resistance).

The Test Variables

The test variables considered for this study were the test wheels (pneumatic and the rigid wheels), four levels of dynamic loads (98.1 N, 196.2 N, 392.4 N and 588.6 N), by taking into consideration the average weight of human being of 60kg (588.6 N) and the load bearing capacity of the selected tyre. Two test surfaces (tilled and the wet surfaces), and the three levels of towing velocities (4.44 km/h, 6.3 km/h and 8.28 km/h) were selected to investigate the effect of towing velocity on the motion resistance ratio, as shown in the subsequent section.

The Effect of Towing Velocity

Three levels of towing velocities of 4.44 km/h, 6.3 km/h and 8.28 km/h were selected. This is as a result of different agricultural operations requiring different operating velocities (speeds). The motion resistances and soil cone indices were taken with regard to the empirical and semi-empirical approaches for the determinations of the motion resistance ratios. The process was repeated three times and the average data were taken and recorded for each level of towing velocities for both the pneumatic and the rigid wheel. The tyre inflation pressure of

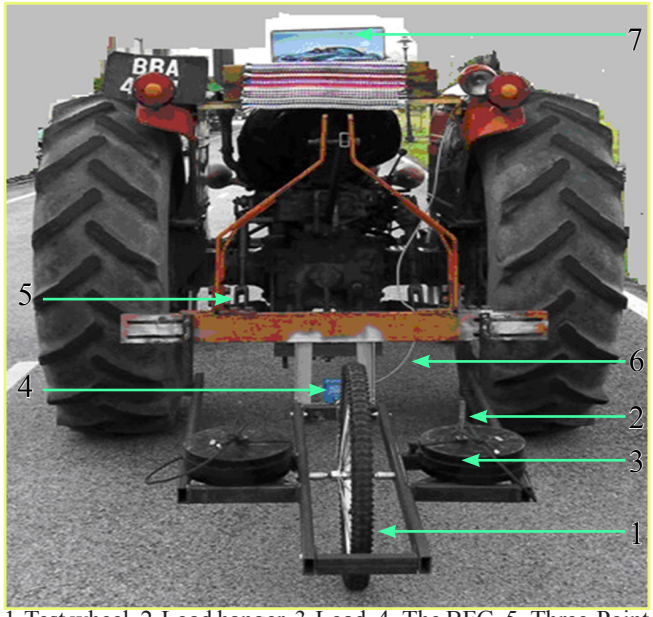

1-Test wheel, 2-Load hanger, 3-Load, 4- The BFG, 5- Three-Point Hitch Frame, 6-connecting cable and 7- Notebook PC

Fig.1: The complete Test Rig attached to the Towing Tractor

the pneumatic wheel was kept at a constant inflation pressure of 414 kPa, as this pressure was assumed to be equal to the tyre surface of the rigid wheel. Meanwhile, the inflation pressure of the tyre was continuously checked to ensure that it was constant throughout the study.

Rigid Wheel Description

The tyre and tube of the 660 mm diameter steel rim pneumatic wheel were removed. A length of 2075 mm of galvanised sheet plate (1.5 mm in thickness and 50 mm in width) was welded round the circumference of the rim. The 50 mm width tyre having the same thread pattern as the pneumatic wheel with equal length as the sheet metal plate was cut and glued onto the sheet metal covering the rim. For rigidity, the two materials were also joined at the edge by a number of bolts and nuts at an interval of 100 mm round the wheel. Fig.2 shows a schematic diagram of the rigid wheel.

Test Surface Preparation

The preparation for data acquisition on the different test surfaces was different. The tests were conducted in one direction only, with the aim to maintain the same test surface condition (slope) for all the tests.

The undisturbed soil of 45 m x 20 m, located at Taman Pertanian Universiti (TPU-University Agricultural Park), was first ploughed and after 48 hours, the rotavator was used to break the large clods into smaller soil clods which were similar to soil bed preparation ready for planting operation. The tests conducted afterwards used the soil moisture probe that was attached to the *Eijkelkamp (Netherlands)* soil penetrologger series (series 06.15.SA) for *in situ* moisture content measurement. The average soil moisture content was then calculated and the range is as stated in Table 3. The field was re-prepared by using a rotavator to make

Fig.2: The Constructed Rigid Bicycle Wheel

the soil surface even and loose to ensure uniform test conditions. The distance of tractor travel during the test from the starting to the end point was set at 35 m for all the tests conducted on the tilled surface.

A bottom-opened box of a size of 20 m x 0.6 m x 0.2 m was installed in the same tilled field. The dimensions of the box, especially the width and the height, were chosen with reference to the test tractor chassis (wheel base and the height). For the tests conducted on the wet surface, the test distance was set at 20m, which is the length of the box. Prior to the test and in between the test, the box was flooded with water and mixed with the soil so as to get the desired wet surface condition. The average soil moisture contents recorded on the wet surface during the test are as stated in Table 3.

Procedure for Data Acquisition

The tractor towing the test rig was prepared to be in a very good condition for the test. The test rig was assembled (i.e. the test wheel was fixed to the test rig). The first level of an added dynamic load (dead weight) of 98.1 N (10kg) was screwed to the load hanger and the tyre inflation pressure of 414 kPa was maintained. The data acquisition system was put on to facilitate real-time data transfer to the Dataplot software installed on the notebook PC for data acquisition. The test distance (between the starting and ending points) was marked. The tractor was allowed to attain a steady velocity of 4.44 km/h for all the tests, except for the tests conducted to investigate the effects of towing velocities before the starting point, while the start icon on the Dataplot environment was also initiated. The real-time data acquisition to measure the towing force (N) against the time taken (seconds) in the form of Force –Time graph was taken progressively until the end point, i.e. when the stop icon was also clicked to stop the data transfer and the plot. The minimum, maximum and the average towing forces (motion resistance) were obtained from the dataplot. Each of the treatments was replicated three times and the average of at least 95% was taken of the measured data around the mean ($\mu \pm 2\delta$).

The Analytical Prediction Method (Semi-empirical Approach)

The mobility number models derived by Brixius (1987) were used for the prediction of the motion resistance ratio, which was also derived by Brixius (1987). Equations 4 and 5 present the Brixius (1987) models for mobility number and motion resistance ratio respectively. However, Equation 5 had been modified (as presented in Equation 6) as the slip component of that equation is zero (0) for the towed wheels (Gee-Clough *et al*., 1978; Naderi *et al*., 2008).

$$Bn = \frac{CIbd}{W}\left[\frac{1+5\frac{\delta}{h}}{1+3\frac{b}{d}}\right] \quad [4]$$

$$M_{RR} = 0.04 + \frac{1}{B_n} + \frac{0.5}{\sqrt{B_n}} \quad [5]$$

$$M_{RR} = 0.04 + \frac{1}{B_n} \quad [6]$$

Equations 5 and 6 are dependent upon Equation 4; therefore, the mobility number was determined from Equation 4, and the value substituted into Equation 6 to determine the motion resistance ratio.

Procedure for Data Acquisition for the Semi-empirical Approach Method

These soil resistances to penetration were measured on the surfaces (path) where the motion resistances were already measured experimentally using the cone penetrologger. Three readings were taken as applicable to the empirical method and the average values were processed for the prediction of the mobility number and the motion resistance ratio.

The procedure for the empirical measurement of the motion resistance on the wet surface was similar to that of the tilled surface. The cone indices were also measured in a similar way to those obtained for the tilled surface. However, the surface of the test wheel, which was in contact with the test surface, was cleaned after every test to ensure similar tyre surface. The test surface was regularly reconditioned to the original state by closing the rut formed during the test and disturbing the test surface and making the surface moist to give uniform test condition.

The sectional width and the sectional height at 414 kPa tyre inflation pressure were measured using the *Mitutoyo* (UK) vernier calliper (series 573) with an accuracy of 0.01cm. The loaded and unloaded radii during the field tests were also measured using the meter rule. The difference is a measure of the tyre deflection, according to Equation 7.

$$\delta = U_R - L_R \quad [7]$$

U_R is the unloaded radius, while L_R is the loaded radius, and δ is the tyre deflection. The rigid wheel has a zero deflection.

RESULTS AND DISCUSSION

From the initial analysis of the experimental data, the analysis of variance showed that at 20kg (196.2 N) added dynamic load, there were significant differences between the mean of the motion resistances measured at 414 kPa inflation pressure and at all levels of the dynamic loads. On this basis, the overall wheel diameter of 660 mm was chosen for this study at 196.2 N added dynamic load and 414 kPa similar to the hard surface of the rigid wheel.

The tyre design parameters, the average soil resistance to penetration, the various dynamic loads are recorded against the respective average moisture contents, as shown in Tables 4a and b. These parameters were substituted into Equation 4 so as to obtain the mobility number for each of the test combinations and these values were substituted into Equation 5 to get the motion resistance ratios. The motion resistance ratio (measured by the empirical methods) and the corresponding dynamic loads were also substituted into Equation 3 to determine the motion resistance ratios. The motion resistance ratios obtained from the two approaches at a constant towing velocity of 4.44 km/h and at varying dynamic loads are presented in Tables

TABLE 4(a): Tyre parameters, soil parameters and dynamic loads on the tilled surface

Test Combinations	Total dynamic load (N)	Motion resistance (N)	Tyre design parameters				Average CI (MPa)	Average mc (%wb)
			d, mm	b, mm	h, mm	δ, mm		
D_pL_1	321.768	28.2374	660	49.3	42.5	5.00	0.60	5.70
D_pL_2	419.868	46.5037	660	49.3	42.5	7.00	0.83	6.00
D_pL_3	616.068	64.1054	660	49.3	42.5	10.00	0.90	11.00
D_pL_4	812.268	90.6656	660	49.3	42.5	13.00	1.20	11.00
D_RL_1	325.201	57.8055	580	49.5	4.0	0	1.23	14.00
D_RL_2	423.301	72.1290	580	49.5	4.0	0	1.43	12.00
D_RL_3	619.501	112.5968	580	49.5	4.0	0	1.10	7.00
D_RL_4	815.701	198.3133	580	49.5	4.0	0	0.90	14.00

*D_P-pneumatic wheel, D_R- rigid wheel, L_{1-4} –additional load (98.1N, 196.2 N, 392.4 N and 588.6N)

TABLE 4(b): Tyre parameters, soil parameters and dynamic loads on the wet surface

Test Combinations	Total dynamic load (N)	Motion resistance (N)	Tyre design parameters				Average CI (MPa)	Average mc (%wb)
			d, mm	b, mm	h, mm	δ, mm		
D_pL_1	321.768	81.7383	660	49.3	42.5	5.00	1.0333	42
D_pL_2	419.868	94.4724	660	49.3	42.5	7.00	1.2000	44
D_pL_3	616.068	143.6779	660	49.3	42.5	10.00	1.3000	43.7
D_pL_4	812.268	157.9837	660	49.3	42.5	13.00	1.2667	42.3
D_RL_1	325.201	103.4037	580	49.5	4.0	0	0.8000	37
D_RL_2	423.301	148.7016	580	49.5	4.0	0	0.9000	35.7
D_RL_3	619.501	161.3703	580	49.5	4.0	0	1.0333	41.3
D_RL_4	815.701	215.0599	580	49.5	4.0	0	1.3000	45

*D_P-pneumatic wheel, D_R- rigid wheel, L_{1-4} –additional load (98.1N, 196.2 N, 392.4 N and 588.6N)

5a and 5b. Table 6 shows the motion resistances of the pneumatic and the rigid bicycle wheels, with respect to dynamic loads.

The motion resistances measured on the tilled and wet surface revealed that the rigid wheel had a higher motion resistance and motion resistance ratios than the pneumatic wheel. The motion resistance of the rigid wheel on the tilled surface was about 50% greater than those of the pneumatic wheel. However, on the wet surface, the motion resistances of the rigid wheel were greater than those of the pneumatic wheel by 11-37%. The motion resistance ratios predicted from the Brixius model were lower than those determined using the experimental approach on both the test surfaces. This result is not at variance with the findings of Gee-Clough *et al*. (1978), Perdok (1978), and Islam (1986). The motion resistances determined empirically for both wheels were found to have increased with the increase in the dynamic load, whereas the motion resistance ratios of both the wheels were shown to have decreased with the increase in the dynamic load on wet surfaces, and increased with the increase in the dynamic loads on the tilled surface. Nonetheless, the motion resistances ranged between good and fair according to the Saarilahti (2003) classifications, with the exception of the rigid wheel at lower additional

TABLE 5(a): Motion resistance ratios obtained from the empirical approach

Added Dynamic Load (N)	Tilled Surface		Wet Surface	
	Pneumatic	Rigid	Pneumatic	Rigid
98.1	0.0878	0.1778	0.2540	0.3180
196.2	0.1108	0.1704	0.2250	0.3513
392.4	0.1041	0.1818	0.2332	0.2605
588.6	0.1116	0.2431	0.1945	0.2637

TABLE 5(b): Motion resistance ratios obtained from the analytical approach

Added Dynamic Load (N)	Tilled Surface		Wet Surface	
	Pneumatic	Rigid	Pneumatic	Rigid
98.1	0.1091	0.1052	0.0903	0.1245
196.2	0.1014	0.1098	0.0897	0.1323
392.4	0.0977	0.1431	0.0934	0.1472
588.6	0.1002	0.1792	0.0984	0.1503

TABLE 6: Motion resistances of pneumatic and rigid wheels measured empirically

Added Dynamic Load (N)	Tilled Surface		Wet Surface	
	Pneumatic	Rigid	Pneumatic	Rigid
98.1	28.2374	57.8055	81.7383	103.4037
196.2	46.5073	72.1290	94.4724	148.7016
392.4	64.1054	112.5968	143.6779	161.3703
588.6	90.6656	198.3133	157.9837	215.0599

dynamic loads which showed poor mobility.

From the semi-empirical approach, it is difficult to conclude the nature of the relationships that existed between the motion resistance ratios and the dynamic loads. However, the motion resistance ratios predicted were directly proportional to the added dynamic load for both the wheels, except for the pneumatic wheel which exhibited an inverse relationship between the motion resistance ratio and the added dynamic load. The motion resistance ratios under this condition fell under a good mobility classification.

Fig.3 and Fig.4 show the graphical relationships between the motion resistance ratios and the towing velocities of both the wheels on the tilled and wet surfaces, respectively, based on the empirical data. The mathematical relationships between the motion resistance ratio and their towing velocities are presented in Equations 8 to 11. On the tilled surface, the motion resistance ratios of both the wheels had direct relationships with the towing velocity. This could also be inferred from the equation having positive coefficient of towing velocity (v). The pneumatic wheel also showed a similar relationship on the wet surface with a higher coefficient of regression. As shown in Fig.4, when the towing velocities increased, the motion resistance ratio of the rigid wheel would decrease. This can also be seen in Equation 11, where

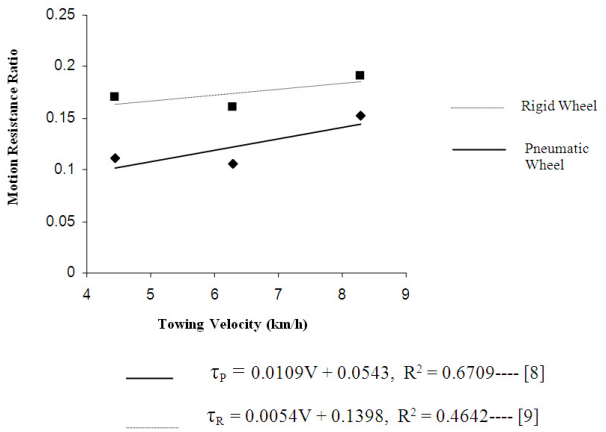

$\tau_P = 0.0109V + 0.0543,\ R^2 = 0.6709$---- [8]

$\tau_R = 0.0054V + 0.1398,\ R^2 = 0.4642$---- [9]

Fig.3: A Comparison of the Motion Resistance Ratio of Pneumatic and Rigid Wheels on the Tilled Surface in terms of Towing Velocity

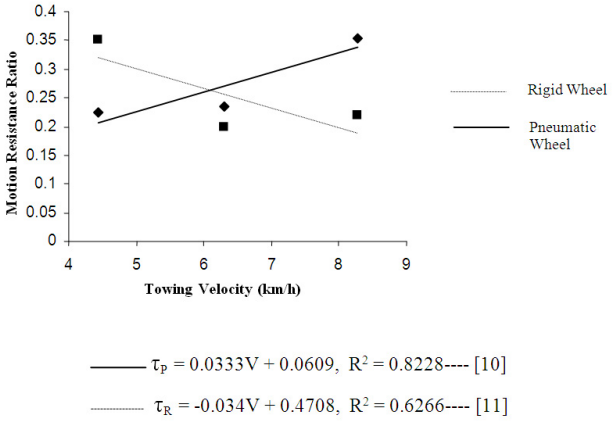

$\tau_P = 0.0333V + 0.0609,\ R^2 = 0.8228$---- [10]

$\tau_R = -0.034V + 0.4708,\ R^2 = 0.6266$---- [11]

Fig.4: A Comparison of the Motion Resistance Ratio of Pneumatic and Rigid Wheels on Wet Surface in terms of Towing Velocity

the towing velocity, v, had a negative coefficient.

Fig.5 and Fig.6, as well as Equations 12 to 15, present the relationships between the motion resistance ratios of both the wheels obtained from the semi-empirical approach on the tilled and wet surfaces. The relationships between the motion resistance ratios and the towing velocities from the two approaches were found to differ. In particular, the motion resistance ratio of the pneumatic wheel is indirectly proportional to the towing speed at 0.8943 coefficient of regression, while the rigid wheel shows a direct relationship at a very low coefficient of regression on the tilled surface. However, the relationship on the wet surface is similar to that obtained from the empirical method. The motion resistance ratio of the rigid wheel is indirectly proportional to the towing velocity, while the pneumatic wheel has a direct relationship. From these findings, it can be concluded that the rigid wheel is a better traction member on wet surfaces.

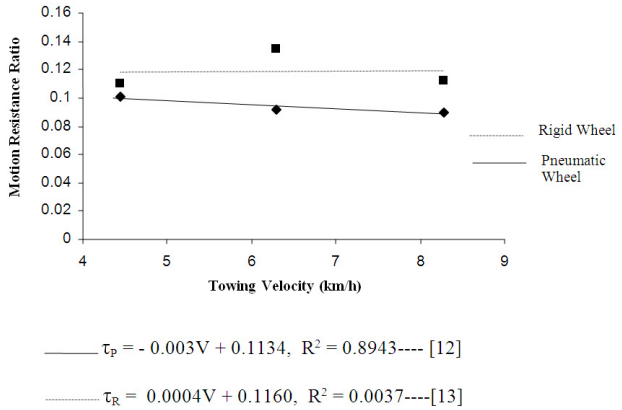

Fig.5: A Comparison of the Motion Resistance Ratio of Pneumatic and Rigid Wheels on Tilled Surface in terms of Towing Velocity: the Analytical Approach

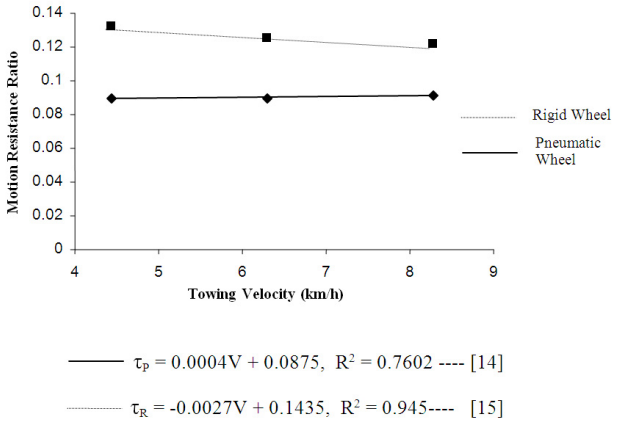

Fig.6: A Comparison of the Motion Resistance Ratio of Pneumatic and Rigid Wheels on Wet Surface in terms of Towing Velocity: The Analytical Approach

The motion resistance ratios, measured by the empirical and the semi-empirical methods, also differed. The motion resistance ratios predicted from the Brixius equation were found to be lower than those measured experimentally, and the main reason for this could be attributed to the size of the tyre used to derive the model. Therefore, a multiplying factor was used to derive the new motion resistance ratio models for the pneumatic and rigid bicycle wheels on two deformable terrains. The factors are stated in Tables 7 and 8, and the models are presented in Equations 16 to 19.

From Brixius' (1987) equation for bias-ply tractor tyres, the motion resistance ratio is as stated in Equation 5. Therefore, for the 660 mm pneumatic bicycle wheels at 414 kPa inflation pressure, the motion resistance ratio was derived, as follows:

$$MRR\ (Bicycle) = 2.0254.\ (0.04 + \frac{1}{B_n})$$

$$MRR\,(Bicycle) = 0.0810 + \frac{2.0254}{B_n} \qquad [16]$$

TABLE 7: Determination of the factors between motion resistance ratio of the pneumatic wheel obtained by empirical and analytical methods at different dynamic loads and 414 kPa

Dynamic Load	A: MRR (Empirical)		B: MRR (Analytical)		C: Factors (A/B)	
(N)	Tilled	wet	Tilled	Wet	Tilled	Wet
98.1	0.0878	0.2540	0.0527	0.0474	1.6660	5.3586
196.2	0.1108	0.2250	0.0504	0.0472	2.1984	4.7669
392.4	0.1041	0.2332	0.0518	0.0482	2.0097	4.8382
588.6	0.1116	0.1945	0.0501	0.0495	2.2275	3.9293
Mean					2.0254	4.7233
Coefficient of variation					12.758%	12.52%

Inflation Pressure, P = 414 kPa and Overall Wheel Diameter (metallic rim), D = 660mm.

Field Condition: Tilled Surface (Sandy-Clay-Loam Soil)

Added Dynamic Load range: 98.1 – 588.6 N

TABLE 8: Determination of the factors between motion resistance ratio of the rigid wheel obtained by empirical and analytical methods at different dynamic loads

Dynamic Load	A: MRR (Empirical)		B: MRR (Analytical)		C: Factors (A/B)	
(N)	Tilled	wet	Tilled	Wet	Tilled	Wet
98.1	0.1778	0.3180	0.0515	0.0578	3.4524	5.5017
196.2	0.1704	0.3513	0.0529	0.0606	3.2212	5.7970
392.4	0.1818	0.2605	0.0646	0.0662	2.8142	3.9350
588.6	0.2431	0.2637	0.0797	0.0675	3.0502	3.9067
Mean					3.1345	4.7851
Coefficient of variation					8.60%	21%

Field Condition: Tilled Surface (Sandy-Clay-Loam Soil)

Added Dynamic Load range: 98.1 – 588.6 N

Field condition: Wet soil (sandy-clay-loam soil) surface
Added dynamic load range: 98.1 – 588.6 N

From Brixius' (1987) equation for bias-ply tractor tyres, the motion resistance ratio is as stated in Equation 5. Therefore, for the 660 mm pneumatic bicycle wheels at 414 kPa inflation pressure, the motion resistance ratio was derived as follows:

$$MRR\ (Bicycle) = 4.7233\ (0.04 + \frac{1}{B_n})$$
$$MRR(Bicycle) = 0.1889 + \frac{4.7233}{B_n} \quad [17]$$

From Brixius' (1987) equation for bias-ply tractor tyres, the motion resistance ratio is as stated in Equation 5. For the rigid bicycle wheel on tilled surface, the motion resistance ratio was therefore derived as follows:

$$MRR\ (Bicycle) = 3.1345.\ (0.04 + \frac{1}{B_n})$$
$$MRR\,(Bicycle) = 0.1254 + \frac{3.1345}{B_n} \quad [18]$$

Field condition: Wet soil (sandy-clay-loam soil) surface
Added dynamic load range: 98.1 – 588.6 N

From Brixius' (1987) equation for bias-ply tractor tyres, the motion resistance ratio is as stated in Equation 5. Therefore, for the rigid bicycle wheel, the motion resistance ratio was derived as follows:

$$MRR\ (Bicycle) = 4.7841.\ (0.04 + \frac{1}{B_n})$$
$$MRR\,(Bicycle) = 0.1914 + \frac{4.7841}{B_n} \quad [19]$$

CONCLUSION

In conclusion, the motion resistance and motion resistance ratios of 660 mm pneumatic and the rigid bicycle wheels were determined both empirically and analytically on tilled and wet surfaces. The motion resistances measured on the wet surface by both the wheels were greater than those obtained on the tilled surface with the rigid wheel leading in all the cases. The motion resistance ratios obtained through empirical methods were greater than those of the semi-empirical ones. Hence, different relationships between motion resistance ratios, the dynamic loads and the towing velocities exist on different surfaces with different wheel types. The rigid wheel is a better traction member on the wet surface at any forward velocity compared with its pneumatic counterpart. The semi-empirical approach under-predicted the motion resistance ratios compared to the empirical method. Based on this, a new set of motion resistance ratio models were derived for predicting motion resistance ratios of pneumatic and rigid bicycle wheels on deformable surfaces (tilled and wet surfaces).

ACKNOWLEDGEMENTS

This research project is classified under the Institute of Higher Learning, IHL (FRGS-Fundamental Research Grant Scheme) 1/ 2007 KOS 55235435.ihlrm7 IRPA Project No. 01-02-04. The authors are very grateful to the authority of Universiti Putra Malaysia for granting the fund for this research project.

REFERENCES

Arregoces, A. (1985). *Rolling resistance of bicycle wheels: Measurement and trends investigation* (Unpublished M.Sc. Thesis), Silsoe College.

American Standard for Test and Measurements (ASTM) D. 4318(2005) Liquid Limit. *Plastic Limit, and Plasticity Index of Soils*. ASTM.

Bernstein, R. (1913): *Problem Experimental Motorflugmech*, 16.

Brixius, W. W (1987). *Traction prediction equations for bias ply tyres*. ASAE Paper No 87-1662, ASAE, St. Joseph, MI.

Code, O. (2003, R2009). General Terminology for Traction of Agricultural Traction and Transport Devices and Vehicles. ANSI/ASABE S296.5 (ASABE Standard), 1-5.

Elwaleed, A. K. (1999). *Motion resistance, Net traction ratio, and tractive efficiency of riceland type tyre* (Unpublished M.Sc Thesis), Biological and Agricultural Engineering, Faculty of Engineering, Universiti Putra Malaysia, Serdang, Selangor.

Gee-Clough, D., McAllister, M., Pearson, G., & Evernden, D. W. (1978). The empirical prediction of tractor-implement field performance. *Journal of Terramechanics, 15*(2), 81-94.

Gheissari, M. H., & Loghavi, M. (2010). *Evaluation of Agricultural Tire Traction Prediction Model Using a Single Wheel Tester* (ASABE Paper No 1009100). Presented at the 2010 ASABE Annual Meeting, David Lawrence Convention centre, Pittsburgh, Pennsylvania. David L. Lawrence Convention Center, Pittsburgh, Pennsylvania: (ASABE Paper No. 1009100) St. Joseph, Mich. ASABE.

Gotteland, P., & Benoit, O. (2006). Sinkage tests for mobility study, modelling and experimental validation. *Journal of Terramechanics, 43*(4), 451-467.

Islam, M. S. (1986). *Off-road performance of bicycle wheels: With special emphasis on Rolling Resistance*. Silsoe College, England.

Kawase, Y., Nakashima, H., & Oida, A. (2006). An indoor traction measurement system for agricultural tires. *Journal of Terramechanics, 43*(3), 317-327.

Macmillan, R. H. (2002). Mechanics of tractor-implement performance; Theory and Worked examples. In *A textbook for Students and Engineers*. Place Published. Retrieved July 3, 2009 from http://www.eprints.unimelb.edu.au.

Naderi, M., Alimardani, R., Abbaszadeh, R., & Ahmadi., H. (2008). Assessment of dynamic load equations through drive wheel slips measurement. *American- Eurasian Journal of Agriculture and Environmental Sciences 3*(5): 778-784.

Pandey K. P., Tiwari, G. (2006). Rolling Resistance of Automobile Discarded Tyres for Use in Camel Carts in Sand. Paper read at 2006 Annual international meeting of ASABE, 9-12 July, 2006, at Oregon Conventional center Portland, oregon.

Perdok U. D. (1978). A prediction model for the selection of tyres for towed vehicles on tilled soil. *Journal of Agricultural Engineering Research 23*(4), 369-383.

Plackett, C. W. (1985). A review of force prediction methods for off-road wheels. *Journal of Agricultural Engineering Research, 31*(1), 1-29.

Pope, R. G. (1971). The effect of wheel speed on rolling resistance. *Journal of Terramechanics, 8*(1), 5-5.

Saarilahti, M. (2003). Soil interaction model. *ECOWOOD studies made at the University of Helsinki. University of Helsinki, Faculty of Agriculture and Forestry, Department of Forest Resource Management Publication, 31*, 2003-07.

Schreiber, M., & Kutzbach H. D. (2007). Comparison of different zero-slip definitions and a proposal to standardize tire traction performance. *Journal of Terramechanics, 44*(1), 75-79.

Turnage, G. W. (1972). *Using dimensional prediction terms to describe off-road wheel vehicle performance*. ASAE paper No. 72-634. St. Joseph, MI.49085.

Wang Z., & Reece, A. R. (1984). The performance of free rolling rigid and flexible wheels on sand. *Journal of Terramechanics, 21*(4), 347-360.

Wismer, R. D., & Luth, H. J. (1974). Off-road traction prediction for wheeled vehicles. *Transactions of the ASAE, 17*(1), 8-10.

Wong, J. Y. (1984). On the study of wheel-soil interaction. *Journal of Terramechanics, 21*(2), 117-131.

Yahya, A., Zohadie, M., Ahmad, D., Elwaleed, A. K., & Kheiralla, A. F. (2007). UPM indoor tyre traction testing facility. *Journal of Terramechanics, 44*(4), 293-301.

Pertanika J. Sci. & Technol. 21 (1): 75 - 96 (2013)

SCIENCE & TECHNOLOGY

Journal homepage: http://www.pertanika.upm.edu.my/

Assessment of Heavy Metal Pollution in the Straits of Johore by Using Transplanted Caged Mussel, *Perna viridis*

Eugene Ng, Y. J.[1], Yap, C. K.[1]*, Zakaria, M. P.[2] and Tan, S. G.[3]

[1]*Department of Biology, Faculty of Science, Universiti Putra Malaysia, 43400 Serdang, Selangor, Malaysia*

[2]*Department of Environmental Sciences, Faculty of Environmental Studies, Universiti Putra Malysia, 43400 Serdang, Selangor, Malaysia*

[3]*Department of Cell and Molecular Biology, Faculty of Biotechnology and Biomolecular Science, Universiti Putra Malysia, 43400 Serdang, Selangor, Malaysia*

ABSTRACT

In this study, a polluted site at Kg. Pasir Puteh was assessed for heavy metal pollution by using transplanted caged mussel (*Perna viridis*) from a relatively clean population, Sg. Melayu; both are located in the Strait of Johore. For control purposes, the *P. viridis* from Kg. Pasir Puteh were also simultaneously transplanted in Sg. Melayu at the same time. It was found that Zn was the metal which got accumulated fastest in the transplanted mussel while Cd was the slowest. This study indicated that the byssus of *Perna viridis* was most effective for biomonitoring of Cd, Ni, Pb and Zn, while the shell could be used for the biomonitoring of Cu, Ni and Pb and the total soft tissue for the biomonitoring of Ni since they were able to accumulate and eliminate the respective metals well. By using mussel as a biomonitor, the present study found that Kg. Pasir Puteh, which is located in the eastern part of the Strait of Johore, had significantly higher contamination and bioavailabilities of Cd, Cu, Fe, Ni, Pb and Zn. Therefore, the use of the transplanted caged mussels is very useful for heavy metal assessment purposes since it can increase the validity of data interpretation by minimizing ecological factors.

Keywords: Heavy metal, *Perna viridis*, Strait of Johore, transplant

INTRODUCTION

Anthropogenic activities have been increasing as the population of humans grows rapidly. The increase of anthropogenic activities has always caused heavy metal pollution in coastal waters. Monitoring of coastal waters which are exposed to chemical pollution due to industrial production and high urbanization

Article history:
Received: 27 April 2011
Accepted: 22 November 2011

E-mail addresses:
enyj@msn.com (Eugene Ng, Y. J.),
yapckong@hotmail.com (Yap, C. K.),
mpauzi@env.upm.edu.my (Zakaria, M. P.),
sgtan@biotech.upm.edu.my (Tan, S. G.)
*Corresponding Author

ISSN: 0128-7680 © 2013 Universiti Putra Malaysia Press.

(Giarratano *et al*., 2010) by using mussels has been widely reported in the literature. However, a more efficient and practical approach for assessing heavy metal pollution is needed. Recently, to define the areas of metal pollution, caged or transplanted mussels have been employed in many coastal waters such as Ushuaia Bay, Argentina (Giarratano *et al*., 2010), North West of Mediterranean Sea (Faverney *et al*. 2010), Boston Harbour, United States (Hunt & Slone, 2010) and New Caledonia Lagoon in the South Pacific of France (Hedouin *et al*., 2011).

The Johore Strait is a narrow strait that separates the Malaysian state of Johore from Singapore and it is separated into two distinct portions by a causeway which connects Peninsular Malaysia and Singapore. It is an important area for fishing and aquaculture activities (Yap *et al*., 2006; Zulkifli *et al*., 2010). Furthermore, the existence of mangrove, sea grass, coral and mudflat ecosystems also make the Johor Straits an important strait (Zulkifli *et al*., 2010). Oil pollution has been identified as the major contributor to the pollution of the water in the Straits of Johor (DOE, 1994; Moradi, 2001; Shahbazi *et al*., 2010). Shipping activities involving tankers and other vessels can easily be found in the Strait of Malacca, while land-based industrial and urban sources have been recognised as the sources of pollutants for the strait (Abdullah *et al*. 1996). The eastern part of the straits is more polluted than the western part since marina, petrochemical plants and port activities such as Pasir Gudang Port (ranked 82nd in 2007 global TEU), Tanjung Pelepas Port (ranked 18th in 2007 global TEU) and Tanjung Langsat Port (a new petrochemical port) are located on the eastern coast (Bayen *et al*., 2003; Yap *et al*., 2004, 2006). Kg. Pasir Puteh, which is located in the eastern part, is reported as a highly polluted site, where large shipyard repair and construction facilities, fossil fuel fired electrical power plants and shipping dock activities can be found (Yap *et al*., 2003d, 2004; Zulkifli *et al*., 2010). On the other hand, Kg. Sg. Melayu in the western part is considered as a site with low human activities and the only activities which can be found there are fish and mussel aquaculture (Yap *et al*., 2006). Owing to its strategic location and ecological importance, the Johore Strait has become a hotspot for pollution studies (DOE, 2007; Shazili *et al*., 2006; Wood *et al*., 1997).

Francesco and Enzo (1994) noted that the accumulations of Pb, Fe and Mn in the mussels, which were transplanted from a clean site to a heavy metal polluted environment, would reach a steady state only after 2 weeks. The results showed that mussels could easily equilibrate with polluted coastal waters. However, the time-integration capacity of mussels might vary for different metals. In fact, many important biological processes associated with metal exposures have generally been studied under laboratory conditions but not in field experiments (Regoli, 1992; Yap *et al*., 2003a). In this respect, mussel transplantation is a more practical approach to be used in monitoring the metal accumulation of mussels at fixed sites.

Marine mussels are suitable for transplantation experiments because they are cost effective and reliable (Farverney *et al*., 2010). In particular, *P. viridis* fulfils the necessary criteria which are sedentary lifestyle, enough tissues for metal analysis, suspension feeder, tolerant of high heavy metal concentrations (Yap *et al*. 2003a) and prone to bioaccumulate and magnify such metals (Yap *et al*. 2004) and of relatively low genetic differentiation (Yap *et al*., 2002a,b).

The advantages of adopting transplantation are mainly due: (1) to the fact that the monitoring sites may be chosen independently of the presence of natural populations (Hedouin *et al*., 2011), (2) to access the status of bioaccumulation in hard-to-reach areas such as in different strata of the water column (Hunt & Slone, 2010; Giarratano *et al*., 2010), (3) it can

be site-specific, (4) control exposure times, depth of transplantation, age, size, stage of sexual maturity of mussels, which can interfere with and affect the accumulation rate (Alfonso *et al*., 2010), and (5) usually with low genetic variation and in the same phase of the reproductive cycle since they are abundant and easily available from commercial markets (Gorbi *et al*., 2007). The use of transplanted mussels has been proven to be a useful strategy for biomonitoring marine pollution (Nasci *et al*., 2002; Romeo *et al*., 2003; Regoli *et al*., 2004; Nigro *et al*., 2006).

By using transplanted mussels, the effects of external and internal factors such as seasonal variations, size or age, which can cause bias in data comparison, are minimized (Regoli & Orlando, 1994; Hedouin *et al*., 2011). Since there has been no study which reported on heavy metals in transplanted mussels in Malaysia, the objective of this study was to assess the heavy metal pollution in the Strait of Johore by using transplanted mussels.

MATERIALS AND METHODS

Transplantation of Mussel Populations

About 200 individuals of *P. viridis* were collected from a polluted site at Kg. Pasir Puteh and transplanted to a relatively unpolluted site at Sg. Melayu, in the Strait of Johore on 28 November 2009. On the same day, the same amount of mussels were also collected from Sg. Melayu and transplanted to Kg Pasir Puteh. After the mussels had been collected, the whole cluster was rinsed 3 times using seawater to get rid of any visible sediment on the mussel shells. The mussels were then divided randomly into sub-groups of 40 individuals and each sub-group was placed in a polyethylene cage of 20 x 15 x 18 cm which permitted water circulation through it. Four cages were used per site and left suspended in the water column at an average depth of 1.5 m using a rope which was modified from Faverney *et al*. (2010). The samples of mussels were taken at the beginning of the experiment (t=0), at 2 (t=2), 6 (t=6) and 10 (t=10) weeks time of the exposure. The collected mussels had been rinsed with seawater before they were transported back to the laboratory in an ice compartment. However, at week 10, all the mussel samples died and no soft tissues were found. Thus, only byssus and shells were analysed at week 10.

Seawater

The physico-chemical readings of the seawater from Sg. Melayu and Kg. Pasir Puteh at around 1.5 m depth were recorded *in situ* at the beginning of the experiment (t=0), at weeks 2 (t=2), 6 (t=6) and 10 (t=10) for temperature (°C), specific conductivity (ms/cm), salinity (ppt) and dissolved oxygen (mg/L) during the transplantation experiment using YSI brand Physico-chemical meter (PCM) model no. 556 MPS.

Pre-treatment of the Samples

Sediment samples at each site were also collected by using an Ekmen Grab (16 cm x 16 cm) and these samples were stored in polyethylene bags and transported in an ice compartment back to the laboratory. The samples were dried until constant weights at 105°C for at least 16 hours (Tanner *et al*., 2000). The samples were then sieved through 63µm stainless steel aperture

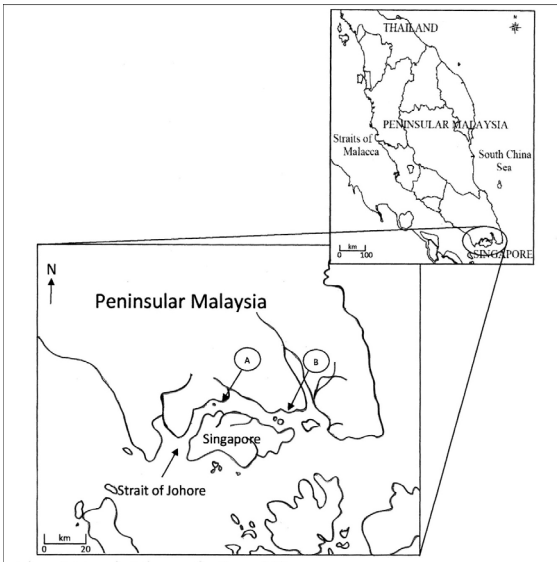

Fig.1: Map showing the transplantation sites for *Perna viridis*
Note: A- Sungai Melayu B- Kampung Pasir Puteh

and vigorously shaken to produce homogeneity. All individuals of *P. viridis* were dissected into byssus, total soft tissue and shell. Half gram of the samples was digested in concentrated nitric acid (AnalaR grade, BDH 69%) in a hot-block digestor first at a low temperature (40°C) for 1 hour before the temperature was increased to 140°C for 3 hours. The digested samples were later diluted in 40ml double distilled water (DDW). The sample was then filtered through Whatman No. 1 filter paper and the filtrate was stored in an acid-washed pill box until metal determination. For the analyses of the total heavy metal concentrations in sediment samples, the open digestion method was used. About 1g of each dried sample was digested in a combination of concentrated nitric acid (AnalaR grade, BDH 69%) and perchloric acid (60%) in the ratio of 4:1. On top of that, the geochemical fractions of Cd, Cu, Fe, Ni, Pb and Zn in the sediments were obtained by using the modified Sequential extraction technique (SET), as described by Yap *et al*. (2002). The first fraction was EFLE (Easily, freely, leacheable or exchangeable). About 10g of the sample was continuously shaken for 3 hours with 50ml 1.0M ammonium acetate (NH_4CH_3COO) at pH 7.0 at room temperature for this fraction. The second fraction was 'Acid-reducible'. The residue from fraction 1 was continuously shaken for 3 hours with 50ml 0.25M hydroxylammonium chloride ($NH_2OH.HCL$) acidified to pH 2 with HCL at room temperature, and this was followed by the third fraction which was 'Oxidisable-organic'. The residue from fraction 2 was first oxidized with 30% H_2O_2 in a water bath at 90–95°C. After cooling, the metal released from the organic complexes was continuously shaken for 3 hours with 1.0M ammonium acetate (NH_4CH_3COO) acidified to pH 2.0 with HCL at room temperature. 'Resistant' was the last fraction where the residue from fraction 3 was digested in a combination of concentrated nitric acid (AnalaR grade, BDH 69%) and perchloric acid (AnalaR grade, BDH 60%), as performed in the open digestion method.

TABLE 1: Size of mussels in average (mean ± SE, mm), condition index (CI) and physico-chemical characteristics of the water samples at different time intervals at Kg. Pasir Puteh

Sg. Melayu – Kg. Pasir Puteh

	Sizes of mussel (mean±SE, mm)										PCM				
Week	Length			Width			Height			CI	Temp (°C)	SC (ms/cm)	Sal (ppt)	DO (mg/L)	pH
0	30.45	±	2.64	9.07	±	1.04	14.64	±	1.54	21.53	29.26	45.17	29.11	4.57	7.52
2	56.67	±	3.68	16.77	±	3.67	23.94	±	3.19	23.54	30.01	38.61	24.42	3.14	7.15
6	68.88	±	4.51	20.67	±	3.92	29.22	±	2.06	21.19	30.61	44.47	28.56	7.59	7.68
10	79.94	±	6.37	24.38	±	2.83	35.17	±	3.17	20.61	29.96	39.90	25.33	13.82	7.03

TABLE 2: Size of mussels in average (mean ± SE, mm), condition index (CI) and physico-chemical characteristics of the water samples at different time intervals at Sungai Melayu

Kg. Pasir Puteh – Sg. Melayu

	Sizes of mussel (mean±SE, mm)										PCM				
Week	Length			Width			Height			CI	Temp (°C)	SC (ms/cm)	Sal (ppt)	DO (mg/L)	pH
0	34.46	±	1.33	10.22	±	1.26	15.66	±	2.37	26.18	30.04	41.54	26.49	3.88	7.15
2	53.17	±	3.14	16.96	±	3.11	22.39	±	3.88	24.22	29.06	46.31	29.94	5.85	7.16
6	66.15	±	4.57	19.37	±	4.31	29.61	±	4.32	21.39	29.06	46.31	29.94	5.74	7.16
10	78.74	±	5.39	23.41	±	3.94	35.10	±	4.16	17.45	29.97	41.59	26.53	4.22	7.15

TABLE 3: A comparison of heavy metal concentrations (µg/g dry weight) between measured values and certified values in the Certified Reference Materials (CRM) for dogfish liver DOLT-3

Metals	Certified values (C)			Measured value (M)			Percentage of recovery [(M/C) x 100]
Cu	31.20	±	1.00	26.81	±	0.25	85.93
Cd	19.40	±	0.60	14.68	±	0.34	75.67
Fe	1484.00	±	57.00	1213.42	±	10.67	81.77
Ni	2.72	±	0.35	3.37	±	0.20	123.90
Pb	37.38	±	12.81	29.37	±	0.33	78.56
Zn	86.60	±	2.40	76.12	±	0.81	99.90

TABLE 4: A comparison of heavy metal concentrations (µg/g dry weight) between measured values and certified values in the Certified Reference Materials (CRM) for Soil China (NSC DC73319)

Metals	Certified values (C)			Measured value (M)			Percentage of recovery [(M/C) x 100]
Cu	21.00	±	2.00	18.28	±	0.74	87.05
Cd	4.30	±	0.40	4.64	±	0.14	107.91
Ni	20.40	±	1.80	17.16	±	0.51	84.12
Pb	98.00	±	6.00	110.8	±	9.39	113.06
Zn	680.00	±	25.00	566.76	±	6.39	83.35

Note: CRM for Fe was not available.

Metal Analysis

After filtration, the samples were analysed for Cd, Cu, Fe, Ni, Pb and Zn using an air-acetylene flame atomic absorption spectrophotometer (AAS), Perkin-Elmer Model AAnalyst 800. The data are presented in $\mu g.g^{-1}$ dry weight. To avoid possible contamination, all the glassware and equipment used were acid-washed and the accuracy of the analysis was checked against blanks. For data validation, Certified Reference Material (CRM) was checked with the samples for dogfish liver (DOLT-3, National Research Council Canada) and Soil China (NSC DC73319, China National Analysis Centre), as shown in Tables 3 and 4.

Condition Index

To examine the individual Condition Index (CI) of mussels, 5 specimens were taken at each exposure time to obtain an estimate of the ratio of weight of the soft parts to shell volume. Soft tissues were separated from the shell and dried at 60°C until constant weight was achieved. Condition index (g/cm^3) of each mussel was calculated according to Lares and Orians (1997):

$$\text{Condition index} = \frac{\text{dry tissue weight (g)}}{\text{shell length (cm) x shell width (cm) x shell height (cm)}} \text{x1000}$$

Data Analysis

The concentration factor (CF) was calculated according to Yap *et al*. (2003a).

$$CF = \frac{\text{Metal level}_{\text{end of metal accumulation}}}{\text{Metal level}_{\text{initial}}}$$

The elimination factor (EF) was also calculated according to Yap *et al*. (2003a).

$$EF = \frac{\text{Metal level}_{\text{end of metal elimination}}}{\text{Metal level}_{\text{initial}}}$$

The rate of metal accumulation was calculated according to a formula proposed by Yap *et al*. (2003a), as follows:

$$\text{Rate of metals accumulation} = \frac{\text{Metal level}_{\text{exposed}} - \text{Metal level}_{\text{initial}}}{\text{Day(s) of metal exposure}}$$

Meanwhile, the rate of metal elimination was calculated according to the following formula (Yap *et al*., 2003a):

$$\text{Rate of metals elimination} = \frac{\text{Metal level}_{\text{exposed}} - \text{Metal level}_{\text{initial}}}{\text{Day(s) of metal elimination}}$$

Note: $\text{Metal level}_{\text{end of metal accumulation}}$ = heavy metals value at week 6 or week 10.

$\text{Metal level}_{\text{end of metal elimination}}$ = heavy metals value at week 6 or week 10.

$\text{Metal level}_{\text{initial}}$ = heavy metals value at week 0.

$\text{Metal level}_{\text{exposed}}$ = heavy metals value at weeks 2, 6 or 10.

Statistical Analysis

The statistical analyses were done by using STATISTICA version 8.0 for Windows. In addition, analysis of variance (ANOVA) was applied to find the differences between the means of heavy metal concentrations in the different parts of the mussels during the transplantation. Students-Newman-Kuel was applied to compare the mean values of heavy metal concentrations between the different parts of the mussels. T-test was carried out to test between the means of the end of the metal exposures and the initial metal exposures. The mean differences between Kg. Pasir Puteh and Sg. Melayu were tested using the Mann-Whitney test (Zar, 1996).

RESULTS AND DISCUSSION

Physico-chemical Parameters and Sediment Data

The physico-chemical parameters from Kg. Pasir Puteh and Sg. Melayu were found to be similar during the 10-week transplantation (see Tables 1 and 2), with ranges of 29.06-30.61°C for temperature, 38.61-46.78 ms/cm for specific conductivity, 24.42-30.24 ppt for salinity, 3.14-13.82 mg/L for dissolved oxygen and 7.03-7.68 for pH. As for sediment, heavy metal concentrations in both the studies sites are presented in Table 5. For Kg Pasir Puteh, the concentrations (µg/g dry weight) for the sediment data ranged from Cd (2.73-3.24), Cu (105.71-112.71), Fe (1.83-2.00%), Ni (45.20-52.46), Pb (61.90-73.47) and Zn (225.83-289.61). On the other hand, the concentration ranges obtained from Sg. Melayu, (µg/g) for the sediment data were Cd (1.42-1.80), Cu (31.39-60.20), Fe (1.74-1.80%), Ni (26.27-37.19), Pb (31.97-42.21) and Zn (83.21-95.18).

The sediment data obtained from Kg. Pasir Puteh in this study were generally higher, although not significantly, as compared to the sediment data reported by Yap *et al*. (2002) for Cd (1.45 µg/g), Cu (104 µg/g), Pb (70 µg/g) and Zn (170 µg/g) from the same sampling site of the sediments collected in 2002. All the metal concentrations (except for Fe) in Kg Pasir Puteh were significantly (Mann-Whitney Test, $p < 0.05$) higher than those of Sg. Melayu. This indicated that Kg. Pasir Puteh was more contaminated by metals than Sg. Melayu. The cause of the high availability of metals, especially Cu, Pb, Zn at Kg. Pasir Puteh, was probably due to the presence of shipyards which used biofouling paints (Bayen *et al*., 2003).

TABLE 5: Heavy metal concentrations (μg/g dry weight) in the surface sediments collected from Sg. Melayu and Kg. Pasir Puteh

		Cd			Cu			Fe			Ni			Pb			Zn		
Weeks		P.Puteh	Sg Melayu	M-W Test	P.Puteh	Sg Melayu	M-W Test	P.Puteh	Sg Melayu	M-W Test	P.Puteh	Sg Melayu	M-W Test	P.Puteh	Sg Melayu	M-W Test	P.Puteh	Sg Melayu	M-W Test
0	Aqua-regia	2.90	1.62	$p>0.05$	105.71	60.20	$p<0.05$	1829.57	1775.22	$p>0.05$	46.62	27.57	$p<0.05$	61.90	31.97	$p<0.05$	225.83	83.21	$p< 0.05$
	F1	0.68	0.23	$p>0.05$	1.07	0.42	$p>0.05$	1.49	2.43	$p>0.05$	1.42	1.18	$p>0.05$	1.76	1.97	$p>0.05$	20.56	2.26	$p< 0.05$
	F2	0.72	0.57	$p>0.05$	0.18	0.33	$p>0.05$	0.08	0.13	$p>0.05$	1.36	2.02	$p>0.05$	2.33	2.98	$p>0.05$	78.90	2.12	$p< 0.05$
	F3	0.84	0.50	$p>0.05$	71.20	9.67	$p<0.05$	601.50	669.41	$p>0.05$	27.27	13.87	$p<0.05$	31.17	15.13	$p<0.05$	109.07	58.78	$p< 0.05$
	F4	0.16	0.13	$p>0.05$	15.49	6.62	$p<0.05$	494.81	657.76	$p<0.05$	4.63	3.62	$p>0.05$	15.44	10.02	$p>0.05$	35.32	15.73	$p< 0.05$
4	Aqua-regia	NC	1.42		NC	31.39		NC	1735.29		NC	37.19		NC	42.21		NC	95.18	
	F1	NC	0.25		NC	0.97		NC	13.88		NC	2.30		NC	2.64		NC	2.80	
	F2	NC	0.64		NC	0.52		NC	10.49		NC	4.25		NC	2.49		NC	2.35	
	F3	NC	0.57		NC	15.29		NC	561.66		NC	16.58		NC	16.54		NC	62.18	
	F4	NC	0.07		NC	9.68		NC	524.25		NC	6.15		NC	11.43		NC	17.61	
6	Aqua-regia	3.24	1.80	$p<0.05$	112.71	36.83	$p<0.05$	1944.11	1795.78	$p>0.05$	52.46	26.27	$p<0.05$	73.47	39.61	$p<0.05$	253.37	94.80	$p< 0.05$
	F1	0.73	0.17	$p<0.05$	2.20	0.99	$p>0.05$	18.29	2.50	$p<0.05$	4.09	1.43	$p<0.05$	3.64	3.07	$p>0.05$	23.08	2.66	$p< 0.05$
	F2	0.63	0.50	$p>0.05$	0.40	0.47	$p>0.05$	0.88	0.42	$p>0.05$	2.89	2.66	$p>0.05$	3.58	4.14	$p>0.05$	84.63	2.18	$p< 0.05$
	F3	0.99	0.47	$p>0.05$	91.87	20.24	$p<0.05$	884.20	727.54	$p>0.05$	34.11	21.16	$p<0.05$	43.91	20.54	$p<0.05$	116.00	55.15	$p< 0.05$
	F4	0.28	0.33	$p>0.05$	19.79	12.19	$p<0.05$	699.10	744.04	$p>0.05$	6.87	6.63	$p>0.05$	23.19	13.00	$p<0.05$	51.73	15.38	$p< 0.05$
10	Aqua-regia	2.73	NC		109.85	NC		2008.96	NC		45.20	NC		63.27	NC		289.61	NC	
	F1	0.70	NC		1.53	NC		3.15	NC		1.82	NC		3.06	NC		22.29	NC	
	F2	0.82	NC		0.18	NC		1.46	NC		1.63	NC		3.98	NC		84.79	NC	
	F3	0.93	NC		94.47	NC		868.70	NC		38.93	NC		44.09	NC		130.00	NC	
	F4	0.18	NC		18.09	NC		729.17	NC		5.57	NC		23.18	NC		38.37	NC	

Note: F1: easily, freely, leacheable or exchangeable; F2: Acid-redicible; F3: Oxidisable-organic; F4: Resistant; NC: sample were not collected; M-W Test; Mann-Whitney test.

Metal Accumulation in the Mussels

During the 10-week duration of transplantation from Sg. Melayu to the sampling site at Kg. Pasir Puteh, all the metal concentrations were generally found to have increased from 1.49 to 6.93 µg/g for Cd, 7.31 to 25.63 µg/g for Cu, 29.27 to 3150.06 µg/g for Fe, 17.13 to 33.98 µg/g for Ni, 6.13 to 43.59 µg/g for Pb and 8.19 to 184.73 µg/g for Zn (see Fig.2 to Fig.7). In specific, the heavy metal concentrations for all the metals in Kg. Pasir Puteh were significantly higher than those in Sg. Melayu (independent t-test, $p< 0.05$). Meanwhile, Fe accumulated the highest in the byssus and the total soft tissue while Pb accumulated the highest in the shells of the mussels transplanted from Sg. Melayu to Kg. Pasir Puteh.

As for Cd, significant differences (one-way ANOVA, SNK, $p< 0.05$) were registered between the tissues for the mussels transplanted from Sg. Melayu to Kg. Pasir Puteh for T_0 and T_2. However, starting from T_6, the total soft tissue and byssus were significantly different from the shell. For Cu, the shell and byssus were significantly different from the total soft tissues during the transplant period, i.e. from T_0 to T_{10}. Meanwhile, significant differences were found between byssus, shell and total soft tissues for Fe concentrations. The Ni concentrations did not register any significant difference between TST, byssus and shell. For both sites, significant differences (one-way ANOVA, SNK, $p< 0.05$) were registered between the shell and byssus from the total soft tissues for Pb concentrations from T_0 to T_{10}. On the other hand, the Zn levels of byssus and total soft tissue were significantly different (one-way ANOVA, SNK, $p< 0.05$) from the shell in both the transplanted mussels.

Table 6 shows the rate of accumulation for all the metals in the different parts of the mussels transplanted from Sg. Melayu to Kg. Pasir Puteh according to weeks. The rates of the metal accumulation were fastest in all the mussel parts in week 2 (T=2) but these became slower in the following weeks and up to week 10 (T=10). During the first 6 weeks of transplantation, the total soft tissues showed the highest concentration factors (CF) in Cd (2.06), Cu (1.81) and Fe (2.04) but the lowest CF in Ni (1.11). Meanwhile, byssus showed the highest CF in Pb (2.28) and Zn (2.28), and the shell showed the highest CF in Ni (1.80). For the period of 10-week transplantation, the total soft tissues showed the highest concentration factorss (CF) in Cd (2.06), Cu (1.81) and Fe (2.22). Byssus showed the highest CF in Pb (3.17) and Zn (3.30), while the shell showed the highest CF in Ni (1.98). These indicated that TST accumulated the highest Cd and Cu concentrations, while byssus accumulated the highest Pb and Zn concentrations and the shell accumulated the highest Ni concentration.

The concentrations of Cd in the shell and Ni in TST in the transplanted *P. viridis* at week 10 reached the values similar to those measured in the initial *P. viridis* (T_0). Similar findings had previously been reported for Cu and Zn in the soft tissues of the mussel *Mytilus edulis* transplanted to a temperate polluted bay (Roesijadi *et al*., 1984) and Cr and Cu in *Isognomon isognomon* and Co, Ni and Zn in *Gafrarium tumidum* transplanted from a polluted site to a clean site in a New Caledonia lagoon (Hedouin *et al*., 2011). As for Ni in byssus, Fe in TST, Pb in byssus and shell and Zn in TST from the transplanted mussels (T_{10}), the levels significantly increased during the transplantation period but did not reach the values measured in the initial *P. viridis* (T_0). This could be due to the transplantation period being not long enough for the transplanted mussels to accumulate the metals completely. Comparable results had been

TABLE 6: Concentration factor (CF), rates of accumulation (µg/g per day) of Cd, Cu, Fe, Ni, Pb and Zn in byssus, total soft tissue and shell of transplanted *P. viridis* from Sg. Melayu to Kg. Pasir Puteh

		Week				
		CF		Rate of accumulation		
	Parts	6	10	2	6	10
Cd	Byssus	1.114	1.134	0.010	0.009	0.006
	TST	1.815	2.060	0.033	0.029	0.023
	Shell	1.061	1.098	0.011	0.009	0.009
Cu	Byssus	1.443	1.498	0.161	0.090	0.061
	TST	1.666	1.807	0.316	0.225	0.164
	Shell	1.490	1.720	0.145	0.085	0.075
Fe	Byssus	1.742	1.898	48.662	29.330	21.286
	TST	2.041	2.218	17.309	13.826	9.706
	Shell	1.295	1.535	0.379	0.205	0.224
Ni	Byssus	1.322	1.460	0.378	0.157	0.134
	TST	1.081	1.109	0.149	0.059	0.048
	Shell	1.802	1.984	0.774	0.327	0.241
Pb	Byssus	2.279	3.172	0.231	0.419	0.426
	TST	1.736	1.862	0.232	0.108	0.076
	Shell	1.187	1.345	0.196	0.120	0.133
Zn	Byssus	2.756	3.299	2.642	2.342	1.839
	TST	1.918	2.270	2.653	1.388	1.153
	Shell	1.518	1.867	0.134	0.101	0.102

previously reported for the oyster *Crassostrea rhizophorae* (Wallner-Kersanach *et al*., 2000), as well as oyster *Isognomon isognomon* and clam *Gafrarium tumidum* from the New Caledonia lagoon (Hedouin *et al*., 2011). However, Cd in byssus did not show any significant increase during the transplantation from Sg. Melayu to Kg. Pasir Puteh. This corresponded with similar observations for the Cd and Zn concentrations in *Crenomytilus grayanus* after two months of transplantation (Shulkin *et al*., 2003). The lack of Cd accumulation in the transplanted *P. viridis*, as observed in the current study, suggested that this particular element was rather poorly bioavailable for them or that *P. viridis* had efficient regulation mechanisms preventing these metals from being accumulated (Hedouin *et al*., 2011).

For the mussels transplanted from Sg. Melayu to Kg. Pasir Puteh, the metal levels in all

the parts had decreased. The high CF values in the metals (Table 6) showed that *P. viridis* was capable of accumulating these metals. In particular, TST was highly capable of accumulating Cd and Cu while the byssus was capable of accumulating Pb and Zn and the shell accumulated the highest Ni concentration. The total soft tissues of *P. viridis* showed the highest CF values for most of the metals, and this indicated that it is useful for monitoring metal contamination in coastal waters. The results obtained in the present study are also comparable to those of Yap *et al*. (2003a, 2004) which showed that *P. viridis* is a good accumulator for Cd, Pb and Zn. This test revealed the ability of *P. viridis* to accumulate and eliminate metals in short periods of time. Among the CF values for week 6 and week 10, Zn was the one which was accumulated the fastest while Cd was the slowest.

Metal Elimination in Mussels

Fig.2 to 7 show that all the metal concentrations in the mussels transplanted from Kg. Pasir Puteh to Sg. Melayu had decreased starting from T_0 to $T_{10.}$ The Cd level decreased from 6.55 to 2.3 µg/g, Cu from 37.81 to 2.84 µg/g, Fe from 2909.69 to 14.98 µg/g, Ni from 55.06 to 13.64, Pb from 46.43 to 16.01 µg/g and Zn from 176.24 to 7.05 µg/g. Similar findings were also reported by Gabr and Gab-Alla (2008) for clams (*Ruditapes decussatus* and *Venerupis pullastra*) transplanted from a polluted site to a clean site.

As for the mussels transplanted from Kg. Pasir Puteh to Sg. Melayu, there was no significant difference (one-way ANOVA, SNK, $p< 0.05$) observed for all the tissues in the Cd concentrations for T_0, starting from T_2, however, the shell was found to be significantly different from the total soft tissue and byssus. As for Cu, the total soft tissue and byssus were significantly different from the shell from T_0 to T_{10}. On the other hand, the total soft tissue and byssus were significantly different from the shell for the Fe concentration from T_0 to T_{10}.

The rate of elimination (Table 7) for all the metals in the different parts of the transplanted mussels from Kg. Pasir Puteh to Sg. Melayu was the fastest in all the mussel parts in week 2 (T=2) and this became slower in the subsequent weeks until week 10 (T=10). For byssus, the rate of elimination was 0.23(T=2), 0.084 (T=6) and 0.033 (T=10) in Cd. During the first 6 weeks of transplantation, the elimination factor (EF) in byssus was the fastest for Cd (0.42) and Ni (0.49). Meanwhile, the EF in shell was the fastest in Cu (0.22) and Pb (0.35) and slowest in Cd (0.80). The EF in TST was the fastest for Cu (0.69), Fe (0.65), Pb (0.72) and Zn (0.74). During the 10-week transplantation, the elimination factor (EF) in byssus was the fastest for Cd (0.38), Ni (0.25) and Zn (0.37). Meanwhile, the EF in shell was fastest for Cu (0.19), Fe (0.42) and Pb (0.34) and the slowest for Cd (0.80). These results indicated that byssus eliminated Cd, Ni concentrations the fastest while shell eliminated Cu and Pb the fastest.

At week 6, the concentrations of Cd in TST, Cu in byssus and TST, Ni in byssus and shell, Fe in byssus and TST, Pb in byssus and TST and Zn in byssus and TST were far from reaching the concentrations measured in the initial population (T_0). At week 10, only Cu, Fe, Pb and Zn in byssus and Ni in shell were far from reaching the concentrations measured in the initial population (T_0). Such findings had also been reported by several authors when organisms from polluted areas were transplanted to clean areas such as Zn in the mussel *M. edulis* (Roseijadi *et al*., 1984; Simpson, 1979), Cd and Cu in the oyster *Crassostrea gigas* (Geffard *et al*., 2002), Cr,

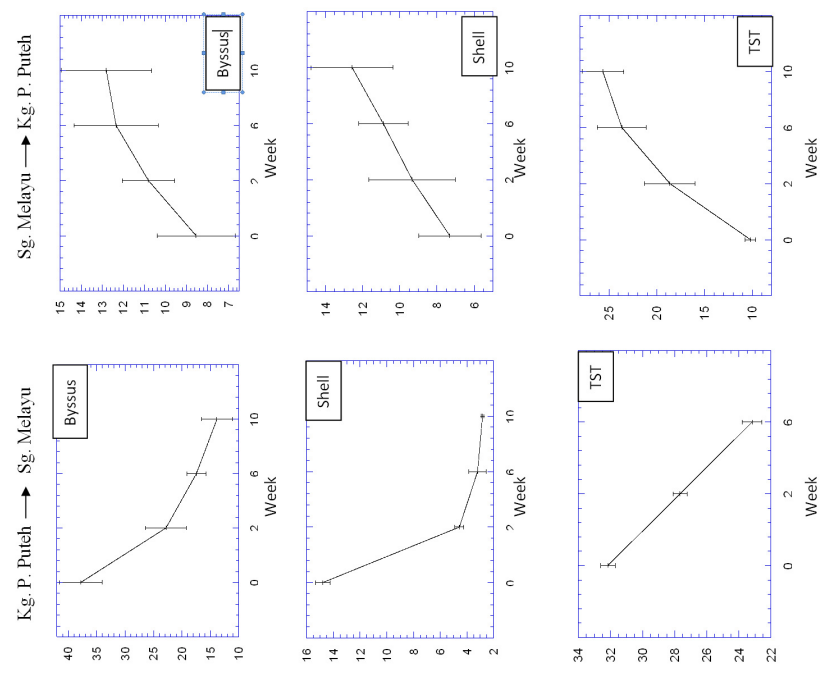

Fig.2: Comparison of Cd concentrations (mean± SE, µg/g dw; N=3) for *Perna viridis* transplanted from Kg. Pasir Puteh to Sg. Melayu and from Sg. Melayu to Kg. Pasir Puteh

*0= Initial, 2=2 weeks, 6= 6 weeks, 10= 10 weeks.
Note: TST= Total soft tissue

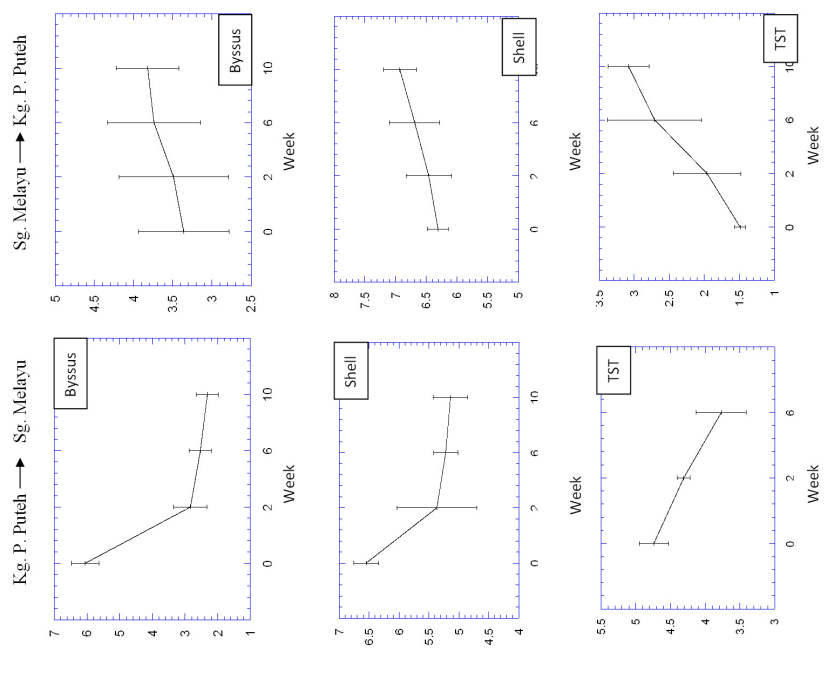

Fig.3: Comparison of Cu concentrations (mean± SE, µg/g dw; N=3) for *Perna viridis* transplanted from Kg. Pasir Puteh to Sg. Melayu and from Sg. Melayu to Kg. Pasir Puteh

*0= Initial, 2=2 weeks, 6= 6 weeks, 10= 10 weeks.
Note: TST= Total soft tissue

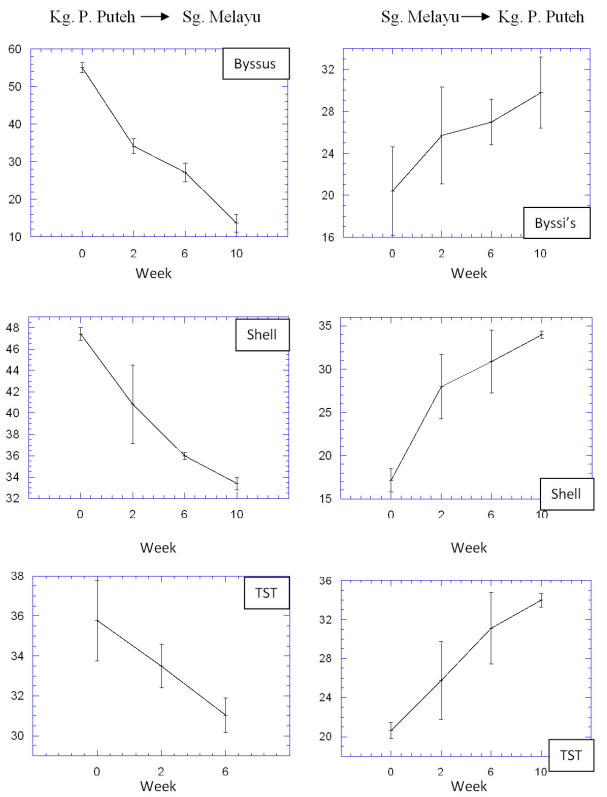

Fig.4: Comparison of Ni concentrations (mean± SE, µg/g dw; N=3) for *Perna viridis* transplanted from Kg. Pasir Puteh to Sg. Melayu and from Sg. Melayu to Kg. Pasir Puteh

*0= Initial, 2=2 weeks, 6= 6 weeks, 10= 10 weeks.
Note: TST= Total soft tissue

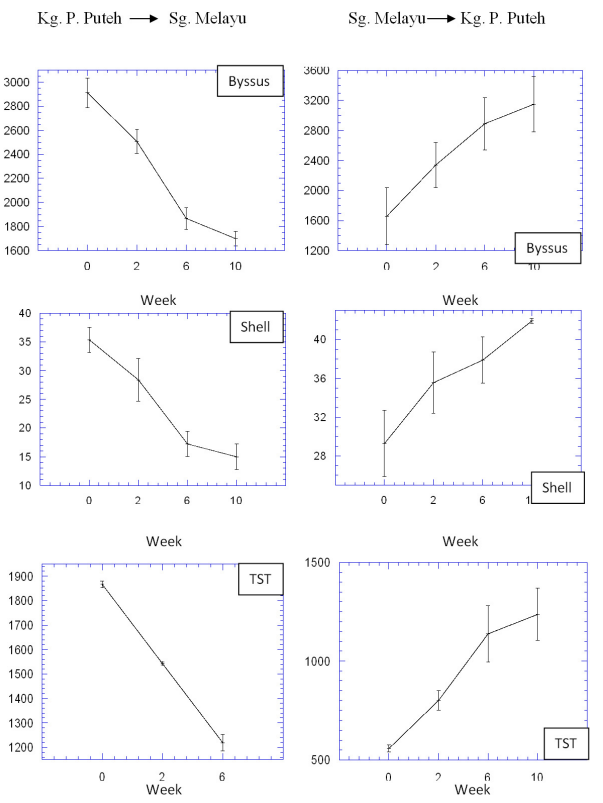

Fig.5: Comparison of Fe concentrations (mean± SE, µg/g dw; N=3) for *Perna viridis* transplanted from Kg. Pasir Puteh to Sg. Melayu and from Sg. Melayu to Kg. Pasir Puteh

*0= Initial, 2=2 weeks, 6= 6 weeks, 10= 10 weeks.
Note: TST= Total soft tissue

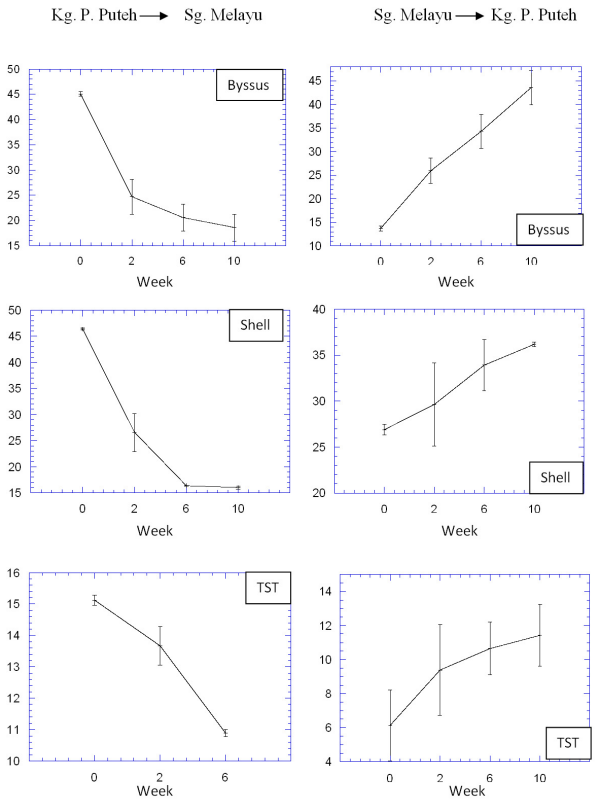

Fig. 6: Comparison of Pb concentrations (mean± SE, µg/g dw; N=3) for *Perna viridis* transplanted from Kg. Pasir Puteh to Sg. Melayu and from Sg. Melayu to Kg. Pasir Puteh

*0= Initial, 2=2 weeks, 6= 6 weeks, 10= 10 weeks.
Note: TST= Total soft tissue

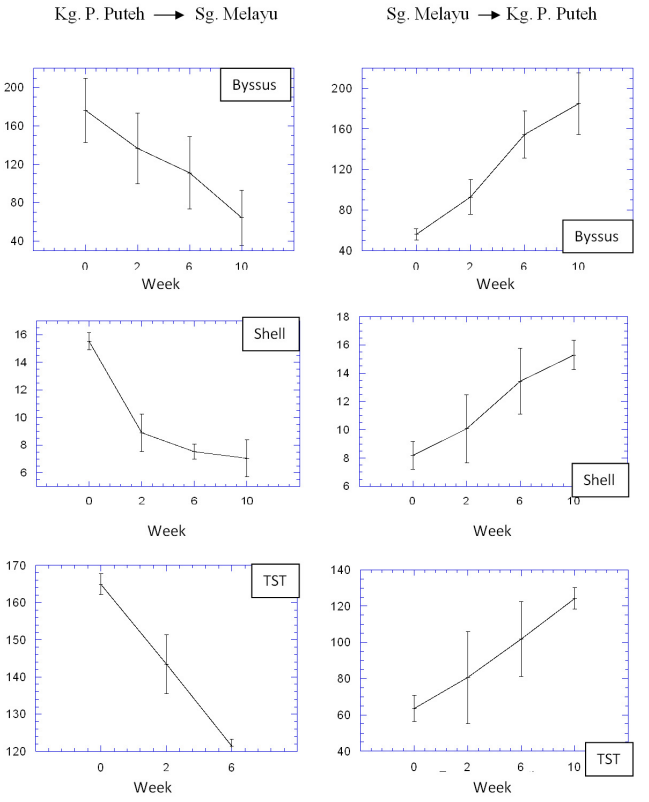

Fig.7: Comparison of Zn concentrations (mean± SE, µg/g dw; N=3) for Perna viridis transplanted from Kg. Pasir Puteh to Sg. Melayu and from Sg. Melayu to Kg. Pasir Puteh

*0= Initial, 2=2 weeks, 6= 6 weeks, 10= 10 weeks.
Note: TST= Total soft tissue

TABLE 7: Elimination factor (EF), rates of elimination (µg/g per day) of Cd, Cu, Fe, Ni, Pb and Zn in byssus, total soft tissue and shell of transplanted *P. viridis* from Kg. Pasir Puteh to Sg. Melayu

		Week				
		EF		Rate of elimination		
	Parts	6	10	2	6	10
Cd	Byssus	0.4177	0.383	0.2298	0.084	0.0331
	TST	0.7954	NC	0.0307	0.0231	NC
	Shell	0.7969	0.8	0.0843	0.0317	0.0749
Cu	Byssus	0.4612	0.3663	1.0724	0.4851	0.1979
	TST	0.69	NC	0.1779	0.2374	NC
	Shell	0.217	0.192	0.7303	0.2758	0.0406
Fe	Byssus	0.6417	0.5844	28.6902	24.8251	24.2906
	TST	0.6531	NC	23.1779	15.4255	NC
	Shell	0.4868	0.4235	0.4982	0.4323	0.214
Ni	Byssus	0.4931	0.2477	1.4939	0.6646	0.1949
	TST	0.868	NC	0.1629	0.1124	NC
	Shell	0.9275	0.7044	0.1141	0.0818	0.4771
Pb	Byssus	0.4558	0.4118	1.4579	0.5843	0.2653
	TST	0.7202	NC	0.1036	0.1007	NC
	Shell	0.3519	0.3448	1.4182	0.7165	0.2287
Zn	Byssus	0.6309	0.3653	2.8325	1.5489	0.9196
	TST	0.736	NC	1.5321	1.0367	NC
	Shell	0.4846	0.4543	0.4734	0.1904	0.1007

Note: TST = total soft tissue, NA = reading is not available because mussels samples had died.

Cu and Zn in the clam *Mercenaria mercenaria* (Behrens & Duedall, 1981), Ag, Co and Ni in the oyster *Isognomon isognomon* (Hedouin *et al*., 2011). When a comparison was made between weeks 6 and 10, more metals in week 6 were far from reaching the concentrations measured in the initial population (T_0) due to the accumulation being dependent on the transplantation period (Hedouin *et al*., 2011). This indicated that the eliminations of the metals were not complete throughout the 10-week period of transplantation for *P. viridis*. Other studies (e.g., Andres *et al*., 1999; Hickey *et al*., 1995; Martincic *et al*., 1992; Wallner-Kersanach *et al*., 2000) found that the equilibration of the trace metals in bivalves with their environment could range between 30 days to 77 days and even longer for some other species. Such a wide range in the equilibration times among the species could be due to previous exposure histories, different

life stages of bivalve, associated metabolic activities with adjustments to a new environment, temperature changes, and food availability (Burt *et al*., 2007).

On the other hand, for the mussels transplanted from Kg. Pasir Puteh to Sg. Melayu, the metal levels in all the parts showed decreases in heavy metal levels. During the transplantation, the accumulation rate and the elimination rate were the highest at T_2, which later decreased from T_2 to T_{10}. According to Yap *et al*. (2003a), the rates of accumulation and elimination were higher during the initial period due to detoxification process. After that, the mussels had slower rates of accumulation and elimination after 2 weeks, which could be caused by some tightly bound compartments, such as metallothionein and lysosomes for Pb. According to Amiard *et al*. (2006), Marigómez *et al*. (2002) and Viarengo *et al*. (2003), metallothionein plays an important role in the elimination of metals in mussels. The high rates of accumulation and elimination were also found in byssus at both sites, indicating that this organ could act as an excretion route for Pb, as reported by Yap *et al*. (2003b,c). The low EF value in the metals (Table 7) showed that *P. viridis* was capable of eliminating these metals. The EF for 6 weeks and 10 weeks showed that byssus was good at eliminating Cd and Ni, while shell was capable of eliminating Cu and Pb in the shortest time. The EF value indicated that Ni was the metal which was eliminated the fastest at week 6, while Cd was eliminated the fastest in week 10. However, Cu was eliminated the slowest in both week 6 and week 10.

Levels of Metals in the Different Parts of P. viridis *after the Transplantation*

Similar patterns of accumulation and elimination of metals found in both total soft tissue and byssus suggested that the metal levels in these parts of *P. viridis* were mainly due to metabolic pathways rather than the direct contact with the surrounding seawater. This finding is on par with the results reported by Ikuta (1986a), Szefer (1999) and Yap *et al*. (2003b) for the byssus of *M. edulis* and *P. viridis,* especially the high EF values in Fe and Zn for byssus. When the heavy metal levels in the soft tissue were high, these metals would be transferred metabolically to the byssus (Ikuta, 1986b; Yap *et al*., 2003b) due to the metal level regulation in the soft tissue. Regulation and sequestration are important mechanisms (Phillips & Rainbow, 1989; Rainbow, 1997; Phillips, 1995) to minimize the harmful effects of high levels of these metals. The high metal accumulation found in the byssus could also be due to the material for byssus formation. The byssus was secreted from a byssal gland in the foot and is composed of a protein component, collagen. These protein components contain some potential metal binding sites, largely composed of glycine and proline amino acid residues (Szefer *et al*., 1999; Yap *et al*., 2003b).

The highest level of Pb was accumulated in the transplanted mussel shell. This result is comparable with those of Yap *et al*. (2003a) and it could be due to the chemical composition of the shells. The present study revealed that the shells of bivalves were accumulative of non-essential metals such as Cd, Ni and Pb. The results obtained by Yap *et al*. (2004) showed that the metals found in the shells of gastropod could be due to the substitution of the calcium ions in the crystalline phase of the shell or were associated with the organic matrix of the shell. In particular, shells accumulated higher concentrations of metals initially due to surface adsorption. According to Wang (2010), uptake of perfluorinated compounds by shell starts with adsorption

or passive deposition of the target chemicals to the shell organic matrix, and this is followed by a biomineralisation process. Therefore, the contaminants bound to the organic matrix in the shell microstructure were sequestrated and hard to release. Meanwhile, the high levels of metals accumulated in the total soft tissue could also be due to the synthesis of metallothionein (Yap *et al*., 2004). This is the reason why the mussels eaten could be a source of metals and why mussels can survive and accumulate high level of metals in their soft tissues in highly contaminate sites.

High levels of Cu and Zn accumulations were found in the TST of the transplanted mussels. These results are similar with those of Yap *et al*. (2011) for *Anadara granosa*. The soft tissues of bivalves were found to be able to induce metallothionein-like protein production at high metal concentrations (Chan *et al*., 2002). The secretion of metallothionein was to counteract metal toxicity at high metal concentrations (Phillips & Rainbow, 1993). MT is generally accepted to be involved in the regulation of essential metals such as Cu and Zn for cell growth and development, although their functions are still not fully understood (Mackay *et al*., 1993). On the other hand, Cu and Zn are also known as essential metals for metabolic functions (Mackay *et al*., 1993) and they can be regulated in bivalves (Yap *et al*., 2003a). This could explain why the concentrations of Cu and Zn were high in the TST.

CONCLUSION

The data reported in this paper clearly demonstrated that Kg. Pasir Puteh was a more polluted site than Sg. Melayu based on the sediment and *P. viridi*s samples for all the six metals. Among the six metals, Zn was the one which was accumulated at the fastest rate, while Cd was the slowest. As for elimination, Ni was the fastest at week 6, while Cd was the fastest at week 10 and Cu was the one with the slowest elimination rate at both weeks 6 and 10. The byssus of *P. viridi*s could be used as a good monitor for Cd, Ni, Pb and Zn, while shell could be used to monitor Cu, Ni and Pb. However, to get more accurate levels of heavy metal pollutions in coastal waters, studies with longer transplantation periods should be carried out since some of the metals needed longer time periods for elimination and to reach equilibrium levels.

ACKNOWLEDGEMENTS

The authors wish to acknowledge the financial support provided through a Research University Grant Scheme (RUGS), [Vot no: 91986], by Universiti Putra Malaysia.

REFERENCES

Abdullah, A. R., Woon, W. C., & Bakar, R. A. (1996). Distribution of Oil and Grease and Petroleum Hydrocarbons in the Straits of Johor, Peninsular Malaysia. *Bulletin of Environmental Contamination and Toxicology*, *57*, 155-162.

Alfonso, S., Giulia, R., Francois, G., Bruno, A., Marina, A., Pierpaolo, G., Josep, C., Monica, C., Juan, A.C., Jose, B.A., Alessandro, C., Samir, B., Cherif, S., Salud, D., Mostefa, B., & Franco, G. (2010). Western Mediterranean coastal waters—Monitoring PCBs and pesticides accumulation in *Mytilus galloprovincialis* by active mussel watching: the Mytilus project. *Journal of Environmental Monitoring*, *12*, 924-935.

Amiard, J. C., Amiard-Triquet, C., Barka, S., Pellerin, J., & Rainbow, P. S. (2006). Metallothioneins in aquatic invertebrates: their role in metal detoxification and their use as biomarkers. *Aquatic Toxicology, 76*, 160–202.

Andres, S., Baudrimont, M., Lapaquellerie, Y., Ribeyre, F., Maillet, N., Latouche, C., & Boudou, A. (1999). Field transplantation of the freshwater bivalve *Corbicula fluminea* along a polymetallic contamination gradient (River Lot, France): I. Geochemical characteristics of the sampling sites and cadmium and zinc bioaccumulation kinetics. *Environmental Toxicology and Chemistry*, *18*, 2462-2471.

Bayen, S., Thomas, G. O., Lee, H. K., & Jeffrey, P. O. (2003). Organochlorine, pesticides and heavy metals in green-lipped mussel, *Perna viridis* in Singapore. *Water, Air, and Soil Pollution*, *155*, 103-116.

Behrens, W. J. & Duedall, I. W. (1981). The behaviour of heavy metals in transplanted hard clams, *Mercenaria mercenaria*. *Journal du Conseil International pour l'Exploitation de la Mer*, *39*, 223-230.

Burt, A., Maher, W., Roach, A., Krikowa, F., Honkoop, P., & Bayne, B. (2007). The accumulation of Zn, Se, Cd, and Pb and physiological condition of *Anadara trapezia* transplanted to a contamination gradient in Lake Macquarie, New South Wales, Australia. *Marine Environmental Research, 64*, 54–78.

Chan, M. K., Othman, R., Zubir, D., & Salmijah, S. (2002). Induction of a putative metallothionein gene in the blood cockle, *Anadara granosa*, exposed to cadmium. *Comparative Biochemistry and Physiology Part C*, *131*, 123-132.

Department of Environment (1994). *Environmental quality report, 1994*. Ministry of Science, Technology and the Environment, Malaysia.

Department of Environment (2007). *Annual Report 2006*. Ministry of Science, Technology and the Environment, Malaysia.

Faverney, C. R., Guibbolini-Sabatier, M. E., & Francour, P. (2010). An ecotoxicological approach with transplanted mussels (*Mytilus galloprovincialis*) for assessing the impact of tyre reefs immersed along the NW Mediterranean Sea. *Marine Environmental Research*, *70*, 87-94.

Francesco, R., & Enzo, O. (1994). Acumulation and subcellular distribution of metals (Cu, Fe, Mn, Pb and Zn) in the Mediterranean mussel *Mytilus galloprovincialis* during a field transplant experiment. *Marine Pollution Bulletin*, *28*(10), 592-600.

Gabr, H. R., & Gab-Alla, A. A-F. A (2008). Effect of transplantation on heavy metal concentrations in commercial clams of Lake Timsah, Suez Canal, Egypt. *Oceanologia, 50*(1), 83-93.

Giarratano, E., Duarte, C. A., & Amin, O. A. (2010). Biomarkers and heavy metal bioaccumulation in mussels transplanted to coastal waters of the Beagle Channel. *Ecotoxicology and Environmental Safety*, *73*, 270-279.

Goh, B. P. L., & Chou, L. M. (1997). Heavy metal levels in marine sediments of Singapore. *Environmental Monitoring and Assessment, 44*, 67–80.

Gorbi, S., Lamberti, C. V., Notti, A., Benedetti, M., Fattorini, D., Moltedo, G., & Regoli, F. (2007). An ecotoxicological protocol with caged mussels, *Mytilus galloprovincialis*, for monitoring the impact of an offshore platform in the Adriatic Sea. *Marine Environmental Research 65,* 34–49.

Hedouin, L., Pringault, L., Bustamante, P., Fichez, R., & Warnau, M. (2011). Validation of two tropical marine bivalves as bioindicators of mining contamination in the New Caledonia lagoon: Field transplantation experiments. *Water Research*, *45*, 483-496.

Hickey, C. W., Roper, D. S., & Buckland, S. J. (1995). Metal concentrations of resident and transplanted freshwater mussels *Hyridella menziesi* (Unionacea: Hyriidae) and sediments in the Waikato River, New Zealand. *Science of the Total Environment, 175*, 163–177.

Hunt, C. D., & Slone, E. (2010). Long-term monitoring using resident and caged mussels in Boston Harbor yield similar spatial and temporal trends in chemical contamination. *Marine Environmental Research*, *70*, 343-357.

Ikuta, K. (1986a). Metal concentrations in byssuses and soft bodies of bivalves. *Bulletin Faculty Agriculture Miyazaki University, 33*, 255–264.

Ikuta, K. (1986b). Correlations between ratios of metal concentrations in byssuses to those in soft bodies and metal concentrations in soft bodies of bivalves. *Bulletin Faculty Agriculture Miyazaki University, 33*, 265– 273.

Lares, M. L., & Orians, K. J. (1997). Natural Cd and Pb variations in *Mytilus californianus* during the upwelling season. *Science of The Total Environment*, *197*, 177-195.

Mackay, E. A., Overnell, J., & Dunbar, B. (1993). Complete amino acid sequences of five dimeric and four monomeric forms of metallothionein from the edible mussel, *Mytilus edulis*. *European Journal of Biochemistry*, *218*, 183-194.

Marigómez, I., Soto, M., Cajaraville, P. M., Angulo, E., & Giamberini, L. (2002). Cellular and subcellular distribution of metals in molluscs. *Microscopy Research and Technique*, *56*, 358–392.

Martincic, D., Kwokal, Z., Peharec, Z., Margus, D., & Branica, M. (1992). Distribution of Zn, Pb, Cd and Cu between seawater and transplanted mussels (*Mytilus galloprovicialis*). *The Science of the Total Environment*, *119,* 211–230.

Moradi, M. A. (2001). *The kinetics of uptake and release of polycyclic aromatic hydrocarbons in the green-lipped mussel (Perna viridis) for biomonitoring of marine pollution* (Ph. D Thesis dissertation). Universiti Putra Malaysia, Serdang, Selangor, Malaysia.

Nasci, C., Nesto, N., Monteduro, R. A., & Da Ros, L. (2002). Field application of biochemical markers and a physiological index in the mussel, Mytilus galloprovincialis: transplantation and biomonitoring in the Lagoon of Venice (NE Italy). *Marine Environmental Research, 54*, 811–816.

Nigro, M., Falleni, A., Barga, I. D., Scancelli, V., Lucchesi, P., Regoli, F., & Frenzilli, G. (2006). Cellular biomarkers for monitoring estuarine environments: transplanted versus native mussels. *Aquatic Toxicology, 77*, 339–347.

Phillips, D. J. H. (1995). The chemistries and environmental fates of trace metals and organchlorines in aquatic ecosystems. *Marine Pollution Bulletin*, *31*, 193– 200.

Phillips, D. J. H., & Rainbow, P. S. (1989). Strategies of trace metals sequestration in aquatic organisms. *Marine Environmental Research*, *28*, 207–10.

Phillips, D. J. H., & Rainbow, P. S. (1993). *Biomonitoring of Trace Aquatic Contaminants*. London: Elsevier Science Publishers.

Phillips, D. J. H., & Segar, D. A. (1986). Use of bioindicators in monitoring conservative contaminants: programme design imperatives. *Marine Pollution Bulletin*, *17*, 10-17.

Rainbow, P. S. (1997). Trace metal accumulation in marine invertebrates: marine biology or marine chemistry. *Journal of the Marine Biological Association of the United Kingdom*, *77*, 195– 210.

Regoli, F. (1992). Lysosomal responses as a sensitive stress index in biomonitoring heavy metal pollution. *Marine Ecology Progress Series*, *84*, 63-69.

Regoli, F., Frenzilli, G., Bocchetti, R., Annarumma, F., Scancelli, V., Fattorini, D., & Nigro, M. (2004). Time-course variations of oxyradical metabolism, DNA integrity and lysosomal stability in mussels, Mytilus galloprovincialis, during a field translocation experiment. *Aquatic Toxicology, 68*, 167–178.

Regoli, F., & Orlando, E. (1994). Seasonal variation of trace metal concentrations (Cu, Fe, Mn, Pb, Zn) in the digestive gland of the Mediterranean mussel *Mytilus galloprovincialis:* comparison between a polluted and a non polluted site. *Archives of Environmental Contamination and Toxicology*, *27*, 36-43.

Romeo, M., Hoarau, P., Garello, G., Gnassia-Barelli, M., & Girare, J. P. (2003). Mussel transplantation and biomarkers as useful tools for assessing water quality in the NW Mediterranean. *Environmental Pollution, 122*, 369–378.

Roseijadi, G., Young, J. S., Drum, A. S., & Gurtisen, J. M. (1984). Behaviour of trace metals in *Mytilus edulis* during a reciprocal transplant field experiment. *Marine Ecology Progress Series, 18*, 155-170.

Shahbazi, A., Zakaria, M. P., Yap, C. K., Tan, S. G., Surif, S., Mohamed, A. R., Sakari, M., Bakhtiari, A. R., Bahry, P. S., Chandru, K., & Mirsadeghi, S. A. (2010). Use of different tissues of *Perna viridis* as biomonitors of polycyclic aromatic hydrocarbons in the coastal water of Peninsular Malaysia. *Environmental Forensics*, *11*, 248-263.

Shazili, N. A. M., Yunus, K., Ahmad, A. S., Abdullah, N., & Rashid, M. K. A. (2006). Heavy metal pollution status in the Malaysian aquatic environment. *Aquatic Ecosystem Health*, *9*, 137–145.

Shulkin, V. M., Presley, B. J., & Kavun, V. I. (2003). Metal concentrations in mussel *Crenomytilus grayanus* and oyster *Crassostrea gigas* in relation to contamination of ambient sediments. *Environment International*, *29*(4), 493-502.

Simpson, R. D. (1979). Uptake and loss of zinc and lead by mussels (*Mytilus edulis*) and relationships with body weight and reproductive cycle. *Marine Pollution Bulletin*, *10*(3), 74-78.

Szefer, P., Ikuta, K., Frelek, K., Zdrojewska, I., & Nabrzyski, M. (1999). Mercury and other trace metals (Ag, Cr, Co, and Ni) in soft tissue and byssus of *Mytilus edulis* from the east coast of Kyushu Island, Japan. *The Science of the Total Environment, 229*, 227-234.

Tanner, P., Leong, L. S., & Pan, S. M. (2000). Contamination of heavy metals in marine sediment cores from Victoria Harbour, Hong Kong. *Marine Pollution Bulletin*, *40*, 769-779.

Viarengo, A., Palmero, S., Zanicchi, G., Capelli, R., Vaissiere, R., & Orunesu, M. (2003). Role of metallothioneins in Cu and Cd accumulation and elimination in the gill and digestive gland cells of *Mytilus galloprovincialis* (Lam.). *Marine Environmental Research***,** *16,* 23-36.

Wallner-Kersanach, M., Theede, H., Eversberg, U., & Lobo, S. (2000). Accumulation and Elimination of trace metals in a transplantation experiment with *Crassostrea rhizophorae*. *Archives of Environmental Contamination and Toxicology*, *38,* 40–45.

Wang, L. (2010). Can shells be biomonitor of contaminants in the environment: an investigation study of perfluorinated compounds in bivalve shells of China. *Geophysical Research Abstracts, 12*.

Wood, A. K., Ahmad, Z., Shazili, N. A. M., Yaakob, R., & Carpenter, R. (1997). Geochemistry of sediments in Johor Strait between Malaysia and Singapore. *Continental Shelf Research*, *17*, 1207–1228.

Yap, C. K., Ismail, A., & Tan, S.G. (2003d). Background concentrations of Cd, Cu, Pb and Zn in the green-lipped mussel *Perna viridis* (Linnaeus) from Peninsular Malaysia. *Marine Pollution Bulletin 46*, 1035-1048.

Yap, C. K., Ismail, A., Edward, F. B., Tan, S. G., & Siraj, S.S. (2006). Use of different soft tissues of *Perna viridis* as biomonitors of bioavailability and contamination by heavy metals (Cd, Cu, Fe, Pb, Ni, and Zn) in a semi-enclosed intertidal water, the Johore Straits. *Toxicological & Environmental Chemistry*, *88*(4), 683–695.

Yap, C. K., Ismail, A., Omar, H., & Tan, S. G. (2003a). Accumulation, depuration and distribution of cadmium and zinc in the green-lipped mussel *Perna viridis* (Linnaeus) under laboratory condition. *Hydrobiologia, 498*, 151-160.

Yap, C. K., Ismail, A., Tan, S. G., & Ismail, A. R. (2004). Assesment of different soft tissues of the green-lipped mussel *Perna viridis* (Linnaeus) as biomonitoring agents of Pb: Field and laboratory studies. *Water, Air and Soil Pollution, 153*, 253-268.

Yap, C. K., Ismail, A., Tan, S. G., & Omar, H. (2002). Correlations between speciation of Cd, Cu, Pb and Zn in sediment and their concentrations in total soft tissue of green-lipped mussel *Perna viridis* from the west coast of Peninsular Malaysia. *Environmental International*, *28*, 117-126.

Yap, C. K., Ismail, A., Tan, S. G., & Rahim I. A. (2003b). Can the byssus of green-lipped mussel *Perna viridis* (Linnaeus) from the west coast of Peninsular Malaysia be a biomonitoring organ for Cd, Pb and Zn? Field and laboratory studies. *Environmental International, 29*, 521-528.

Yap, C. K., Muhamad Azlan, A. G., Cheng, W. H., & Tan, S. G. (2011). Accumulation and Depuration of Cu and Zn in the Blood Cockle *Anadara granosa* (Linnaeus) under Laboratory Conditions. *Pertanika Journal of Tropical Agricultural Science*, *34*(1), 75 – 82.

Yap, C. K., Tan, S. G., Ismail, A., & Omar, H. (2002). Genetic variation of green-lipped mussel *Perna viridis* (Linnaeus) from the west coast of Peninsular Malaysia. *Zoological Studies 41*(1), 376-387.

Zar, J. H. (1996). Biostatistical Analysis (3rd Ed.). Upper Saddle River, New Jersey: Prentice-Hall, pp. 662.

Zulkifli, S. Z., Ismail, A., Mohamat-Yusuff, F., Arai, T., & Miyazaki, N. (2010). Johor Strait as a Hotspot for Trace Elements Contamination in Peninsular Malaysia. *Bulletin of Environmental Contamination and Toxicology*, *84*, 568-573.

Pertanika J. Sci. & Technol. 21 (1): 97 - 110 (2013)

SCIENCE & TECHNOLOGY

Journal homepage: http://www.pertanika.upm.edu.my/

Physico-Chemical and Electrical Properties of Bismuth Chromate Solid Solutions

Wong Y. C.[1,2] and Tan Y. P.[1,2]*

[1]*Centre of Excellence for Catalysis Science and Technology, Universiti Putra Malysia, 43400 Serdang, Selangor, Malaysia*

[2]*Department of Chemistry, Faculty of Science, Universiti Putra Malysia, 43400 Serdang, Selangor, Malaysia*

ABSTRACT

Bismuth chromium solid solutions, with a general formula $Bi_{6-x}Cr_2O_{\delta}$, where $-1 \leq x \leq 2$, were successfully synthesized via the conventional solid state method. The phases of the synthesized samples were determined by X-ray diffraction (XRD) analysis. The properties of single-phase compounds were characterized by using differential thermal analysis (DTA), thermal gravimetric analysis (TGA), AC impedance spectroscopy, and inductively coupled plasma-atomic emission spectroscopy (ICP-AES). The occurrence of phase transitions was confirmed by DTA and TGA, where a thermal event was observed by DTA at around 800°C. In addition, TGA studies also showed that there was a weight loss at around 800°C. Elemental analysis of $Bi_6Cr_2O_{15}$ and its solid solutions by ICP-AES showed a good agreement between the expected value and the experimental value on the compositions, with no evidence of any systematic deviation from stoichiometric. Electrical properties of $Bi_6Cr_2O_{15}$ and its solid solutions were investigated by using AC impedance spectroscopy from 300°C to 650°C. Ionic conductivity increased with the increasing temperature and bismuth content, and the best ionic conductivity was observed for $Bi_7Cr_2O_{16.5}$. The activation energy (E_a) of $Bi_6Cr_2O_{15}$ and its solid solutions were in the range of 1.22-1.32 eV.

Keywords: Bismuth oxide, Chromium oxide, Impedance spectroscopy

INTRODUCTION

Magneto-electric materials, in which magnetic and ferroelectric orders coexist, are currently attracting more and more attention owing to their potential applications and intriguing physics. Bi-based 3d-transition metal oxides with distorted perovskite structures, such as $BiMnO_3$ and $BiFeO_3$, are important magneto-

Article history:
Received: 18 May 2011
Accepted: 21 December 2011

E-mail addresses:
stevenwongyc@hotmail.com (Wong Y. C.),
yptan@science.upm.edu.my (Tan Y. P.),
*Corresponding Author

ISSN: 0128-7680 © 2013 Universiti Putra Malaysia Press.

electric materials (Chi *et al.*, 2007; Li *et al.*, 2006; Selbach *et al.*, 2010; Yang *et al.*, 2007). It is believed that the lone-pair electrons of Bi play a crucial role in ferroelectricity. The Bi_2O_3–Cr_2O_3 system was investigated to explore novel magneto-electric compounds.

The phase diagram of the Bi_2O_3-Cr_2O_3 system consisted of three compounds which were synthesized by solid-state reactions: $Bi_{18}CrO_{30}$ (tetragonal, a = b = 7.74 Å, c = 5.72 Å), $Bi_6Cr_2O_{15}$ (orthorhombic, a = 5.55 Å, b = 5.76 Å, c = 5.50 Å), and $BiCrO_3$ (orthorhombic, a = 10.52 Å, b = 17.63 Å, c = 9.995 Å) (Liu *et al.*, 2008). Later, the phase diagram of the pseudo-binary system Bi_2O_3-Cr_2O_3 was reconstructed based on the x-ray diffraction measurement and differential thermal analysis by Liu *et al.* (2008). Four intermediate phases were determined in this system, namely, $Bi_{14}CrO_{24}$-based solid solutions (space group I4Im), $Bi_{10}Cr_2O_{21}$-based high temperature solid solutions (orthorhombic symmetry), a new compound Bi_2CrO_6 (monoclinic symmetry) and the stoichiometric compound $Bi_6Cr_2O_{15}$ (orthorhombic symmetry, with unit cell parameters, a = 12.3018 Å, b = 19.8749 Å, and c = 5.8816 Å and space group Ccc2) (Liu *et al.*, 2008).

In term of ionic conductivity, the compound $Bi_6Cr_2O_{15}$ could be expected to be a good oxygen ion conductor, in view of its structural similarity to the solid solution $Bi(Bi_{12-x}Te_xO_{14})Mo_{4-x}V_{1+x}O_{20}$ ($0 \leq x \leq 2.5$), which exhibits a conductivity as high as $\sigma = 8.0 \times 10^{-3}$ $(\Omega\ cm)^{-1}$ at 750°C (x = 1) with an activation energy, $E_a = 0.84$ eV. It is, however, found to be considerably modest oxygen ion conductor. It is speculative to attribute this to any structural difference between the phases, but it seems to imply that the high oxygen ion mobility in the column phases is not provided solely by the presence of the column, but also significantly depends on the atoms and the arrangement between the columns (Grins *et al.*, 2002).

Previously, the thermogravimetric analyses done by Esmaeilzadeh *et. al.* (2001) showed that upon heating mixtures of Bi_2O_3 and Cr_2O_3 in air, an irreversible increase in weight began at 450-500 °C and reached, depending on the Cr concentration, a plateau at 650 to 900°C. The weight increase corresponded well to that of a complete oxidation of Cr^{3+} to Cr^{6+}. This oxidative behaviour is quite unusual for Cr-containing materials in air, at normal pressure, and these high temperatures. Magnetic susceptibility measurements confirmed an oxidation state of +6 for Cr, as no or only very weak paramagnetic signals were observed (Colmont *et al.*, 2010).

In this work, the focus was placed on synthesizing $Bi_6Cr_2O_{15}$ and its solid solutions, as well as investigating their physico-chemical and electrical properties.

EXPERIMENTAL

Powder sample of bismuth chromate ($Bi_6Cr_2O_{15}$) and its solid solutions were prepared via solid state reactions using Bi_2O_3 (Aldrich, 99.999%) and Cr_2O_3 [Johnson Matthey (JM), 99.999%] as starting materials. The samples were heat-treated at 600°C for 48-72 hours with intermediate grindings. The phase identity and purity of the synthesized samples were determined by X-ray diffraction (XRD) analysis (Shimadzu diffractometer XRD-6000), which was equipped with a diffracted-beam graphite monochromator using CuKα radiation. The morphology of the samples was studied using scanning electron microscopy (LEO 1455 VP SEM).

The thermal properties of the samples were determined by using the differential thermal analysis, DTA (Perkin-Elmer instrument, model DTA 7) and thermal gravimetric analysis, TGA (Mettler Toledo Star SW 7.01). Inductively coupled plasma-atomic emission spectroscopy (ICP-

AES) (Perkin-Elmer P1000) was used to carry out the elemental analysis. Fourier-transform infrared (FT-IR) spectrometer (Perkin-Elmer model 1725x), with the wavenumber range in the region of 4000 and 400 cm^{-1}, was used for the structural analysis. The electrical properties of the pelleted samples were studied by using AC impedance analyzer (Hewlett-Packard Impedance Analyzer HP 4192A). The frequency range of 5 Hz to 13 MHz with an applied voltage of 100 mV was used. The measurements were made between 300°C and 650°C by increment steps of 50°C with 30 minutes stabilization time. The measurements were carried out on heat-cool thermal cycles.

RESULTS AND DISCUSSION

XRD and SEM Results

Fig.1 shows the XRD pattern of $Bi_6Cr_2O_{15}$ and its solid solutions prepared via conventional solid state method. $Bi_6Cr_2O_{15}$ and its solid solutions were indexed using the orthorhombic system with lattice parameters: a = 12.30184 Å, b = 19.87492 Å, c = 5.88162 Å, and in space group of Ccc2 (Grins *et al.*, 2002; Liu *et al.*, 2008). From the results obtained, the limit of the solid solutions in Bi_2O_3-Cr_2O_3 system was in the range 4 to 7. The four single phase solid solutions that crystallized in orthorhombic system were $Bi_4Cr_2O_{12}$, $Bi_5Cr_2O_{13.5}$, $Bi_6Cr_2O_{15}$ and $Bi_7Cr_2O_{16.5}$. As for $Bi_3Cr_2O_{10.5}$, two extra peaks were observed at 24.5 ° and 33.6°. These two peaks were due to the formation of chromium oxide (ICDD card number, 01-070-3765). Meanwhile, there were seven extra peaks observed in $Bi_8Cr_2O_{18}$, in the positions of 31.0778 °, 32.6381 °, 45.4703 °, 46.5948 °, 53.2193 °, 54.6160 °, and 55.2515 °. All these peaks were attributed to the formation of δ-bismuth oxide (δ-Bi_2O_3) (ICDD card number: 01-074-1633, 00-027-0052, 00-051-1161).

As the composition varies, the solid solutions may undergo a small contraction or expansion. According to Vegard's law, unit-cell parameters should change linearly with the composition. The evolution of the unit-cell parameters versus composition was plotted and is shown in Fig.2 to Fig.4. All the parameters *a*, *b* and *c* underwent a regular increase from x = 4 to x = 7. This general increase of all unit-cell parameters can be expected, since a smaller cation, Cr (ionic radius = 0.51 Å), is being substituted for by a larger Bi (ionic radius = 1.20 Å) (Bëguë *et al.*, 2002).

Fig.5(a), (b), (c), and (d) show the scanning electron microscopy (SEM) images of the samples. All the samples have displayed a similar morphology where the microstructures were homogeneously distributed in the lattice. No secondary phase was observed in the structure, and therefore, the samples synthesized were in the single phase. Some pores were also observed in the inter-granular area, indicating a moderate connection between the grains.

Structural Analysis

The IR absorption spectra of the single-phase orthorhombic structure compounds, $Bi_xCr_2O_\delta$, $4 \leq x \leq 7$, have similar patterns as shown in Fig.6. A broad, diffuse band was observed at ~850 cm^{-1} and ~792 cm^{-1} in the IR spectra of all the compounds. This may be due to the Cr-O-Cr bond vibration and Cr-O stretching (Brown *et al.*, 1967; Jezowska-Trzebiatowska *et al.*, 1968).

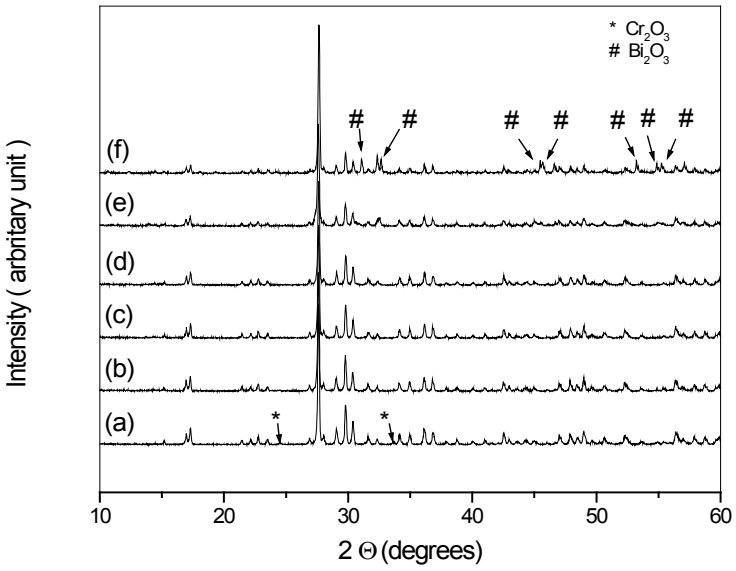

Fig.1: The XRD patterns of (a) $Bi_3Cr_2O_{10.5}$, (b)$Bi_4Cr_2O_{12}$, (c) $Bi_5Cr_2O_{13.5}$, (d) $Bi_6Cr_2O_{15}$, (e) $Bi_7Cr_2O_{16.5}$, and (f) $Bi_8Cr_2O_{18}$ prepared at 600°C

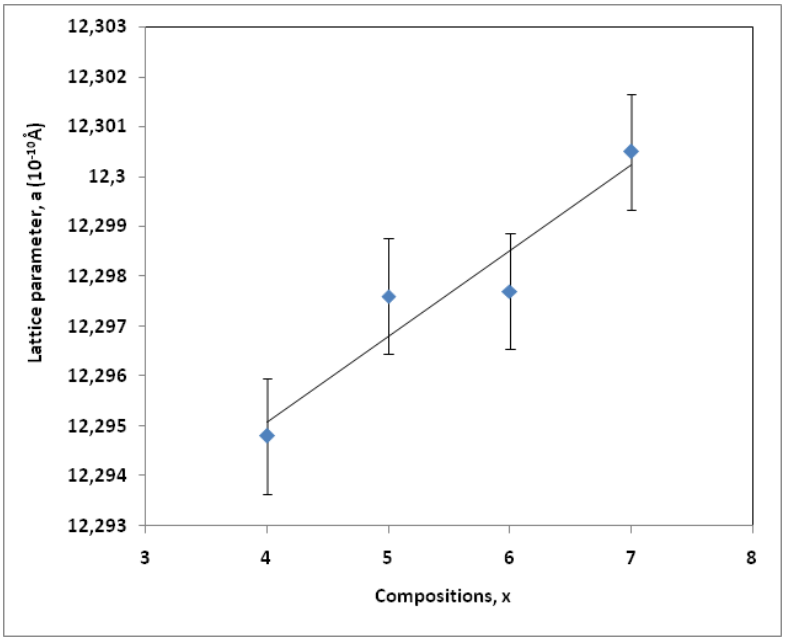

Fig.2: Variation of the lattice parameter, *a*, with composition, x, in $Bi_xCr_2O_\delta$, $4 \leq x \leq 7$

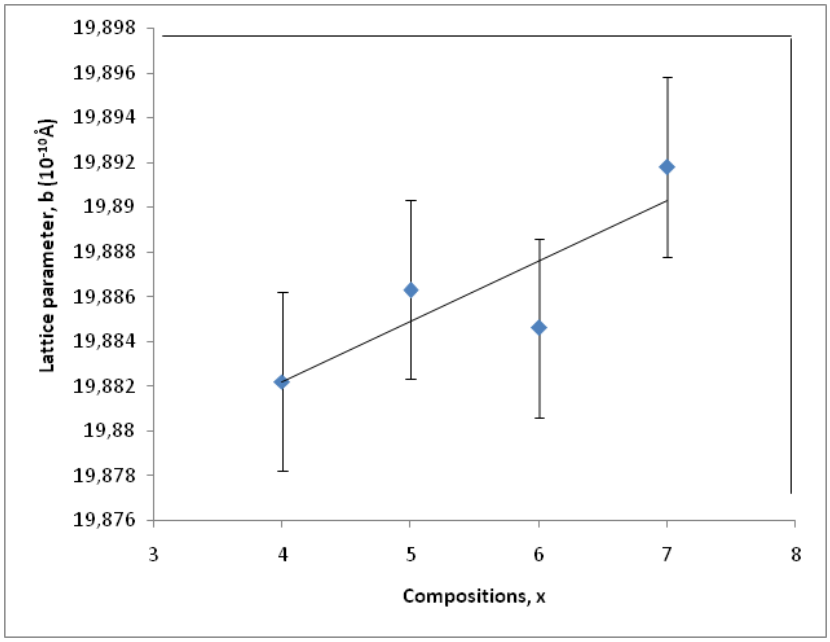

Fig.3: Variation of the lattice parameter, *b*, with composition, x, in $Bi_xCr_2O_\delta$, $4 \leq x \leq 7$

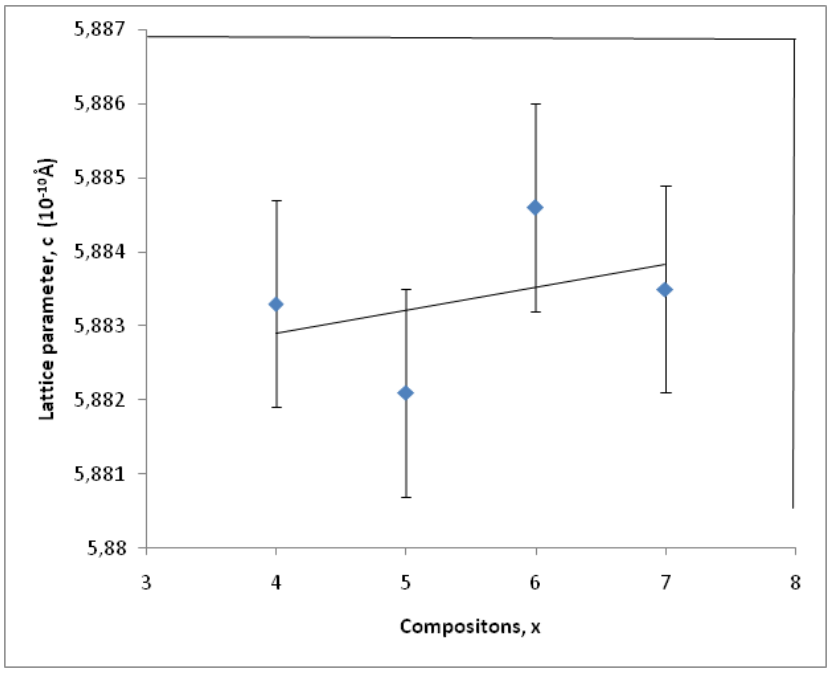

Fig.4: Variation of the lattice parameter, *c*, with composition, x, in $Bi_xCr_2O_\delta$, $4 \leq x \leq 7$

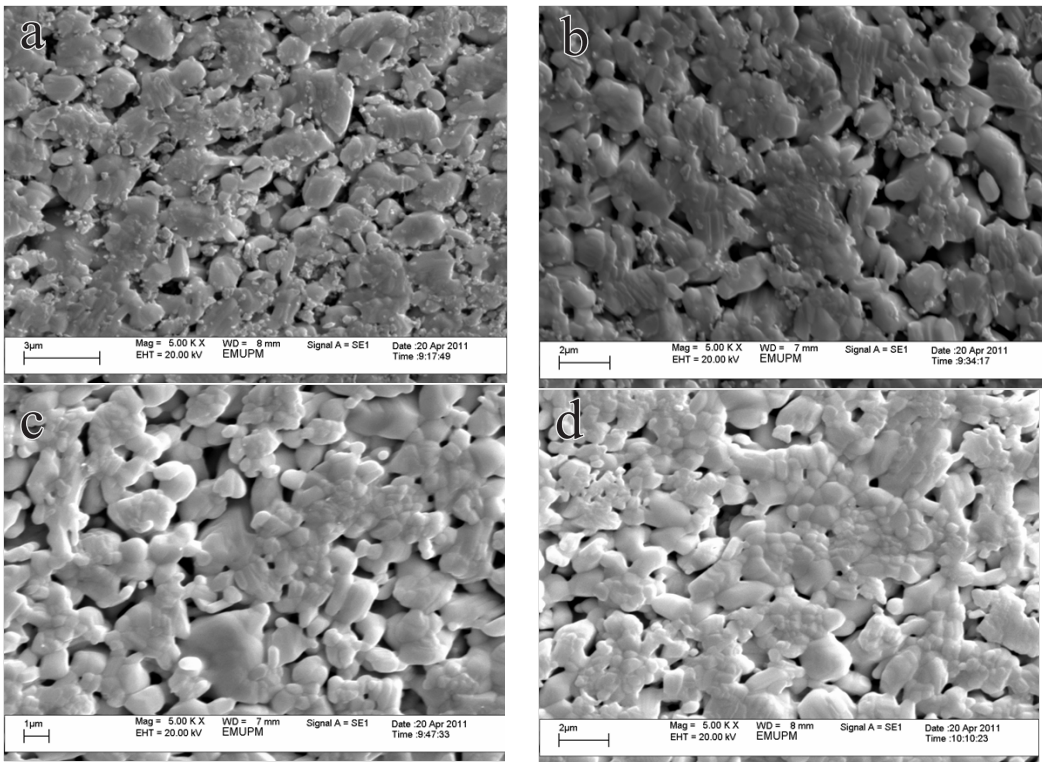

Fig.5: The SEM image for (a) $Bi_4Cr_2O_{12}$, (b) $Bi_5Cr_2O_{13.5}$, (c) $Bi_6Cr_2O_{15}$, and (d) $Bi_7Cr_2O_{16.5}$, sintered at 600°C

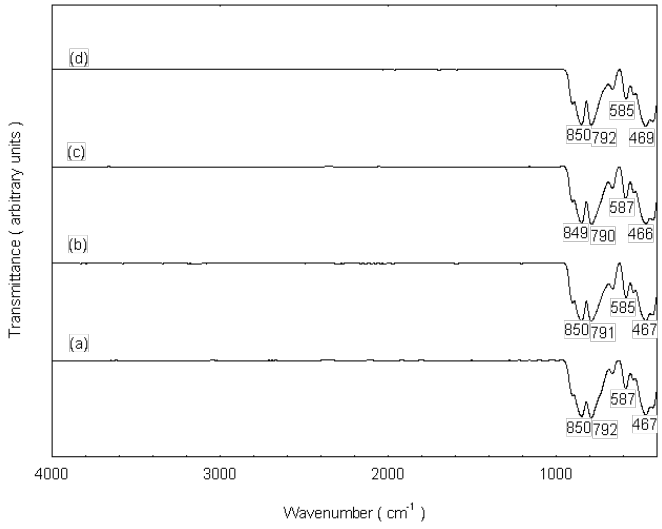

Fig.6: The FT-IR spectra of (a) $Bi_4Cr_2O_{12}$, (b) $Bi_5Cr_2O_{13.5}$, (c) $Bi_6Cr_2O_{15}$, and (d) $Bi_7Cr_2O_{16.5}$

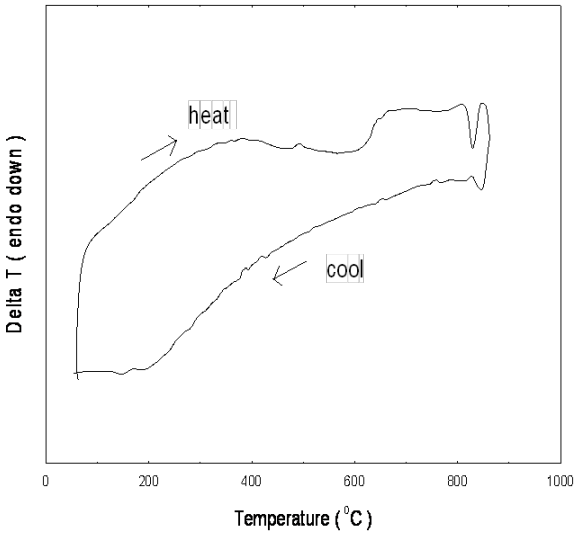

Fig.7: DTA thermogram of $Bi_6Cr_2O_{15}$

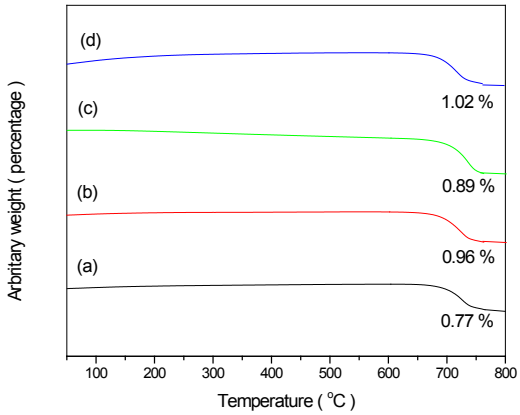

Fig.8: The TGA thermographs of (a) $Bi_4Cr_2O_{12}$, (b) $Bi_5Cr_2O_{13.5}$, (c) $Bi_6Cr_2O_{15}$, and (d) $Bi_7Cr_2O_{16.5}$ with their respective percentage weight loss

However, no shift was observed in the wavenumbers of Cr-O-Cr bond vibration, as well as Cr-O stretching with the variation of the Cr content. The band of ~ 587 cm^{-1} and ~ 467 cm^{-1} in the IR spectra was attributed to the vibration of Bi-O and Bi-O-Bi vibrations of $[BiO_6]$ octahedral units, respectively (Cheng *et al.*, 2006; Rico-Fuentes *et al.*, 2005).

The atomic weight of Bi is about four times larger than that of Cr. Moreover, the ionic radius of Bi^{3+} (1.20 Å) is larger than that of Cr^{3+} (0.69 Å). Thus, Bi-O bond length is expected to be longer and weaker compared to Cr-O bond. This may lead to the lowering of wavenumber (υ) at 587 cm^{-1} and 467 cm^{-1}. The Bi contents for the compounds $Bi_xCr_2O_\delta$, $4 \leq x \leq 7$ are different and it is expected that υ would decrease with increasing Bi content. However, from the IR spectra obtained, the υ does not decrease with the increasing Bi content. It may due to Bi-O

bond existed in the form of [BiO_6] octahedral units which restricted its vibration (Ardelean *et al.*, 2008).

Thermal Properties

The DTA thermograms of all solid solutions exhibited a similar pattern. Here, only the thermogram of $Bi_6Cr_2O_{15}$ (Fig.7) is shown for discussion. The endothermic peak around 600°C was due to the oxidation of Cr^{3+} into Cr^{6+}, which began at 450°C to 600°C (Esmaeilzadeh *et al.*, 2001). Besides, an endothermic peak was also observed at the temperature around 800°C on the heating cycle, which ascribed to the transformation of orthorhombic $Bi_6Cr_2O_{15}$ into the high temperature solid solution, face-centred orthorhombic $Bi_{10}Cr_2O_{21}$. It was an irreversible transformation, where the face-centred orthorhombic $Bi_{10}Cr_2O_{21}$, once formed at 800°C, could not be transformed back into the orthorhombic $Bi_6Cr_2O_{15}$ on cooling (Liu *et al.*, 2008).

All the solid solutions showed a similar TGA thermograph pattern (Fig.8). In particular, Thermogravimetric measurements did not show any weight loss when the samples were heated up until 700°C. After 700°C, a weight loss was observed, indicating $Bi_6Cr_2O_{15}$ and its solid solutions had undergone phase transition from orthorhombic to face-centred orthorhombic structure (Liu *et al.*, 2008). It further confirmed the DTA results that the phase transition occurred at high temperature.

Elemental Analysis

The compositions of the solid solutions were examined by using ICP-AES and the data are shown in Table 1. With the increasing chromium content in the order of $Bi_7Cr_2O_{16.5}$ to $Bi_4Cr_2O_{12}$, both $Bi_4Cr_2O_{12}$ and $Bi_5Cr_2O_{13.5}$ were unable to dissolve either in concentrated hydrochloric acid (HCl) or hydrofluoric acid (HF). Therefore, the elemental analysis for the chromium content in these two samples was ignored. These two samples were tested only for bismuth composition. In general, the experimental values for the composition are in good agreement with the calculated values, with no evidence of any systematic deviation from the stoichiometric. Thus, the stoichiometric compositions of the single phase materials were confirmed.

TABLE 1: Composition determination of solid solutions in the Bi_2O_3-Cr_2O_3 system

Sample	Elements	Atomic %	
		Calculated	Experimental
$Bi_4Cr_2O_{12}$	Bi	73.85	76.78 ± 0.56
	Cr	-	-
	O	-	-
$Bi_5Cr_2O_{13.5}$	Bi	76.56	76.57 ± 0.60
	Cr	-	-
	O	-	-

TABLE 1: (continued)

$Bi_6Cr_2O_{15}$	Bi	78.47	78.70 ± 0.19
	Cr	6.51	6.34 ± 0.48
	O	15.02	14.96
$Bi_7Cr_2O_{16.5}$	Bi	79.90	81.93 ± 0.72
	Cr	5.68	5.54 ± 0.61
	O	14.42	12.53

Electrical Properties

The conductivity values of the materials were extracted from complex plane plots. In general, the complex plane plots of the four solid solutions were similar, and therefore, the parent compound ($Bi_6Cr_2O_{15}$) was selected for the discussion. The conductivity measurements of solid solutions were reproducible on heating and cooling. The complex plane plot of $Bi_6Cr_2O_{15}$ at 450°C (Fig.9) showed that the resistance (R) of the material was 2.3871 x 10^5 ohm cm. Thus, the semicircle has an associated capacitance (C_b) (calculated from $\omega RC = 1$, where ω is the frequency of maximum loss) of 6.67 x 10^{-12} F cm^{-1}, which is a typical value for bulk component. The conductivity of the material at 450°C was 4.189 x 10^{-6} Ω^{-1} cm^{-1}. The moderate ionic conductivity of the samples was due to the moderate connection between the grains, as a result of the presence of pore in the inter-granular area, as shown in the SEM image (Fig.5). As the temperature increased, the intercept at the real component of impedance, Z' (resistive) axis shifted towards lower value and gave the lower resistance value. Hence, the conductivity

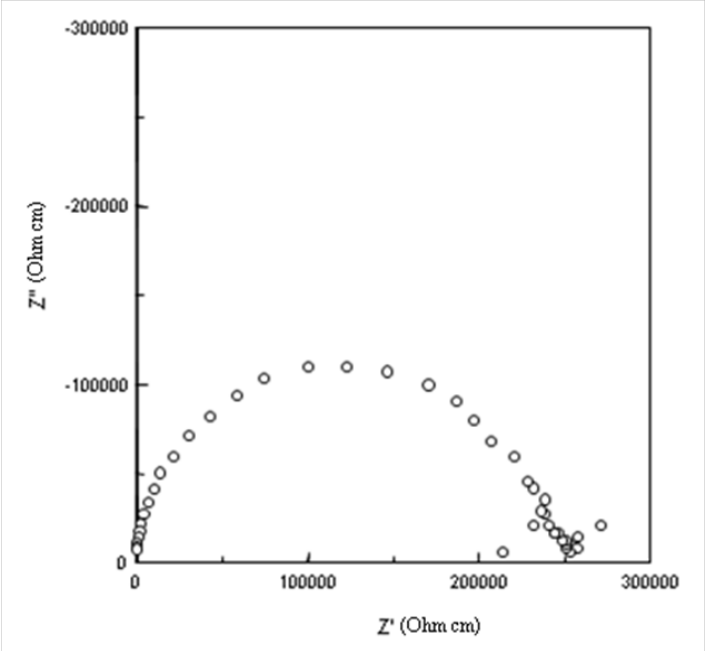

Fig.9: A complex plane plot of $Bi_6Cr_2O_{15}$ at 450°C

increased with the increasing temperature. The optimum conductivity of $Bi_6Cr_2O_{15}$ was observed at 650°C with a conductivity value of 4.456 x 10^{-4} Ω^{-1} cm^{-1}.

The homogeneity of the materials can be observed from the complex plane plots. A single semicircle observed indicated that this material was homogeneous. The homogeneity of the materials can also be determined from the combined spectroscopic plots of electric modulus, M", and the imaginary components of impedance, -Z" versus log f (where f was frequency). Fig.10 shows the combined spectroscopic plots of M", -Z" versus log f of $Bi_6Cr_2O_{15}$ at 450°C. It showed a single peak and the frequency maxima of Z" and M" coincided at a higher frequency, where the full width at half maximum (FWHM) of the Z" peaks was approximately 1.4 decade. Thus, this material can be considered as homogeneous and the conductivity was purely attributed by bulk.

Ionic conductivity is temperature dependence and is related by the Arrhenius equation:

$$\sigma = A\exp(-E/RT) \quad (1)$$

where σ is ionic conductivity, *A* is pre-exponential factor, E is activation energy, R is constant and T is temperature. When the temperature increases, the mobility of ions also increases and thus the ionic conductivity increases.

Fig.11 shows the combination of the Arrhenius plots of all pure phase solid solutions in Bi_2O_3-Cr_2O_3 system. The conductivity behaviour is similar for all materials studied and is temperature dependence. The conductivity increased in the order of $Bi_4Cr_2O_{12} < Bi_5Cr_2O_{13.5} \sim Bi_6Cr_2O_{15} < Bi_7Cr_2O_{16.5}$. The conductivity increased with the increasing bismuth content in the stoichiometric equation. Meanwhile, the ionic radius of bismuth is larger than chromium, and therefore enlarging the cell volume of the materials and making the passage of charge carriers through more feasible cells (Galy *et al.*, 2003).

A linear straight line was observed from 400°C up to 650°C. Below 400°C, a curvature was observed. The curvature in the plot may be due to a temperature dependence of the activation energy (e.g., $E_a = E_{a0} - E_{a1}.T^2$) or to different conduction mechanisms dominating at lower and higher temperatures (Grins *et al.*, 2002). Deviation at high temperature can correlate to the phase transformation from $Bi_6Cr_2O_{15}$ to face-centred orthorhombic $Bi_{10}Cr_2O_{21}$ and monoclinic Bi_2CrO_6 above 650°C (Liu *et al.*, 2008). From the linear range of the plot, the activation energies (E_a) calculated were in the range within 1.22 eV to 1.32 eV. The best ionic solid has an activation energy of 1 eV (96 kJ $mole^{-1}$) or lower. For example, Bi_5NbO_{10} and $Bi_{26}Mo_{10}O_{\delta}$, which are good ionic conductors, have E_a of 0.94 eV and 0.47 eV, respectively (Hou *et al.*, 2010; Begue *et al.*, 1998). Hence, solid solutions in Bi_2O_3-Cr_2O_3 system were considered as moderate oxide ion conductors.

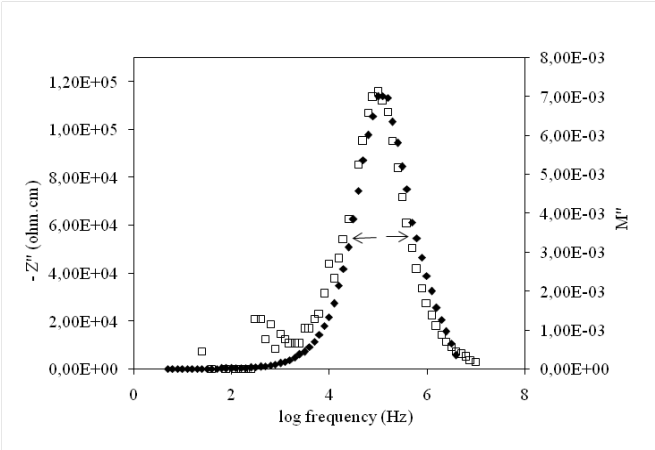

Fig.10: The modulus spectroscopic plot of M", -Z" versus log f of $Bi_6Cr_2O_{15}$ at 450°C

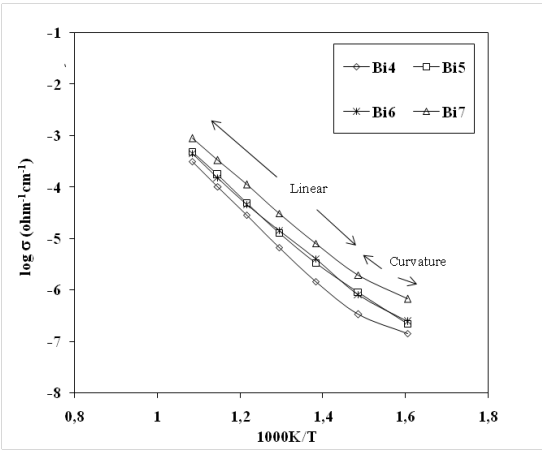

Fig.11: The Arrhenius conductivity plots of $Bi_xCr_2O_\delta$ ($4 \leq x \leq 7$)

CONCLUSION

The solid solutions in the $Bi_2O_3 - Cr_2O_3$ system have been successfully synthesized via conventional solid state method. Among the compounds synthesized in which Bi:Cr ratio range from 1.5:1 to 4:1 and as determined from the X-ray diffraction (XRD) analyses, only four were in the pure phase with the orthorhombic structure, i.e. $Bi_4Cr_2O_{12}$, $Bi_5Cr_2O_{13.5}$, $Bi_6Cr_2O_{15}$ and $Bi_7Cr_2O_{16.5}$. The SEM image showed a homogeneous dispersion of microstructure and the presence of pores in the inter-granular area. The occurrence of the phase transitions at high temperatures was confirmed by the thermal analyses. The thermal analyses showed an irreversible endothermic peak at temperature ~ 800°C on heating cycle. Besides, the TGA results showed that there is a weight loss after 700°C.

The activation energy for the solid solution in Bi_2O_3-Cr_2O_3 system is in the range 1.22 eV- 1.32 eV. The moderate ionic conductivity of the samples can be related to the moderate

connection between the grains, which is due to the presence of pores in the inter-granular area. However, conductivity increases with the increasing temperature and bismuth content. The conductivity of the solid solutions increased in the order of: $Bi_4Cr_2O_{12} < Bi_5Cr_2O_{13.5} \sim Bi_6Cr_2O_{15} < Bi_7Cr_2O_{16.5}$. Among the solid solutions, $Bi_7Cr_2O_{16.5}$ is the best ionic conductor and has the highest conductivity. From the results of the electrical measurement, the solid solutions for Bi_2O_3-Cr_2O_3 system can be concluded as moderate oxide ion conductors at the temperature above 350°C.

ACKNOWLEDGEMENTS

The authors are grateful for the financial support given by the Ministry of Science, Technology, and Innovation (MOSTI) via Science Fund.

REFERENCES

Ardelean, I., Cora, S., & Rusu, D. (2008). EPR and FT-IR spectroscopic studies of Bi_2O_3–B_2O_3– CuO glasses. *Physica B*, *403*, 3682– 3685.

Begue, P, Rojo, J. M., Enjalbert, R., Galy, J., & Castro, A. (1998). Ionic conductivity of the new oxide family $Bi[Bi_{12-x}Te_xO_{14}]Mo_{4-x}V_{1+x}O_{20}$. *Solid State Ionics, 112*, 275–280.

Bëguë, P., Rojo, J.M., Iglesias, J. E., & Castro, A. (2002). Different $[Bi_{12}O_{14}]_n$ columnar structural types in the Bi-Mo-Cr-O system: synthesis, structure, and electrical properties of the solid solution $Bi_{26}Mo_{10-x}Cr_xO_{69}$. *Journal of Solid State Chemistry, 166*, 7-14.

Brown, D. A., Cunningham, D., & Glass, W. K. (1967). The infrared and Raman spectra of chromium (III) oxide. *Spectrochimita Acta Part A: Molecular Spectroscopy, 24*, 965- 968.

Cheng, Y., Xiao, H. N., Guo, W. M., & Guo, W. M. (2006). Structure and crystallization kinetics of Bi_2O_3–B_2O_3 glasses. *Thermochimica Acta, 444*, 173–178.

Chi, Z. H., Yang, H., Feng, S. M., Li, F. Y., Yu, R. C., & Jin, C. Q. (2007). Room-temperature ferroelectric polarization in multiferroic $BiMnO_3$. *Journal of Magnetism and Magnetic Materials, 310*, e358-e360.

Colmont, M., Drache, M., & Roussel, P. (2010). Synthesis and characterization of $Bi_{31}Cr_5O_{61.5}$, a new bismuth chromium oxide, potential mixed-ionic-electronic conductor for solid oxide fuel cells. *Journal of Power Sources, 195*, 7207-7212.

Esmaeilzadeh, S., Lundgren, S., Haslenius, U., & Grins, J. (2001). $Bi_{1-x}Cr_xO_{1.5+1.5x}$, $0.05 \leq x \leq 0.15$: A new high-temperature solid solution with a three-dimensional incommensurate modulation. *Journal of Solid State Chemistry, 156*, 168-180.

Galy, J., Enjalbert, R., Rozier, P., & Millet, P. (2003). Lone pair stereoactivity versus anionic conductivity. Columnar structures in the Bi_2O_3–MoO_3 system. *Solid State Sciences, 5*, 165-174.

Grins, J., Esmaeilzadeh, S., & Hull, S. (2002). Structure and ionic conductivity of $Bi_6Cr_2O_{15}$, a new structure type containing $(Bi_{12}O_{14})^{8n+}_n$ columns and CrO^{2-}_4 tetrahedra. *Journal of Solid State Chemistry, 163*, 144–150.

Hou, J. G., Vaisha, R., Qu, Y. F., Krsmanovic, D., Varma, K. B. R., & Kumar, R. V. (2010). Dielectric relaxation and electrical conductivity in Bi_5NbO_{10} oxygen ion conductors prepared by a modified sol–gel process. *Journal of Power Source, 195*, 2613-2618.

Jezowska-Trzebiatowska, B., Hanuza, J., Wojciechowski, W., & Nawojska, J. (1968). Spectroscopic studies and structural chemistry of Cr^{III}/Cr^{VI} compounds in the solid state. *Inorganica Chimica Acta*, *2*, 202-207.

Li, M.C., Judith, D., Liu, L. H., & Zhao, L. C. (2006). The phase transition and phase stability of magnetoelectric BiFeO3. *Materials Science and Engineering A*., *438-440*, 346-349.

Liu, Y. H., Li, J. B., Liang, J. K., Luo, J., Ji, L. N., Zhang, J. Y., & Rao, G. H. (2008) Phase diagram of the Bi_2O_3-Cr_2O_3 system. *Materials Chemistry and Physics*, *112*, 239–243.

Rico-Fuentes, O., Sanchez-Aguilera, E., Velasquez, C., Ortega-Alvarado, R., Alonso, J. C., & Ortiz, A. (2005). Characterization of spray deposited bismuth oxide thin films and their thermal conversion to bismuth silicate. *Thin Solid Films, 478*, 96– 102.

Selbach, S. M., Tybell, T., Einarsrud, M-A., & Grande, T. (2010). Phase transitions, electrical conductivity and chemical stability of $BiFeO_3$ at high temperatures. *Journal of Solid State Chemistry, 183*, 1205-1208.

Yang, C. H., Koo, T. Y., & Jeong, Y. H. (2007). Orbital order, magnetism, and ferroelectricity of multiferroic $BiMnO_3$. *Journal of Magnetism and Magnetic Materials*, *310*, 1168–1170.

Pertanika J. Sci. & Technol. 21 (1): 111 - 118 (2013)

SCIENCE & TECHNOLOGY

Journal homepage: http://www.pertanika.upm.edu.my/

Application of Computer Vision in the Detection of Chilling Injury in Bananas

Norhashila Hashim[1,2]*, Rimfiel B. Janius[1], Russly Abdul Rahman[3], Azizah Osman[3], Mahendran Shitan[4] and Manuela Zude[2]

[1]Department of Biological and Agricultural Engineering, Faculty of Engineering, Universiti Putra Malaysia, 43400 Serdang, Selangor, Malaysia

[2]Department Horticultural Engineering, Leibniz Institute for Agricultural Engineering Potsdam-Bornim (ATB), Max-Eyth-Allee 100, 14469 Potsdam-Bornim, Germany

[3]Faculty of Food Science and Technology, Universiti Putra Malysia, 43400 Serdang, Selangor, Malaysia

[4]Faculty of Science, Universiti Putra Malaysia, 43400 Serdang, Selangor, Malaysia

ABSTRACT

Bananas were chilled at 6°C and the appearance of brown spots when exposed to ambient air, a phenomenon known as chilling injury (CI), was detected using computer vision. The system consisted of a digital colour camera for acquiring images, an illumination set-up for uniform lighting, a computer for receiving, storing and displaying of images and software for analyzing the images. The RGB colour space values of the images were transformed into that of HSI colour space which is intuitive to human vision. Visual assessment of CI by means of a browning scale was used as a reference and correlation between this reference values and hue was investigated. Results of the computer vision study successfully demonstrate the potential of the system in substituting visual assessment in the evaluation of CI in bananas. The results indicate significant influence, at α=0.05, of treatment days and temperature on hue. A strong correlation was also found between hue and visual assessment with R>0.85.

Keywords: Computer vision, imaging, chilling injury, banana, hue

Article history:
Received: 20 May 2011
Accepted: 4 October 2011

E-mail addresses:
shila@eng.upm.edu.my (Norhashila Hashim),
janius@eng.upm.edu.my (Rimfiel B. Janius),
russly@putra.upm.edu.my (Russly Abdul Rahman)
azosman@putra.upm.edu.my (Azizah Osman)
mahendran@science.upm.edu.my (Mahendran Shitan),
zude@atb-potsdam.de (Manuela Zude)
*Corresponding Author

INTRODUCTION

The computer vision system (CVS) has been used increasingly for inspection and grading of agricultural produce in recent years. Articles regarding the feasibilities of the system and their reviews have been published by researchers since a decade ago (Tillet, 1991; Gunasekaran, 1996; Chen *et al*., 2002; Brosnan & Sun, 2004; Du & Sun, 2004). The

ISSN: 0128-7680 © 2013 Universiti Putra Malaysia Press.

effectiveness of the system has been shown on many kinds of fresh produce and food such as cherries (Beyer *et al*., 2002), tomatoes (Lana *et al*. 2006), mangoes (Kang *et al*., 2008), bananas (Roberto *et al*. 2009), pizzas (Du & Sun, 2005) and salmon fillets (Quevedo *et al*., 2010).

A digital colour camera in the CVS system generates RGB (red-green-blue) images that are device dependent (Yam & Papadakis, 2004; Mendoza *et al*., 2006; Cubero *et al*., 2011). To overcome this problem, the colours are transformed to other colour space such as the HSI (hue-saturation-intensity) and the L*a*b*. Hue is a commonly used colour coordinate in image processing because it is more intuitive to human vision (Cheng *et al*., 2001; Du & Sun, 2005). Generally, hue is considered as the angle between the reference line and the colour point in RGB space. The hue value varies from 0° to 360°, reflecting colours ranging from blue, yellow, green to magenta (Cheng *et al*., 2001). The method of using hue coordinates for colour evaluation is highly effective with more than 90% accuracy achieved in the inspection of potatoes and apples (Tao *et al*., 1995) and bell peppers (Shearer & Payne, 1990). Meanwhile, an accuracy of 96.7% was achieved in pizza classification (Du & Sun, 2005) and average error of approximately 2° in colour measurement was obtained in different curvatures of mangoes (Kang *et al*., 2008).

The application of computer vision in the detection of chilling injury (CI) in bananas is, however, still limited. CI is one of the physiological disorders that can appear if an agricultural produce is stored at low temperatures and the banana is one of the chilling sensitive produce that may show CI symptoms when exposed to a temperature below 10°C (Murata, 1969; Abd El-Wahab & Nawwar, 1977; Broughton & Wu, 1979; Nguyen *et al*., 2003). The symptoms may appear most severe at 6°C (Nguyen *et al*., 2003) but can tolerate well to a temperature range of 13-14°C (Zhang *et al*., 2010).

The most common visual symptom of CI is colour change. The quantification and characterization processes which are usually made by visual inspection may lead to considerable variation in results due to the differences in human evaluation, perception and human error. This has encouraged scientists to look for various ways of quantifying colour changes involving computer-based techniques.

Hence, the application of computer vision to replace the conventional method is investigated and subsequently suggested. The objectives of this paper are: i) to investigate colour changes due to CI in bananas using computer vision; and ii) to compare the performance of hue against visual assessment as a CI indicator.

MATERIALS AND METHODS

Materials

A batch of good quality hands of ripe bananas (*Musa Cavendish*) were obtained from a local market in Potsdam, Germany. The bananas were then transported to the laboratory at Leibniz Institute of Agricultural Engineering Potsdam-Bornim, Germany. Sixteen fingers of bananas were selected for the experiment. Images of the bananas were taken and visual assessment was also immediately carried out before storage (i.e. beginning of day 1). Then, eight bananas were allowed to ripen in a control temperature at 13°C, while another eight were stored at 6°C (rH 90-95%) for 2 days to induce CI. At the end of day 2 (i.e. beginning of day 3), the bananas

were taken out and their images were taken and visual assessment carried out immediately upon exposure to ambient temperature (15-20°C). This was repeated after one day of exposure to ambient temperature (i.e. beginning of day 4).

Visual Assessment

Visual assessment was conducted immediately after image acquisition. The assessment was based on browning scale as described by Nguyen *et al*. (2003). The browning scale was rated as follows: 1 = no chilling injury symptoms appear; 2 = mild chilling injury symptoms in which the injury can be found in between the epidermal tissues; 3 = moderate chilling injury symptoms in which the brown patches begin to become visible, larger and darker; 4 = severe chilling injury symptoms in which the brown patches are visible, larger and darker than at scale 3; 5 = very severe chilling injury symptoms in which the patches are relatively large on the surface.

Computer Vision System

A computer vision system developed by the Institute of Agricultural Engineering, Potsdam, Germany with CCD camera JVC KY-F50E (zoom lens F2.5 and focal lengths of 18-108 mm) was used to capture the images of bananas. The size of the captured image was 720x576 pixels by 24 bits. The bananas were illuminated using four fluorescent lamps arranged as front lighting at a height of 35cm above the samples in the form of a square for uniform effect. The angle between the camera lens axis and the lamps was 45° since diffused reflections responsible for colour occurred at 45° from the incident light. Optimas grabber board (Bioscan Inc., USA) software was used to acquire the images directly on the computer display and store them in the computer in bmp format.

All the acquired images were processed and analysed using Matlab software. The overall process is as presented in Fig.1.

A segmentation process was applied to separate the part of interest (the true image of a banana) from the background. This process is critical in image processing and it is done to eliminate the influence of the background pixel information on the RGB value of the banana. The threshold value used was obtained from a histogram of the gray-scale image (Fig.2), which is the conversion image of the original image of the banana. Morphological dilation was performed to remove background noise, and this was followed by a mask operation to get back the original colour of the segmented image resulting in a binary image and finally the true image of the bananas (Fig.3). The RGB values were then extracted from the image and converted to hue value using the following transformation:

$$H = \begin{cases} 2\pi - \cos^{-1}\left\{\dfrac{[(R-G)+(R-B)]}{2\sqrt{(R-G)^2+(R-B)(G-B)}}\right\}, & B > G \\ \cos^{-1}\left\{\dfrac{[(R-G)+(R-B)]}{2\sqrt{(R-G)^2+(R-B)(G-B)}}\right\}, & otherwise \end{cases} \qquad \text{[Equation 1]}$$

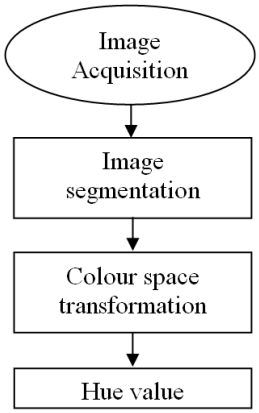

Fig.1: A schematic representation of the colour transformation process

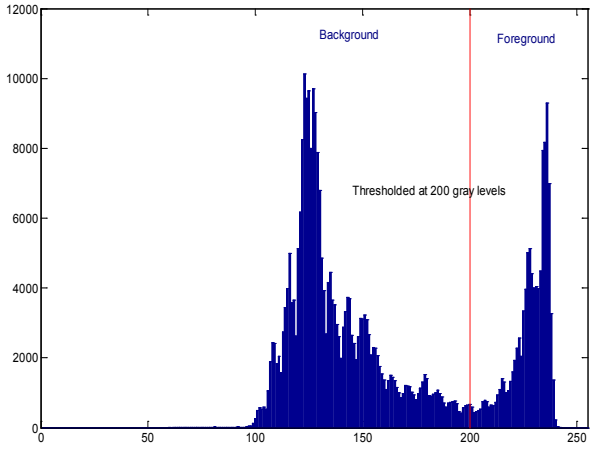

Fig.2: Histogram of gray-scale image

Statistical Analysis

Statistical analysis was performed using the SAS statistical software. Meanwhile, the analysis of variance (ANOVA) was used to compare the mean values of the sample hues at different treatment factors (treatment days and temperature). Then, the mean comparison test using Least Significant Difference (LSD) was conducted to compare the treatment group means after the ANOVA results had been shown to be significant. Finally, a correlation analysis between the hue and visual assessment values was conducted to find the relationship between them.

RESULTS AND DISCUSSION

Colour Change

The colour of bananas stored at 6°C changed from bright yellow at the beginning of the experiment to brown after being exposed to ambient temperature. The change in the colour was parallel to the change in the hue values (Fig.4).

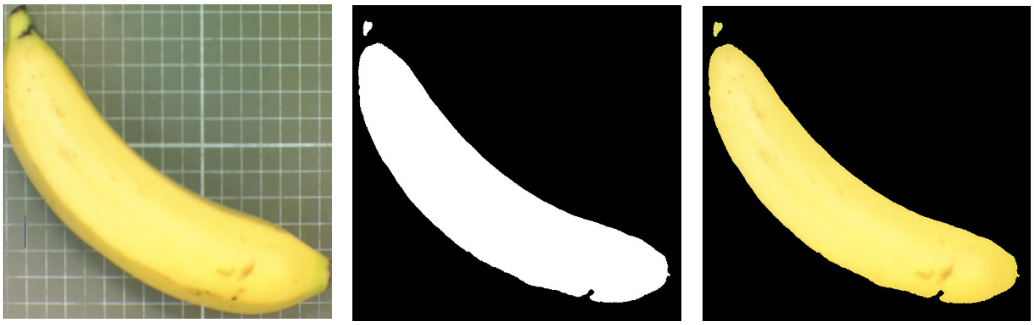

(a) (b) (c)

Fig.3: Banana images: (a) an original image, (b) a binary image and (c) a true image of the banana

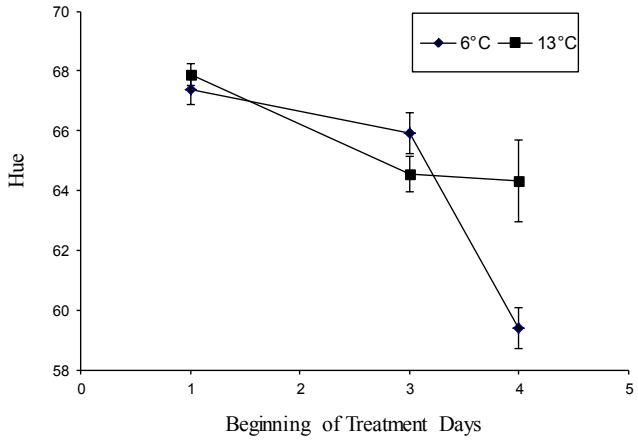

Fig.4: Change of hue values by treatment days

The change became severe when the exposure was prolonged. This is illustrated by the steep slope of the plot between the beginning of day 3 and day 4. At the beginning of day 4, i.e. after one day of exposure to ambient temperature, the hue value dropped to below 60°, which corresponded to brown in the HSI colour chart. Meanwhile, no change was observed on the control samples. The slight decrease that was shown in the hue value on the control samples was basically due to the normal ripening process.

The results of ANOVA revealed that the individual main effects, i.e., treatment days and temperature were statistically significant at $\alpha = 0.05$ (Table 1). In agreement with Skog (1998), the results also showed that there was a significant interaction ($p<0.05$) between the treatment days and the level of temperatures. In other words, the treatment days, the level of temperature and the interaction between them significantly affected the hue values and are thus important factors contributing towards the severity of CI in bananas. The lower the temperature is below the threshold temperature, the sooner and the more severe will be the resulting injury. The longer the duration of exposure to lower temperature, the more severe will be the CI.

Further analysis using the LSD test indicates that the day(s) of treatment was statistically different from each other (Table 2). Similar response was observed in the temperature analysis.

Post-hoc analysis showed that both the levels of temperature were statistically different (Table 3). This means that each level of temperature gives different effects to the CI symptoms. Bananas stored at 6°C were severely affected by CI, while bananas stored at 13°C were not affected and ripened normally.

TABLE 1: ANOVA of CI factors

Source	DF	Mean Square	F Value	Pr > F
Treatment Days	2	134.5183099	138.71	<.0001
Temperature	1	21.9351723	22.62	<.0001
Treatment days*temperature	2	41.7632839	43.06	<.0001

TABLE 2: Comparison of means of treatment days

t Grouping	Mean	Treatment days
A	67.6403	1
B	65.2408	3
C	61.8685	4

TABLE 3: Comparison of means of level of temperature

t Grouping	Mean	Temperature
A	65.5925	13
B	64.2405	6

Correlation

Correlation studies indicated the existence of a relationship between hue values and visual assessment, with R = 0.852. The correlation result is significant at $\alpha = 0.05$. Thus computer vision could be a feasible substitute for visual assessment in the evaluation of CI in bananas. At the end of the experiment, the brown patches became larger and darker, indicating an increasingly severe CI on the bananas. Parallel to the colour changes, the value of hue increased until a maximum value of 68.23 was reached. Descriptive statistics for hue and visual assessment is illustrated in Table 4. Meanwhile, the variation in hue with visual assessment is illustrated in Fig.5.

TABLE 4: Descriptive statistics of visual assessment and hue

Variable	Mean	Standard Deviation	Sum	Minimum	Maximum
Visual assessment	2.4792	1.1839	59.5000	1.0000	4.0000
Hue	64.2405	3.6494	1542	58.4071	68.2317

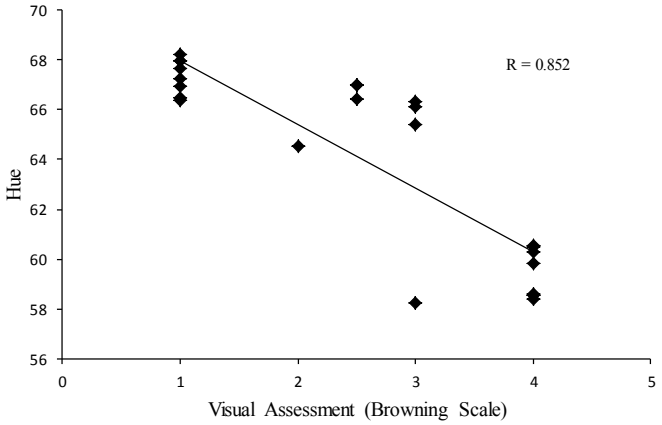

Fig.5: The correlation between hue values and visual assessment

CONCLUSION

The results of this study have successfully demonstrated the potential of applying computer vision in the detection of CI in bananas. In particular, treatment days and temperature level are important factors affecting the severity of the CI symptoms. The correlation between hue and visual assessment values indicates a high potential for the system to replace the conventional method and to offer objectivity in and automation possibility to the sorting process.

ACKNOWLEDGMENTS

The authors are grateful for the financial support received from the Ministry of Higher Education Malaysia, Universiti Putra Malaysia and Leibniz Institute for Agricultural Engineering Potsdam-Bornim (ATB), Germany, for this project.

REFERENCES

Abd El-Wahab, F. K., & Nawwar, M. A. M. (1977). Physiological and biochemical studies on chilling-injury of banana. *Scientia Hoticulturae*, *7*(4), 373-376.

Beyer, M., Hahn, R., Peschel, S., Harz, M., & Knoche, M. (2002). Analysing Fruit Shape in Sweet Cherry (*Prunus avium* L.). *Scientia Horticulturae*, *96*(1-4), 139–150.

Brosnan, T., & Sun, D.-W. (2004). Improving Quality Inspection of Food Products by Computer Vision-a Review. *Journal of Food Engineering*, *61*, 3-16.

Broughton, W. J., & Wu, K. F. (1979). Storage condition and ripening of two cultivars of banana. *Scientia Horticulturae*, *10*(1), 83-93.

Chen, Y. R., Chao, K., & Kim, M. S. (2002). Machine Vision Technology for Agricultural Applications. *Computers and Electronics in Agriculture, 36*, 173-191.

Cheng, H. D., Jiang, X. H., Sun, Y., & Wang, J. (2001). Color Image Segmentation: Advances and Prospects. *Pattern Recognition*, *34*(12), 2259-2281.

Cubero, S., Aleixos, N., Moltó, E., Gómez-Sanchis, J., & Blasco, J. (2011). Advances in Machine Vision Applications for Automatic Inspection and Quality Evaluation of Fruits and Vegetables. *Food and Bioprocess Technology, 4*(4), 487-504.

Du, C. –J., & Sun, D. –W. (2004). Recent Developments in the Applications of Image Processing Techniques for Food Quality Evaluation. *Trends in Food Science and Technology*, *15*(5), 230-249.

Du, C. -J., & Sun, D. -W. (2005). Comparison of three methods for classification of pizza topping using different colour space transformations. *Journal of Food Engineering, 68*(3), 277–287.

Gunasekaran, S. (1996). Computer Vision Technology for Food Quality Assurance. *Trends in Food Science and Technology*, *7*(8), 245-256.

Kang, S. P., East, A. R., & Trujillo, F. J. (2008). Colour Vision System Evaluation of Bicolour Fruit: A Case Study with 'B74' Mango. *Postharvest Biology and Technology*, *49*(1), 77-85.

Lana, M. M., Tijskens, L. M. M., & van Kooten, O. (2006). Effects of storage temperature and stage of ripening on RGB colour aspects of fresh-cut tomato pericarp using video image analysis. *Journal of Food Engineering, 77*(4), 871–879.

Mendoza, F., Dejmek, P., & Aguilera, J. M. (2006). Calibrated Colour Measurements of Agricultural Foods Using Image Analysis," *Postharvest Biology and Technology*, *41*(3), 285-295.

Murata, T. (1969). Physiological and biochemical studies of chilling injury in bananas. *Physiologia Plantarum, 22*(2), 401–411.

Nguyen, T. B. T., Ketsa, S. & van Doorn, W. G. V. (2003). Relationship between browning and the activities of polyphenol oxidase and phenylalanine ammonia lyase in banana peel during low temperature storage. *Postharvest Biology and Technology*, *30*(2), 187-193.

Quevedo, R. A., Aguilera, J. M., & Pedreshi, F. (2010). Color of Salmon Fillets By Computer Vision and Sensory Panel. *Food and Bioprocess Technology, 3*, 637-643.

Roberto, Q., Oscar, D., Betty, R., Franco, P., & Jose, M. G. (2009). Description of the kinetic enzymatic browning in banana (*Musa cavendish*) slices using non-uniform color information from digital images. *Food Research International, 42*(9), 1309–1314.

Shearer, S. A., & Payne, F. A. (1990). Color and Defect Sorting of Bell Peppers Using Machine Vision. *Transactions of the ASAE*, *33*, 2045–2050.

Skog, L. J. (1998). *Factsheet: Chilling injury of horticultural crops*. Horticultural Research Institute of Ontaria, University of Guelph.

Tao, Y., Heinemann, P. H., Varghese, Z., Morrow, C. T., & Sommer III, H. J. (1995). Machine Vision for Color Inspection of Potatoes and Apples. *Transactions of the American Society of Agricultural Engineers*, *38*(5), 1555-1561.

Tillet, R. D. (1991). Image Analysis for Agricultural Processes: A Review of Potential Opportunities. *J. Agric. Engng. Res., 5*, 247-258.

Yam, K. L., & Papadakis, S. E. (2004). A Simple Digital Imaging Method for Measuring and Analyzing Color of Food Surfaces. *Journal of Food Engineering*, *61*(1), 137-142.

Zhang, H., Yang, S., Joyce, D. C., Jiang, Y., Qu, H., & Duan, X. (2010). Physiology and Quality Response of Harvested Banana Fruit to Cold Shock. *Postharvest Biology and Technology*, *55*(3), 154-159.

Pertanika J. Sci. & Technol. 21 (1): 119 - 126 (2013)

SCIENCE & TECHNOLOGY

Journal homepage: http://www.pertanika.upm.edu.my/

On the Integral Solutions of the Diophantine Equation $x^4 + y^4 = z^3$

S. Ismail* and K. A. Mohd Atan

Institute for Mathematical Research, Universiti Putra Malaysia,43400 Serdang, Selangor, Malaysia

ABSTRACT

This paper is concerned with the existence, types and the cardinality of the integral solutions for diophantine equation $x^4 + y^4 = z^3$ where x, y and z are integers. The aim of this paper was to develop methods to be used in finding all solutions to this equation. Results of the study show the existence of infinitely many solutions to this type of diophantine equation in the ring of integers for both cases, $x = y$ and $x \neq y$. For the case when $x = y$, the form of solutions is given by $(x, y, z) = (4n^3, 4n^3, 8n^4)$, while for the case when $x \neq y$, the form of solutions is given by $(x, y, z) = (un^{3k-1}, vn^{3k-1}, n^{4k-1})$. The main result obtained is a formulation of a generalized method to find all the solutions for both types of diophantine equations.

Keywords: Integral solutions, diophantine equation, hyperbolic equation, prime power decomposition, coprime integers

INTRODUCTION

Hyperbolic equation has been studied since ancient times; one of which was started as early as 350 years ago by Fermat who showed that the equations $x^4 + y^4 = z^2$ and $x^4 + y^4 = z^4$ have no solution in integers by using the method of proof of infinite descent (for example, refer to Dudley, 1978). Nonetheless, much of work has been done to examine various kinds of hyperbolic equations until the present time and since the variation of these equations exists, this activity will be continued into the future.

Cross (1993) studied the diophantine equation $\alpha^4 + \beta^4 \neq \gamma^4$ in Gaussian integers. In his paper, the author used cyclotomic integers by considering the special case $n = 3$ of the Fermat's Last Theorem to prove that no triplet (α, β, γ) of the non-zero members of Gaussian integers exists, $\mathbb{G}$ with $\gcd(\alpha, \beta) = 1$ such that $\pm\alpha^4 \pm \beta^4 = \pm\gamma^4$. The proof given by the author is a version of Fermat's method of infinite descent.

Similarly, Dieulefait (2005) also proved that with p a prime, $p \not\equiv -1 \ (mod\ 8)$ and

Article history:
Received: 5 March 2012
Accepted: 3 May 2012

E-mail addresses:
sha_fulica@yahoo.com.my (S. Ismail),
kamel@putra.edu.my (K. A. Mohd Atan)
*Corresponding Author

ISSN: 0128-7680 © 2013 Universiti Putra Malaysia Press.

p > 13, the diophantine equation $x^4 + y^4 = z^p$ has no solutions x, y, z with $(x, y) = 1$ and $(x, y) \neq 1$. In the same publication, the author proved that if p is a prime, $p \geq 211$, the equation $x^4 + y^4 = z^p$ would have no primitive solution in non-zero integers. Later on, the author generalized the form of equation studied and considered the following equation, $x^4 + y^4 = qz^p$. He gave a method to solve this equation for some prime values of q and every prime p bigger than 13. The author proved that the diophantine equation, $x^4 + y^4 = qz^p$, does not have any primitive solutions for $q = 73, 89$ and 113 and $p > 13$.

Grigorov and Rizov (1998) studied the diophantine equation, $x^4 + y^4 = cz^4$. In their paper, the authors gave a precise explicit estimates for the difference of the Weil height and the Neron Tate height on the elliptic curve, $v^2 = u^3 - cu$. They later applied this to prove that if $c > 2$ is a fourth power free integer and the rank of $v^2 = u^3 - cu$ is 1, the diophantine equation $x^4 + y^4 = cz^4$ would have no non-zero solution in integers.

In his publication, Poonen (1998) proved that the equation $x^n + y^n = z^m$ has no non-trivial primitive solution for $n \geq 4$. At the same time, by assuming the Shimura-Taniyama conjecture, he also proved that the equation $x^n + y^n = z^3$ has no non-trivial primitive solution for $n \geq 3$.

Motivated by the works on the equation of Fermat's equation of degree four and its variations, this research was undertaken to study the equation $x^4 + y^4 = z^3$ and to find its solutions in the ring of integers. Our quest here was to determine whether the infinitely many solutions to the equation $x^4 + y^4 = z^3$ do exist, and to solve this diophantine equation in the integer domain.

The cases of non-existence of solutions for this equation have been discussed earlier by some authors. For examples, Cohen (2002) gave an assertion as stated in Lemma 1.1. It is easy to show that the solution set of the equation $x^4 + y^4 = z^3$ is non-empty whenever $\gcd(x, y, x) > 1$. For example, $(x, y, x) = (4, 4, 8), (289, 578, 4913)$ is in the solution set. Theorem 1.1 gives a general proof of this particular assertion. Since the solution set is non-empty, we are interested to know the form of integers that satisfies this equation. However, the general forms of the solutions for such equation have not been discussed extensively. Hence, using the elementary methods in this study, we determined some explicit forms of solutions to the equation $x^4 + y^4 = z^3$ when $\gcd(x, y, x) > 1$.

RESULTS AND DISCUSSION

This paper is outlined as follows. There are three theorems discussed. Theorem 1.1 shows that the solution set of $x^4 + y^4 = z^3$ is always non-empty whenever $\gcd(x, y, x) > 1$. Theorem 1.2 deals with the case when $x = y$ and $\gcd(x, y, x) > 1$, while Theorem 1.3 deals with the case when $x \neq y$ and $\gcd(x, y, x) > 1$. We reproduced an assertion of Cohen (2002) in Lemma 1.1, which deals with the equation $x^4 + y^4 = z^3$, whereby $\gcd(x, y, x) = 1$. In addition, two corollaries are also discussed in this paper. Corollary 1.1 gives the forms of solutions for the triplet (a, b, c) when $n = u^4 + v^4$ for a pair of integers u and v is a cube in which there exist infinitely many solutions to the equation $x^4 + y^4 = z^3$. Also, Corollary 1.2 in this paper gives the form of solutions for (a, b, c), when $w = n^k$, where $w = \frac{c}{\gcd(a, b, c)}$, and n and k are positive integers.

We will show that the solution set of the equation in which $\gcd(x, y, x) > 1$ is always non-empty in the following theorem. It shows that a solution set can always be constructed from a given pair of integers.

Theorem 1.1

Suppose u and v are integers and $n = u^4 + v^4$. Let k be an integer such that $k \equiv 2(\mathrm{mod}\, 3)$. Then, $a = un^k$, $b = vn^k$ and $c = n^{\frac{4k+1}{3}}$ is in the solution set of the equation $x^4 + y^4 = z^3$.

Proof:

By multiplying both sides of the equation $n = u^4 + v^4$ with n^{4k}, the following is obtained:

$$n^{4k} \cdot n = (n^{4k} \cdot u^4) + (n^{4k} \cdot v^4)$$

or

$$n^{4k+1} = (n^k u)^4 + (n^k v)^4$$

Since $k \equiv 2(\mathrm{mod}\, 3)$, we have $4k + 1 \equiv 0(\mathrm{mod}\, 3)$.

Thus, there exists integer m such that $4k + 1 = 3m$.

It follows that

$$n^{3m} = (n^k u)^4 + (n^k v)^4$$

or

$$(n^m)^3 = (n^k u)^4 + (n^k v)^4$$

Hence, $a = un^k$, $b = vn^k$ and $c = n^m$ satisfy the equation $x^4 + y^4 = z^3$. We obtain the assertion by putting $m = \dfrac{4k+1}{3}$.

A corollary obtained from the above theorem is as shown below. The forms of solutions for the triplet (a, b, c) are obtainable when n is a cube in which case there exist infinitely many solutions to the following equation, $x^4 + y^4 = z^3$.

Corollary 1.1

Suppose u and v are integers and $n = u^4 + v^4$. Suppose $n = r^3$ for some integer, r. Let k be a positive integer. Then $a = un^k$, $b = vn^k$ and $c = n^{\frac{4k+1}{3}}$ is in the solution set of $x^4 + y^4 = z^3$.

Proof:

From the proof of Theorem 1.1, it can be shown that:

$n^{4k+1} = (n^k u)^4 + (n^k v)^4$

Let $n = r^3$, then the following will be obtained:

$(r^{4k+1})^3 = (n^k u)^4 + (n^k v)^4$

Hence, $a = un^k$, $b = vn^k$ and $c = n^{\frac{4k+1}{3}}$ is in the solution set of $x^4 + y^4 = z^3$, if n is a cube.

The following theorem gives the form of solutions to the following equation, when $x = y$ and $\gcd(a,b,c) > 1$.

Theorem 1.2:

Suppose the triplet (a,b,c) in which $a = b$ and $\gcd(a,b,c) > 1$ is a non-trivial solution to $\gcd(a,b,c) > 1$. Then a,b,c is of the form $a = b = 4n^3$ and $c = 8n^4$ for some integer, n.

Proof:

First, suppose that the triplet (a,b,c) is a solution in which $a = b$. Then, the equation will become:

$$2a^4 = c^3 \tag{1.1}$$

Clearly $2 \mid c^3$ which implies that c is even.

Hence, there exists q_j in the prime power decomposition of c such that $q_j = 2.$

Rearranging the prime power decomposition of c, let $q_1 = 2$, we will have the following:

$c = 2^{f_1} \prod_{j=2}^{m} q_j^{f_j}$ where q_j are odd primes and $f_j \geq 1$ for $1 \leq j \leq m$

Similarly, let $p_1 = 2$ in the prime power decomposition of a. Then, the following will be obtained:

$a = 2^{e_1} \prod_{i=2}^{l} p_i^{ei}$ in which q_j are odd primes, $e_1 \geq 0$, $e_i \geq 0$ for $2 \leq i \leq l$

Substituting the above expression for a and c into (1.1), the following will be obtained:

$$2^{4e_1+1}(\prod_{i=2}^{l} p_i^{4e_i}) = 2^{3f_1}(\prod_{j=2}^{m} q_j^{3f_j}) \tag{1.2}$$

By uniqueness of the prime power decomposition of a and c, we will have for each i, the integer j in such a way that $p_i = q_j$ and vice versa for $2 \leq i \leq l$, $2 \leq j \leq m$, and $l = m$.

Also, we will have $2^{4e_1+1} = 2^{3f_1}$, which implies that $4e_1 + 1 = 3f_1$

or $$3f_1 + (-4)e_1 = 1$$

Since $\gcd(3,-4) = 1$, many integral solutions to this equation do exist.

Meanwhile, we can see that $e_1 = 1$, and $f_1 = 3$ is a particular solution that satisfies this equation.

Thus, all the solutions for this equation are given by:

$$e_1 = 2 - 3t_1 \qquad \text{and} \qquad f_1 = 3 - 4t_1 \tag{1.3}$$

where t_1 is the integer.

Since e_1 and f_1 are positive integers, $t_1 \leq 0$.

Now for each $t_1 < 0$, the integer $s_1 > 0$ exists in such a way that $t_1 = -s_1$. Thus, from (1.3), we will obtain the following:

$$e_1 = 2 + 3s_1 \quad \text{and} \quad f_1 = 3 + 4s_1$$

Similarly from (1.2), by uniqueness of prime power decomposition of a and c, we will have by considering the odd prime factors of a and c that l, $p_i = q_j$ and $4e_i = 3f_j$ for some i and j, where $i, j = 2, 3, ...m$.

From here, we can see that $4 \mid 3f_j$ and $3 \mid 4e_i$.

Since $\gcd(4,3) = 1$, the integers r_j and s_i exist in such a way that $f_j = 4r_j$ and $e_i = 3s_i$.

It follows that $s_i = r_j$.

Then, the prime power decomposition of a, b and c will respectively be:

$$a = b = 2^{2+3s_1} \prod_{i=2}^{l} p_i^{3s_i} = 2^2 (2^{s_1} \prod_{i=2}^{l} p_i^{3s_i})^3$$

and

$$c = 2^{3+4s_1} \prod_{i=2}^{l} p_i^{4s_i} = 2^3 (2^{s_1} \prod_{i=2}^{l} p_i^{s_i})^4$$

Let $n = 2^{s_1} \prod_{i=2}^{l} p_i^{s_i}$ in this case.

Thus, $a = b = 4n^3$ and $c = 8n^4$ could be obtained as asserted, where n is an integer.

Now if $t_1 = 0$, we will obtain $e_1 = 2$ and $f_1 = 3$ from (1.3).

Then, the prime power decomposition of a, b and c will respectively be as follows:

$$a = b = 2^2 \prod_{i=2}^{l} p_i^{3s_i} = 2^2 (\prod_{i=2}^{l} p_i^{3s_i})^3$$

and

$$c = 2^3 \prod_{i=2}^{l} p_i^{4s_i} = 2^3 (\prod_{i=2}^{l} p_i^{s_i})^4$$

Let $n = \prod_{i=2}^{l} p_i^{s_i}$ in this case.

Thus, $a = b = 4n^3$ and $c = 8n^4$ could be obtained as asserted, where n is an integer.

Hence, the triplet $(4n^3, 4n^3, 8n^4)$ is a solution to the equation $x^4 + y^4 = z^3$, when $x = y$.

In Theorem 1.1 (i.e. where the solutions are of the form $(a,b,c) = (un^k, vn^k, n^{\frac{4k+1}{3}})$ and in Theorem 1.2 [where the solutions of this equation in which $x = y$ is $(a,b,c) = (4n^3, 4n^3, 8n^4)$], it is clear that $\gcd(a,b,c) > 1$. The subsequent Theorem 1.3 gives the forms of integral solution to the equation $x^4 + y^4 = z^3$, in which $x \neq y$ and $\gcd(a,b,c) > 1$ also. The cases in which $\gcd(x,y,z) = 1$ have been discussed by a number of earlier authors. For example, Cohen (2002) showed that non-trivial integral solutions did not exist in such cases. Thus, this assertion was reproduced in the following Lemma 1.1, the proof of which could be found in Cohen (2002).

Lemma 1.1

The equation $x^4 \pm y^4 = z^3$ has no solutions in the non-zero coprime integers, x, y, x.

The following theorem gives the form of solutions to the equation $x^4 + y^4 = z^3$ in cases when $\gcd(a,b,c) > 1$ and $x \neq y$ in terms of n, where $n = \left(\frac{x}{\gcd(x,y,z)}\right)^4 + \left(\frac{y}{\gcd(x,y,z)}\right)^4$ and $\gcd(x,y,z) = n^{3k-1}$, where k is a positive integer with $k \geq 1$.

Theorem 1.3:

Suppose the triplet (a,b,c) with $a \neq b$ and $\gcd = (a,b,c) = d$ is a solution to the equation, $x^4 + y^4 = z^3$. Let $u = \frac{a}{d}$, $v = \frac{b}{d}$ and $n = u^4 + v^4$. Let k be a positive integer. If $d = n^{3k-1}$, then $a = un^{3k-1}$, $b = vn^{3k-1}$ and $c = n^{4k-1}$.

Proof:

Since $a = du$, $b = dv$ and $d = n^{3k-1}$, we have clearly $a = un^{3k-1}$ and $b = vn^{3k-1}$.

From the following equation $a^4 + b^4 = c^3$, it follows that:

$(un^{3k-1})^4 + (un^{3k-1})^4 = c^3$ or $(n^{3k-1})(u^4 + v^4) = c^3$

Since, $n = u^4 + v^4$, we have $(n^{4k-1})^3 = c^3$

which implies that $c = n^{4k-1}$

Hence, $a = un^{3k-1}$, $b = vn^{3k-1}$ and $c = n^{4k-1}$ if $d = n^{3k-1}$, where $n = u^4 + v^4$

A corollary was obtained from the above theorem, as shown below. The forms of solution for the triplet (a,b,c) are obtainable when $w = \frac{c}{d} = n^k$.

Corollary 1.2

Suppose the triplet (a,b,c) with $a \neq b$ and $\gcd = (a,b,c) = d$ is the solution to the equation $x^4 + y^4 = z^3$. Let $u = \frac{a}{d}$, $v = \frac{b}{d}$, $w = \frac{c}{d}$ and $n = u^4 + v^4$. If $w = n^k$, then $a = un^{3k-1}$, $b = vn^{3k-1}$ and $c = n^{4k-1}$.

Proof:

From the equation, we have $a^4 + b^4 = c^3$.

It follows that $d^4(u^4 + v^4) = d^3 n^{3k}$.

Since $u^4 + v^4 = n$, we will have the following:

$$dn = n^{3k} \qquad \text{or} \qquad d = n^{3k-1}$$

From Theorem 1.3, we have then $a = un^{3k-1}$, $b = vn^{3k-1}$ and $c = n^{4k-1}$ since $d = n^{3k-1}$.

Table 1 below shows some example solutions $(a,b,c) = (un^{3k-1}, vn^{3k-1}, n^{4k-1})$ that were obtained for Theorem 1.3 for various values of k.

TABLE 1: Some examples of the integer solutions for the diophantine equation $x^4 + y^4 = z^3$ when $x \neq y$ and $\gcd(x,y,z) > 1$ for various values of k.

k	$a = un^{3k-1}$	$b = vn^{3k-1}$	$c = n^{4k-1}$	$d = n^{3k-1}$
1	$a = un^2$	$b = vn^2$	$c = n^3$	$d = n^2$
2	$a = un^5$	$b = vn^5$	$c = n^7$	$d = n^5$
3	$a = un^8$	$b = vn^8$	$c = n^{11}$	$d = n^8$
4	$a = un^{11}$	$b = vn^{11}$	$c = n^{15}$	$d = n^{11}$
5	$a = un^{14}$	$b = vn^{14}$	$c = n^{19}$	$d = n^{14}$
⋮	⋮	⋮	⋮	⋮

Note: The solution set obtained from Theorem 1.3, where $d = n^{3k-1}$ with $k \geq 1$ as represented in Table 1 is also the solution set obtainable from the forms of solutions in Theorem 1.1, in which $k \equiv 2 (\mathrm{mod}\, 3)$. In this study, the assertions of Theorem 1.1, Theorem 1.2 and Theorem 1.3 have been illustrated by showing the actual solutions for the integers (x,y,z), as in Table 2 that satisfy this equation using the C language in integer domain.

TABLE 2: Some examples of the integer solutions generated by the C language for the diophantine equation $x^4 + y^4 = z^3$ when $x = y$ and $x \neq y$.

x	y	z
4	4	8
32	32	128
108	108	648
256	256	2048
289	578	4913
500	500	5000
4000	4000	80000
6724	20172	551368
18818	28227	912673
391876	1959380	245314376
821762	2054405	263374721
340707	454276	38272753
66049	264196	16974593
⋮	⋮	⋮

CONCLUSION

From the discussion above, the non-trivial integral solutions for the diophantine equation $x^4 + y^4 = z^3$ was shown to exist when $\gcd(x, y, z) > 1$. Suppose u and v are the integers and $n = u^4 + v^4$ and k are the integer in such that $k \equiv 2 (\mathrm{mod}\, 3)$. Then, $a = un^k$, $b = vn^k$ and $c = n^{\frac{4k+1}{3}}$ are the solutions to this equation. Also, suppose u and v are the integers and $n = u^4 + v^4$. If n is a cube, the many solutions of the forms $a = un^k$, $b = vn^k$ and $c = n^{\frac{4k+1}{3}}$ would infinitely exist. As for the case when $x = y$, the triplet $(x, y, z) = (4n^3, 4n^3, 8n^4)$ where n is any integer is a solution to this equation. For the case when $x \neq y$, we have $x = un^{3k-1}$, $y = vn^{3k-1}$ and $z = n^{4k-1}$, where $n = u^4 + v^4$ and $d = n^{3k-1}$. This work points towards a future direction in the determination of solutions to a more generalized equation $x^4 + y^4 = p^k z^3$, where p is a prime and k is any positive integer.

ACKNOWLEDGEMENTS

The authors would like to acknowledge the Laboratory of Theoretical Studies, Institute of Mathematical Research (INSPEM), Universiti Putra Malaysia for supporting this research.

REFERENCES

Cohen, H. (2002). The Super-Fermat Equation. In *Graduate Texts in Mathematics: Number Theory, Volume II: Analytic and Modern Tools* (6th Edn.), 463-477. New York: Springer-Verlag, Chapter 6.

Cross, J. T. (1993). In the Gaussian Integers $\alpha^4 + \beta^4 \neq \gamma^4$. *Mathematics Magazine, 66*(2), 105-108.

Dieulefait, L. V. (2005). Modular congruences, Q-curves, and the diophantine equation $x^4 + y^4 = z^p$. *Bull. Belg. Math. Soc. Simon Stevin*., *12*(13), 363-369.

Dieulefait, L. V. (2005). Solving diophantine equations $x^4 + y^4 = qz^p$. *Acta Arith, 117*(3), 207-211.

Dudley, U. (1978). *Elementary Number Theory* (2nd Edn.) San Francisco: W. H. Freeman and Company.

Grigorov, G., & Rizov, J. (1998). *Heights on elliptic curves and the diophantine equation* $x^4 + y^4 = cz^4$. *1-9*.

Poonen, B. (1998). Some diophantine equations of the form $x^n + y^n = z^m$. *Acta Arith, LXXXVI, 3*, 193-205.

Pertanika J. Sci. & Technol. 21 (1): 127 - 134 (2013)

SCIENCE & TECHNOLOGY

Journal homepage: http://www.pertanika.upm.edu.my/

Radiation-Induced Formation of Acrylated Palm Oil Nanoparticle Using Pluronic F-127 Microemulsion System

Tajau, R.[1]*, Wan Yunus, W. M. Z.[2], Mohd Dahlan, K. Z.[3], Mahmood, M. H.[1], Hashim, K.[4], Ismail, M.[5], Salleh, M.[1] and Che Ismail, R.[1]

[1]*Synthesis and Radiation Curing Group, Division of Radiation Processing Technology (BTS), Malaysian Nuclear Agency, Bangi, 43000 Kajang, Selangor, Malaysia*

[2]*Department of Chemistry, Centre For Defence Foundation Studies, National Defence University Malaysia, 57000 Sungai Besi Camp, Kuala Lumpur, Malaysia*

[3]*Division Director's Office, Division of Radiation Processing Technology (BTS), Malaysian Nuclear Agency, Bangi, 43000 Kajang, Selangor, Malaysia*

[4]*Polymer Modification Radiation Group, Division of Radiation Processing Technology (BTS), Malaysian Nuclear Agency, Bangi, 43000 Kajang, Selangor, Malaysia*

[5]*Laboratory of Molecular Biomedicine, Institute of Bioscience, Universiti Putra Malaysia, 43400 Serdang, Selangor, Malaysia*

ABSTRACT

This study demonstrated the utilization of radiation-induced initiator methods for the formation of nanoparticles of Acrylated Palm Oil (APO) using aqueous Pluronic F-127 (PF-127) microemulsion system. This microemulsion system was subjected to gamma irradiation to form the crosslinked APO nanoparticles. Dynamic light scattering (DLS), Fourier Transform Infrared (FTIR) spectroscopy and Transmission Electron Microscopy (TEM) were used to characterize the size and the chemical structure of the nanoparticles. As a result, the size of the APO nanoparticle was decreased when the irradiation dose increased. The decrease in size might be due to the effects of intermolecular crosslinking and intramolecular crosslinking reactions of the APO nanoparticles during irradiation process. The size of the nanoparticle is in the range of 98 to 200 nanometer (nm) after irradiation using gamma irradiator. This radiation-induced method provides a free initiator induced and easy to control process as compared to the classical or chemical initiator process. The study has shown that radiation-induced initiator methods, namely, polymerization and crosslinking in the microemulsion, were promising for the synthesis of nanoparticles.

Keywords: Acrylated palm oil, nanoparticle, radiation crosslinking, ionizing radiation

Article history:
Received: 28 July 2011
Accepted: 13 January 2012

E-mail addresses:
rida@nuclearmalaysia.gov.my (Tajau, R.),
wanmdzin@gmail.com (Wan Yunus, W. M. Z.),
khairul@nuclearmalaysia.gov.my (Mohd Dahlan, K. Z.)
hilmi@nuclearmalaysia.gov.my (Mahmood, M. H.),
kbhashim@nuclearmalaysia.gov.my (Hashim, K.),
maznah@medic.upm.edu.my (Ismail, M.),
mekzah@nuclearmalayisa.gov.my (Salleh, M.),
rosley@nuclearmalaysia.gov.my (Che Ismail, R.)
*Corresponding Author

ISSN: 0128-7680 © 2013 Universiti Putra Malaysia Press.

INTRODUCTION

A high energy radiation, i.e. gamma-rays (γ-rays), provides in principle an ideal initiator for emulsion polymerization because of its high degree of penetration (Stannett & Stahel, 1991). The radiation-induced polymerization method offers more benefits as compared to the thermal decomposition of chemical initiators method due to its (gamma-ray) ability to induce polymerization, which can be controlled more easily when the homogenously γ-ray irradiation is penetrating through the sample. The system is independence of temperature and no additional component has been introduced in the system that might influence the reaction (Chen & Zhang, 2007).

There are studies which have reported that the nanogels and microgels (nanoparticle and microparticle) can be synthesized by combination of polymerization and cross-linking process, usually in the emulsion system (e.g., Ravi Kumar *et al*., 2004; Rosiak *et al*., 2003; Ulanski *et al*., 2002). Ulanski and co-workers (1998) reported that the nanogels and microgels produced using the radiation technique are suited for biomedical applications. In more specific, they described that this method or process is free of initiators, monomers and any other additives and it can be used to produce a drug carrier for controlled drug delivery system. Besides that, this method is able to control the size and composition of the microscopic polymer structure through a proper selection of the polymer concentration, type of the irradiation and dose rate (Rosiak *et al*., 2003).

Furthermore, natural polymers, such as vegetable oils, have been used in developing nanoparticles as a carrier for controlled drug delivery. The microemulsion-based plant and vegetable oil formulations have been found promising in a number of drug delivery applications (Corswant *et al*., 1998). In this work, Acrylated Palm Oil (APO) microemulsion mainly contains the water, while modified palm oil and the PF-127 were used to produce the APO nanoparticle. The microemulsion system was chosen to formulate this APO nanoparticle due to its unique characteristic, whereby its dispersed phase consists of small droplets with a diameter in the range of 100-1000 Armstrong (A^o) (Sharma & Shah, 1985). Besides that, miniemulsion system using water as the dispersed phase is a plentiful, nontoxic, environmental friendly and inexpensive system (Wang *et al*., 2007).

Thus, in the present study, the focus of research was to develop nanoparticle of Acrylated Palm Oil (APO) that could sustainably be used as drug carriers through the radiation-induced initiator method. The work includes examining the effects of concentration of polymer and radiation dose on the size, microstructure and the physiochemical structure of nanoparticles.

MATERIALS AND METHODS

Materials

An APO was produced in the Radiation Technology Division, Malaysian Nuclear Agency (Nuclear Malaysia) Bangi, 43000 Kajang, Selangor, Malaysia and PF-127 purchased from Sigma Aldrich was used as a surfactant. Double distilled and deionized water prepared at Nuclear Malaysia was used to prepare the microemulsion.

Preparation of the APO Nanoparticles

A standard microemulsion system consisting of three components [water, oil (APO) and non-ionic surfactant (PF-127)] was developed to formulate the APO nano-droplets. One concentration of PF-127 surfactant at 0.00039M was used to develop the micellar. Then, two volumes of APO (i.e. 0.18% and 1.8%) were added to the micellar system, respectively. The samples were stirred for one hour at 400 rpm using a magnetic stirrer. Then, they were stirred continuously using a high speed mechanical stirrer (Dispermat, VMA-Getzmann GMBH) for at least one hour at 3000 rpm. The vessels were closed tightly using Para film and degassed for 30 minutes using nitrogen gas. After degassing, the vessel was screwed capped immediately. The samples were then irradiated at 0.36, 0.5, 1, 5, 10, 15 and 25 kiloGray (kGy) using gamma irradiation for fabrication of nanoparticles of the cross-linked APO.

Characterization of the Nanoparticles

The samples were ultrafiltered using a disposable polytetrafluoroethylene (PTFE) teflon filter for removing suspended materials or impurity. The filtrates were collected to determine their size. The filtrates were placed in 1 cm quartz cell before the measurement was done. The mean diameter of the samples was determined by photon cross correlation spectroscopy (PCCS) using a dynamic light scattering (Sympatec Nanophox). The wavelength for this PCCS was at 632 nm. Infra-red spectrum was performed using Fourier Transform Infrared (FTIR) spectroscopy (Perkin Elmer). The FTIR spectroscopy was used to characterize the carbon double bond (C=C) crosslinking transformation of the sample. The Perkin Elmer Spectrophotometer was set-up at spectra in the range of 4000 cm^{-1} to 500 cm^{-1}. The dried samples were analyzed using Attenuated Total Reflectance (ATR) method. The Transmission Electron Microscopy (TEM) images were obtained using a Zeiss microscope (JEOL, Japan) and analyzed at the voltage range of 80-120 kilovolt (kV). The dried samples were placed on a copper grid prior to analysis.

RESULT AND DISCUSSIONS

Formation of APO Nanoparticles

Table 1 tabulated the size of the APO nanoparticle before and after irradiation, as characterized by the dynamic light scattering (DLS). This study found that the size of the APO nanoparticle decreased when increasing the irradiation dose. This was due to the intraparticle crosslinking of the radicals and the hampered diffusion of monomer molecules to the structure (Ulanski & Rosiak, 2004). The intermolecular crosslinking of the nanoparticles was dominant at irradiation process of 1 kGy or lower of the irradiation dose. However, above 1 kGy, the crosslingking reaction of the particles might involve both intermolecular and intramolecular crosslinking proceses. This study revealed that the sample underwent crosslinking, leading to the formation of smaller size of the APO nanoparticles (see Table 1). After the sample had been exposed to the gamma irradiation, the water molecule underwent hydrolysis. As a result, initial reactive intermediates were formed, such as hydroxyl radicals ($^{\bullet}OH$), H-atoms ($H^{\bullet}$) and hydrated electrons (Equation 1). Then, the OH radicals and the H atoms reacted with APO macromolecules by hydrogen abstraction. As a result of this process, a radical was formed on

the acrylate's carbon double bond of the APO macromolecule C=C-C- → •C-C-C- (Equation 2). Afterward in the APO molecular structure, these radicals •C-C-C- underwent crosslinking reaction and this resulted in the formation of networking between the APO chains after being subjected to the maximum dose of gamma irradiation (Equation 3). In this study, the maximum dose for the APO nanoparticle to undergo the crosslinking was approximately between 10 to 25 kGy using gamma irradiation. Ulanski and Rosiak (1999) reported that the nanogel dimensions became smaller as compared to the parent (origin) polymer because of the shrinkage of the initial loose and mobile polymer coils into a more tightly bound entities. In this study, the smallest size of the APO particle formation was approximately 98.70 nm at 25 kGy in the 0.18% of the APO/PF-127 system. Besides that, the study also showed that the higher APO content sample produced bigger particle size, as shown in Table 1.

TABLE 1: Size of the PF127/APO nanoparticles upon irradiation

Dose (kGy)	Particle Size, nm	
	0.18% APO	1.8% APO
0	184.74	219.45
0.36	172.94	192.72
0.50	122.29	173.48
1	115.36	132.36
5	114.99	132.35
10	99.37	130.65
15	99.45	133.05
25	98.70	141.80

**kGy-kiloGray, nm-nanometer*

$$H_2O \xrightarrow{\gamma} {}^{\bullet}OH,\ H^{\bullet},\ e^-_{aq},\ H^+,\ OH^-,\ H_2O_2,\ H_2 \qquad \text{[Equation 1]}$$

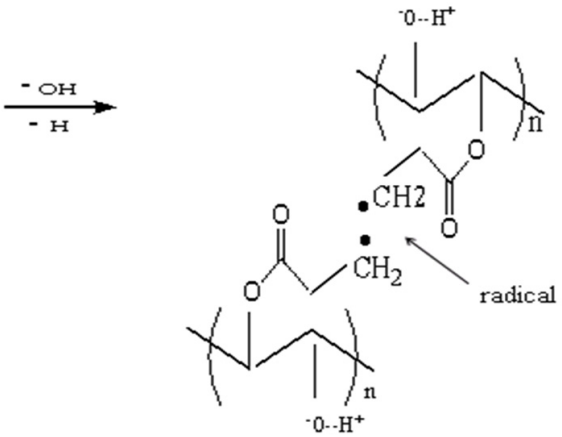

"radical generation"

[Equation 2]

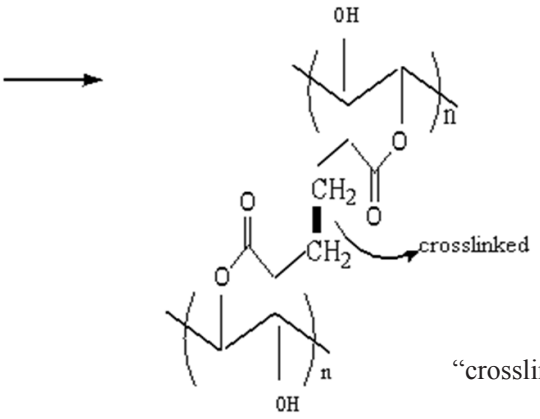

"crosslinking"

[Equation 3]

Fourier Transform Infra-red (FTIR) Spectra Analysis

Fig.1 shows the spectrum of the APO nanoparticle before and after irradiation. The spectrum clearly showed that the IR peaks of the APO nanoparticle underwent transition schematically from 0 kGy, 1 kGy, until the 25 kGy. As detected by the IR spectrum in Fig.1 (*see* the spectrum before irradiation at 0 kGy), it was demonstrated that the peaks at 2921 -2856 cm^{-1} represented -CH stretching from the PF-127 and the APO mixture, whereby these peaks consequently illustrated the existence of the microemulsion hydrocarbon or the micellar core. Furthermore, the peaks of 3432, 1741, 1638, 1404, 985, 810 and 1282-1243 cm^{-1} represent the APO's functional groups such as -OH (alcohol), C=O (carbonyl), C=C (acrylate's carbon-carbon

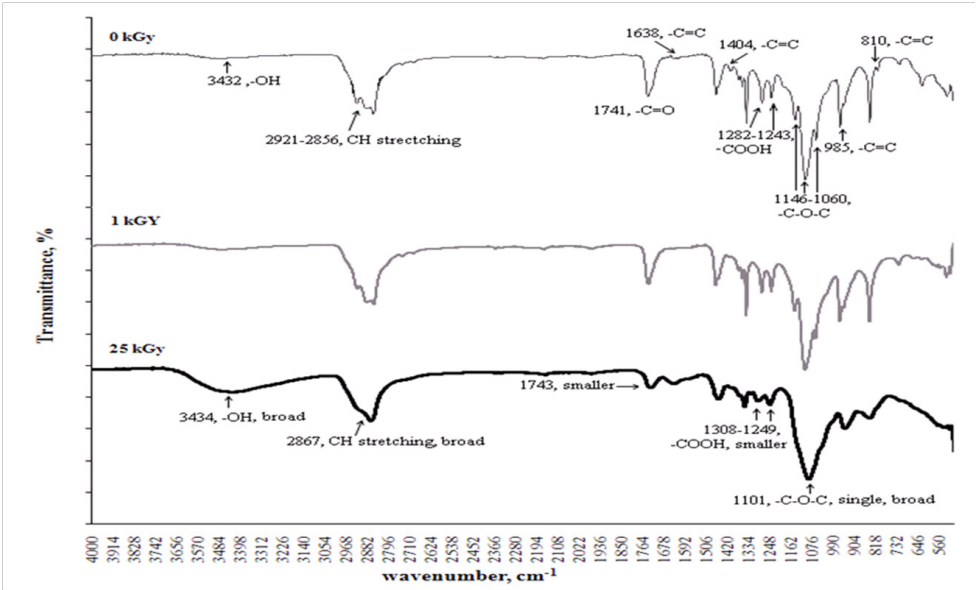

Fig.1: FTIR spectra of the APO/PF127 nanoparticle, before (at 0 kGy) and after irradiation at 1 kGy and 25 kGy, respectively.

double bond) and COOH (carboxylic). The bands at 1146 to 1060 cm^{-1} were due to the presence of PO (propylene oxide) chains (C-O-C) of hydrocarbon chains of the PF-127.

After irradiation, the peaks slowly underwent transition at 1 kGy (see Fig.1, spectrum at 1 kGy). When the irradiation dose increased to 25kGy, the carbon double bond (C=C) peaks disappeared at 1638, 1404, 985 and 810 cm^{-1}, confirming that the APO nanoparticle was completely crosslinked (see Fig.1, spectrum at 25 kGy). Besides that, the height peak of -OH at 3434 cm^{-1} was increasing and becoming broader due to the increasing amount of APO networking chains. The occurrence of the interaction between the hydrocarbons chains of PO and APO was illustrated by the appearances of the broad and single -CH stretching peaks at 2867 cm^{-1}. Meanwhile, the existence of C-O-C of the PO group was demonstrated by the appearance of the single and broad peak at 1101 cm^{-1}. Furthermore, the C=O and COOH peaks were also shown to be smaller and broader at 1743 cm^{-1} and 1308-1249 cm^{-1}, respectively. This study revealed that the polymerization and the crosslinking process to form the APO nanoparticle seemed to be completed at 25 kGy.

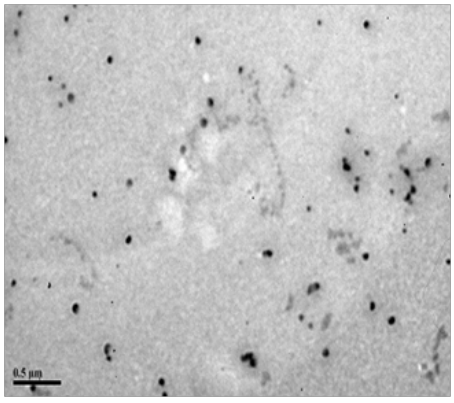

120 kV, magnification: 5000
(a) Before irradiation

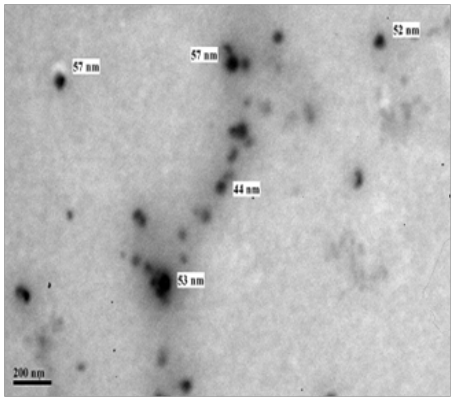

120 kV, magnification: 10 000
(b) Before irradiation

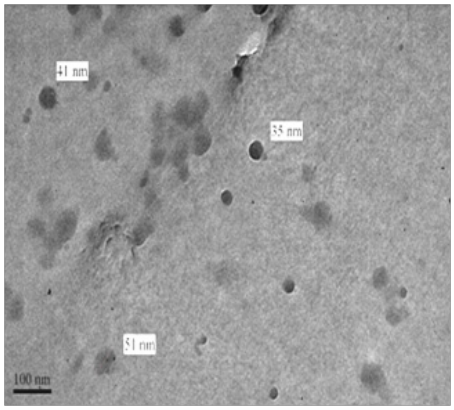

80 kV, magnification:20 000
(c) After irradiation at 1kGy

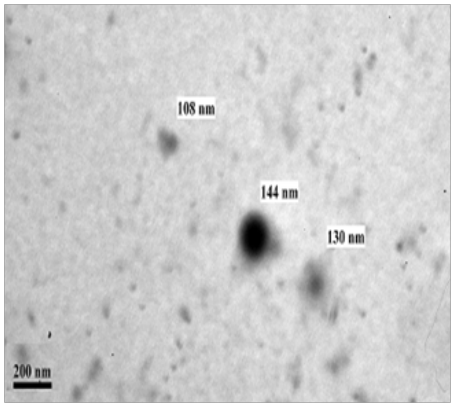

120kV, magnification:10 000
(d) After irradiation at 25kGy

Fig.2: The TEM images of the APO/PF-127 nanoparticles formulated with 1.8% w/v EPOLA in 0.00039 M PF-127, before (*a*,*b* at 0 kGy) and after irradiation (*c* at 1 kGy and *d* at 25 kGy)

Transmission Electron Microscopy (TEM) Images

Fig.2 shows images of the APO nanoparticle before and after irradiation. As illustrated in the figure, the size of the nanoparticle was approximately in the range of 44-57 nm (Fig.2b) for the before irradiation, 35-51 nm (Fig. 2c) and 108-144 nm (Fig.2d) for the after irradiation at 1 and 25 kGy, respectively. The shape of the APO nanoparticle was spherical and its size distribution was not uniform. The main factor of the particle size enlargement after irradiation at 25 kGy (Fig. 2d) was due to the diffusion of the hydrophobic core of PO and APO, in addition to the growth of C=C crosslinked chains in the nanoparticle.

CONCLUSION

This study has shown that the APO nanoparticles were successfully developed by using the radiation-induced initiator method in the microemulsion system. The results obtained revealed that the size of the APO nanoparticle produced in this study was in the nanometer and submicron, which was below 200 nm particle size after irradiation using gamma-rays. The size of the APO nanoparticles depended upon the irradiation doses and the microemulsion formulations.

ACKNOWLEDGMENTS

The authors are indebted to the Government of Malaysia through the Ministry of Science, Technology and Innovation (MOSTI) and the Public Service Department (JPA) for their financial (SCIENCEFUND: 03-03-01-SF0052 and HLP) and technical supports in implementing this study. In particular, the author gratefully acknowledged the grants (HCD Fund-RMK9) provided by the Malaysian Nuclear Agency (Nuclear Malaysia) for the project (MINT R&D 05-025-01).

REFERENCES

Chen, J., & Zhang, Z. C. (2007). Radiation-induced polymerization of methyl methacrylate in microemulsion with high monomer content. *Journal of European Polymer*, *43*, 1188-1194.

Corswant, C. V., Thorean, P., & Engstrom, S. (1998). Triglyceride-based microemulsion for intravenous administration of sparingly soluble substances. *Journal of Pharmaceutical Sciences*, *87*(2), 200-208.

Ravi Kumar, M. N. V., Sameti, M., Kneuer, C., Lamprecht, A., & Lehr, C. M. (2004). Polymeric Nanoparticles for Drug and Gene Delivery. *Encyclopedia of Nanoscience And Nanotechnology*, *9*, 1-9.

Rosiak, J. M., Janik, I., Kadlubowski, S., Kozicki, M., Kujawa, P., Stasica, P., & Ulanski, P. (2003). Nano-, Micro- And Macroscopic Hydrogels Synthesized By Radiation Technique. *Nuclear Instruments and Methods in Physics Research B*, *208*, 325-330.

Sharma, M. K., & Shah, D. O. (1985). *Macro- and Microemulsions: Theory and Applications*. Washington: American Chemical Society.

Stannett, V. T., & Stahel, E. P. (1991). *Radiation Processing (An Overview in Radiation Processing of Polymers)*. New York: Hanser Publishers.

Ulanski, P., Janik, I., & Rosiak, J. M. (1998). Radiation Formation of Polymeric Nanogels. *Radiation Physics and Chemistry, 52*, 1-6.

Ulanski, P., & Rosiak, J. M. (1999). The use of radiation technique in the synthesis of polymeric nanogels, *Journal of Nuclear Instruments and Methods in Physics Research (B)*, *151*, 356-360.

Ulanski, P., Kadlubowski, S., & Rosiak, J. M. (2002). Synthesis of Poly (acrylic acid) Nanogels by Preparative Pulse Radiolysis. *Radiation Physics and Chemistry, 63*, 533-537.

Ulanski, P., & Rosiak, J. M. (2004). Polymeric Nano/Microgels. *Encyclopedia of Nanoscience and Nanotechnology*, *X*, 1-26.

Wang, S., Wang, X., & Zhang, Z. (2007). Preparation of polystyrene particles with narrow particle size distribution by γ–ray initiated miniemulsion polymerization stabilized by polymeric surfactant. *Journal of European Polymer*, *43*, 178-184.

Pertanika J. Sci. & Technol. 21 (1): 135 - 140 (2013)

SCIENCE & TECHNOLOGY

Journal homepage: http://www.pertanika.upm.edu.my/

Induced Tensile Properties With EB- Cross Linking of Hybridized Kenaf/Palf Reinforced HDPE Composite

Aji, I. S.[1]*, Zinudin, E. S.[2], Khairul, M. Z.[3], Abdan, K.[4] and S. M. Sapuan[1]

[1]Department of Mechanical and Manufacturing Engineering, Faculty of Engineering, Universiti Putra Malysia, 43400 Serdang, Selangor, Malaysia

[2]Institute of Tropical Forestry and Forest Products, Laboratory of Biocomposite technology, Universiti Putra Malysia, 43400 Serdang, Selangor, Malaysia

[3]Polymer and Radiation Division, Malaysian Nuclear Agency, Bangi, 43000 Kajang, Selangor, Malaysia

[4]Department of Biological and Agricultural Engineering, Universiti Putra Malaysia, 43400 Serdang, Selangor, Malaysia

ABSTRACT

Electron beam irradiation, without any addition of cross-linking agents, was investigated at varying doses of EB-Irradiation to develop an environmentally friendly hybridized kenaf (bast)/ pineapple leaf fibre (PALF) bio-composites. Improvement in tensile property of the hybrid was achieved with the result showing a direct proportionality relationship between tensile properties and increasing radiation dose. Statistical analysis software (SAS) was employed to validate the result. HDPE has been shown to have self-cross-linked, enabling interesting tensile properties with irradiation. Statistical analysis validated the results obtained and also showed that adequate mixing of fibres and matrix had taken place at 95% confidence level. Hybridization and subsequent irradiation increased the tensile strength and modulus of HDPE up to 31 and 185%, respectively, at about 100kGy. Meanwhile, SEM was used to view the interaction between the fibres and matrix.

Keywords: Hybrid, cross linking, EB-irradiation, tensile properties, statistical analysis

INTRODUCTION

For many years, research has been carried out on the use of natural fibres for both automobile and structural applications. This has helped to reduce the use of synthetic materials for the sake of our environment. Nowadays, natural fibres are used to reinforce polymers that serve as matrix. Several factors have aided the

Article history:
Received: 23 July 2011
Accepted: 13 January 2012

E-mail addresses:
suleimanaji@yahoo.com (Aji, I. S.),
edisyam@gmail.com (Zinudin, E. S.),
khairul@nuclearmalaysia.gov.my (Khairul, M. Z.),
khalina@eng.upm.edu.my (Abdan, K.),
sapuan@eng.upm.edu.my S. M. Sapuan)
*Corresponding Author

ISSN: 0128-7680 © 2013 Universiti Putra Malaysia Press.

use of these natural fibres, including low cost, light weight, environmental friendliness, ease of formulation, availability in most countries, specific strength, relative non-abrasiveness to processing equipments (George *et al*., 2001; Lee *et al*., 2005; Li *et al*., 2008; Aji *et al*., 2009), just to mention a few. Meanwhile, some marketable reasons in replacing synthetic fibres with natural ones include low cost (~1/3 of glass fibres), lower density (~1/2 of glass), as well as acceptable specific strength properties and enhance energy recovery, CO_2 sequesterization and its natural tendency to degrade (Kim *et al*., 2007).

Electron beam irradiation (EBI) technique is gaining increased attention as a surface modifier and properties enhancer of various polymers, natural and synthetic fibre composites. This is because the process is devoid of wet conditions, while its clean and cold process gives rise to energy saving and high-speed enhancement of properties.

It has been reported by Han *et al*. (2006) that the presence of inner pore structure of natural fibril can be maintained by the use of EBI treatment unlike its destruction when fibres undergo alkali treatment. These pore structures can serve as insulators and collision absorbers when such composites are used in automobile and structural part. Similarly, to achieve superior strength in natural fibre composite, there is a basic need to improve fibre/matrix adhesion, and the use of adequate coupling agents and EB-Irradiation is one of the ways to achieve this (Czvikovszky, 1996). However, hybridization has been shown to be one of the ways to achieve this objective (Aji *et al*., 2011).

This work presents the response of Hybridized Kenaf/PALF reinforced HDPE Composite's tensile properties to EB-Irradiation without the addition of cross linking agents to develop an environmentally friendly bio-composite.

MATERIALS AND METHOD

Materials

Pineapple leaf (*Ananas comosus*) was bought from Perniagaan Benang Serat Nanas M&Z, with the source from Johor pineapple plantation, Malaysia. It was manually decorticated from the PALF variety of "*Josephine"*. Kenaf (*Hibiscus cannabinus*) of variety V36, which was purchased from KEFI Malaysia Sdn. Bhd., was utilized in this research. These fibres were reinforced with high density polyethylene, which was also purchased from KEFI Malaysia. The tensile strength and modulus of HDPE used as tested by us using ASTM D-638 was 29.44 MPa and 287.70 MPa, with a melting point of 180 – 240^{o}C, in addition to a melt mass flow rate of 0.10/10min (190^{o}C/2.16 kg) and a density of 0.95 g/cm^3.

Preparation of the Composite

The fibres of Kenaf and PALF (at a ratio of 1:1) and the fibre length of 0.25 mm were utilized for this particular experiment. The fibres were carefully and thoroughly mixed together in a Brabender Plasticod at a fibre loading of 50%, in 190^{o}C, at 40 rpm processing speed and for 25 minutes operating (Aji *et al*., 2011). The mixed composite obtained from the internal mixer was cut into pellets and compressed in a compression-moulding machine set at 170^{o}C, with 7 min preheat, 5 min full press, 10 seconds of venting process, and 5 min cooling of the

compressed hybrid composite sheet. Thereafter, a Dog-bone tensile specimen of 10 mm X 1.5 mm X 1 mm was cut out using a pneumatic tensile sample cutter. The test specimens were conditioned in an oven for 21 hrs at 105^{o}C prior to the tensile test.

Electron Beam Irradiation

The tensile specimens produced as described earlier were irradiated using an electron beam (EB) accelerator EPS Model-3000 at a dose range of 10–100 kGy in the sequence of 10, 20, 30, 40, 60, 80 and 100 kGy at 10 kGy per pass. All the samples were irradiated at room temperature, with accelerator energy of 2 MeV, beam current of 2 mA, and conveyor speed of 1.88 m/m.

Tensile Testing

The tensile measurement of the hybrid composite specimen was conducted using a 5 kN Bluehill INSTRON universal testing machine according to ASTM D638 as the test condition. 2 mm/min crosshead speed was used to run the machine.

RESULT AND DISCUSSIONS

The effect of radiation on the hybrid composite produced without the addition of cross-linkers is shown in Fig.1. It is clear that the tensile strength and modulus of the composite increased with the increase in the radiation dose. Although the strength of the composite dropped as compared to pure HDPE, it increased after exposure to radiation at 10 kGy and above. The increases of the tensile strength and the modulus of the hybrid composite upon irradiation are due to the fact that HDPE is a radiation cross-linkable polymer (Wilson & Burton, 1974; Singh & Silverman, 1992a; Singh, 2001). The EB irradiation of agro-fibres has been shown to induce formation of radicals that may undergo subsequence radical-radical reactions that lead to chemical bonding or may undergo radical induced chain scission that leads to degradation upon exposure to high energy radiation (Singh & Silverman, 1992b). In the current system, the radical formation of HDPE and agro-fibres led to the cross-linking between the two materials and contributed to the enhancement of the properties at lower dose of about 10 kGy. However, at higher doses, the competition between cross-linking and degradation, in particular for agro-fibres, is prominent and hence there is no significant increase in the properties of the hybrid composites between 20 kGy and 100 kGy.

SAS was used to analyze the tensile properties obtained so that statistical validation of the results can be obtained. This can help to see if adequate mixing of the hybrid has been achieved because it is the pre-requisite to achieving optimum mechanical properties. The GLM procedure and Duncan multiple range test results are shown in Table 1 for both strength and modulus. It is clear that an adequate mixing of fibres and matrix had taken place although at a probability of 5%, the replication of the specimen produced and tested is significant at lower doses. Increasing the radiation dose on the hybrid has also shown to significantly assist in improving the tensile property of the hybrid, especially in terms of the hybrid's modulus. The results have also shown that for tensile modulus, even at a probability of 1%, increasing the amount of irradiation dose is very significant in improving hybrid's modulus. Duncan's grouping

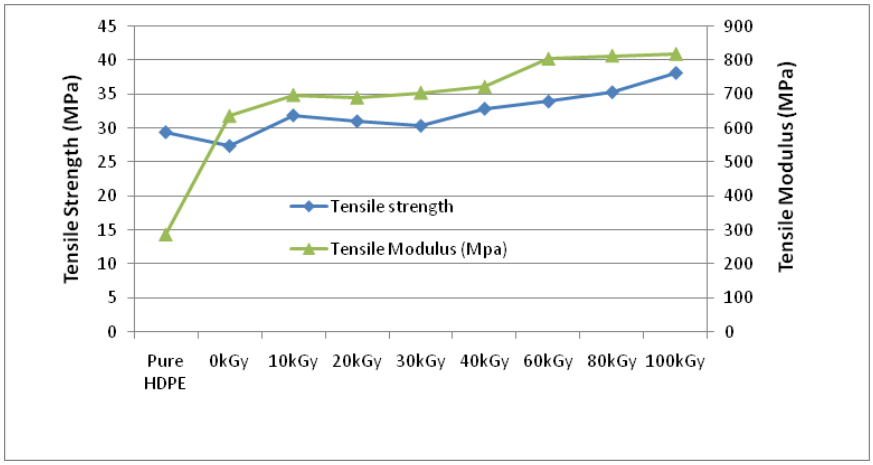

Fig.1: Variation in the tensile properties of hybridized composite

has also shown that lower dosed hybrid is closely interacting with each other. This meant that the dose applied to the hybrid was not significantly different between 10 and 40 kGy until about 60 kGy onward, where significant formation of the radicals that underwent subsequence radical-radical reactions led to increase chemical bonding, leading to greater improvement in properties, especially that of the hybrid's modulus. Hybridization and subsequent irradiation increased the tensile strength and modulus of HDPE to 31 and 185%, respectively, at about 100 kGy.

Fig.2 and Fig.3 show that this close interaction took place within the composite at lower and higher doses. This must have been the reason why there was a direct proportionality relationship between the amount of dose and the tensile properties obtained in the hybrid composite produced. It is clear that there is a tendency for higher tensile properties with the increase in dose that can be received by this kind of hybrid.

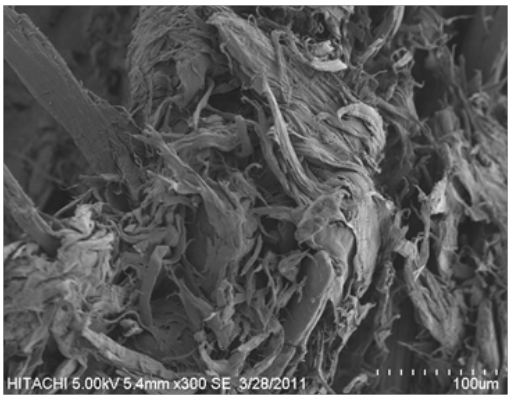

Fig.2: Tensile specimen at 10kGy without cross linking

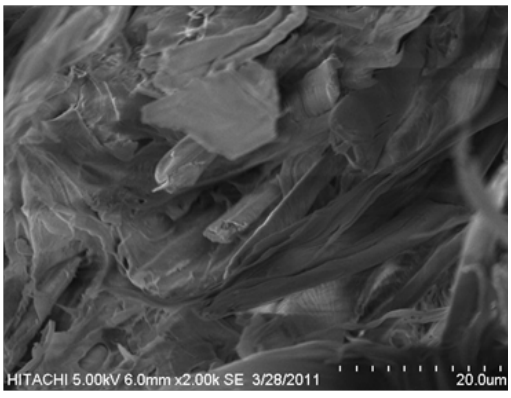

Fig.3: Tensile specimen at 100kGy without cross linking

TABLE 1: The SAS analysis for Tensile strength and Modulus: Means with the same letter are not significantly different (alpha = 0.5)

Dependent Variable: TStrength (Alpha = 0.5)

Source	DF	Sum of Squares	Mean Square	F Value	Pr > F
Model	12	497.709442	41.475787	2.05	0.0605
Error	26	524.918198	20.189161		
Corrected Total	38	1022.627640			

R-Square	Coeff Var	Root MSE	TStrength Mean
.486697	14.03633	4.493235	32.01146

Source	DF	Type I SS	Mean Square	F Value	Pr > F
Rep	4	115.6834183	28.9208546	1.43	0.2514
Trt	8	382.0260238	47.7532530	2.37	0.0463

Duncan Grouping	Mean	N	Trt
A	38.099	3	100kGy
B A	36.124	4	80kGy
B A C	33.916	5	60kGy
B A C	32.870	4	40kGy
B A C	31.899	4	10kGy
B A C	31.041	5	20kGy
B C	30.369	4	30kGy
B C	29.445	5	Neat HDPE
C	27.419	5	Un-irradiated Hybrid

TModulus

Source	DF	Sum of Squares	Mean Square	F Value	Pr > F
Model	12	1060713.996	88392.833	9.30	<.0001
Error	26	247137.190	9505.277		
Corrected Total	38	1307851.186			

R-Square	Coeff Var	Root MSE	Tstrength Mean
0.811036	14.43587	97.49501	675.3662

Source	DF	Type I SS	Mean Square	F Value	Pr > F
Rep	4	62140.6451	15535.1613	1.63	0.1956
Trt	8	998573.3508	124821.6689	13.13	<.0001

Duncan Grouping	Mean	N	Trt
A	819.90	3	100kGy
A	814.92	4	80kGy
A	805.82	5	60kGy
B A	723.01	4	40kGy
B A	705.56	4	30kGy
B A	699.12	4	10kGy
B A	691.14	5	20kGy
B	637.16	5	un-irradiated hybrid
C	287.70	5	Neat HDPE

CONCLUSION

In the current study, electron beam irradiation, without the addition of any cross linking agents, was investigated at varying doses of EB-Irradiation to develop environmentally friendly bio-composites. Improvement in the tensile properties of the hybrid was achieved, with the result showing a direct proportionality relationship between tensile properties and increased radiation dose. In particular, HDPE has been shown to be self-cross-linked, enabling interesting tensile properties with irradiation. Meanwhile, the statistical analysis conducted validated the results obtained and showed that an adequate mixing of fibres and matrix had taken place at very significant level in tensile modulus of the hybrid.

REFERENCES

Aji, I. S., S. M. Sapuan, E. S. Zainudin, & K. Abdan. (2009). Kenaf fibres as reinforcement for polymeric composites: a review. *International Journal of Mechanical and Materials Engineering (IJMME), 4*, 239–248.

Aji, I. S., E. S. Zainuddin, A. Khalina, & S. M. Sapuan. (2011). Optimizing Processing Parameters for Hybridized Kenaf/PALF Reinforced HDPE Composite. *Key Engineering Materials, 471*, 674–679.

Aji, I. S., E. S. Zainudin, A. Khalina, S. M. Sapuan, & M. D. Khairul. (2011). Studying the effect of fiber size and fiber loading on the mechanical properties of hybridized kenaf/PALF-reinforced HDPE composite. *Journal of Reinforced Plastics and Composites, 30*, 546 -553.

Czvikovszky, T. (1996). Electron-beam processing of wood fiber reinforced polypropylene. *Radiation Physics and Chemistry, 47*, 425–430.

George, J., Sreekala, M. S., & Thomas, S. (2001). A review on interface modification and characterization of natural fiber reinforced plastic composites. *Polymer Engineering & Science, 41*, 1471-1485.

Han, Y. H., Han, S. O. Cho, D., & Kim, H. I. (2006). Henequen/unsaturated polyester biocomposites: electron beam irradiation treatment and alkali treatment effects on the henequen fiber. *Macromolecular Symposia, 245-246*, 539–548.

Kim, S. W., Oh, S., & Lee, K. (2007). Variation of mechanical and thermal properties of the thermoplastics reinforced with natural fibers by electron beam processing. *Radiation Physics and Chemistry, 76*, 1711–1714.

Lee, S. M., Cho, D., Park, W. H., Lee, S. G., Han, S. O., & Drzal, L. T. (2005). Novel silk/poly (butylene succinate) biocomposites: the effect of short fibre content on their mechanical and thermal properties. *Composites Science and Technology, 65*, 647–657.

Li, Y., Hu, C., & Yu, Y. (2008). Interfacial studies of sisal fiber reinforced high density polyethylene (HDPE) composites. *Composites Part A, 39*, 570–578.

Singh, A. (2001). Irradiation of polymer blends containing a polyolefin. *Radiation Physics and Chemistry, 60*, 453–459.

Singh, A., & Silverman, J. (1992a). *Radiation processing of polymers*. Hanser Munich.

Singh, A., & Silverman, J. (1992b). *Radiation processing of polymers*. Hanser Munich.

Wilson, J. E., & Burton, M. (1974). Radiation chemistry of monomers, polymers, and plastics. *Physics Today, 27*, 50.

Pertanika J. Sci. & Technol. 21 (1): 141 - 150 (2013)

SCIENCE & TECHNOLOGY

Journal homepage: http://www.pertanika.upm.edu.my/

Thermal Properties of Alkali-Treated Sugar Palm Fibre Reinforced High Impact Polystyrene Composites

D. Bachtiar[1]*, S. M. Sapuan[1], E. S. Zainudin[2], A. Khalina[3] and K. Z. H. M. Dahlan

[1]Department of Mechanical and Manufacturing Engineering, Faculty of Engineering, Universiti Putra Malaysia, 43400 Serdang, Selangor, Malaysia

[2]Institute of Tropical Forest and Forest Products, Universiti Putra Malaysia, 43400 Serdang, Selangor, Malaysia

[3]Department of Biological and Agricultural Engineering, Faculty of Engineering, Universiti Putra Malaysia, 43400 Serdang, Selangor, Malaysia

[4]Radiation Processing Division, Malaysian Nuclear Agency, Bangi, 40300 Kajang, Selangor, Malaysia

ABSTRACT

Thermal characterization of sugar palm fibre (SPF), reinforced high impact polystyrene (HIPS) composites, was studied by means of thermogravimetric analysis. The effects of alkaline treatment and compatibilizing agent on the thermal stability of the composites were evaluated. Alkaline treatment was carried out by soaking the fibres in 4 and 6% of NaOH solution, while treatment with compatibilizing agent was employed by adding 2 and 3% maleic anhydride-graft-polystyrene (MA-g-PS) to the composites. Both the treatments were aimed to improve the mechanical performance of the composites. From the study, the thermal stability of the treated composites was found to be higher than that of untreated composites. It is shown that the incorporation of sugar palm fibre influences the degree of thermal stability of the composites. The treatments on composites also contributed to shifting the peak temperature of degradation of the composites. In other words, there are strong chemical reactions between the components of the treated composites. The thermal stability of the composites, with alkaline treatment and compatibilizing agent, was found to be better as compared to those of the untreated composites.

Keywords: Thermal stability, sugar palm fibre, high impact polystyrene, thermogravimetry

Article history:
Received: 28 July 2011
Accepted: 13 January 2012

E-mail addresses:
dandibachtiar@gmail.com (D. Bachtiar),
sapuan@eng.upm.edu.my (S. M. Sapuan),
edisyam@gmail.com (E. S. Zainudin),
khalina@eng.upm.edu.my (A. Khalina),
khairul@nuclearmalaysia.gov.my (K. Z. H. M. Dahlan)
*Corresponding Author

INTRODUCTION

The application of natural fibres in the production of thermoplastic composites is highly beneficial as these materials have been shown to improve toughness, stiffness and strength of plastic. Moreover, these materials are cheap, biodegradable and also flexible. As

ISSN: 0128-7680 © 2013 Universiti Putra Malaysia Press.

a substitute for glass fibre materials, they also reduce the wear of machinery. They are of low density and produce environmentally friendly goods (Bledzki & Gassan, 1999; George *et al*., 2001). Various types of natural fibres have been widely recognized in the study of reinforcement of thermoplastics such as sisal, abaca, kenaf, sugar palm, pineapple leaf, jute, flax, hemp, and sugarcane fibres (John & Thomas, 2008; Bledzki *et al*., 2007; Malkapuram *et al*., 2009; Joffe & Andersons, 2008).

Although natural fibre based reinforcement of thermoplastics has shown satisfactory results in some aspects, there are still problems at the interface between the fibre and matrix. They are not fully integrated due to the fact that natural fibres are hydrophilic and thermoplastics are hydrophobic. This caused poor adhesion, and thereby, stress is not fully transferred at the interface when loading takes place onto the material. In order to overcome this drawback, some treatments were usually applied. Mercerization was one famous treatment on the surface of natural fibres. Many studies by researchers everywhere have been reported on the improvement on the mechanical properties of the natural fibre composites after mercerization or alkaline treatment (Li *et al*., 2007). Another common treatment used to enhance the performance of natural fibre composites was the application of a compatibilizing agent such as maleic-anhydride to the thermoplastics matrix. The difference of this with that of the alkaline treatment is that maleic anhydride is not only used to modify the surface of fibre but also the thermoplastic matrix so as to achieve better interfacial bonding and mechanical properties in composites (Joseph *et al*., 2003). Meanwhile, dispersion of the fibres in polymer matrix was enhanced by this compatibilizing agent, and it also improved the quality of interfacial interaction that promoted adhesion of fibres and polymeric matrix.

Recently, the authors reported on the tensile properties (Bachtiar *et al*., 2011) of short sugar palm fibre reinforced high impact polystyrene composites. However, no work has reported on the thermal properties of these composites. Thermal analysis is an important analytical method in understanding the structure–property relationships and thermal stability of composite materials. Thermal analysis can be used to determine moisture content and volatile component present in composites. Since moisture content and volatile components have deteriorating effects on the properties of the composite, these studies are of great importance. Thermogravimetric (TG) analysis is one of the common methods used in assessing thermal properties of polymeric materials. The data indicate a number of stages of thermal breakdown, weight loss of the material in each stage and threshold temperature. Both TG and derivative thermogravimetry (DTG) provide information about the degree of degradation of the material (Joseph *et al*., 2003).

In the present paper, the results report on the present studies on the thermal properties of short sugar palm fibre reinforced high impact polystyrene composites under TG analysis after alkaline treatment and treatment with compatibilizing agent. The objective of the study was to look at the effects of the alkaline treatment and compatibilizing agent on the thermal stability of the composites.

MATERIALS AND METHOD

Materials

The high impact polystyrene (HIPS) used as the matrix polymer was Idemitsu PS HT 50, supplied by the Petrochemical (M) Sdn. Bhd., Pasir Gudang, Johor, Malaysia. The sugar palm fibre (SPF) was obtained from a traditional market in Aceh, Indonesia. The fibres were crushed with a pulverisette machine for shortening and sieved through 30 and 50 mesh screens. There were two types of treatment used in this study: (1) mercerization using an alkali solution and (2) polystyrene-block-poly(ethylene-ran-butylene)-block-poly(styrene-graft-maleic-anhydride) which was as a compatibilizing agent. NaOH and the MA-g-PS compatibilizing agent were supplied by Aldrich Chemical Company, Malaysia.

Treatment Processing

The first treatment was mercerization or alkali treatment. It was carried out by immersing the short fibres in NaOH solution for 1 hour at room temperature. Four and 6% NaOH were used as soaking solutions for the modification of the surface of the fibres. The fibre/solution ratio used was 1:20 (w/v). The treated fibres were then washed with distilled water to remove residual NaOH thoroughly. The drying process of the fibres was done using an oven at 100°C for 2 days. The second treatment included applying two different weight concentrations (2 and 3 wt. %) of the compatibilizing agent.

Composite Processing

The sugar palm fibres (40 wt. %) were mixed with the HIPS matrix using a common method as previously reported (Bachtiar *et al*., 2011). The HIPS (58 wt. % and 57 wt. %) and compatibilizing agent (2 wt. % and 3 wt. %) were first premixed at room temperature for 3 minutes. The HIPS and the compatibilizing agent were then placed in a mixing chamber for about 2 minutes at 50 rpm, followed by the addition of the SPF for another 10 min. of mixing. The resulting material was then compressed in the mould using a Carver laboratory press with a metal frame size of 150 mm x 150 mm x 1mm at 100 bars and 165°C of temperature. Thereafter, it was subjected to a process of pre-heating for 5 minutes and full press-heating for 5 minutes. The processing pressure is 100 kg/cm^2. This was followed by cooling for 5 minutes using circulated water in a temperature of 20^{o}C, and the final resulting composite was formed into sheets. The same technique was also applied for the alkali-treated sugar palm fibres, with a mixing composition of 40 wt. % alkali-treated fibre and 60 wt. % HIPS matrix.

Thermogravimetric Analysis

Thermogravimetric (TG) analysis is a common method used in understanding the relationship between the structure-property and thermal stability of composite materials. This testing was carried out on the specimens to calculate the degradability of weight in relation to change in the temperature. A TGA/SDTA 851^e Mettler Toledo device was used. The specimens were observed from 30 to 600^{o}C at a heating rate of 20 deg. C/min. and the nitrogen gas flow was 50 mL min. The weight of the samples varied from 6 mg to 20 mg.

RESULTS AND DISCUSSION

The TG analysis of sugar palm fibre, HIPS polymeric matrix, untreated SPF-HIPS composites and treated SPF-HIPS composites were studied as a function of % weight loss with the increase in temperature. Fig.1 and Fig.2 show the TG and Derivative TG curves of sugar palm fibre, neat HIPS and the untreated SPF-HIPS composites, respectively. The degradation level of sugar palm fibre was almost similar to that of other natural fibres. It was differentiated by the variability of three main natural fibre components, namely, hemicelluloses, cellulose and lignin, while sugar palm fibre was subjected to the heating decomposition of each component that takes place in three steps. The first one was initial weight loss at 56 to 165°C, known as moisture evaporation and the loss of volatile extractives. Kim *et al*. (2004) reported that the initial mass loss took place from 50 to 150°C for natural fibre from rice husk and wood fibre. Meanwhile, Ishak *et al*. (2011) found that the range for this step was 45 to 123°C and Zainudin *et al*. (2009) stated their findings at 35 to 115°C for banana pseudo-stem fibre. These differences occurred due to the diversity of water and volatile extractive content in the fibres. The TG analysis data showed that at 56°C, the initial mass loss was at 99.7% weight and at 165°C, the weight was 89%. These findings indicated that 10.7% moisture and volatile extractive content had been removed from the fibre.

The second step was the decomposition of hemicelluloses components at temperature ranging from 238 to 306°C, and the peak temperature for this phase was 287.4°C. This result was almost similar to that of Yang *et al*. (2007) who reported that the temperature ranging from 220 to 318°C and peak temperature was at 281°C for hemicelluloses component. The degradation of the cellulose component started from 306°C and ended at 387.4°C, with a peak temperature of 344.46°C. The lignin degradation was not clearly seen in this curve. Yang *et al*. (2007) reported in their work that lignin is tough and the degradation of lignin takes place from 165°C up to 900°C. It was difficult to show the peak temperature for lignin degradation because the maximum mass loss rate was less (i.e. about 0.1 %/min.). From this study, it is worth saying that lignin starts to decompose at about 238°C, whereas hemicelluloses starts to degrade at 238°C. The degradation of lignin gradually takes place during the heating process

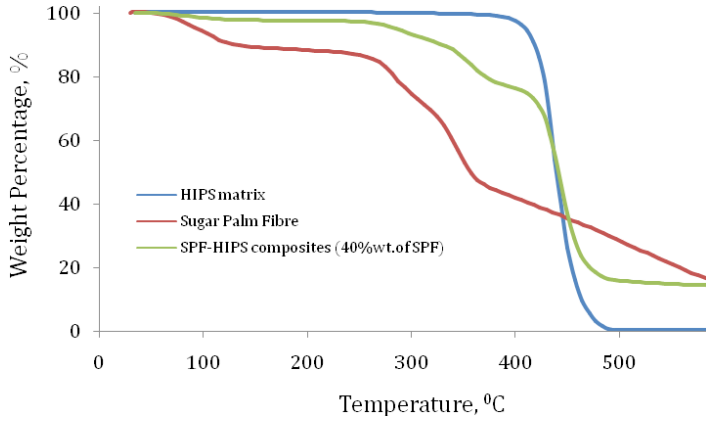

Fig.1: TGA curve of sugar palm fibre, HIPS polymer matrix and SPF-HIPS composites.

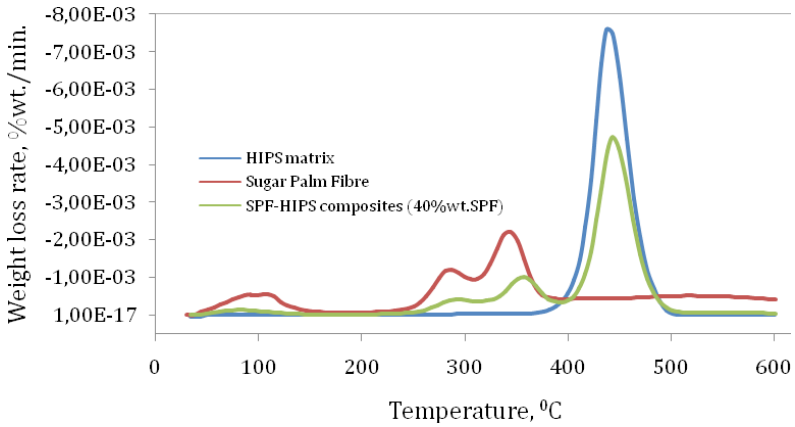

Fig.2: Derivative TG curve of sugar palm fibre, HIPS polymer matrix, and SPF-HIPS composites.

until the end at 600°C. The degradation of lignin was unidentifiable as an individual peak in the DTG curve, and this was probably because it had overlapped with the hemicelluloses and cellulose decomposition (Reed & Williams, 2004).

Thermal decomposition of HIPS matrix takes place in one single stage between 365°C and 500°C, when the polymeric chains break down and evolve into the gaseous phase (see Fig.1 and Fig.2). Almost similar results were also exhibited by other researchers (see Siregar *et al*., 2011; Vilaplana *et al*., 2007; Agung *et al*., 2011). The peak of thermogram indicating the temperature of the maximum decomposition rate appears at around 437.86°C. Vilaplana *et al*. (2007) studied the degradation of several recycle HIPS polymer. The onset (initial) temperature of the thermal decomposition has similar values for all the HIPS materials at around 365°C. Meanwhile, the temperature of the maximum decomposition rate appears at around 430°C for all the samples (Vilaplana *et al*., 2007). A summary of all the decomposition stages for sugar palm fibre, HIPS matrix and the composites is shown in Table 1.

TABLE 1: Decomposition stages of sugar palm fibre, HIPS matrix and untreated SPF-HIPS composites.

Stage	Temperature	Sugar Palm Fibre, in °C	Neat HIPS, in °C	Untreated SPF-HIPS composites (40%wt.), in °C
1	Initial weight loss, T_i	56	-	42
	Final weight loss, T_f	165	-	146
	Temp. at max. degrad., T_m	109.3	-	79.5
2	Initial weight loss, T_i	238	-	266.8
	Final weight loss, T_f	306	-	321
	Temp. at max. degrad., T_m	287.4	-	291
3	Initial weight loss, T_i	306	-	329.97
	Final weight loss, T_f	387.4	-	387.5
	Temp. at max. degrad., T_m	344.46	-	356.25

TABLE 1: (continue)

	Initial weight loss, T_i	-	365	405.4
4	Final weight loss, T_f	-	500	510
	Temp. at max. degrad., T_m	-	437.86	439.74

The degradation temperatures for the natural fibre reinforced composites usually fall between the degradation temperatures for the matrix and the fibres (Singha & Thakur, 2008). The same behaviour is also exhibited by the untreated sugar palm fibre reinforced with high impact polystyrene composites. It has been observed that for composites that the initial decomposition temperature is at 42°C and the final decomposition of the composite at 600°C, indicating that the presence of cellulose fibres does affect the degradation process. The whole degradation of the untreated composites occurs in four stages. The first stage is the moisture evaporation which starts at 42°C and ends at 146°C, with the peak temperature at 79.6°C. In this step, it can be seen that the moisture content was less, as indicated by a tiny peak at DTG curve. The second stage of weight loss occurred at 266.8°C to 321°C, with the peak of this transition at 291°C. This step of degradation indicated the decomposition of hemicelluloses content in the composites. The third step indicated the degradation of cellulose that occurred from 329.97 to 387.5°C, with the temperature at the maximum degradation at 356.25°C. The fourth step indicated the degradation of the HIPS polymer part in the composites that occurred from 405.4 to 510°C and the peak of this transition was observed at 439.74°C. The value is slightly higher than the peak transition of neat HIPS matrix. Hence, it can be stated that the thermal stability of SPF-HIPS composites is better than the neat HIPS.

TGA/DTG for the Treated SPF-HIPS Composites

Fig.3 represents the TG analysis of the SPF-HIPS composites after the treatments, while Fig.4 depicts the DTG thermogram. The compatibilizing agent and alkali-treated SPF fibre on the composites slightly influence the characteristics of the thermal degradation of the composites.

For 2% MA-g-PS and 3% MA-g-PS composites, the degradation occurs in three stages, as also shown by the degradation of the untreated composites. The first stage is believed to be the decomposition of the hemicellulose component, with an initial decomposition temperature at 260°C and the final temperature at 320°C, while the peak of transition occurs at 291°C. The second stage is the decomposition of cellulose component ranging from 331°C to 417°C, and the peak was observed at about 359.38°C and 359.46°C for 2%MA-g-PS and 3%MA-g-PS composites, respectively. The last stage is the degradation of HIPS polymer in the composites that occurs initially at 416°C to 500°C, and the peak of transition temperature occurs at about 444°C. Meanwhile, at the peak temperature transition for the untreated composites (439°C), it was clearly seen that the TG curve of the compatibilizing agent modified composites was higher as compared to the untreated composites.

The compatibilizer was found to improve the thermal resistance of the composites due to the good interaction between the natural fibre and the polymer matrix that was caused by the formation of a covalent bond at the interface (Doan *et al*., 2007).

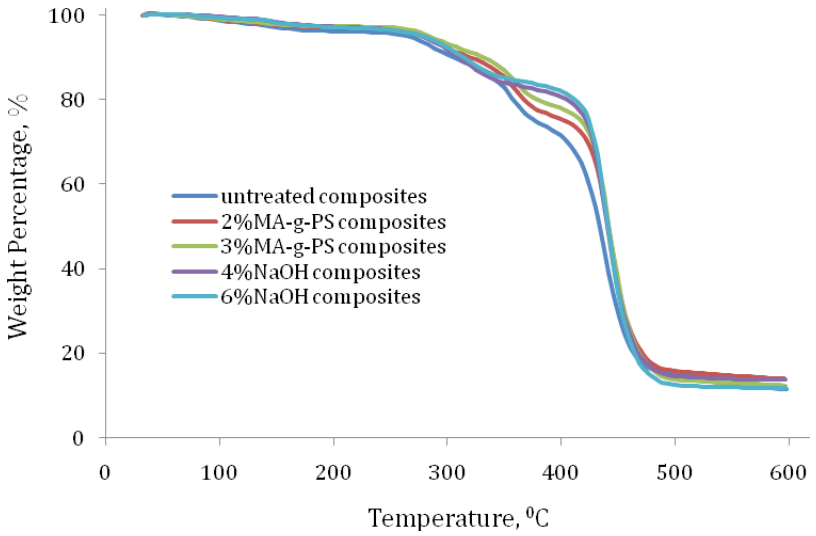

Fig.3: The TG analyses of the untreated and treated SPF-HIPS composites

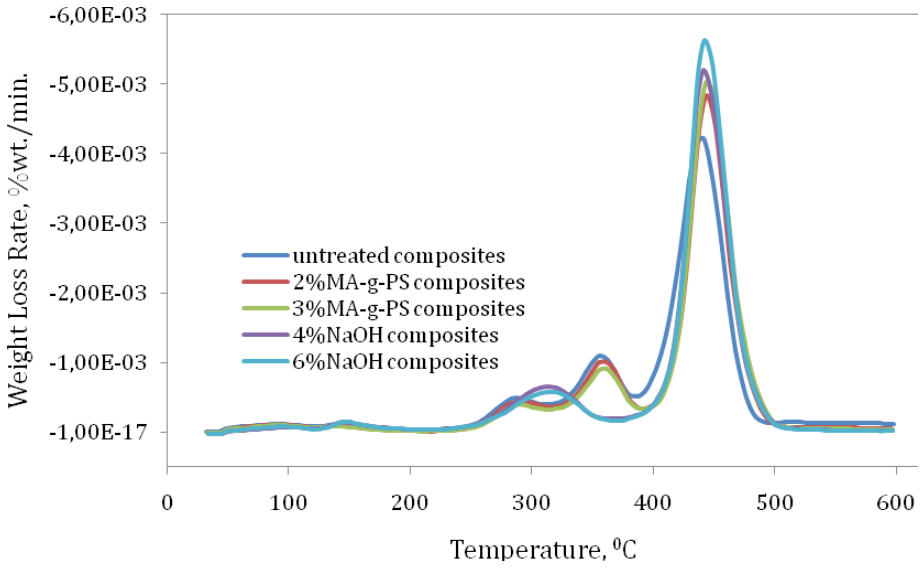

Fig.4: The DTG curve of the untreated and treated SPF-HIPS composites

The TG and DTG thermograms of the thermal decomposition treated fibre composites, with 4% and 6% of NaOH, showed different curves as compared to the TG and DTG curves of the untreated and compatibilizing agent treated composites. Only two stages appeared in the DTG curve during the degradation of the composites process. In general, this treatment removed natural and artificial impurities, produced a rough surface topography and made fibre fibrillation (Alawar *et al*., 2009). Moreover, the alkali treatment changes the structure of the fibres, removes weak amorphous components (hemicellulose and lignin) so that the

fibre retains crystalline components (cellulose) (Reddy *et al*., 2012). It was believed that the structure change in the sugar palm interior due to the DTG curve exhibits the single step for degradation of hemicellulose and cellulose components. The initial degradation of this transition was at about 261°C to the final transition temperature at about 360°C, and the peak transition temperature occurred at about 311°C. It showed a lower value than the peak transition temperature of the untreated and Ma-g-PS treated composites for the degradation of cellulose component. Otherwise, the peak transition temperature in the next step is for the HIPS matrix component in the composites which shows an almost similar value to the Ma-g-PS treated composites which was about 442°C. However, all the peak transition temperatures of the treated composites at the degradation step of the HIPS component in the composites show a higher value than the untreated composites. It was worth noting that the thermal stability of the treated composites with alkali and compatibilizing agent was higher than that of the untreated composites. The degree of thermal stability was also exhibited by the residue that remained after the heating process. Table 2 represents the percentage weight of the sample at several temperature processes. Meanwhile, Table 3 represents the residue content of the samples at 600°C. On each temperature, it can be seen that the percentage weight of the treated samples has higher values than those of the untreated composites.

TABLE 2: Weight percentage of the samples at various temperatures

Samples	200 ^{0}C (%wt.)	300 ^{0}C (%wt.)	400 ^{0}C (%wt.)	500 ^{0}C (%wt.)
Untreated composites	96.2	90.5	71.6	15.3
2%MA-g-PS composites	97.09	92.2	75.1	15.8
3%MA-g-PS composites	97.37	93.2	78	13.8
4%NaOH composites	97.26	92	80.5	14.6
6%NaOH composites	97.15	92.4	81.9	12.52

TABLE 3: Residue of the samples as the TG analysis results

Samples	Residue at 600°C (% wt.)
Sugar Palm Fibre	14.4
Neat HIPS matrix	0.39
Untreated composites (40%wt.SPF)	11.27
2% MA-g-PS composites	13.89
3% MA-g-PS composites	12.48
4% NaOH composites	13.73
6% NaOH composites	11.82

CONCLUSION

The effects of alkaline treatment and compatibilizing agent on the thermal degradation of sugar palm fibre reinforced high impact polystyrene composites were studied in the current work. The modification of the SPF-HIPS composites, using the compatibilizing agent with different weight concentrations of polystyrene-block-poly(ethylene-ran-butylene)-blockpoly(styrene-graft-maleic anhydride) and the fibres treated with alkali, has brought a slight improvement to the peak temperature of decomposition of composites. It can be stated that the addition of sugar palm fibre and the modification of the composites with alkaline treatment and compatibilizing agent on the high impact polystyrene composites resulted in a higher thermal stability of the composites than the high impact polystyrene polymer alone.

ACKNOWLEDGEMENTS

The authors wish to express their thanks to the Ministry of Agriculture and Agro-Based Industry, Malaysia, for funding the research through the Science Fund Agriculture grant number 05-01-04SF1114. The authors would also like to thank Universiti Putra Malaysia for the financial assistance through the Graduate Research Fellowship for the principal author. Special thanks also go to Mr. Ahmed Ali for proof reading the manuscript.

REFERENCES

Agung, E. H., Sapuan, S. M., Hamdan, M. M., Zaman, H. M. D. K., & Mustofa, U. (2011). Study on abaca (*Musa textilis Nee*) fibre reinforced high impact polystyrene (HIPS) composites by thermogravimetric analysis (TGA). *International Journal of the Physical Sciences*, *6*(8), 2100-2106.

Alawar, A., Hamed, A. M., & Al-Kaabi, K. (2009). Characterization of treated palm tree fibre as composites reinforcement. *Composites: Part B*, *40*, 601-606.

Bachtiar, D., Sapuan, S. M., Zainudin, E. S., Khalina, A., & Dahlan, K. Z. H. M. (2011). Effects of alkaline treatment and compatibilizing agent on tensile properties of sugar palm fibre reinforced high impact polystyrene composites. *Bioresources*, *6*(4), 4815-4823.

Bledzki, A. K., & Gassan, J. (1999). Composites reinforced with cellulose based fibres. *Progress in Polymer Science, 24*(2), 221-274.

Bledzki, A. K., Mamun, A. A., & Faruk, O. (2007). Abaca fibre reinforced PP composites and comparison with jute and flax fibre PP composites. *eXPRESS Polymer Letter*, *1*, 755-762.

Doan, T. T. L., Brodowsky, H., & Mader, E. (2007). Jute fibre/polypropylene composites II. Thermal hydrothermal and dynamic mechanical behaviour. *Composites Science and Technology*, *67,* 2707-2714.

George, J., Sreekala, M. S., & Thomas, S. (2001). A review on interface modification and characterization of natural fibre reinforced plastic composites. *Polymer Engineering & Science, 41*(9), 1471-1485.

Ishak, M. R., Sapuan, S. M., Leman, Z., Rahman, M. Z. A., & Azwar, U. M. K. (2011) Characterization of sugar palm (*Arenga pinnata*) fibres: tensile and thermal properties. *Journal of Thermal Analysis and Calorimetry*, DOI 10.1007/s10973-011-1785-1.

Joffe, R., & Andersons, J. (2008). Mechanical performance of thermoplastic matrix natural-fibre composites. In Kim, & L. Pickering (Eds.), *Properties and performance of natural-fibre composites* (p. 402-459). England: Woodhead Publishing Limited.

John, M. J., & Thomas, S. (2008). Biofibres and biocomposites. *Carbohydrate Polymers, 71*(3), 343-364.

Joseph, P. V., Joseph, K., Thomas, S., Pillai, C. K. S., Prasad, V. S., Groeninckx, G., & Sarkissova, M. (2003). The thermal and crystallization studies of short sisal fibre reinforced polypropylene composites. *Composites Part A: Applied Science and Manufacturing*, *34*(3), 253.

Kim, H. S., Yang, H. S., Kim, H. J., & Park, H. J. (2004). Thermogravimetric analysis of rice husk flour filled thermoplastic polymer composites. *Journal of Thermal Analysis and Calorimetry*, *76*(2), 395-404.

Li, X., Tabil, L. G., & Panighari, S. (2007). Chemical treatments of natural fibre for use in natural fibre-reinforced composites: a review. *Journal of Polymer and Environment, 15*, 25–33.

Malkapuram, R., Kumar, V., & Negi, Y. S. (2009). Recent development in natural fibre reinforced polypropylene composites. *J. Reinforced Plastic and Composites*, *28*, 1169-1189.

Reed, A. R., & Williams, P. T. (2004) Thermal processing of biomass natural fibre wastes by pyrolysis. *International Journal of Energy Research*, *28*, 131-145.

Reddy, K. O., Maheswari, C. U., Shukla, M., & Rajulu, A. V. (2012) Chemical composition and structural characterization of Napier grass fibres. *Materials Letters, 67*, 35–38.

Singha, A. S., & Thakur, V. K. (2008) Mechanical properties of natural fibre reinforced polymer composites. *Bulletin of Materials Science*, *31*(5), 791-799.

Siregar, J. P., Sapuan, S. M., Rahman, M. Z. A., & Dahlan, K. Z. H. M. (2011) Thermogravimetric analysis (TGA) and differential scanning calorimetric (DSC) analysis of pineapple leaf fibre (PALF) reinforced high impact polystyrene (HIPS) composites. *Pertanika Journal Science & Technology*, *19*(1), 161-170.

Vilaplana, F., Ribes-Greus, A., & Karlsson, S. (2007) Analytical strategies for the quality assessment of recycled high-impact polystyrene: A combination of thermal analysis, vibrational spectroscopy, and chromatography. *Analytica Chimica Acta*, *604*(1), 18-28.

Yang, H., Yan, R., Chen, H., Dong, H. L., & Zheng, C. (2007) Characteristics of hemicellulose, cellulose and lignin pyrolysis. *Fuel*, *86*, 1781–1788.

Zainudin, E. S., Sapuan, S. M., Abdan, K., & Mohamad, M. T. M. (2009). Thermal degradation of banana pseudo-stem filled unplasticized polyvinyl chloride (UPVC) composites. *Materials & Design*, *30*(3), 557-562.

Pertanika J. Sci. & Technol. 21 (1): 151 - 160 (2013)

PERTANIKA JOURNALS

SCIENCE & TECHNOLOGY

Journal homepage: http://www.pertanika.upm.edu.my/

FTIR and TGA Analysis of Biodegradable Poly(Lactic Acid)/ Treated Kenaf Bast Fibre: Effect of Plasticizers

N. Maizatul[1]*, I. Norazowa[2], W. M. Z. W. Yunus[3], A. Khalina[2] and K. Khalisanni[4]

[1]Department of Polymer Engineering, School of Materials Engineering, Universiti Malaysia Perlis, 02600 Jejawi, Perlis, Malaysia

[2]Laboratory of Biocomposites Technology, Institute of Tropical Forestry and Forest Product, Universiti Putra Malaysia, 43400 Serdang, Malaysia

[3]Department of Chemistry, Faculty of Science, Universiti Putra Malaysia, 43400 Serdang, Selangor, Malaysia

[4]Department of Chemistry, Faculty of Science, University of Malaya, 50603, Kuala Lumpur, Malaysia

ABSTRACT

A biodegradable composite (PLA/KBF blends) was prepared using melt blending technique in a brabender mixer and characterized with FTIR and TGA analyzer. Five percent of triacetin and glycerol contents were used as plasticizers to plasticise PLA matrix. KBF was treated with 4% NaOH solution, while 30 wt% of fibre loading was used constantly for all the composite samples. From the FTIR analysis, the additions of triacetin and glycerol to PLA composites did not produce any significant difference, and there were no chemical changes in both the plasticized PLA with the treated and untreated KBF, respectively. Observation done on the TGA analysis revealed that both plasticizers did improve the thermal stability of the composites, and this might be due to the modification on the fibre surfaces, which further led to the delay in the degradation of the PLA matrix and to significant stabilization effect.

Keywords: Polylactic acid, kenaf bast fibre, triacetin, glycerol, TGA, FTIR analysis

INTRODUCTION

In the recent years, attention has been focused on the development of technologies that utilise composite materials. However, combining biofibers with a biodegradable and renewable resource-based polymer offers additional sustainability benefits. Kenaf bast fibre (KBF) (Nina *et al.,* 2009) has received considerable interest as an environmental-friendly alternative to glass fibre in polymer

Article history:
Received: 4 August 2011
Accepted: 13 January 2012

E-mail addresses:
maizatulnisa@unimap.edu.my (N. Maizatul),
norazowa@science.upm.edu.my (I. Norazowa),
wanzin@science.upm.edu.my (W. M. Z. W. Yunus),
khalina@eng.upm.edu.my (A. Khalina),
k.khalid@um.edu.my (K. Khalisanni)
*Corresponding Author

ISSN: 0128-7680 © 2013 Universiti Putra Malaysia Press.

composites for excellent mechanical properties, especially when low density and price are taken into account. Undeniably, it has high strength and modulus to weight ratio, as well as fatigue and corrosion resistance (Islam *et al.,* 2010). Hence, great attention has been given to KBF composites, such as KBF reinforced poly(lactic acid) (PLA) composites, in which the effects of triacetin (Mingkang *et al.,* 2010; Yijun *et al.,* 2007) and glycerol (Caroline *et al.,* 2009) were studied.

Triacetin is a renewable resource-based plasticizer compared to glycerol which is a multiple plasticizer. These plasticizers are extensively used in the polymer industry and research has shown that they have the potential to improve the properties of PLA (Caroline *et al.,* 2010; Lima *et al.,* 2008; Oksman *et al.,* 2003). The use of triacetine to plasticize PLA has successfully been found to lower the melting point (Tm) and glass transition (Tg) temperature by 10°C at 25 wt%, after which phase separation occurred and the melting temperature increased. In this phenomenon, triacetine-plasticized PLA films underwent crystallization, and plasticizer molecules migrated towards the surface with storage time due to their low molecular weight resulting in improvement of the elastic properties at the cost of tensile strength (Rahul *et al.,* 2010) and high percentage of nominal strain at break (Marius *et al.,* 2008).

In contrast, glycerol is nearly and systematically incorporated in most of the hydrocolloid films because it lowers Tg and Tm and increases elongation at break (Maharana *et al.,* 2009). It is indeed a highly hygroscopic molecule that is generally added to film-forming solutions to prevent film brittleness. However, as a compromise between film mechanical resistance and flexibility to maintain low solubility and swelling in water, the use of 5–10% glycerol in the finishing cross-linking step was recommended. Concentrations lower than 3% glycerol produced brittle films, while phase separation was observed on the film surface when concentrations higher than 12% glycerol were used (Melissa *et al.,* 2011).

In this study, treated KBF was combined with PLA and impact modifier (plasticizers), a bio-based plastic which is commercially available. These renewable materials can be referred to as biocomposites due to their superior sustainability profile from the perspective of Industrial Ecology, such as calculated using the tools of life cycle analysis (Harding *et al.,* 2007; Martin *et al.,* 2007). Thus, the objective of this study was to determine the effects of triacetin and glycerol on treated KBF reinforced poly(lactic acid) composites.

MATERIALS AND METHODS

Long KBF, with the V36 variety, was obtained from Lembaga Kenaf - Tembakau Negara (LTN) in Kelantan. Meanwhile, the Kenaf stem was chipped before flaking to reduce the size of the kenaf fibre. The KBF used in this study was ground to 75-150µm. After that, the KBF was dried in an oven at 60ºC to a constant weight. This lignocellulosic fibre consists of 65% cellulose and 19% lignin. Triacetin and glycerol (1.158g/cm^3 and 1.262g/cm^3, respectively) were purchased from Sigma Aldrich Chemie GmbH, Steinheim, Germany. Meanwhile, sodium hydroxide pellet grade UN 1823 Pro Analysis consisting of 40g/mol was obtained from MERCK, Germany.

Poly(lactic acid) (PLA) (NatureWorks™ PLA 4060D) in the pellet form was obtained from Natureworks® LLC, Minnetonka, Minnesota. It is important to note that PLA has a specific

gravity of 1.25 and a melt flow index of around 15 g/10 min (190°C/2.16 Kg). Its Tg is 52°C and the melting temperature is 135°C, while its density is 1.24g/cm^3.

Preparation of the Kenaf Treatment

The concentrations of NaOH used were 2, 4, 6 and 8%, respectively. All the solutions of sodium hydroxide (NaOH) were prepared using the pellets of NaOH in deionised water and a stirrer. The fibres were then placed in these solutions for 3 hours at 25ºC. Later, the fibres were washed with distilled water until all the alkali was removed from their surface. After that, the fibres were tested for neutralisation using pH paper to confirm that there was no more alkalinity occurrence. The filter paper was placed under a sieve to avoid the fibres from leaking and being flushed out. After washing, the KBF was dried in air (ambient temperature) for two days. Next, the treated fibres were left to dry in an oven at 60°C for 24 hours.

Preparation of the PLA/Treated KBF with Triacetin and Glycerol

Prior to blending, the polymer and fibres were kept in an oven at 60˚C for 24h. PLA was premixed with several percentages of triacetin and glycerol, respectively, before they were mixed with 30 wt% of the treated KBF content. These mixtures were prepared using the Brabender internal mixer at 170˚C for 10 min at 50rpm. Pure PP was also processed in the same way to obtain a reference material. The blended materials were processed using a hot press to produce sheets of about 1mm thickness. The moulding process was carried out at the moulding temperature of 150˚C, with a 15 minute-preheat time and a pressing at full pressure for 5 minutes, followed by 8 minutes of cooling time at 827.37 kPa.

TABLE 1: The compositions at different triacetin and glycerol contents

Materials	Matrix (wt%)	KBF (wt%)	Tri/Gly (%)	NaOH (%)
Pure	100	0	-	-
Pure PP	100	0	-	-
PLA/KBF	70	30	3	4
PLA/KBF	70	30	5	4
PLA/KBF	70	30	8	4
PLA/KBF	70	30	10	4

Fourier Transform Infrared Spectroscopy (FTIR)

The Fourier Transform Infra Red (FTIR) spectroscopy was carried out using the Perkin Elmer Model 1750x FT-IR spectrometer and KBr method. The transmission of the infrared spectra was obtained in the range between 400 cm^{-1} to 4000 cm^{-1} at room temperature. The difference between the FTIR spectra was studied to find any new form of bond or interaction.

Thermogravimetric Analysis (TGA)

The thermo-stability property of the composite prepared was analysed using the Mettler Toledo TGA/SDTA 851º thermogravimetry analyser. About 10mg of the sample was used for the analysis and was heated from -50ºC to 500ºC at the rate of 10ºC/min, using about 20-25mg of the samples with a nitrogen gas flow rate of 50mL/min. The weight and percentage of the residue were recorded to determine the weight losses of the sample after heating.

RESULTS AND DISCUSSIONS

Characterization Analysis

The infrared spectra for the treated KBF, untreated KBF, plasticized PLA (triacetin), with treated and untreated KBF, are presented in Fig.1, while the results for the treated KBF reinforced plasticized PLA with triacetin (tri) and glycerol (gly) obtained using an FTIR spectrometer are shown in Fig.2.

In the alkali treatment process, the presence of Na^+ in fibre changes the hydrophilic to the hydrophobic fibre properties. Fig.1 shows peak at 3350 cm^{-1} for the untreated and treated KBF, indicating the presence of hydroxyl group. A large band at 3500-3000 cm^{-1} and a small absorption at 2950 cm^{-1} are mainly related to the hydroxyl groups and the bonded O-H stretching vibration present in carbohydrate (Bilba *et al.,* 2007). Meanwhile, the decreased intensity of the OH peak at 3350 cm^{-1} on the treated KBF compared to the untreated KBF could be clearly seen, which was assigned to the hydroxyl group and reduced due to the removal of the hemicellulose component (Ghazanfari *et al.,* 2008). However, there were no chemical changes in both the plasticized PLA with the treated and untreated KBF, respectively.

As depicted in Fig.2, both the plasticized PLA with the treated KBF samples showed that the characteristics of asorption of hydroxyl group around 3500-3200 cm^{-1} were reduced due to the removal of the hemicellulose component. Due to the alcohol group of cellulose OH deformation, another peak appeared at 1310 cm^{-1}, and this was also observed to have been decreased by the alkaline treatment.

The peaks located at 3000-2800 cm^{-1} were attributed to the CH group and this band had a higher absorption of the plasticized PLA composites with the treatment as compared to the untreated spectrum, which was rather expected since the PLA led to -CH_2- and –CH group formation (Ogata *et al.,* 1997). As for the plasticized PLA composites with the untreated and treated samples, all the samples showed the absorption band of carbonyl stretching at 1700cm^{-1}, which corresponded to the hemicelluloses, and this absorption seemed to be smaller for the treated KBF composite samples as compared to the untreated KBF composite samples. The asorption band in the range of 1600-1400 cm^{-1} region in all the composite spectra might be attributed to the presence of aromatic or benzene ring in lignin, whereas the aliphatic or aromatic (C-H) in plane deformation vibration of methyl and methoxy groups in fibres could be seen near 1400-1300 cm^{-1}. The research by Mubarak *et al.* (1993) suggested that the band in the region of 1300-1000 cm^{-1} represented the C-O stretching vibration of aliphatic primary and secondary alcohols in cellulose, hemicelluloses, lignin and primary and secondary aromatic alcohols in lignin. It was observed that there was no absorption peak at 1245 cm^{-1} for the treated

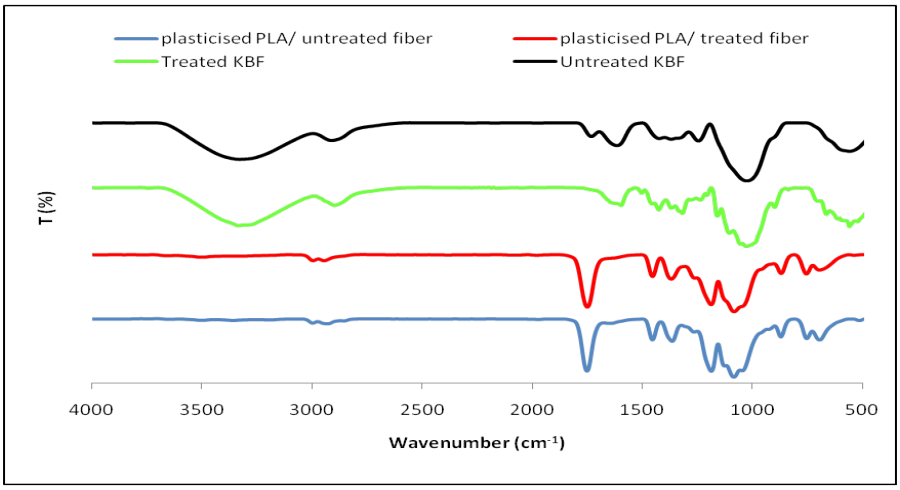

Fig.1: IR spectra for the treated KBF, untreated KBF, and plasticized PLA (tri), with treated and untreated KBF

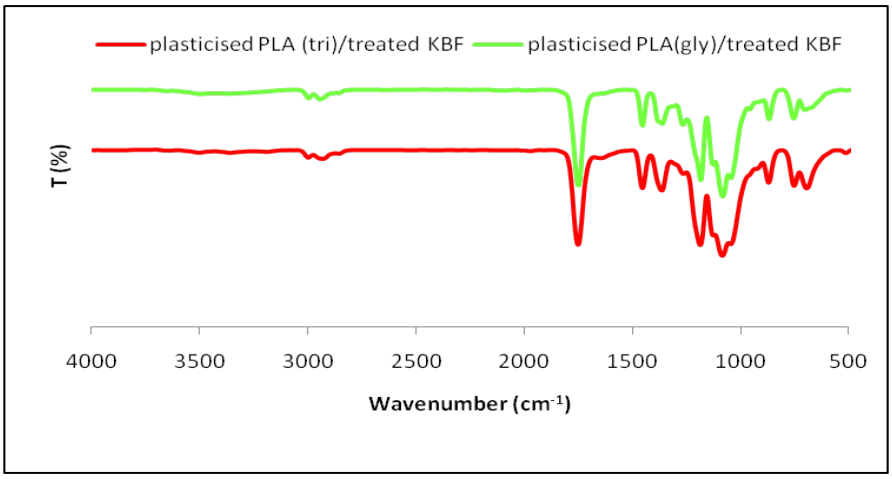

Fig.2: IR spectra of treated KBF reinforced plasticized PLA with Triacetin (tri) and glycerol (gly)

KBF for both types of plasticized PLA composite samples. This happened in the process of the surface modification as the alkaline removed the waxy epidermis tissue, adhesive pectins and hemicelluloses, which bound the fibre bundles together. The C-O-C symmetry glycocidic, stretched at 1100 cm^{-1}, arose from the polysaccharide components that were largely cellulose, and the asorption band widely appeared for the untreated and treated fibre composite systems as compared to the PLA single system.

Thermal Stability Analysis

One of the advantages of the surface modification treatment of KBF is that it makes KBF hydrophobic instead of hydrophilic. Polypropylene (PP) acts as reference to the modified composites. The thermograms depicted in Fig.3 and Fig.4 show only about 2% weight loss at

the temperature below 100°C, indicating that there was less water absorbed in the plasticized PLA (tri)/ treated KBF and plasticized PLA (gly)/treated KBF composite samples as compared to the plasticized PLA/untreated KBF composite sample and pure PLA. Meanwhile, Fig.3 shows the degradation of plasticized PLA with the untreated KBF that occurred between 250°C and 300°C, whereas the degradation of plasticized PLA (tri) with the treated KBF occurred between 350°C and 450°C, leading to a weight loss of 85.5%. The PP sample was used as a reference to the modified composites. The degradation temperature of PP was about at 360ºC.

The plasticized PLA, with the treated KBF, provided a higher decomposition temperature as the addition of the plasticizer had improved the adhesion between the PLA and fibres and prevented the migration and leaching of the plasticizer molecules from the PLA matrix at the same time. This finding is similar to that of Murariu *et al.* (2007), who also found that the decomposition temperature was increased by adding plasticizer to PLA.

The differential gravimetric analysis (DTG curve) indicated that there were decomposition peaks for the plasticized PLA treated KBF with triacetin and glycerol. The first decomposition peak, i.e. at about 300°C to 430°C, is due to thermal depolymerisation of hemicelluloses and the glycosidic linkages of cellulose, as well as α-cellulose decomposition. Lignin degraded first and at a slower rate than other constituents. The second peak occurred at about 450°C, it might also be due to the late degradation of the plasticized PLA with glycerol.

The area under the peak at 270°C for the plasticized PLA with the untreated KBF was found to be greater than both types of the plasticized PLA with the treated KBF. A possible explanation for this is that because of the treatment, which is, part of the lignin was removed from the fibre (Claudia *et al.,* 2004). Hence, this caused a better adhesion between PLA and the treated KBF, and thus influenced the decomposition temperature.

As shown in Fig.4, the thermal stability of the plasticized PLA/ treated KBF with triacetin and glycerol also improved as compared to that of the pure PLA. The increase in the thermal stability in the plasticized PLA with the treated KBF might be due to the modification done on the fibre surfaces, which delayed the degradation of the PLA matrix and to significant stabilization effect.

This can be quite well-distinguished in the interval of temperature 340-420°C in Fig.4. The thermogravimetry analysis (TGA) in Fig.4 showed that the weight loss was due to the volatilization of the plasticizers, and the degradation of the materials monitored as a function of temperature. As compared to pure PP, the thermal stability of both types of plasticized PLA/ treated KBF increased dramatically. The additions of 5% glycerol and triacetin to PLA and the treated KBF were found to have shifted the thermal stability of the composites.

CONCLUSION

The FTIR analysis of the plasticized PLA composites with the untreated and treated samples showed the absorption band of carbonyl stretching at 1700cm^{-1}, which corresponded to the hemicelluloses, and this absorption seemed to be smaller for the treated KBF composite samples as compared to the untreated KBF composite samples. Meanwhile, the additions of triacetin and glycerol to the PLA composites did not produce any significant different, and there were no chemical changes in both the plasticized PLA with the treated and untreated KBF, respectively

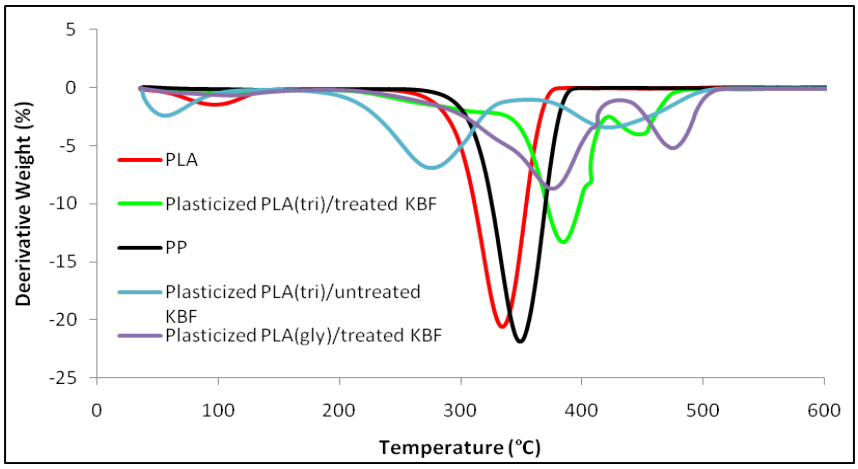

Fig.3: The DTG curves of PP, PLA, plasticized PLA/untreated KBF, and plasticized PLA/treated KBF with triacetin and glycerol

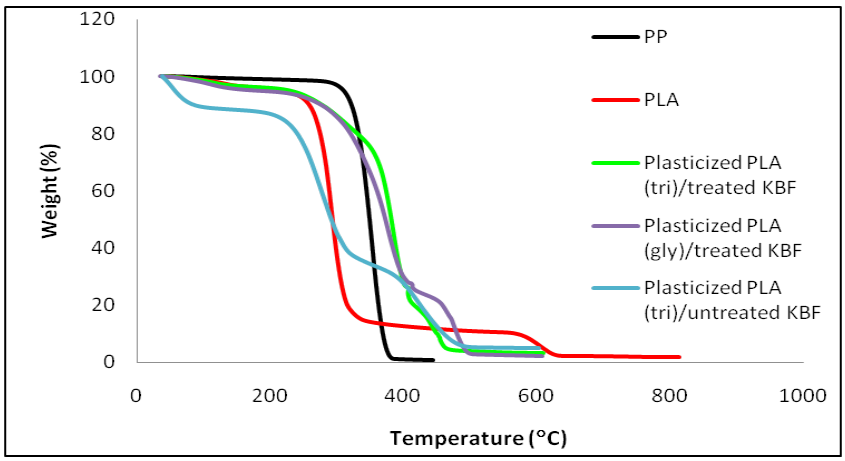

Fig.4: The TGA curves of PP, PLA, plasticized PLA/untreated KBF, and plasticized PLA/treated KBF with triacetin (tri) and glycerol (gly)

Based on the thermogravimetry analysis, an increment was observed in the thermal stability for both the samples of plasticized PLA composites and this was due to the fibre treatment, which further led to the delay in the degradation of the PLA matrix and to significant stabilization effect of the composites.

ACKNOWLEDGEMENTS

The authors would like to acknowledge the Ministry of Science, Technology and Innovation (MOSTI), Malaysia, UPM and UNIMAP for providing the research grant and facilities for the current study.

REFERENCES

Bilba, K., Arseme, M. A., & Ouensanga, A. (2007). Study of banana and coconut fibers: botanical composition, thermal degradation and textural observation. *Bioresources Technol, 98*(1), 58-68.

Caroline, A., Rosemary, A., Carvalho, C., & Grosso, R. F. (2009). Effect of hydrophobic plasticizers on functional properties of gelatin-based films. *Food Research International, 42*, 1113–1121.

Caroline, A., Rosemary, A., Carvalho, C., & Grosso, R. F. (2010). Gelatin-based films containing hydrophobic plasticizers and saponin from *Yucca schidigera* as the surfactant. *Food Research International, 43,* 1710–1718.

Claudia, V., Jose, M.K., Analia, V., & Vivian, P. C. (2004). Effect of chemical treatment of starch-based blends reinforced with sisal fiber. *Journal Composite Materials, 38*, 1387-1392.

Ghazanfari, A., Emami, S., Panigrahi, S., & Tabil, L. G. (2008). Thermal and mechanical properties of blends and composites from HDPE and date pits particles. *Journal of Composites Materials*, *42*, 3452-3459.

Harding, K. G., Dennis, J. S., Blottnitz, H. V., & Harrison, S. T. L. (2007). Environmental analysis of plastic production processes: Comparing petroleum-based polypropylene and polyethylene with biologically-based poly-hydroxybutyric acid using life cycle analysis. *Journal of Biotechnology, 130*, 57–66.

Islam, M. S., Pickering, K. L., & Foreman, N. J. (2010). Influence of accelerated ageing on the physico-mechanical properties of alkali-treated industrial hemp fibre reinforced poly(lactic acid) (PLA) composites. *Polymer Degradation and Stability, 95*, 59-65.

Lima, L. -T., Auras, R., & Rubino, M. (2008). Processing technologies for poly(lactic acid). *Progress in Polymer Science, 33*, 820–852.

Maharana, T., Mohanty, B., & Negi, Y. S. (2009). Melt–solid polycondensation of lactic acid and its biodegradability. *Progress in Polymer Science, 34*, 99–124.

Marius, M., Amália, D. S. F., Miroslaw, P., Leila, B., Michaël, A., & Philippe, D. (2008). Polylactide (PLA)–$CaSO_4$ composites toughened with low molecular weight and polymeric ester-like plasticizers and related performances. *European Polymer Journal, 44*, 3842–3852.

Martin, W., Martin, P., Hermann, H., & Stefan, B. (2007). Applying distance-to-target weighing methodology to evaluate the environmental performance of bio-based energy, fuels, and materials. *Resources, Conservation and Recycling, 50,* 260–281.

Melissa, G. A. V., Mariana, A. D. S., Lucielen, O. D. S., & Marisa, M. B. (2011). Natural-based plasticizers and biopolymer films: A review. *European Polymer Journal, 47,* 254–263.

Mingkang, J., Shaoyang, L., Xin, D., & Yifen, W. (2010). Physical properties and internal microstructures of films made from catfish skin gelatin and triacetin mixtures. *Food Hydrocolloids, 24*, 105–110.

Mubarak, A. K., Idris, A. K., & Basu, S. C. (1993). IR Studies of wood plastic composites. *Journal of Applied Polymer Science*, *49*, 1547-1551.

Murariu, M., Da Silva, F. A., Degee, P. H., Alexandre, M., & Dubois, P. H. (2007). Polylactide compositions, Part I: Effect of filler content and size on mechanical properties of PLA/calcium sulphate composites. *Journal Polymer, 48*, 2613-2618.

Nina, G., Axel, S. H., & Jörg, M. (2009). Natural and man-made cellulose fibre-reinforced poly(lactic acid) (PLA) composites: An overview about mechanical characteristics and application areas. *Composites: Part A, 40*, 810–821.

Ogata, N., Jimenez, G., Kawai, H., & Ogihara, T. J. (1997). Structure and thermal/mechanical properties of poly(l-lactide)-clay blend. *Journal of Applied Polymer Science, 12*, 584-590.

Oksman, K., Skrifvars, M., & Selin, J. -F. (2003). Natural fibres as reinforcement in polylactic acid (PLA) composites. *Composites Science and Technology, 63*, 1317–1324.

Rahul, M. R., Amol, V. J., & Douglas, E. H. (2010). Poly(lactic acid) modifications. *Progress in Polymer Science, 35*, 338–356.

Yijun, L., Edgar, L., James, G., Goodwin, Jr., & Changqing, Lu. (2007). Transesterification of triacetin using solid Brønsted bases. *Journal of Catalysis, 246*, 428–433.

Pertanika J. Sci. & Technol. 21 (1): 161 - 168 (2013)

SCIENCE & TECHNOLOGY

Journal homepage: http://www.pertanika.upm.edu.my/

Content-based Image Retrieval Using Colour and Shape Fused Features

Mas Rina Mustaffa*, Fatimah Ahmad, Ramlan Mahmod and Shyamala Doraisamy

Department of Multimedia, Faculty of Computer Science and Information Technology, Universiti Putra Malaysia, 43400 Serdang, Selangor, Malaysia

ABSTRACT

Multi-feature methods are able to contribute to a more effective method compared to single-feature methods since feature fusion methods will be able to close the gap that exists in the single-feature methods. This paper presents a feature fusion method, which focuses on extracting colour and shape features for content-based image retrieval (CBIR). The colour feature is extracted based on the proposed Multi-resolution Joint Auto Correlograms (MJAC), while the shape information is obtained through the proposed Extended Generalised Ridgelet-Fourier (EGRF). These features are fused together through a proposed integrated scheme. The feature fusion method has been tested on the SIMPLIcity image database, where several retrieval measurements are utilised to compare the effectiveness of the proposed method with few other comparable methods. The retrieval results show that the proposed Integrated Colour-shape (ICS) descriptor has successfully obtained the best overall retrieval performance in all the retrieval measurements as compared to the benchmark methods, which include precision (53.50%), precision at 11 standard recall levels (52.48%), and rank (17.40).

Keywords: CBIR, colour, feature fusion, and shape

INTRODUCTION

Content-based Image Retrieval (CBIR) is developing amazingly due to the increase needs to show, share, organise, search, and retrieve digital imagery. The CBIR technology has been useful in many areas, such as crime prevention, medicine, law, science, fashion and interior design, and a few others. As compared to conventional image retrieval techniques that use image annotations or keywords, CBIR has been able to reduce the many problems associated with retrieving images based on

Article history:
Received: 31 March 2012
Accepted: 31 August 2012

E-mail addresses:
masrina@fsktm.upm.edu.my (Mas Rina Mustaffa),
fatimah@fsktm.upm.edu.my (Fatimah Ahmad),
ramlan@fsktm.upm.edu.my (Ramlan Mahmod),
shyamala@fsktm.upm.edu.my (Shyamala Doraisamy)
*Corresponding Author

ISSN: 0128-7680 © 2013 Universiti Putra Malaysia Press.

text, such as manual image annotations, differences in perceptions and interpretations, and language barrier, where image annotations are usually presented in one language, by retrieving images on the basis of automatically derived low-level features, middle-level features, or high-level features (Datta *et al*., 2008; Vassilieva, 2009; Veltkamp & Tanase, 2002). Among these features, the low-level features are the most popular due to their simplicity compared to the other levels of features plus automatic object recognition and classification which are still among the most difficult problems in image understanding and computer vision.

Apart from utilising the low-level features separately, they can also be integrated whereby in most cases, a single feature will not be suffice to represent the pictorial content of an image and fusing the low-level features will lead to a better performance. According to Forczmański and Frejlichowski (2007), the fusing features can be done either through the sequential approach or parallel approach. Based on the sequential approach, an image will first be processed by one feature descriptor and the output will then be used as the input for the following feature descriptor, and so on until a final feature vector is obtained. The parallel approach, on the other hand, works by allowing an image to be processed by different feature descriptors separately, where each of these descriptors will generate its respective coefficients and these coefficients will be integrated based on a certain scheme to produce the final integrated feature vectors. The sequential approach allows for a filtering procedure, where images which are depicted as very dissimilar by the first feature descriptor, can be omitted for subsequent steps. This can lead to a decrease in future computation time and computation complexity. However, allowing for images to be filtered out at the initial stage may result in false elimination of similar images, thus influencing the end result as well as the effectiveness of the approach. On the contrary, the parallel approach allows for computation time reduction where different methods can be calculated at the same time independently. The integration of the features is usually performed at the final stage where equal or different weights are assigned to each feature. Determining the best weight for the respective feature can be a complex task. However, assigning different weights to each feature will allow a method to stress the contribution of one set of features which may be considered as more important in the application than the rest. Weight distribution is definitely easier to be done in a parallel-based approach. Unlike the sequential-based feature fusion, to stress out a feature is to modify the process flow all together. The sequential and parallel approaches have their own strengths and weaknesses. In practice, the selection between a sequential-based or a parallel-based approach is very much dependent upon the application needs and requirements. There are quite a number of efforts done related to the feature fusion in CBIR to overcome the shortcomings associated with the single-feature methods. Some of the many works can be found in the following references (see Choraś *et al*., 2007; Lee & Yin, 2009; Prasad *et al*., 2001; Schaefer, 2004; J.Y. Wang & Zhu, 2010; Yue *et al*., 2011).

Therefore, this paper aims to contribute to a parallel-based feature fusion method, namely ICS descriptor, which combines colour and shape features to improve the performance of a CBIR system. The remainder of the paper is organised as follows: The methods to extract the respective colour and shape features are first described. Then, the combining strategy is explained following by the description on the experimental setting and discussion of results. Conclusions and future works can be found at the end of the paper.

COLOUR FEATURE BASED ON MJAC

The proposed MJAC is an improved framework by adopting ideas from three previous works in CAC including those by Huang *et al*. (1997), Moghaddam *et al*. (2005) and Williams and Yoon (2007) by implementing the Joint Auto Correlograms in a multi-level resolution. This provides an enhanced method which allows for pixels correlation of several local image features, such as colour, gradient magnitude, rank, and texturedness to be captured at different image scales in the frequency domain. At the beginning, the collected images will go through an extraction process to separate the RGB colour space and the grey-scale colour space. This is followed by the implementation of the Ridgelet transform on both of the RGB colour space and the grey-scale colour space by first calculating the Radon transform, followed by the implementation of the one-dimensional discrete Wavelet transform on the Radon transform coefficients up to four sub-bands. Next, focusing only on scale-3 and scale-4 of the one-dimensional discrete Wavelet transform coefficients, the local image features such as colour, gradient magnitude, rank, and texturedness are extracted, where each of the local image features is treated independently. The colour feature is extracted in the RGB colour space, while the gradient magnitude, rank, and texturedness are extracted in the grey-scale colour space. In order to reduce the feature dimension, a compact representation, as well as ease of coefficient management, these local image features is then quantised. Auto correlogram is then performed on each of the quantised local image features. At the end of this process, feature vectors are generated to represent the images, which are stored in the feature database. The similarity between the query image and the images in the database are measured by comparing the feature vectors of the query image with the feature vectors of all the images in the database using the L_1-norm distance function.

SHAPE FEATURE BASED ON ENRF

ENRF is an extension and improvement to the work done by Chen *et al*. (2006), where the extended descriptor is now resulting in a rotation, scaling, and translation invariant Ridgelet transform for images of various sizes. The first step is by putting the collected images through an initialisation process. During this process, all the images in the collection are assigned with certain constraints. The images will then be made translation and scaling invariant. Only pixels of the translation and scaling invariant images that fall within the ellipse template centred at (M/2, N/2) are considered for the next steps (note that M and N represents the width and height of an image, respectively). A template option is made available after implementing the ellipse template setting, where it allows the algorithm to provide an option in choosing between proceeding with the ellipse template or considering the square template instead when processing the translated and scaled pixels of an image. A square template is used if the percentage of the pixels of the translation and scaling invariant image that fall outside of the ellipse area is more than the threshold value. Otherwise, the ellipse template is utilised. Radon transform is then performed on the shape that has been processed according to the suitable template using 128 points for both the number of samples taken on each radial line as well as the number of orientations. After normalising the Radon transform, the next step is to apply the one-dimensional Discrete Wavelet transform on each of the Radon slices to obtain the Ridgelet

coefficients. In order to make the descriptor invariant to rotation, the one-dimensional Discrete Fourier transform is performed along the angular direction of the scale 3 and scale 4 of the wavelet decomposition levels. For each of the mentioned wavelet decomposition levels, only 15 Fourier magnitude spectrums are captured to represent the shape. These coefficients will be used as the feature vectors for the image which is stored in the feature database. As for the distance function, the L_1-norm is utilised.

SIMILARITY MEASURE

Fig.1 shows the scheme to combine the colour and shape features. According to the L_1- norm distance function concept, the smaller the similarity value between an image and the query image, the more similar the image is to the query image. Meanwhile, between the similarity values generated for both the colour and shape features, it is easier to identify whether an image is similar or not to a query image based on the shape feature similarity values rather than the colour feature similarity values since the shape feature similarity values are in wider range. Due to this reason, the shape feature is being made the benchmark in determining the initial similarity as shown in 'Line 1' of Fig.1 below.

As shown in 'Line 1' of Fig.1, the shape feature similarity values are being multiplied with a threshold value, *Threshold_Value*. The *Threshold_Value* is used to identify the limit of which the *Shape_Similarity_Value* is small enough to make it noteworthy to be retained. Through the experiments, it has been identified that the best *Threshold_Value* is 3000. If the *Shape_Similarity_Value* multiplied by 3000 is below the value of 1, the *Shape_Similarity_Value* is noteworthy enough to be retained. The retention process is done by multiplying the *Shape_Similarity_Value* (range 0.000248 to 0.761901) with the *Colour_Similarity_Value* (range 1.195548 to 9.146877). Since the range of the *Colour_Similarity_Value* is more than 1, when it is multiplied with the *Shape_Similarity_Value* of less than 1, it will always return a sum of less than 1, and hence retaining the small similarity value. If the *Shape_Similarity_Value* multiplied by 3000 is more than the value of 1, the similarity value is no longer noteworthy to be retained, hence an addition is performed.

Based on the literature review, the colour feature is usually superior in image representation compared to other features. Due to this reason, more weights are given to the colour feature compared to the shape feature, as shown in 'Line 2' and 'Line 4' of Fig.1 above. A weight of 0.2 is given to the shape feature while a weight of 0.8 is given to the colour feature ($a + b = 1$). These weights are obtained experimentally.

Line 1: If (*Shape_Similarity_Value* * *Threshold_Value*) < 1
Line 2: (*a* * *Shape_Similarity_Value*) * (*b* * *Colour_Similarity_Value*)
Line 3: Else
Line 4: (*a* * *Shape_Similarity_Value*) + (*b* * *Colour_Similarity_Value*)
Line 5: End If

Fig.1: Algorithm for Combining the Colour and Shape Features

EVALUATION AND ANALYSIS OF THE RESULTS

The objective of this experiment was to evaluate the retrieval effectiveness of the proposed feature fusion descriptor, namely, ICS compared to the proposed colour-only descriptor (MJAC) and the proposed shape-only descriptor (ENRF) based on several retrieval measurements. The retrieval experiments were conducted on an Intel Pentium Dual-Core 2.5 GHz desktop. These methods were tested on 100 SIMPLIcity image dataset where the first 10 images from each of the image classes made up the 100 images (for example, the images labelled 0-9 for the first class, 100-109 for the second class, 200-209 for the third class, etc.) (Wang *et al*., 2001). For each class, all of the 10 images were selected as image queries. In total, there were 100 query images. There are 10 similar images in each image class, which provide the ground truth. The Query-by-Example (QBE) paradigm is employed. Samples of the SIMPLICITY image dataset is shown in Fig.2.

The retrieval effectiveness of the MJAC, ENRF, and ICS was evaluated using three different retrieval measurements, which were the precision at 10, 11 standard precision-recall at 10, and rank at 100.

Table 1 shows a summary of the overall average retrieval effectiveness of the proposed MJAC, ENRF, and ICS for 100 SIMPLIcity image dataset based on three retrieval measurements. It should be highlighted that the proposed feature fusion descriptor (ICS) is able to achieve the best overall performance for all the retrieval measurements. This indicates that the proposed ICS is better in differentiating between similar and dissimilar images when given a query image as well as able to retrieve similar images at higher rank compared to the colour-only MJAC and the shape-only ENRF. The best overall retrieval performance achieved by the ICS in all three retrieval measurements indicates its capability to maintain a good performance across different retrieval measurements compared to the benchmark methods. The consideration of colour and shape information in one descriptor allows or the ICS to perform better compared to the colour-only descriptor and shape-only descriptor. It is common where one feature may not be enough to represent an image since different images may contain colour information but not shapes, and vice versa. Generally, by taking a few features together, they can complement each other, hence contributing to a better descriptor rather than a single feature descriptor.

Fig.2: Samples of the SIMPLIcity image dataset

This work has successfully integrated the colour and shape features and the retrieval results have shown the implication of the proposed feature fusion descriptor (ICS) in improving the retrieval effectiveness.

TABLE 1: Retrieval effectiveness summary between the ICS and its benchmark methods based on various retrieval measurements

Method	Average Precision (p-10)	Average 11 Standard Precision-Recall (p-10)	Average Rank (p-100)
MJAC	0.508000	0.491669	18.409000
ENRF	0.312000	0.325884	36.790000
ICS	0.535000	0.524829	17.403000

From Table 1, it can be concluded that the proposed MJAC is suitable for images that have various colour information with inadequate shape characteristics, while the ENRF performs better on images with obvious shapes or regions but less colour variations. On the contrary, ICS is able to achieve higher precision rate for images with obvious colour and shape information. In general, the SIMPLIcity image dataset contains images with complex shapes and backgrounds. Therefore, it can be observed that the proposed shape descriptor is not able to perform equally to that of the proposed colour descriptor since colour information is definitely more obvious in such images. This has led to a relatively big gap in retrieval performance between the proposed colour and shape descriptors. Since the feature fusion method makes use of these two descriptors, the proposed ICS will generally hold a retrieval rate which gives a balance between these two descriptors. Nevertheless, it can be said that the proposed feature fusion method has successfully achieved a reasonable precision rate for all image classes with either achieving the highest precision rate or the second highest (with mostly achieving small gaps compared to the highest precision rate) in most of the image classes.

CONCLUSION AND FUTURE SUGGESTIONS FOR WORK

In this paper, a new feature fusion approach is proposed. The proposed ICS integrates colour and shape features, where the colour feature is extracted based on the MJAC while the shape information is obtained through the ENRF. These features are combined through a proposed integrated strategy. The feature fusion method is introduced to boost the retrieval performance compared to single-only methods. The results have shown that retrieval effectiveness has been improved by integrating features for image representation. Based on 100 SIMPLIcity images, where all 100 images have been chosen as query images, ICS has successfully obtained the best overall retrieval performance in three different retrieval measurements, which include precision at 10 with 53.50%, 11 standard precision-recall at 10 with 52.48%, and rank at 100 with 17.40. This has proven that the proposed integrated descriptor, which combines the colour and shape features, has contributed to a better retrieval and rank of similar images. Achieving the best overall retrieval performance in all three different retrieval measurements

has also proven the capability of the proposed ICS to maintain a good performance across different retrieval measurements as compared to the benchmark methods. Future work will include providing relevance feedback as well as combining the colour-shape methods with other features such as texture.

ACKNOWLEDGMENTS

Financial support provided by the Ministry of higher Education, Malaysia and Universiti Putra Malaysia during the duration of this research is gratefully acknowledged.

REFERENCES

Chen, G. Y., Bui, T. D., & Krzyżak, A. (2006). Rotation invariant feature extraction using Ridgelet and Fourier transforms. *Pattern Analysis and Applications*, *9*(1), 83-93.

Choraś, R. S., Andrysiak, T., & Choraś, M. (2007). Integrated colour, texture, and shape information for content-based image retrieval. *Pattern Analysis and Applications*, *10*(4), 333-343.

Datta, R., Joshi, D., Li, J., & Wang, J. Z. (2008). Image retrieval: Ideas, influences, and trends of the new age. *ACM Computing Surveys, 40*(2), 1-60.

Forczmański, P., & Frejlichowski, D. (2007). Strategies of shape and colour fusions for content-based image retrieval. *Computer Recognition Systems*, *2*, 3-10.

Huang, J., Kumar, S. R., Mitra, M., Zhu, W. J., & Zabih, R. (1997). Image indexing using colour correlograms. In *Proceedings of the 1997 Conference on Computer Vision and Pattern Recognition (CVPR '97)* (pp. 762-768). Washington, DC, USA: IEEE Computer Society.

Lee, X. F., & Yin, Q. (2009). Combining colour and shape features for image retrieval. In *Universal Access in HCI, Part III, HCII 2009, 5616 of LNCS* (pp. 569-576).

Moghaddam, H. A., Khajoie, T. T., Rouhi, A. H., & Tarzjan, M. S. (2005). Wavelet correlogram: A new approach for image indexing and retrieval. *Pattern Recognition*, *38*(12), 2506-2518.

Prasad, B. G., Biswas, K. K., & Gupta, S. K. (2001). Colour and shape index for region-based image retrieval. In Arcelli, C., Cordella, L. P., & Di Baja, G. S. (Eds.), *Proceedings of the 4th. International Workshop on Visual Form (IWVF-4)*, 28-30 May 2001, Capri, Italy (716-725). London, UK: Springer-Verlag.

Schaefer, G. (2004). CVPIC colour/shape histograms for compressed domain image retrieval. In *DAGM 2004, 3175 of LNCS*, Tubingen, Germany (pp. 424-431).

Vassilieva, N. S. (2009). Content-based image retrieval methods. *Programming and Computing Software, 35*(3), 158-180.

Veltkamp, R. C., & Tanase, M. (2002). *Content-based image Retrieval Systems: A Survey*. Technical Report UU-CS-2000-34, Institute of Information and Computing Sciences, Utrecht University.

Wang, J. Y., & Zhu, Z. (2010). Image retrieval system based on multi-feature fusion and relevance feedback. In *Proceedings of the Ninth International Conference on Machine Learning and Cybernetics*, 11-14 July 2010, Qingdao (pp. 2053-2058).

Wang, J. Z., Li, J., & Wiederhold, G. (2001). SIMPLIcity: Semantics-sensitive integrated matching for picture libraries. *IEEE Transactions on Pattern Analysis and Machine Intelligence*, *23*(9), 947-963.

Williams, A., & Yoon, P. (2007). Content-based image retrieval using joint correlograms. *Multimedia Tools and Applications*, *34*(2), 239-248.

Yue, J., Li, Z., Liu, L., & Fu, Z. (2011). Content-based image retrieval using colour and texture fused features. *Mathematical and Computer Modelling, 54*(3-4), 1121-1127.

Pertanika J. Sci. & Technol. 21 (1): 169 - 182 (2013)

SCIENCE & TECHNOLOGY

Journal homepage: http://www.pertanika.upm.edu.my/

Toward Automatic Semantic Annotating and Pattern Mining for Domain Knowledge Acquisition

Tianyong Hao[1]* and Yingying Qu[2]

[1]*School of Computer Science and Engineering, University of New South Wales, Australia*

[2]*Faculty of the Built Environment, University of New South Wales, Australia*

ABSTRACT

Due to the high complexity of natural language, acquisition of high quality knowledge for the purpose of fine-grained data processing still mainly relies on manual labour at present, which is extremely laborious and time consuming. In this paper, a new automatic approach using semantic annotating and pattern mining is proposed to assist engineers for domain knowledge acquisition. This approach uses Minipar to label sentences processed from domain texts. Based on the dependency relations, structural patterns are extracted and semantic bank is applied to annotate and represent concepts with semantic labels considering sentence contexts. The approach further learns and assigns relations to previously extracted concepts by pattern matching. The involved concepts and semantic labels with learned relations together, as extracted knowledge, enrich domain knowledge base. Preliminary experiments on Yahoo! Data in "heart diseases" category showed that the proposed approach is feasible for automatic domain knowledge acquisition.

Keywords: Knowledge acquisition, semantic annotation, semantic bank, structural pattern, transformation rule

INTRODUCTION

With the mass production of digital information over the web, extracting and snatching knowledge with effectiveness, efficiency and accuracy have become an urgent and challenging tasks (Wang *et al.*, 2006). In recent years, knowledge acquisition from texts has become one of hot research fields in Artificial Intelligence (Tanaka & Jatowt, 2010; Tanaka & Jatowt, 2010; Deng & Han, 2012; Carayannis, 2012; Fan *et al.*, 2012). The task of knowledge acquisition is to extract knowledge for an information system or expert system by setting up sound, perfect, effective knowledge base.

Article history:
Received: 31 March 2012
Accepted: 31 August 2012

E-mail addresses:
haotianyong@gmail.com (Tianyong Hao),
yingyinqu2@gmail.com (Yingying Qu)
*Corresponding Author

ISSN: 0128-7680 © 2013 Universiti Putra Malaysia Press.

In the past several decades, a number of these methods were followed with Cognitive Science and other disciplines.

Due to the high complexity of natural language, i.e. with the huge amount of concepts and relations in free texts being too complicated to be formalized by automatic methods, the acquisition of high quality knowledge for the purpose of fine-grained data processing is still mainly relying on the costly manual labour at present.

In the field of medical informatics, there is a high demand for domain knowledge within a formally specified framework and knowledge based is getting more and more accepted (Campbell *et al.*, 1994; Hull & Gomez, 1999; Cao, 2001; Dawoud *et al.*, 2012). It requires medical knowledge to be expressed in a sound and consistent manner. Knowledge engineering in an ontologically coherent (sub) domain makes use of existing knowledge compilations, such as ICD-10, SNOMED, MESH, UMLS, as much as possible. Due to the insufficiency of formal specification and levels of granularity, only a limited amount of the knowledge can be reused even if they are judged transferable in principle (Carenini & Moore, 1993; Firdaus *et al.*, 2012).

Most knowledge is contained in a large collection of unstructured textual documents. Ordinary approaches are to acquire knowledge from the documents manually and then formalize the knowledge at the conceptual level. However, this acquisition procedure mainly relies on a large number of knowledge engineers' manual efforts, which is rather labour intensive, time consuming and troublesome. Moreover, the huge amounts of concepts and relations in domain texts are extremely complicated to be formalized by knowledge engineers. Thus, automated or semi-automated knowledge acquisition techniques are urgently required (Wang *et al.*, 2006; Firdaus *et al.*, 2012).

In this paper, a novel automatic method is proposed for domain knowledge acquisition from domain text corpus by semantic annotating and pattern mining. After pre-processing the corpus by splitting into sentences and removing the noise data, the proposed method analyzes the corpus by using Minipar to label sentences. The nouns and noun phrases, regarded as the concepts, are extracted along with structural patterns. In order to improve matching and learning efficiency, frequent patterns are mined based on these structural patterns using a sequence-based Apriori algorithm. The concepts are then annotated with semantic labels by WordNet and a further defined semantic bank containing unit annotations and context annotations.

With regard to training on annotated data, the method can generate structural patterns to match with a group of frequent patterns previously extracted. The concepts and their annotated relations in each pattern can be applied into the sentences with the same matched frequent pattern to derive more concepts with similar relations, or to learn more relations with the same concepts. The automatically extracted concepts, semantic labels and relations can thus dramatically enrich domain knowledge bases.

We used Yahoo! Answers (2012) corpus as of 10/25/2007 as an experimental dataset. It contained 4,483,032 questions and their correct answers, which are reliable domain text sources as the answers were rated by human users. Furthermore, the dataset contained a small amount of metadata such as best answers on human selection. Finally, 19,622 questions were extracted with their best answers in the "heart diseases" category as the domain corpus. By proposing a number of knowledge transformation rules, the preliminary experiments showed that the annotations could be transformed to standard knowledge representation formats such as OWL

accurately and stably. Therefore, the method is feasible for domain knowledge acquisition aiming at knowledge sharing.

The rest of this paper is organized as follows: Section 2 introduces the proposed framework of automatic knowledge acquisition. Section 3 presents sentence labelling and pattern mining. Section 4 describes semantic annotating of the concepts and relation learning by pattern matching. In Section 5, preliminary experiments with knowledge transformation rules are discussed, and Section 6 summarizes this paper and discusses future work.

THE FRAMEWORK OF DOMAIN KNOWLEDGE ACQUISITION

Admittedly, human-based knowledge acquisition can ensure the high quality of extracted knowledge. However, it is a long-term laborious work with high cost. Thus, automatic acquisition methods are more preferable, especially for quick acquisition demand. In this paper, an automatic method was proposed to extract domain knowledge based on semantic annotating and frequent pattern mining.

Through this method, domain corpus was firstly pre-processed to separate the text paragraphs into sentences and to remove noisy data such as Mathematics formulas. Sentences were then analyzed and labelled by Minipar to extract nouns, noun phrases and structural patterns. By using the sequence-based Apriori algorithm, the frequent patterns were mined from those extracted structural patterns to improve learning efficiency. Regarding those nouns or noun phrases as concepts, these concepts were then annotated by WordNet and a semantic bank which contained unit annotations and context annotations, as a semantic label annotation technique. After that, the patterns with their conceptual relations, learned from annotated training resources, were matched with the mined frequent patterns. According to the matched parts, the corresponding relations could be applied to the concepts associated with the mined frequent patterns. With defined knowledge transformation rules, these concepts and relations can be further transformed into standard knowledge representation formats such as OWL thus to enrich domain knowledge bases. The related framework is shown Fig.1.

The automatic knowledge acquisition method contains seven main steps, which are shown in the fig.1:

Step 1: Pre-processing a domain corpus by formatting, removing noisy data, and splitting text paragraphs into sentences;

Step 2: Labelling all sentences to extract all nouns, noun phrases, and structural patterns;

Step 3: Mining frequent patterns from the structural patterns using a sequence-based frequent pattern mining algorithm;

Step 4: Annotating all the concepts with semantic labels based on WordNet and a semantic bank-based annotation method;

Step 5: Training annotated resources to match with the frequent patterns;

Step 6: Assigning relations extracted from matched patterns to the previously extracted concepts;

Step 7: Presenting all the concepts and relations using OWL or RDF, aided by knowledge transformation rules to enrich domain knowledge bases.

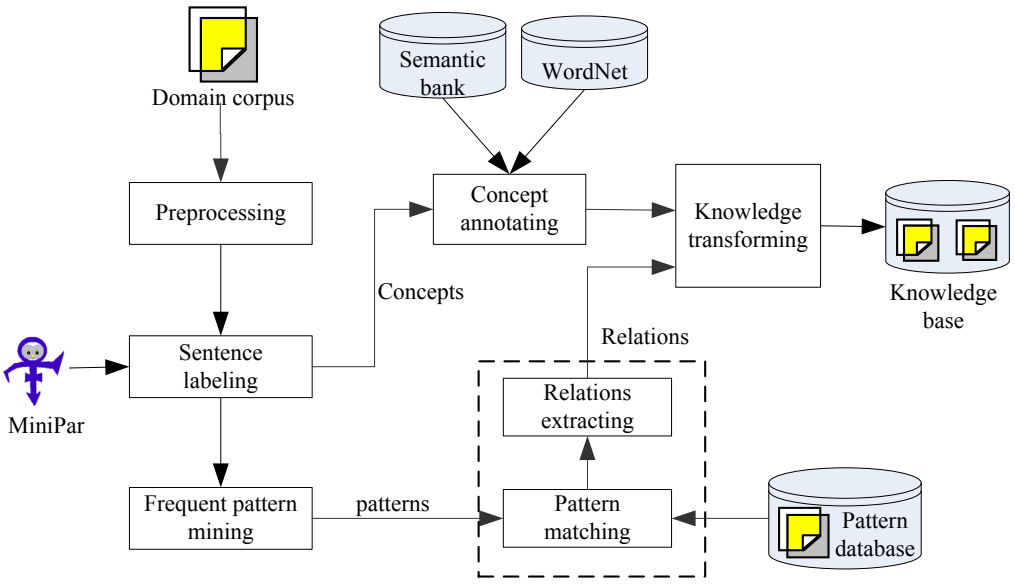

Fig.1: A framework of the automatic domain knowledge acquisition

With the previous processing steps, the framework can discover concepts with their relations, which are then transformed to be formal knowledge representations. Furthermore, this framework can be extended to more corpora or web documents to extract a large amount of knowledge automatically.

SENTENCE LABELING AND FREQUENT PATTERN MINING

The pre-processed sentences from domain corpus are used for sentence structure labelling and frequent structural pattern mining. A pattern is defined as the core structure of a sentence, which can then be extended as the generalization of similar sentences that shares the similar structure.

Sentence Labeling

There are many syntax analysis tools, such as TreeTagger (2012) and OpenNLP (2012), to label sentences by identifying nouns and verbs. However, most of these tools parse sentences by part-of-speech tagging without considering the relations between the objects in the sentences, making it difficult to find the core structures. Dependency Grammar (2012) is a class of syntactic theories developed by Lucien Tesnière. Sentence structure is determined by the relations between a word (a head) and its dependents, which are distinct from phrase structure grammars. The dependency relationship in this model is an asymmetric relationship between a word called head (governor) and another one called modifier. This kind of relationship can be used to analyze the dependency thus to acquire the main structure and nouns of a sentence effectively.

In this study, Minpar was used as a dependency parser tool to analyze sentence relationship in the paper. Minipar is a principle-based broad-coverage parser for the English language (Berwick *et al.*, 1991). Like Principar, Minipar represents its grammar as a network where nodes represent grammatical categories and links represent types of syntactic (dependency) relationships. The output of Minipar is a dependency tree. The links in the diagram represent dependency relationships. The direction of a link is from the head to the modifier in the relationship. Labels associated with the links represent the types of dependency relations. Furthermore, according to the evaluation with the SUSANNE corpus, Minpar achieves about 88% precision and 80% recall, in relation to dependency relationships (2012). The reliable performance ensures the quality of sentence labelling work.

By using Minipar, the sentences in corpus can be labelled with part-of-speech and dependency relations. Therefore, the core sentence structure, which includes nouns, verbs and other meaningful terms, could be extracted. For example, the sentence "what are the risks of plugging a hole in the heart?" was analyzed by using Minipar and the result is shown in Table 1 below.

TABLE 1: Minipar output on the example sentence

E1	(()	fin	C	*	*)*	
1	(what	~	N	E1	*whn*	(gov fin))
2	(are	be	VBE	E1	*i*	(gov fin))
E4	(()	what	N	4	*subj*	(gov risk)
3	(the	~	Det	4	*det*	(gov risk))
4	(risks	risk	N	2	*pred*	(gov be))
5	(of	~	Prep	4	*mod*	(gov risk))
E0	(()	vpsc	C	5	*pcomp-c*	(gov of))
E2	(()	~	N	E0	*s*	(gov vpsc))
6	(plugging	plug	V	E0	*i*	(gov vpsc))
E5	(()	~	N	6	*subj*	(gov plug)
7	(a	~	Det	8	*det*	(gov hole))
8	(hole	~	N	6	*obj*	(gov plug))
9	(in	~	Prep	8	*mod*	(gov hole))
10	(the	~	Det	11	*det*	(gov heart))
11	(heart	~	N	9	*pcomp-n*	(gov in))
12	(?	~	U	*	*punc)*	

In order to facilitate high speed pattern extraction, the output of Minipar is firstly converted into XML format. The nodes in XML are aligned with hierarchical structure, which can dramatically speed up pattern extraction. The XML format of the example is shown in Fig.2.

After the analysis, a group of nouns such as "risk", "hole" and "heart", as well as noun phrases, could be obtained. With the tagged relations, "risk" has the relation of "gov" to "be", "hole" has the relation of "gov" to "plug", and "heart" has the relation of "gov" to "in". Since "gov" means the actual word that it refers to, the structural patterns can be acquired level by

```
<?xml version="1.0" encoding="utf-8" ?>
- <node label="E3" category="U">
  - <node label="E1" category="C" word="" root="fin">
      <node label="1" category="N" word="what" root="what" relation="whn" />
    - <node label="2" category="VBE" word="are" root="be" relation="i">
      - <node label="4" category="N" word="risks" root="risk" relation="pred">
          <node label="E4" category="N" word="" root="what" relation="subj" />
          <node label="3" category="Det" word="the" root="the" relation="det" />
        - <node label="5" category="Prep" word="of" root="of" relation="mod">
          - <node label="E0" category="C" word="" root="vpsc" relation="pcomp-c">
              <node label="E2" category="N" word="" root="~" relation="s" />
            - <node label="6" category="V" word="plugging" root="plug" relation="i">
                <node label="E5" category="N" word="" root="~" relation="subj" />
              - <node label="8" category="N" word="hole" root="hole" relation="obj">
                  <node label="7" category="Det" word="a" root="a" relation="det" />
                - <node label="9" category="Prep" word="in" root="in" relation="mod">
                  - <node label="11" category="N" word="heart" root="heart" relation="pcomp-n">
                      <node label="10" category="Det" word="the" root="the" relation="det" />
                    </node>
                  </node>
                </node>
              </node>
            </node>
          </node>
        </node>
      </node>
    </node>
    <node label="12" category="U" word="?" root="?" relation="punc" />
  </node>
```

Fig.2: The Minipar output of the example in XML format

level. In each level, incremental part, which is the content extended compared with the previous pattern, is judged if it contains a noun or noun phrase. Only the patterns that fulfil constraints are regarded as qualified structural patterns. On the same example, all the extracted structural patterns and their related concepts are shown in Table 2.

TABLE 2: The extracted patterns and their related concepts on the same example

Structural patterns	**Concepts**
what(*gov* fin) be(*gov* fin) [*N1*](*gov* be)	risk
what(*gov* fin) be(*gov* fin) [*N1*](*gov* be) of(*gov N1*) plug(*gov* vpsc) [*N2*](*gov* plug)	risk; hole
what(*gov* fin) be(*gov* fin) [*N1*](*gov* be) of(*gov N1*) plug(*gov* vpsc) [*N2*](*gov* plug) in(*gov N2*) [*N3*](gov in)	risk; hole; heart

Frequent Pattern Mining

Since a single structural pattern may be specific, to improve the performance of matching and learning, frequent patterns are more appropriate to be used for efficient knowledge acquisition. Apriori, as a classic association rule mining method, is applied to mine possible frequent patterns. It is an algorithm for learning association rules and was designed to operate on databases containing transactions (for example, collections of items bought by customers, or details of a website frequentation).

Given a set of item sets (for instance, sets of retail transactions, each listing individual items purchased), Apriori algorithm attempts to find subsets which are common to at least a

minimum number *C* of the item sets. Apriori uses a "bottom up" approach, where frequent subsets are extended one item at a time (a step known as candidate generation), and groups of candidates are tested against the data. The algorithm terminates when no further successful extensions are found. Apriori uses breadth-first search and a tree structure to count candidate item sets efficiently. It generates candidate item sets of length *k* from the item sets of length *k*-1. Then, it prunes the candidates which have an infrequent sub pattern. According to the downward closure lemma, the candidate set contains all frequent *k*-length item sets. After that, it scans the transaction database to determine frequent item sets among the candidates. In this paper, threshold *support* for a pattern candidate *p* is defined as the number of pattern candidates that contain *p*.

In frequent pattern learning, those candidates whose occurrences are lower the *support* threshold are removed. Furthermore, two corollaries are applied to reduce calculation complexity. Let *X*, *Y*, *Z* be any three pattern candidates, and observe that if $X \subseteq Y$ and $Y \subseteq Z$, then $support(X) \geq support(Y) \geq support(Z)$, which leads to the following two corollaries: 1) If *Z* is frequent, then any subset *X* or *Y* is also frequent; 2) If *X* is not frequent, then any superset *Y* or *Z* cannot be frequent.

Regarding a structural pattern as an item set, a pattern can be split into several items thus can be sent to Apriori for mining. However, the sequences, as order information between items, need be fully considered. After sequence-based Apriori algorithm, the patterns whose recorded occurrence values larger than a threshold are mined as frequent patterns, which are further used in the next section.

SEMANTIC ANNOTATING AND RELATIONS LEARNING

Semantic Annotating

There are a large amount of nouns and noun phrases acquired from corpus labelling. Regarding them as concepts here, it is an essential step to annotate these concepts for semantic representation. In order to annotate them, semantic labels were used as annotation labels based on WordNet (2012), which provides a large database of English lexical items available online.

A semantic label here is defined as [*Concept1*] \ [*Concept2*], where these two concepts *(Concept1* and *Concept2)* have a relation with *Sub*(*Concept2*, *Concept1*), which means *Concept2* is the sub concept of *Concept1*. The purpose is to assign a label with a super concept label as constraint to reduce potential ambiguities. In this semantic label definition, concepts can be retrieved and labelled using WordNet. For instance, in the following sentence "What is the exact relationship between pulse rate and systolic pressure?", "pulse rate" have two senses, and thus the super concepts are: 1) "vital sign", "sign", "evidence", "information", and so on; and 2) "rate", "magnitude relation", "relation", and so on. Hence, the semantic labels of the "pulse rate" are tagged as "[sign\ vital sign]" and "[magnitude relation \rate]" finally.

The annotated concepts with semantic labels are important sources to enrich or even construct the basis of domain knowledge base. To improve annotation efficiency and label concepts in a complex context, these annotated concepts are represented in the form of semantic bank, which can be transferred into knowledge format directly as described in the following section. The idea of semantic bank is from one of our research work (Hao *et al.*, 2009). The

semantic bank is a kind of database to store concepts, corresponding semantic labels, and context annotation data. It consists of two parts: 1) unit annotation; and 2) context annotation.

The unit annotation part contains single concepts with their semantic labels. For example, the concept "pulse rate" is tagged as "[sign\ vital sign]" and "[magnitude relation \rate]". The format of the unit concept is represented as follows:

[*Concept***] HAVING [***Semantic labels***]**

The context annotation is a type of representation of unit annotation and occurrences in a specific context. For example, the concept "pulse rate" has two semantic labels. However, in the example sentence, the semantic label of "systolic pressure" was identified as "[vital sign\ blood pressure]". In this context, the "pulse rate" was assigned with the semantic label "[sign\ vital sign]". The format of context annotation is represented as follows:

([*Term1***] HAVING [***Semantic labels 1***] WITH [***Term2***] HAVING**

[*Semantic labels 2***]):** *Occurrence*

The *Semantic labels* in [*Semantic labels*] can be modified and the *Occurrence* can be increased and updated when there are new semantic labels used for the current concepts. An example of the context annotation is shown in Table 3, in which "pulse rate" has two different labels in different sentence contexts. From the context annotation, the probability model can be used to calculate the possible semantic senses in certain context.

TABLE 3: An example of context annotation

Concept$_1$ with label	*Concept$_2$ with label*	*Occurrence*
pulse rate **HAVING** [sign\vital sign]	systolic pressure **HAVING** [vital sign\blood pressure]	1
pulse rate **HAVING** [magnitude relation\rate]	valve **HAVING** [body part\structure]	2

With the semantic bank, the concordance of concepts and their semantic labels are recorded with occurrences. When the data are large enough, they can be used to determine the semantic labels for a given new sentence. A naïve Bayesian formulation was used with the hypothesis that each word in a sentence was thought to be independently distributed to determine the semantic label. The probability of the semantic label for each concept can be calculated by using the following equation:

$$P_{c_i}(label_n \mid \prod_{j \neq i} c_j) = \frac{P_{c_i}(label_n) \prod_{j \neq i} P_{c_i}(c_j \mid label_n)}{P_{c_i}(\prod_{j \neq i} c_j)} \quad (2)$$

where the left part denotes that the probability of concept c_i is distinguished by the semantic label $label_n$ on the condition that c_i co-occurs with c_j. $P_{c_i}(label_n)$ is the prior probability of c_i, which is distinguished by semantic label $label_n$. The denominator means the probability of c_i co-occurs with each c_j and $P_{c_i}(c_j \mid label_n)$ gives the probability of appearing c_j when c_i is labeled by $label_n$. Noting that the denominator remains constant when c_i and $label_n$ are fixed, as a result, we only need to calculate the product of each $P_{c_i}(c_j \mid label_n)$ and $P_{c_i}(label_n)$ to determine the semantic label of c_i using the following equation:

$$label = Max \arg_n [P_{c_i}(label_n) \prod_{j \neq i} P_{c_i}(c_j \mid label_n)] \quad (3)$$

The concept annotation method based on the semantic bank is further implemented in our system, which can analyze a sentence and annotate concepts with semantic labels automatically.

Relation Learning

Since the acquired frequent patterns have a larger coverage of sentences than normal structural patterns, and they can be used to extract more concepts having similar relationship theoretically. With annotated and validated training data, our method can learn the patterns and their relations so as to be applied into the extraction of more concepts extracted from the original domain corpus. The detailed method is as follows:

Given an annotated sentence with knowledge representation as a training sentence s_t, the method first analyzes the sentence by Minipar to acquire structural patterns p_t and corresponding relation r_t. After that, the pattern is matched with each pattern in the frequent pattern set. If there is a pattern p_f matched, the r_t is then applied to the relation representation of all nouns extracted from p_f. The detailed equation for this purpose is shown in the following:

$$MScore(p_t) = \frac{2 \times \left| MS_{p_t} \cap MS_{p_f} \right|}{\left| MS_{p_t} \right| + \left| MS_{p_f} \right|} \quad (4)$$

p_t and p_f are firstly split into items MS_{p_t} and MS_{p_f} and these items are then used to match with each other. The matching score, as *MScore* for the pattern p_t, is calculated based on the counting matched items with all the items.

From Equation (4), the frequent pattern matched best to the current structural pattern was obtained compared with a matching threshold. If there is no frequent pattern fulfils the current structural pattern still can be applied to pattern learning though its question matching coverage is less than the frequent patterns.

For example, there is training sentence "the signs of a heart attack are chest discomfort, discomfort in other areas of the upper body, shortness of breath, and other symptoms". Its annotation is shown in the following:

<heart attack>
<Has_attribute_Signs rdf:resource="# *chest discomfort, discomfort in other areas of the upper body, shortness of breath, and other symptoms* "/>
</ heart attack>

The structural pattern of the example sentence is "the(*gov* [*N1*]) [*N1*](*gov* be) of(*gov N1*) [*N2*](gov *N1*) be(*gov* fin) [*N3*](*gov* be)". Therefore, the pattern can be matched with the whole pattern set. Suppose there is a frequent pattern matched and its covered sentences include "The benefits of red wine are reducing coronary heart diseases, maintains the immune system, polyphenols, resveratrol, flavonoids, anti-bacterial activity, anti-stress". The relation is then applied in the sentence, and thus, a relation is learned automatically, as follows:

<red wine>
<Has_attribute_benefits rdf:resource="# *reducing coronary heart diseases, maintains the immune system, polyphenols, resveratrol, flavonoids, anti-bacterial activity, anti-stress* "/>
</red wine>

By this way, all the possible relations related to the concepts in our domain sentences could be acquired, especially using the previous semantic bank. Therefore, the semantic annotations of concepts with their relations can be used to enrich or built a domain specific knowledge base.

PRELIMINARY EXPERIMENTS

In this study, the automatic knowledge acquisition method was implemented in a Windows-form application. The domain was selected as "heart diseases" from Yahoo! Answers (2012) as of 10/25/2007, which was used as corpus since it contained huge amount of data (4,483,032 items) and also tagged with rated answers. These human-based answers are favourable domain text source. Furthermore, the dataset contained a large amount of metadata, i.e., which answer was selected as the best answer, as well as the category and sub-category that were assigned to this question. Therefore, the questions with their best answers were selected in the "Heart Diseases" category as our domain dataset, containing 19,622 items in total. The example data in the domain are shown in Fig.3.

After pre-processing the corpus into sentences, Minipar was applied to automatically identify the concepts and dependency relations. In this experiment, the focus was mainly placed on recognizing nouns and noun phrases, in which the latter has higher priority since the noun phrases can convey more specific semantic information. After that, the system extracted all the possible structural patterns. With the sequence-based Apriori algorithm, the frequent patterns are mined and extracted. WordNet is further applied to annotate the nouns and nouns phrases as the format of unit annotation and context annotation. In order to annotate a sentence more accurately, all the semantic labels and items were recorded with their occurrences into a semantic bank. These statistical data were further used to assist annotation on specific sentences.

```
12993  What is the name of the blood vessels which carry blood to the heart?
12994  I have had a stroke,diabetis and now parkinsons. Which one is keeping
       me awake at nights?
12995  How can you cure SVT ( supra-ventricular tachycardia) ?
12996  What is the Medical Term for an Enlarged Heart?
12997  What is a septal infarct and what is the maximum period of getting
       cardiac enzymes for infarct diagnosis?
12998  Has any one ever heard of Athlete's heart? I was told by a doctor I
       have it but offered no treatment or any a
12999  What do ththe meaning of Ballooning?When it is needed to do ballooning
       in our heart?
13000  What could cause extreme pounding of heart while at sleep?
```

Fig. 3: Question Examples in "Heart Diseases" category

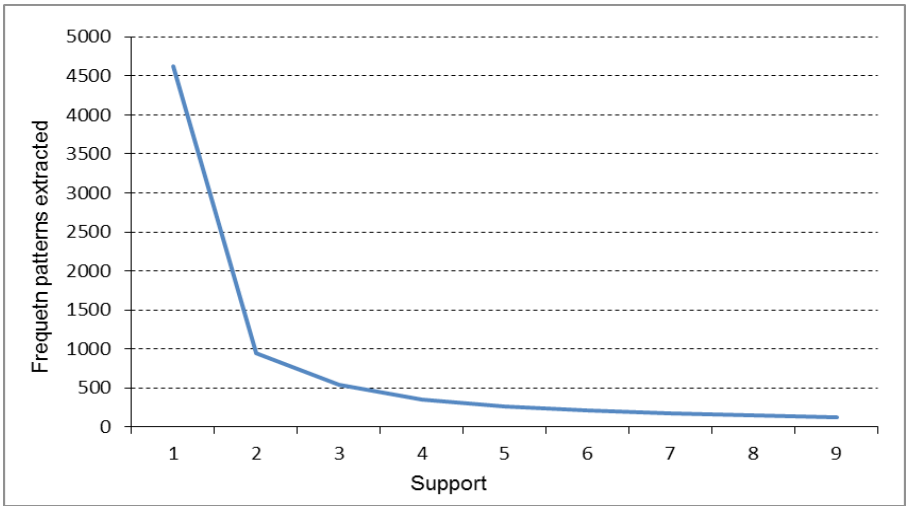

Fig.4: The extracted frequent patterns by different support values

From a total of 19,622 question items, 10.3 words were allocated for each question on average. Using the proposed pattern extraction method, 56,118 structural patterns were finally extracted in total, indicating that 2.86 patterns for each sentence on average. With different values of the *support* threshold, the number of the extracted frequent patterns changed dramatically, and the distribution is shown in Fig. 4.

Since it was difficult to find annotated knowledge resources in this domain as the training data, 100 sentences were randomly selected from the domain dataset and they were also manually annotated for this preliminary experiment. On these training data, the structural patterns and concepts were firstly extracted automatically by sentence labelling. After that, all the concepts and related semantic labels that are automatically annotated by the semantic bank and WordNet were randomly selected. The relations in the training data were also annotated and applied into the sentences where the matched patterns had been generated from. Based on the training data, there were a total of 272 structural patterns extracted. With regard to the pattern matching on all the other sentences in the whole dataset, 1,929 new concepts and 632 relations were finally acquired in total, and the results are shown in Table 4. The preliminary

experiment showed that the proposed method could effectively extract knowledge by using the proposed semantic annotating and pattern mining method. With more training sentences involved, the number of knowledge pieces extracted from domain dataset could dramatically increase so as to enrich or even build a new domain knowledge base.

TABLE 4: Extracted concepts and relations based on 100 training data

Patterns extracted	Sentences matched	Concepts extracted	Relations extracted
272	1,297	1,929	632

With relation learning based on the training data, the annotated relations and semantic bank are potentially desirable to be added into knowledge base. To represent them in a standard knowledge format, two formal knowledge representations - Resource Description Framework (RDF) and Web Ontology Language (OWL) - are applied. RDF is a family of World Wide Web Consortium (W3C) specifications, which were originally designed as a metadata model. It has come to be used as a general method for conceptual description or modelling of information. OWL is a family of knowledge representation languages for authoring ontologies, and is endorsed by W3C (Smith *et al.*, 2004). In this study, the OWL Full was used as our knowledge representation method since it provides compatibility with RDF Schema.

The annotated data, either in semantic bank or other relation representation ways, need to be transformed into OWL format. Therefore, a set of knowledge transformation rules (KTR) was defined for this purpose. KTR is an intermediate description logic language, which can be transformed into first-order logic. The involved semantic labels are converted using the following rule and the *SubClassOf* relation is then represented in OWL, as follows:

KTR	$\forall x, there\ exist\ [x / concept_1] \rightarrow SubClassOf\ (concept_1, x)$
OWL format	*<owl:Class rdf:ID=" #[x]">* *<rdfs:subClassOf rdf:resource="#[concept$_1$]"/>* *</owl:Class>*

In the same way, the unit annotation in semantic bank can be converted by the following rule into OWL. It is important to mention that the relation inside a semantic label is already converted using the previous rule. Therefore, the following rule only considers the sub-class outside the semantic labels.

KTR	$\forall y, there\ exist\ [y\ HAVING\ \ concept_1 / concept_2]$ $\rightarrow SubClassOf\ (y, concept_2)$
OWL format	*<owl:Class rdf:ID=" #[y]">* *<rdfs:subClassOf rdf:resource="#[concept$_2$]"/>* *</owl:Class>*

The context annotation in semantic bank is more complicated since the words inside a sentence are concordant. Thus, "restriction" was used to represent and the corresponding KTR was defined as follows:

KTR	$\forall x \forall y, there\ exist\ [x\ HAVING\ \ concept_1 / concept_2]$ $WITH\ [y\ HAVING\ \ concept_3 / concept_4]$ $\rightarrow SubClassOf\ (x, concept_2)\ with\ constraint : SubClassOf\ (y, concept_4)$ ...
OWL format	*<owl:Class rdf:ID="#[x]">* *<rdfs:subClassOf rdf:resource="#[concept$_2$]" />* *<owl:Restriction>* *<owl:onCondition rdf:resource="#[y]" />* *<rdfs:subClassOf rdf:resource="#[concept$_4$] " />* *</owl:Restriction>* *</owl:Class>*

Similarly, the relations can also be transformed into knowledge representation format. In this way, the extracted knowledge can be represented in a standard way automatically and can be applied to enrich domain knowledge base directly.

CONCLUSION AND FUTURE WORK

A novel method for automatic knowledge acquisition from domain texts is proposed in this paper. Taking "heart disperses" from Yahoo! Answers as the source domain corpus, this method makes use of Minipar to label sentences and extract structural patterns. A semantic bank is further proposed to annotate concepts regarding to sentence context based on WordNet to enhance the semantic representation. With regard to the pattern matching, the relations extracted from training data were applied to the previously extracted concepts. Thus, the concepts, annotated labels, and relations can be converted by knowledge transformation rules to enrich domain knowledge base automatically. As for further development, more experiments with larger dataset and evaluation/comparison of the performances of knowledge extraction will be taken into consideration in the future.

REFERENCES

Berwick, R. C., Abney, S. P., & Tenny, C. (1991). *Principle-Based Parsing: Computation and Psycholinguistics*. Kluwer Academic Publishers.

Campbell, K., Das, A., & Musen, M. (1994). A Logical Foundation for Representation of Clinical Data. *Journal of the American Medical Informatics Association*, *1*(3), 218-232.

Cao, C. G. (2001). Medical Knowledge Acquisition From Encyclopedic Texts. *LNCS*, *2101*, 268-271. Berlin.

Carayannis, E. G. (2012). Knowledge Arbitrage, Serendipity, and Acquisition Formality: Their Effects on Sustainable Entrepreneurial Activity in Regions. *IEEE Transactions on Engineering Management*, *58*(3), 546-577.

Carenini, G., & Moore, J. (1993). Using the UMLS Semantic Network as a Basis for Constructing a Terminological Knowledge Base: a preliminary report. *In Proceedings of Annual Symposium on Computer Applica-tions in Medical Care*, pp. 725-729.

Dawoud, K., Qabaja, A., Shang Gao, Alhajj, R., & Rokne, J. (2012). Identifying Cancer Biomarkers by Knowledge Discovery From Medical Literature. In *Proceeedings of IEEE International Conference on Computational Advances in Bio and Medical Sciences*.

Deng, H., & Han, J. (2012). Uncertainty Reduction for Knowledge Discovery and Information Extraction on the World Wide Web. *Proceedings of the IEEE*, Vol. 100, Issue: 9, pp. 2658-2674.

Dependency grammar. (2012). Retrieved from http://en.wikipedia.org/wiki/Dependency_grammar/.

Fan, J., Kalyanpur, A., Gondek, D. C., & Ferrucci, D. A. (2012). Automatic Knowledge Extraction From Documents. *IBM Journal of Research and Development*, *56*(3.4), 5:1- 5:10.

Firdaus, O. M., Suryadi, K., Govindaraju, R., & Samadhi, T. M. A. A. (2012). Medical Knowledge Sharing Guideline: A Conceptual Model. In *Proceedings of International Conference on ICT and Knowledge Engineering*, pp. 22- 26.

Hao, T. Y., Ni, X. L., Quan, X. J., & Liu, W. Y. (2009). Automatic Construction of Semantic Dictionary for Question Categorization. *Journal of Systemics, Cybernetics and Informatics*, *7*(6), 86-90.

Hull, R., & Gomez, F. (1999). Automatic Acquisition of Biographic Knowledge From Encyclopedic Texts. *Expert Systems with Applications*, *16*(3), 261-270.

Minpar Evaluation. (2012). http://www.cs.ualberta.ca/~lindek/downloads.htm.

OpenNLP. (2012). http://opennlp.sourceforge.net/projects.html.

Smith, M. K., Welty, C., & McGuinness, D. L. (2004). OWL Web Ontology Language Guide. *W3C*.

Tanaka, K., & Jatowt, A. (2010). Automatic Knowledge Acquisition from Historical Document Archives: Historiographical Perspective. *LNCS*, *6259*, 161-172.

TreeTagger. (2012). Retrieved from http://www.ims.uni-stuttgart.de/projekte/corplex/TreeTagger/.

Wang, Y. M., Johanna, V., & Haase, P. (2006). Towards Semi-automatic Ontology Building Supported by Large-scale Knowledge Acquisition. In *AAAI Fall Symposium On Semantic Web for Collaborative Knowledge Acquisition*, Vol. FS-06-06, pp.70-77.

WordNet. (2012). Retrieved from http://wordnet.princeton.edu/.

Yahoo! Answers. (2012). Retrieved from http://answers.yahoo.com/.

Pertanika J. Sci. & Technol. 21 (1): 183 - 192 (2013)

SCIENCE & TECHNOLOGY

Journal homepage: http://www.pertanika.upm.edu.my/

Issues on Trust Management in Wireless Environment

Abubakr Sirageldin*, Baharum Baharudin and Low Tang Jung

Computer and Information Science Department, University Technology Petronas, Bandar Seri Iskandar, 31750 Tronoh, Perak, Malaysia

ABSTRACT

Developing a trust management scheme in mobile computing environment is increasingly important, and the effective trust management model is a challenging task. Business, education, military, and entertainment have motivated the growth of ubiquitous and pervasive computing environments, which are always available due to the widespread of portable and embedded devices. Wireless and mobile computing are good example of ubiquitous and pervasive computing environments. Due to the uncertainty and mobility in such environments, the issue of trust has been regarded as an important security problem. Malicious nodes are a major threat to these networks; the trust system can monitor the behaviour of nodes and accordingly rewards well-behaved nodes and punishes misbehaving ones. At present, there are a lot of endeavours on the trust model of the pervasive computing environment. In this paper, a trust management framework for mobile computing is presented. The hybrid framework is based on a fusion of the support vector machine (SVM) and fuzzy logic system. From the results, it can be stated that the framework is effective, dynamic, lightweight, and applicable.

Keywords: Trust management, support vector machine, fuzzy logic, membership, interaction, pervasive, recommendation, central node, relationship

INTRODUCTION

Due to the rapid growth in network and communication technology, and the widespread of various types of computing devices, and the constant availability of services, security, confidentiality and the reliability are required in such an environment. Devices interact, collect and transfer information with simplicity, and minimal technical expertise without being previously introduced to each other. This necessitates a certain concept of security such as trust. In order to maintain a secure, dependable, and reliable environment, a smart security system without or with the least human participation is

Article history:
Received: 31 March 2012
Accepted: 31 August 2012

E-mail addresses:
abubakrsirag@gmail.com (Abubakr Sirageldin),
baharbh@petronas.com.my (Baharum Baharudin),
lowtanjung@petronas.com.my (Low Tang Jung)
*Corresponding Author

ISSN: 0128-7680 © 2013 Universiti Putra Malaysia Press.

needed. Therefore, both privacy and security challenges are confronting security professionals, because in such environments, a chance is available for bad intent entities to launch attacks to others easily (Mieso *et al.*, 2010). The traditional security models are based on the integration of, authentication, authorization, and access control to provide a secure environment. These traditional solutions can be useful in wired infrastructures. However, they are not efficient in pervasive and wireless infrastructures due to the dynamic topology of the wireless network that changes quickly, and the scalability of the wireless networks needs to be considered as well (Boukerche *et al*., 2008). Many studies have been conducted in this field. The previous works used different methods to achieve the objectives of the trust management system, and these can be briefly summarized as the trust models based on Bayesian approach and probabilistic theory (Almenarez *et al*., 2011), and trust models based on fuzzy logic (Wenshuan *et al*., 2007), trust model based on Dempster-Shafer and the theory of evidence (Zeng *et al*., 2010), and some approaches based on game theory. Despite these previous efforts, the optimum solution has not been reached. In this paper, a combination of two methods is proposed to recover the limitations of the existing ones. In particular, a trust management scheme is proposed by implementing a fusion of support vector machine (SVM) and fuzzy logic. The main motivation of the proposed scheme in using SVM is to predict the optimal relationship values for approximation purpose. Those approximated values will then relate the fuzzy basis functions for uncertainty resolving purpose, and the inference rules are invited for evaluating the trustworthiness of the devices.

The Previous Work

Trust in pervasive computing environments has obtained wide attention and become a challenge, with both wireless and mobile networks growing in a complex way. Many solutions have been proposed to solve the issue. Among other, Wenshuan *et al*. (2007) proposed a trust framework for pervasive computing using statistical distribution. The framework is composed of three models, namely, trust, security, and a risk model to resolve the uncertainty problem. Meanwhile, Boukerche *et al*. (2008) proposed a security system based on the trust management model using linear functions. The model assigns credentials to nodes, updates private keys, calculates trustworthiness for a node, as well as presents authority policy and access rights. Dong *et al*. (2010) presented a lightweight multilevel trust management framework based on the Bayesian formalization to produce trust assessments based on direct and recommended interaction. Mieso *et al*. (2010) investigated their previous probabilistic trust management scheme, and identified the possibility of a device to choose another for interaction by assessing its trustworthiness according to the current interaction and recommendations. Similarly, Shuai *et al*. (2010) proposed a dynamic trust model using the Dempster-Shafer for the set hypothesis on trust evaluation based on the accumulation of evidence. The model expresses the relationship between entities as direct, indirect, and integrated trust. Using their model, anonymous object can participate in the interaction with other trusted parties without any central security control.

Denko *et al*. (2008) proposed a model which utilizes probability distribution. The trust value is a probability of satisfactory interactions between any two neighbours. The distributed model uses filtering methods for recommendations. The weighting method is used for measuring the effect of time on the current behaviour of the devices. Wu (2011) proposed a Stable Group-

based trust Management Scheme by considering geographic position, analysing the mobility patterns of nodes, and evaluating the trustworthiness without relying on any specific networking architecture. Meanwhile, Rhymend *et al*. (2010) proposed an approach that utilizes fuzzy logic for different trust characteristic's integration, whereby the trust values are calculated based on the interaction of the devices with the environment, and the model also uses a global data store point. Nonetheless, some drawbacks have been observed in the existing approaches; these include assuming transitivity of the trust, ignorance of the vagueness and uncertainty, and ignorance of the network traffic nature. Despite these previous efforts, an optimum solution has not been reached yet. In this work, a combination of two approaches is made using SVM to cope with network traffic nature and fuzzy logic as well as to cope with uncertainty problem. Accordingly, the model has shown the expected results.

Trust Concept

Trust concept occurs in many fields. The meaning of trust is tailored to its specific use in a particular application domain (Walt Yao, 2004). In computing, trust is an essential foundation for information security, where the security is concerned with the correct operations of software and hardware. The challenge of exploiting trust in computing lies in extending the use of trust based solutions. First to artificial entities such as software agents or subsystems, then to the human user's subconscious choice (Punam *et al*., 2008). In Social, trust is often used by people in a very broad sense. Its interpretation depends on many issues such as past experiences, associated risks, recommendations from other parties, the reputation of the trusted parties, or even cultural background (Walt Yao, 2004). The basis of this form of trust lies in familiarity, bonds of friendship and common faith and values. In networks, the relationships among participating entities are extremely needed for reliability and security of the collaborative environment. In this context, trust is defined as a set of relations among entities that participate in a protocol. These relations are based on the evidence generated by the previous interactions of entities Jin-Hee *et al*. (2011). Based on the above discussions, some sources that assist the establishment of trust are discussed.

Experience: The past record provides a good indication of future interactions. Depending on the knowledge recorded from the previous interactions, the degree of trust may either increase or decrease. Experiences can involve some trusted parties, and they may be as useful in recommendations.

Recommendation: It is a third party evaluation, and it depends on its source. In real life, a recommendation is employed to assist decision-making in daily situations. It helps decision makers by providing evaluations from others.

Reputation: is another popular mechanism that people employ to deal with unfamiliar parties. Similar to the recommendation, it does not require any prior experience with the party for a reputation to be used to infer trustworthiness (Walt Yao , 2004). Some previous research mentioned some features of trust such as exist on uncertain and risky environment, context dependent, requires previous knowledge and experience, quantitative, based on reputation and opinion, subjective, not necessarily transitive, asymmetric, and dynamic.

THE APPROACH AND METHODS

In our approach, a centralized environment is considered. Each centre operates autonomously and collaborates with another centre, and takes the responsibility of disconnecting or establishing a connection, and evaluates the trustworthiness of each node. We have two types of trust, namely, direct trust (the history of interactions in the environment as motivated by Sanjeev *et al*., 2010) and others) and indirect trust (or recommendations, as motivated by Zhong *et al*. (2010), Trcek (2011) and others. In order to understand the model architecture in a simple way, let us consider the relationship between two nodes, namely, A and B. The trust of A to B is $V_{A,B}$ and the trust of B to A is $V_{B,A,}$ as shown in Fig.1. If *A* sends to *B*, and *B* sends to *A*, then the relationship is established, and values initiated. Each node has (*N-1*) relationships with the others. The total number of the relationships in the network is *N**(*N-1*) relationship.

Direct Trust Computation

The previous interactions are taken under consideration in the context, such as the history of interactions H_{AB} between *A* and *B* is computed numerically in the range [0, 1], based on satisfactory/ unsatisfactory interactions, and good/bad packets sent. Let *Ps* be the number of good packets, *Pu* is number of bad packets, *S* is the number of satisfactory interactions, and *U* is the number of satisfactory interactions, while *S* and *U* are calculated as:

$$S = \frac{P_s}{P_s + P_u} \tag{1}$$

The history of interaction value, H, is:

$$H = \frac{\text{number of Satisfactory Interactions}}{\text{Total Number of Interactions}} \tag{2}$$

For each node, the average of interactions {*H1, H2, H3...Hm*} with another node where *m* is the number of previous interactions that is computed as:

$$H_{average} = \sum_{i=1}^{m} H_i \tag{3}$$

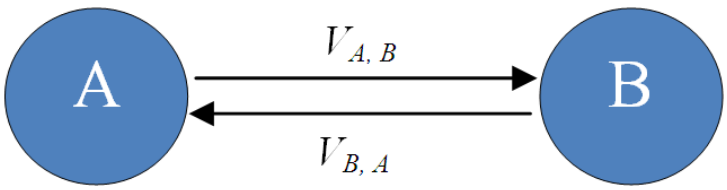

Fig.1: The simple trust relation between nodes

The average value then forms the relationship value. In a network of *N* nodes, each node has (*N-1*) relationships, the total number of relationships in the network is *N**(*N-1*). Now, these relationships are forming an *NxN* matrix of real number. The rows are the values given to other nodes in the environment by node *i*, and the columns are the values given to node *i* by others. Where H_{ij} denotes the history of interaction value for node *i* to node *j*, and the diagonal of the matrix H_{ii} is the accumulated interaction values for the node, *i*.

Indirect Trust Computation

In fact, the recommendation is the history of interaction of a node in other environments. In this study, the average value of recommendations is used. Let $R = \{R_1, R_2, R_3 ... R_k\}$ be the set of K's centre recommendations, then:

$$R_{average} = \frac{\sum_{i=1}^{k} R_i}{k} \tag{4}$$

The average recommendation is the accumulated relationship value from outside the environment.

The Hybrid Computation

The previously mentioned matrix, which constructed by *N**(*N-1*) relationships, is now the kernel trick matrix. The matrix is fed into the support vector machine for prediction purpose based on the relationship values. A suitable kernel trick function such as $k(x,y)=(<\Phi(x),\Phi(y)>)$ is used.

Where the input data are the relationship values forming the kernel matrix. The SVM technique approximates the total value for each node according to the relationship values in the kernel matrix. The expensive calculations can be reduced by using a suitable kernel trick decision formula.

$$f(x) = \text{sgn}\left[\sum_{i=1}^{n} y_i \alpha_i . k(x, y)\right] \tag{5}$$

The output results in a vector of N elements describe the predicted value for each node, and this vector contains values range in an interval [0 1]. These values imply fuzziness and uncertainty expression for evaluating trustworthiness of a node. Among the various fuzzy logic (MFs), the simple trapezoid MF is used to reduce execution overhead in order to make a lightweight model. The fuzzy sets designed for this model are VU, UT, TW, and VW, which represent Very Untrustworthy, Untrustworthy, Trustworthy, and Very Trustworthy, respectively. Therefore, there are a total of four MFs, as shown in Fig.2.

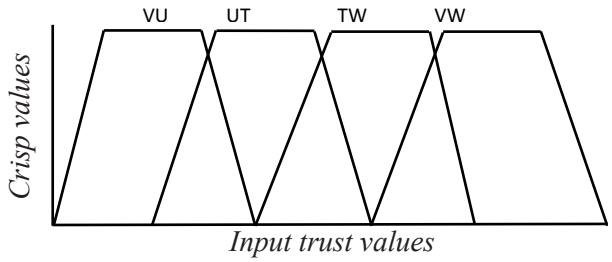

Fig.2: Trapezoid Fuzzy set membership functions

The trapezoid MF is described by four numerical parameters (a, b, c, and d), with d-c shoulder which is expressed by the following formula:

$$f(x,a,b,c,d) = \max\left\{\min\left(\frac{f(x)-a}{b-a},1,\frac{d-f(x)}{d-c}\right),0\right\} \quad (6)$$

The MF expression generates two crisp values in different MFs. The first value denoted as lower bound MF and the second denoted as upper bound MF. If the upper bound MF value is greater than the threshold value, the decision will then be upper bound MF, or else, the decision is the lower bound MF. The inference rules are playing a role in the final decision manifesto.

Performance Evaluation

In this section, the performance of the hybrid scheme SVM-Fuzzy is tested. In particular, the dynamic characteristic of the model is examined, while the values are collected perfectly. The data type is a real number, and the values are in a range [0 1]. Any connection request managed by the centre and all well-trusted nodes participate in the interaction without any obvious involvement of the centre. The completely new node implies constructing a new record on the environment, so the new identified node is verified by retrieving its record as recommendations from the other centres. In fact, the recommendation is the past interaction history of the new node in these environments. The centre will then validate the retrieved data for the purpose of establishing a connection with another node. The established connection is confirmed by that destination node. The values are dynamic and updated each time the record is altered.

Parameter Setup: In the experimental zone, three parameters are used, namely, the relationship values, the recommended values, and the number of nodes in the network.

Performance Metrics: The model used five metrics. The average relationship value *H* represents the statistical mean of relationship values, and the predicted value *f(x)* of kernel trick. The crisp value represents the trapezoid MF expression *f(a,b,c,d)*, average recommendations, *R*, and the threshold value, *T*.

The Results of the Experiments

The effective of SVM: the model is tested offline, and due to this circumstance, the data are arbitrary initiated in a range between 0 and 1. The number of nodes and the values of α are varied in order to study the performance of SVM.

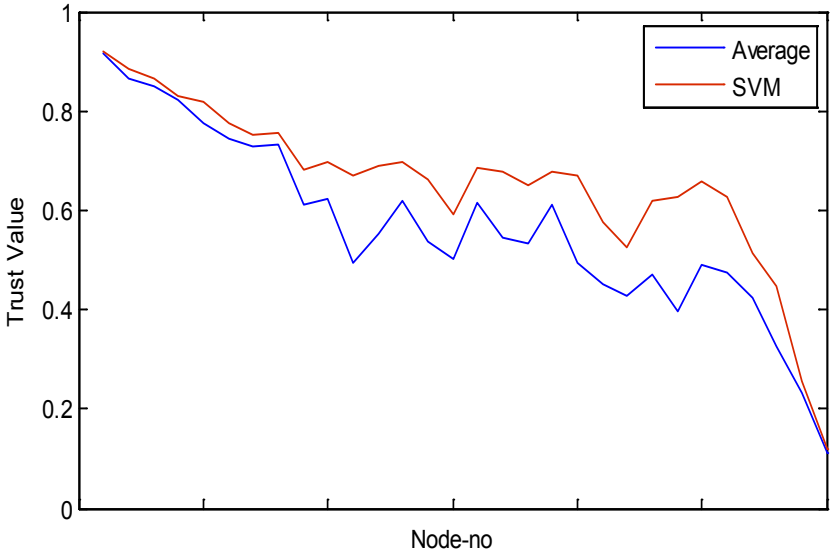

Fig.3: The performance of SVM against basic Statistics (average)

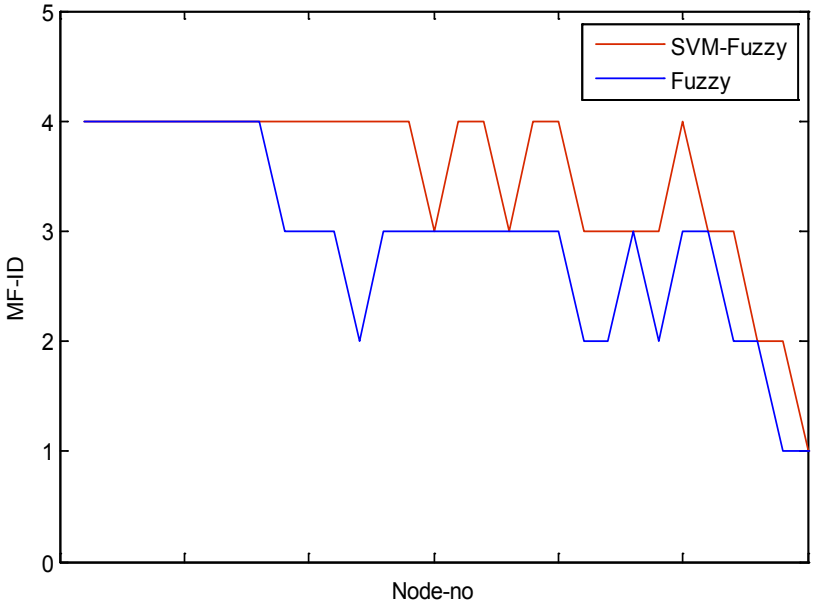

Fig.4: Comparison of SVM-Fuzzy against Fuzzy, the vertical axis 1, 2, 3, 4 represent the four MFs VU, UT, TW, VW, respectively.

The significance of threshold value: In this experiment, the effectiveness of the fuzzy logic performance under different threshold values is argued.

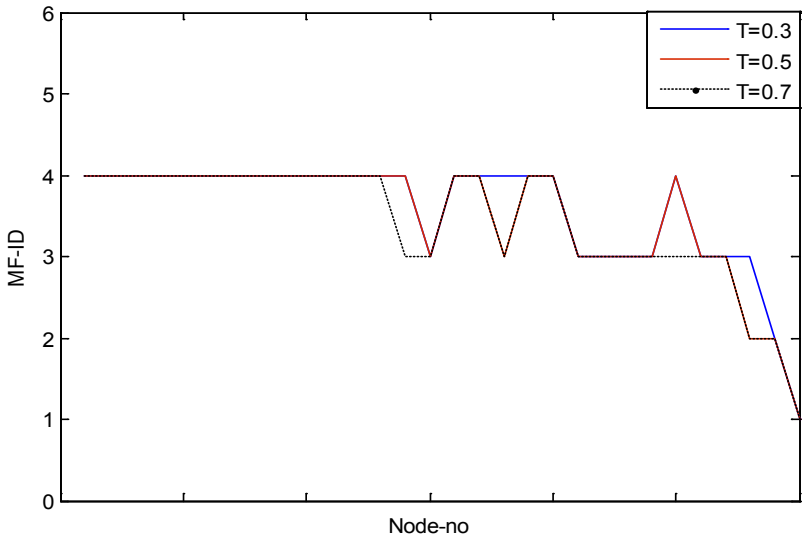

Fig.5: Fuzzy logic Performance

RESULTS AND DISCUSSION

The experiment went as expected without unusual input data that would have introduced errors. The input data were the real values in a range between 0 and 1. The type of the statistical method used has enforced the interaction observations to be in the above-mentioned range. Carefully, the SVM parameters were initialized, and the Gaussian function which led to the predicted values was used to avoid the the execution overhead of the kernel trick. Only one α was assumed for each data-range in the kernel matrix and the graph depicted in Fig.4 reveals the differences. Fig.3 shows the the performance of SVM and the modified values. This modification is almost under the general rules of the trust management policy. The adjustment was done to enhance the average calculation of the interaction history with a single node. In this study, an acceptable rate was chosen due to the relationship values. The result shows a good performance of SVM compared to the statistical average. As a part of this experiment, the predicted values were the input of the fuzzy expression, and the crisp values were accordingly calculated for each node. In this calculation, the values were assumed to be couple according to the trapezoid MF expression. The inference rules were applied to the couple under a predefined threshold value. The comparison between SVM-Fuzzy and Fuzzy (see Fig.5) is exactly different. In Fig.4, the vertical axes 1, 2, 3, 4 represent the four MFs VU, UT, TW, and VW, respectively. The results of the combined SVM-Fuzzy have been studied by comparing them with the performance of the Fuzzy logic alone under a threshold value T=0.5 before the optimization process.

The threshold value is an administrative issue, and it should have been specified previously due to the policy. Fig.5 shows the results of different threshold values (T=0.3, T=0.5, T=0.7). Note that the threshold value is defined according to the trust policy in the entire network. Errors may arise when the relationship values are out of the range, and this indicates that the optimized value may not be precise for the entire range.

Contributions

The main contribution of the current work is the possibility of the use of automated hybrid SVM-fuzzy for trust management. In addition, the framework shows some advantages such as follows: first, it does not conflict with any security infrastructure in the environment; second, it is dynamic as the trust changes according to the activities of the node; third, it is protected against false recommendation that can be given by human; and finally, it lets the autonomous entities interact freely without security management overhead.

CONCLUSION AND RECOMMENDATIONS FOR FUTURE WORK

The issue of trust is really a challenge in ubiquitous and pervasive computing environments, especially for wireless and mobile networks. In this paper, the concept of trust has been presented and the basic of a controlled environment has also been explained. The framework is based on simple statistical methods which are used in interaction computation. Hence, a framework that integrates both the SVM and fuzzy system is proposed. Other than the trust frameworks, the importance of the central point, which is responsible of the trust calculation and evaluation process, have also been taken into consideration. In order to obtain a reliable recommendation, the central point request policy has been adopted. In addition, the framework has the capability of: (1) avoiding conflict with any security infrastructure in the environment, (2) dealing with the dynamic nature of trust, (3) giving protection against the false recommendation, and (4) avoiding security management overhead. A possible future work is the direction towards multidisciplinary approaches due to the complexities in the environments.

REFERENCES

Almenárez, F., Marín, A., Díaz, D., Cortés, A., Campo, C., & García-Rubio, C. (2011). Trust management for multimedia P2P applications in autonomic networking. *Ad Hoc Networks, 9*(4), 687-697.

Bedi, P., & Gaur, V. (2008). Trust based prioritization of quality attributes. *International Arab Journal of Information Technology*, *5*(3), 223-229.

Boukerche, A., & Ren, Y. (2008). A trust-based security system for ubiquitous and pervasive computing environments. *Computer Communications, 31*(18), 4343-4351.

Denko, M. K., Sun, T., & Woungang, I. (2011). Trust management in ubiquitous computing: A Bayesian approach. *Computer Communications, 34*(3), 398-406.

Deno, M. K., & Tao, S. (2008, 17-20 Dec. 2008). *Probabilistic Trust Management in Pervasive Computing*. Paper presented at the Embedded and Ubiquitous Computing, 2008. EUC '08. IEEE/IFIP International Conference.

Jin-Hee, C., Swami, A., & Ing-Ray, C. (2011). A Survey on Trust Management for Mobile Ad Hoc Networks. *Communications Surveys & Tutorials, IEEE, 13*(4), 562-583.

Rhymend Uthariaraj, V., Valarmathi, J., Arjun Kumar, G., Subramanian, P., & Karthick, R. (2010). A Novel Trust Management Scheme Using Fuzzy Logic for a Pervasive Environment. In N. Meghanathan, S. Boumerdassi, N. Chaki & D. Nagamalai (Eds.), *Recent Trends in Networks and Communications* (Vol. 90, pp. 144-152): Springer Berlin Heidelberg.

Sharma, S., Mishra, R., & Kaur, I. (2010, 9-11 July 2010). *New trust based security approach for ad-hoc networks.* Paper presented at the Computer Science and Information Technology (ICCSIT), 2010 3rd IEEE International Conference.

Trcek, D. (2011). Trust Management in the Pervasive Computing Era. *Security & Privacy, IEEE, 9*(4), 52-55.

Wenshuan, X., Yunwei, X., & Guizhang, L. (2007, 21-25 Sept. 2007). *A Trust Framework for Pervasive Computing Environments.* Paper presented at the Wireless Communications, Networking and Mobile Computing, 2007. WiCom 2007.

Wu, X. (2011). A Stable Group–based Trust Management Scheme for Mobile P2P Networks. *International Journal of Digital Content Technology and Its Applications*, *5*(2), February.

Yao, W. (2004). *Trust management for widely distributed systems*. Technical report, UCAM-CL-TR-608. Retrieved from http://www.cl.cam.ac.uk/techreports/UCAM-CL-TR-608.pdf

Zeng, S., Xu, F., Xin, Y., Yand, Y-X., & Hu, Z-M. (2010). Trust Model based on Dynamic Policy Similarity for pervasive Computing Environments. *IEEE,* 978-1-4244-6349.

Zhong, D., Zhu, Y., Lei, W., Gu, J., & Wang Y. (2010). Multilevel Trust Management Framework for Pervasive Computing. *Third International Conference on Knowledge Discovery and Data Mining*. *IEEE*, 978-0-7695-3923.

Pertanika J. Sci. & Technol. 21 (1): 193 - 204 (2013)

SCIENCE & TECHNOLOGY

Journal homepage: http://www.pertanika.upm.edu.my/

A Negation Query Engine for Complex Query Transformations

Rizwan Iqbal* and Masrah Azrifah Azmi Murad

Faculty of Computer Science and Information Technology, Universiti Putra Malaysia, Serdang, Selangor, Malaysia

ABSTRACT

Natural language interfaces to ontologies allow users to query the system using natural language queries. These systems take natural language query as input and transform it to formal query language equivalent to retrieve the desired information from ontologies. The existing natural language interfaces to ontologies offer support for handling negation queries; however, they offer limited support for dealing with them. This paper proposes a negation query handling engine which can handle relatively complex natural language queries than the existing systems. The proposed engine effectively understands the intent of the user query on the basis of a sophisticated algorithm, which is governed by a set of techniques and transformation rules. The proposed engine was evaluated using the Mooney data set and AquaLog dataset, and it manifested encouraging results.

Keywords: Natural language interfaces, ontology, semantic web, negation queries, search engines

INTRODUCTION

Many natural language interfaces have been developed to date. The concept of natural language interfaces is not new. Natural language interfaces were initially used for databases which allowed users to submit their queries in natural language instead of writing in SQL query format. Since the emergence of ontologies in the field of computer science, researchers have started developing interfaces for them. Natural language interfaces facilitate users to express their information needs in natural language that they are familiar with and can consequently populate knowledge bases.

Depending upon the ability to process natural language input, natural language interface can be classified into two categories, namely full natural language interface and restricted natural language interface. Full natural language interfaces provide the ease of inputting a natural language query without any

Article history:
Received: 31 March 2012
Accepted: 31 August 2012

E-mail addresses:
mail.rizwaniqbal@yahoo.com (Rizwan Iqbal),
masrah@fsktm.upm.edu.my (Masrah Azrifah Azmi Murad)
*Corresponding Author

ISSN: 0128-7680 © 2013 Universiti Putra Malaysia Press.

restriction of vocabulary, whereas restricted natural language interfaces contradict the former and restrict users to input a restricted vocabulary.

Natural language interfaces work by converting natural language into formal semantic query (Tablan *et al*., 2008a). Different interfaces rely on distinct techniques and algorithms to translate natural language query into formal semantic query. Some natural language interfaces that support full natural language support are Semsearch (Lei *et al*., 2006), NLP-Reduce (Kaufmann *et al*., 2007), FREya (Damljanovic *et al*., 2010), QuestIO (Tablan *et al*., 2008b), Spark (Zhou *et al*., 2007), Q2Semantic (Wang *et al*., 2008) and NLION (Ramachandran & Krishnamurthi, 2009). Natural language interface that comes under the category of restricted natural language interfaces include Orakel (Cimiano *et al*., 2008), and AquaLog (Vanessa *et al*., 2007).

Natural language queries with negation are a very usual and expected input from the user. In this study, Mooney dataset (MooneyData, 1994), which is widely applied for the evaluation of natural language interfaces and systems (Wang *et al*., 2007; Damljanovic *et al*., 2010; Tablan *et al*., 2008b; Kaufmann *et al.*, 2006; Iqbal *et al.,* 2012) was used. This dataset has a number of negation queries in it. This paper proposes a negation query handling engine, which effectively caters negation natural language queries. The proposed negation query handling engine supports full natural language rather than restricted language. The proposed engine effectively understands the intent of the user's negation query on the basis of a sophisticated algorithm, which is governed by a set of techniques and transformation rules. The rest of this paper is organized as follows. Work related to the current study is discussed in the next section. Then, the motivation for the proposed negation query handling engine is discussed. Later sections cover the design, technical details and evaluation of the proposed engine. Finally, the paper is concluded by the conclusion and future work section.

RELATED WORK

All developed natural language interfaces differ from each other in one way or another. Some natural language interfaces focus on giving users the freedom of entering natural language query using free vocabulary (Lei *et al*., 2006), while others allow users to enter natural language query using a restricted vocabulary (Cimiano *et al*., 2008; Vanessa *et al*., 2007). Other than natural language interfaces, there are also interfaces that allow the user to search knowledge bases by inputting formal language queries. Such search engines are of two types; first is the form-based search engine, which provides web forms as a means of specifying queries (Rocha *et al.,* 2004), and second is the RDF-based querying search engine which supports RDF-based querying languages at the front end (Rocha *et al*., 2004).

SHOE (Heflin & Hendler, 2000) is an interface which comes in the category of form-based semantic search engine. This system is based on a semantic mark-up language. SHOE (Heflin & Hendler, 2000) allows users to define and associate vocabularies which can be understandable by the machines. The system uses knowledge annotator to add up SHOE annotations to the documents. Naive users often feel uncomfortable using SHOE as the web forms require familiarity with the knowledge bases being searched. On the other hand, adding annotations with SHOE is more time consuming as compared to standard XML.

Corese (Corby *et al*., 2004) search engine is from the category of RDF-based querying language fronted search engines. This search engine is dedicated to RDF metadata. The Corese engine internally works on the concept of conceptual graphs (CG). The query and the ontology schema are translated from RDF to conceptual graphs (CG) in order to perform matching operations. The limitation with such search systems is that they require the users to be familiar with both the knowledge base and the querying language used.

The kind of interfaces that take a formal language query for input remains comparatively less preferred by users than the natural language query interfaces. The reason is the fact that users require training of the system as well as reasonable knowledge about the knowledge bases being searched. When talking about the systems that support natural language, SemSearch (Lei *et al*., 2006) is an interface that was designed to take input in natural language from the users. The system has idealized Google for the style of its interface. In particular, SemSearch (Lei *et al*., 2006) uses three heuristic operators to support its search. The use of these heuristic operators helps the system to have a clue of what information exactly the user wants from the knowledge bases. SemSearch relies on simple string matching algorithms rather than using complex techniques like WordNet (Fellbaum, 1998) in order to reduce the response time of the system. The use of the simple string matching algorithms reduces the response time but at the same time, it can be a reason for losing some good matches in certain situations.

AquaLog (Vanessa *et al*., 2007) is a natural language based question-answering system. It takes input in the natural language query and answers on the basis of ontology loaded in the system. AquaLog has a learning mechanism in which it helps to improve the performance over time. Relation Similarity Service (RSS) is a component of AquaLog and it is considered as the backbone of the system. In case of any ambiguity between multiple terms, the RSS module directly interacts with the user to disambiguate between the terms of natural language and the concepts of the knowledge bases. The limitation with AquaLog is that it can at the most translate the query to two triples.

QuestIO (Tablan *et al*., 2008b) is another natural language interface that was designed to take natural language input from the user. It was designed to cater language ambiguities, handle incomplete and grammatically incorrect queries. QuestIO focuses to be an open domain system that does not require any customization by the users, as well as any training to use it. This system uses light weight linguistic processing that allows the user's text to be fully analyzed in the query processing part for the identification of ontology concepts and property names. QuestIO works by finding implicit relations which are not clearly stated in the user query. The limitation is that it only works with directly explored relations (Tablan *et al*., 2008b).

The creators of QuestIO (Tablan *et al*., 2008b) later developed another natural language interface named FREya (Damljanovic *et al*., 2010). The focus of creating FREya was to further reduce customization efforts and to introduce clarification dialogues mechanism to avoid empty results. The clarification dialogue mechanism in FREya helps users to get answers in case the system is not able to find any answer (Damljanovic *et al*., 2010). If the system does not come up with an answer automatically, it will interact with the end users to get a clue for the right answer. The user's selections are saved over time and the system learned to place correct suggestions on top of any similar query next time on the basis of the saved user selections. FREya reported satisfactory results for the learning mechanism in it but its

correctness without clarification dialogues was considerably low as compared to other similar systems like PANTO (Wang *et al*., 2007) for the same data. Damljanovic *et al*. (2010) also reported that FREya was not able to answer some questions correctly while evaluating. The questions that were answered incorrectly included those with negation. PANTO (Wang *et al*., 2007) is another natural language interface that is portable and does not make any assumption about any specific knowledge domain. It functions in a way that it picks the words from the natural language query and map them to entities (concepts, instances, relations) in the ontology.

The architecture of PANTO (Wang *et al*., 2007) relies on the existing tools like WordNet (Fellbaum, 1998) and different string metric algorithm. In PANTO, the Lexicon Builder automatically extracts ontological resources (Classes, Object and Datatype properties, Literals, Instances) from the ontology and constructs the Lexicon. The translator is the core processing engine of PANTO. It receives the processed natural language query from the parser as input and then performs operations to map the natural language entities to the ontological entities.

PANTO uses an off the shelf parser which relies on limited NLP techniques, and this restricts the scope of queries which can be handled by the system (Wang *et al*., 2007). Wang *et al.* (2007) also discussed the limitation of PANTO in relation to the weakness in supporting complex user interactions. The current version of PANTO deals with superlative, comparative, conjunction and negation kind of queries. Nonetheless, PANTO has not discussed how effectively it can deal with the queries. PANTO discusses that it can handle negation queries including "not" and "no". However, Wang *et al.* (2007) have not discussed in detail how effectively PANTO can deal with negation queries or what the precision of the system is in catering particularly with negation queries. From the literature, it is found that all systems have discussed about their supports for catering negation queries. Wang *et al.* (2007) mentioned that it could support negation queries but did not give any detail that to what extent and precision it could cater them. Damljanovic *et al.* (2010) discussed about catering negation cases, and explicitly mentioned that their system had failed to answer some questions correctly and amongst them were questions with negation.

MOTIVATION FOR NEGATION QUERY HANDLING ENGINE

After studying the trend in some natural language interfaces over the years, it is found that the state-of-art interfaces are particularly focusing on some specific features. Some of these features include portability (Wang *et al*., 2007), users' interaction (Damljanovic *et al*., 2010), automated learning (Vanessa *et al*., 2007; Damljanovic *et al*., 2010), lesser customization (Lei *et al*., 2006), detecting and resolving the ambiguity in natural language (Lei *et al*., 2006) and precision in understanding the complexity of the natural language query (Wang *et al*., 2007; Tablan *et al*., 2008a). For a natural language interface to be effective for the user, it is very critical for it to understand the complexity of the natural language query inputted by the user. Over the years, researchers have improved from simple string matching algorithms to advance natural language processing engines which are designed to understand the complexity of natural language.

It was found that natural language interfaces have the capability to deal with different types of queries such as instance superlative, comparative, conjunction and negation. Systems like

PANTO (Wang *et al*., 2007) and FREya (Damljanovic *et al*., 2010) have discussed negation queries. In particular, PANTO has given no details about the extent, details and precision for which it can handle the negation queries. FREya only discussed that the system was not able to answer some questions correctly and amongst them were questions with negation. Natural language queries with negation are very usual and expected input from the user. A review of relevant literature has shown that the Mooney dataset (MooneyData, 1994) and AquaLog dataset (AquaLogData, 2007) are widely used for the evaluation of natural language interfaces (Wang *et al*., 2007; Damljanovic *et al*., 2010; Tablan *et al*., 2008a; Kaufmann *et al*., 2007). These datasets have negation queries in them.

A natural language interface with the capability to handle negation queries must be able to correctly interpret the intent of the user's query to its equivalent formal query language. In order to correctly interpret the intent of the user's query, the natural language interface cannot just rely on simple keyword detection and simple string matching algorithms. An effective negation handling interface must have a sophisticated algorithm that is governed by a set of rules. These rules should give a deeper insight into the natural language interface about the negation query under consideration. An in-depth understanding of the negation query will facilitate the interface to make appropriate transformations of natural language query to its equivalent formal query language, keeping intact the intent of the user.

The absence of such an algorithm focusing to handle negation queries has become a motivation for this research. This research came up with a negation query handling engine which incorporates an algorithm that has been particularly designed to cater negation queries in an effective manner. The next section discusses the design of negation query handling engine in detail.

THE DESIGN OF NEGATION QUERY HANDLING ENGINE

The negation query handling engine was designed to cater effective machine level transformation for the natural language query entered by the user. The engine was designed to perform some processes in a sequential manner. There is also a set of natural language query transformation rules which are implemented according to the structure of the natural language query entered by the user. Fig.1 shows how the negation query handling engine works.

The processes performed by the negation query handling engine

The negation query handling engine performs three processes on the natural language query entered by the user. The first process identifies the negation keywords in the natural language query. The second process is responsible to identify the coordinating conjunctions in the natural language query structure. The final process is responsible to make sure that the natural language keywords are correctly mapped to the corresponding ontological resources (Classes, Object and Datatype properties, Literals, Instances) and the machine level transformations are correctly carried out.

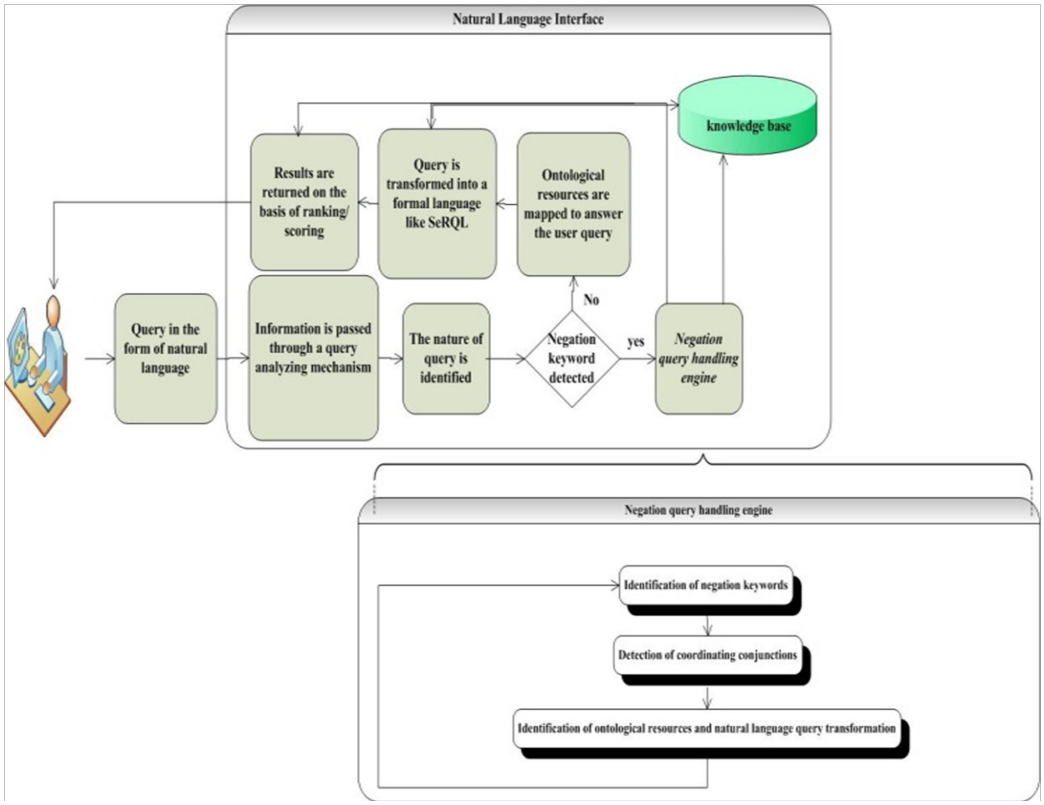

Fig.1: Negation query handling engine

Identification of negation keywords

This process deals with the identification of negation keywords. The engine intelligently identifies keywords with a broad coverage in the aspect of negation. Some previous systems like PANTO (Wang *et al*., 2007) suffer limited support for negation queries. In particular, PANTO handles those queries including "not" and "no". This engine was designed to handle several kinds of queries including those with does not/ do not/ don't/ excluding/ except/ leaving/ none/ and other than. The proposed engine also has provision to handle affirmative-negative and affirmative-negative-pseudorel type of queries, whereby such queries can be found in the AquaLog data set (AquaLogData, 2007). In addition, the proposed engine does not only identify negation keywords but also makes appropriate transformations from the natural language to formal query language (like SPARQL) keeping in integrity the negation sense of the user query.

Detection of coordinating conjunctions

After the occurrence of negation keywords, the engine looks for coordinating conjunctions in the natural language query. Coordinating conjunctions include for, and, nor, but, or, yet, so. If a coordinating conjunction is detected, only the keywords before it will be considered for

query formation. The occurrence of a coordinating conjunction depicts that the query has more than one condition in it. For example, if the Mooney dataset (MooneyData, 1994) which is used as a test data for many natural language interfaces to ontologies is considered, it is found that there are many queries in it which have more than one condition in them. The existence of more than one condition in the user's query makes query transformation a complex task especially when handling negation queries.

Identification of ontological resources and natural language query transformation

This process deals with the identification of ontological resources. After the identification of ontological resources (Classes, Object and Datatype properties, Literals, Instances), the engine performs the transformation of natural language query to its formal query language equivalent. The engine ensures that the transformation is in alignment with the viewpoint of the user. The natural language query transformation rules were designed on the basis of some rules. These rules have been found to be satisfying the negation queries within the Mooney dataset (MooneyData, 1994) and AquaLog dataset (AquaLogData, 2007).

The natural language query transformation rules

The negation query handling engine transforms natural language query to formal query language on the basis of some rules. These rules are applied to the natural language query, depending on the detection of certain scenarios. These rules give an insight into the engine about the intent of the user query and actions which should be applied on the user's query for transforming it into the formal query language equivalent. These rules were tested on the Mooney dataset and AquaLog dataset, and encouraging results were seen while performing the query transformation. Table 1 shows some query transformation rules.

Step-by-step processing of the natural language query

The negation query handling engine performs step-by-step operation on the natural language query inputted by the user. The operations on the natural language query can handle a negation query with two possible cases. The first case deals with explicit negation words like not/ do not/ don't/ excluding/ except/ leaving/ none. The second case deals with affirmative-negative and affirmative-negative-pseudorel type of queries. Below is the step-by-step processing for the first case.

1. A negation keyword is detected in the user's query.
2. After detecting the negation keyword, the engine looks for a coordinating conjunction.
3. If a coordinating conjunction is found, only the keywords before it are considered for query transformation; otherwise, all the keywords are considered for the query transformation.
4. The engine tries to map the literals and instances from the knowledge base to the keywords in the user's query.
5. If the engine fails to find an appropriate match for a literal or an instance, it is then expected that a data or object be detected.

TABLE 1: Query transformation rules

Rules	Actions
Coordination conjunction detected.	The query transformation is not based on a single step. The keywords before the coordinating conjunction are considered for the first step of the natural query transformation. The remaining part of the natural query is treated as the second part of a query transformation. After the completion of the transformation for the first part of the query, the remaining part of the query will be treated as a different part and all the transformation processes will be performed from the beginning.
Coordination conjunction is not detected.	The query transformation is a single step. All the keywords in the natural language query are considered for the natural language query transformation.
Literal or instance is not detected.	The natural language query refers to an object or data property. Matching algorithms are run to find the appropriate matches for the object or data property from a list of ontological resources.
Literal or instance is detected.	The natural language query has detected a literal or an instance. The next step is to find the associated data or object property with the detected literal or instance from a list of ontological resources.
Is/ Does/ Has is detected at the beginning of the Query.	This is the condition that deals with affirmative-negative and affirmative-negative-pseudorel type of queries. The next step is to detect an instance in between Is/ Does/ Has and "?" in the query. If an instance is detected, all the keywords (excluding Is/ Has/ Does) and the instance will then be matched to find the best match for object property associated with the instance.

6. Transformations are based on some predefined rules, depending whether a literal/ instance or a data/object property is detected.
7. If there is a coordinating conjunction detected at step 3, all the steps will be repeated for the remaining part of the query.

The step-by-step processing for the second case is as below.

1. Is/ Does/ Has is detected at the beginning of the query which ends with a “?”.
2. The next step is to look for an instance after the words Is/ Does/ Has.
3. If an instance is found, the next step is to find an object property.
4. Matching is performed by the algorithm, which excludes Is/ Does/ Has, and the instance is to find the best match for the object property associated with the instance.
5. Transformations are performed based on some predefined rules and templates.

EVALUATION OF NEGATION QUERY HANDLING ENGINE

The designed negation query handling engine is evaluated using the negation queries in the Mooney dataset (MooneyData, 1994) and Aqualog dataset (AquaLogData, 2007). The Mooney data set included a total of 88 negation queries. There are 74 negation queries in the job Mooney dataset and 14 negation queries in the geography Mooney dataset. There are a total 24 negation queries in the Aqualog dataset. The Aqualog dataset has divided these negation queries into

three different categories. The category names are affirmative-negative, affirmative-negative-pseudorel and negation. The designed algorithm of the negation query handling engine correctly transformed 72.7% of the negation queries in the Mooney dataset and 41.6% of the negation queries in the Aqualog data set to their formal query language equivalent. Table 2 and Fig.2 show the evaluation of the proposed algorithm.

The designed algorithm of the negation query handling engine manifested encouraging results for the negation queries in the Mooney dataset and AquaLog dataset. All the negation queries in the Mooney dataset and AquaLog data set were parsed through the algorithm of the proposed negation query handling engine. Below are some examples of how every query with negation is individually parsed and the proposed algorithm is evaluated.

Sample Query 1 (Job Mooney data set): **"Are there ada jobs outside austin?"**

Refer to Fig.3 for details of the sequence of processing natural language in the proposed negation query handling engine.

Step 1 : Negation keyword detected: **outside.**

Step 2 : Coordinating conjunction not detected. According to the transformation rules, all the words in the natural language query will be considered for formal language query transformation (SPARQL).

Step 3 : Instances are detected: **"ada"** and **"austin".** According to the query transformation rules (Table 2) if a literal or an instance is detected, the next step is to find the associated data or object property with the detected literal or an instance from the list of ontological resources.

Step 4 : The negation query handling engine will look for the object properties associated with the instances. The engine will find the associated object properties associated with

TABLE 2: Results obtained for query transformation

Dataset	Total negation queries	No of queries correctly transformed to formal query language	% of queries correctly transformed to formal query language
Mooney	88	64	72.7%
Aqualog	24	10	41.6%

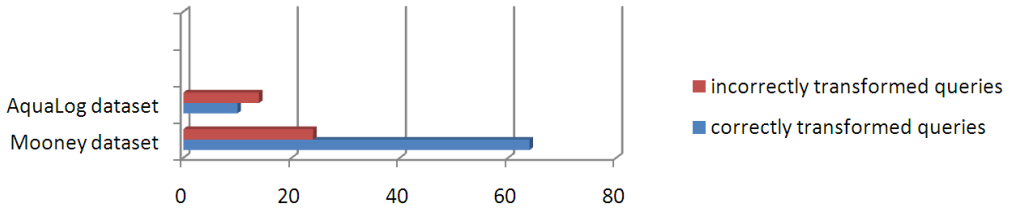

Fig.2: Query transformation results

"ada" and **"austin"**. As for **"ada"**, the system will locate **"useslanguage"** and for **"austin"**, the system will recognize **"isinCity"**.

Step 5: The selected object properties are set into pre-defined template in SPARQL in a specified format. The basic format is as below. The selected object property is set in the following sequence of triple.

?subject name of selected property?Var

FILTER(?Var!=(name of instance or literal))

In the case of the exampled query, the exact query transformation in SPARQL will be in the following format. The negation query handling engine will intelligently identify the intent of the user in the negation sense and will place a "!" in the filter part of the SPARQL query. In the case of the example query, the "?City!=p1:austin" means to exclude all those jobs which are not in "Austin" city.

SELECT ?subject ?Lang ?City

WHERE{?subject a p1:ITJob.

?subject p1:usesLanguage ?Lang.

?subject p1:isInCity ?City.}

FILTER(?Lang=p1:ada && ?City!=p1:austin).

CONCLUSION AND RECOMMENDATIONS FOR FUTURE WORK

This paper has proposed a negation query handling engine that was specifically designed for handling negation queries. The designed negation query handling engine was evaluated using the Mooney dataset (MooneyData, 1994) and AquaLog dataset (AquaLogData, 2007). It was found that the proposed negation query handling engine correctly transformed 72.7% of Mooney dataset and 41.6% of AquaLog dataset negation queries to their formal query language equivalent. The proposed engine demonstrated encouraging results. Hence, it is a step forward towards an effective handling of complex natural language query transformations.

It is an intention for the future to further improve the algorithm so as to bring more correctness in the negation query transformations. An evaluation of the proposed engine on other datasets may also lead to new insights, which can be incorporated in the existing algorithm of the negation query handling engine to make it more effective and robust in handling negation queries.

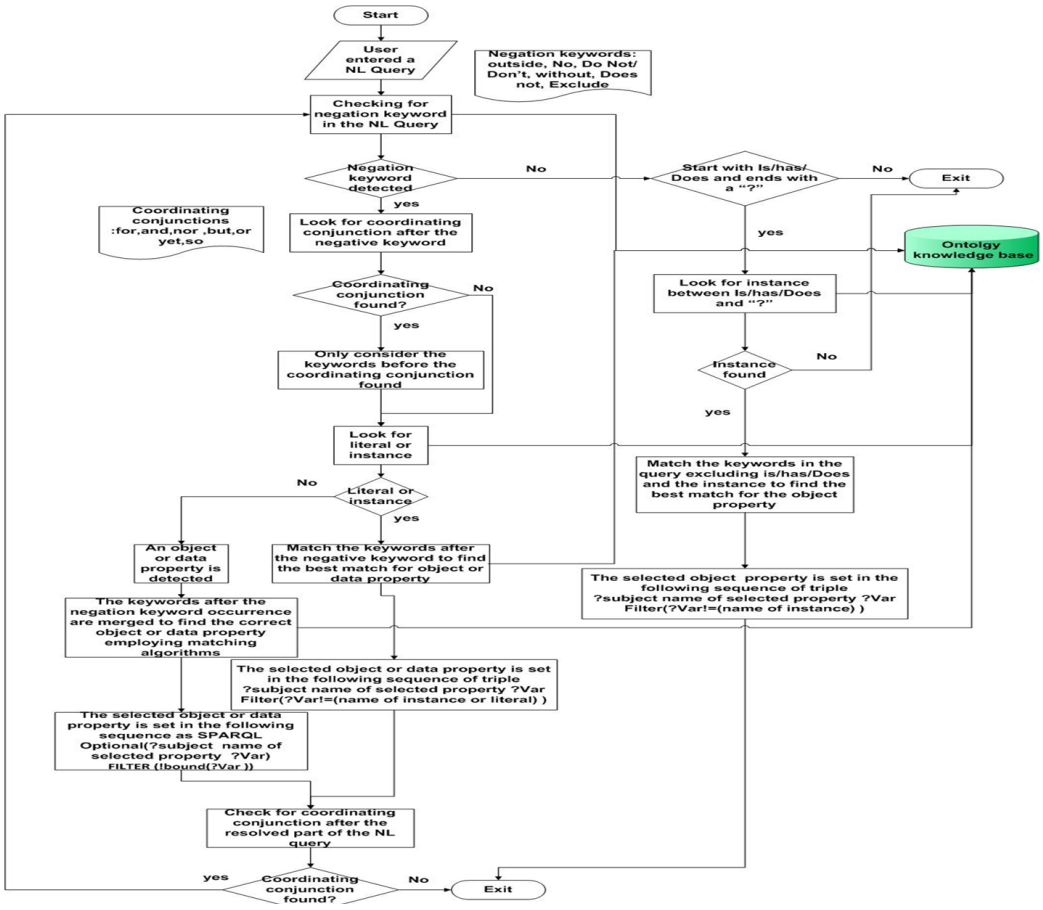

Fig.3: The step-by-step processing of the natural language query

REFERENCES

AquaLogData. (2007). Retrieved from http://kmi.open.ac.uk/technologies/aqualog/examples.html

Cimiano, P., Haase, P., Heizmann, J., Mantel, M., & Studer, R. (2008). Towards portable natural language interfaces to knowledge bases - The case of the ORAKEL system. *Data and Knowledge Engineering*, *65*, 325-354.

Corby, O., Dieng-Kuntz, R., & Faron-Zucker, C. (2004). Querying the Semantic Web with the corese search engine*. 16th European conference on Artificial Intelligence* (ECAI-2004), 705-709.

Cohen, W. W., Ravikumar, P., & Fienberg, S. E. (2003). A Comparison of String Distance Metrics for Name-Matching Tasks. *Workshop on information integration on the Web* (IIWeb-03), 73-78.

Damljanovic, D., Agatonovic,M., & Cunningham, H. (2010). Natural Language interface to ontologies: Combining syntactic analysis and ontology-based lookup through the user interaction. *European Semantic Web Conference* (ESWC 2010), 106-120.

Fellbaum, C. (1998). WORDNET: An Electronic Lexical Database. *MIT Press*, 1998.

Heflin, J., & Hendler, J. (2000). Searching the web with SHOE. *Workshop on AI for Web Search* (AAAI-2000).

Iqbal, R., Murad, M. A. A., Selamat, M. H., & Azman, A. (2012). Negation query handling engine for natural language interfaces to ontologies. *International Conference on Information Retrieval and Knowledge Management (CAMP'12)*, 249-253.

Kaufmann, E., Bernstein, A., & Fischer, L. (2007). Nlp-Reduce: A "naïve" but domain independent natural language interface for querying ontologies. *European Semantic Web Conference* (ESWC 2007).

Kaufmann, E., Bernstein, A., & Zumstein, R. (2006). Querix: A Natural Language Interface to Query Ontologies Based on Clarification Dialogs. *International Semantic Web Conference* (ISWC 2006), Springer, 980-981.

Lei,Y., Uren, V., & Motta, E. (2006). Semsearch: a search engine for the semantic web. *Managing Knowledge in a World of Networks*, *4248*, 238-245.

Motro, A. (1986). Constructing queries from tokens. *SIGMOD international conference on Management of data* (SIGMOD '86), 120-131.

MooneyData. (1994). Retrieved from http://www.cs.utexas.edu/users/ml/nldata.html.

Rocha, C., Schwabe, D., & de Aragao, M. (2004). A Hybrid Approach for Searching in the Semantic Web. *13th International conference on World Wide Web* (WWW'04), 374-383.

Ramachandran, V. A., & Krishnamurthi, I. (2009). NLION: Natural Language interface for querying ontologies. *2nd Bangalore Annual Compute Conference* (COMPUTE' 09), 1-4.

Tablan,V., Damljanovic, D., & Bontcheva, K. (2008a). A natural language query interfaceto structured information. *5th European semantic web conference on The semantic web: research and applications* (ESWC'08), Springer Berlin/Heidelberg, LNCS, 5021, 361–375.

Tablan, V., Damljanovic, D., & Bontcheva, K. (2008b). A natural language query interface to structured information. *European Semantic Web Conference* (ESWC 2008), 361-375.

Vanessa, L., Victoria, U., Motta, E., & Michele, P. (2007). AquaLog: an ontology-driven question answering system for organizational semantic intranets. *Journal of Web Semantics*, *5*, 72–105.

Wang, H., Zhang, K., Liu, Q., Tran, T., & Yu, Y. (2008). Q2semantic: A lightweight keyword interface to semantic search. *European Semantic Web Conference* (ESWC '08), 584–598.

Wang, C., Xiong, M., Zhou, Q., & Yu, Y. (2007). PANTO: A Portable Natural Language Interface to Ontologies. *European Semantic Web Conference* (ESWC '07), 473-487.

Zhou, Q., Wang, C., Xiong, M., Wang, H., & Yu, Y. (2007). Spark: Adapting keyword query to semantic search. *International Semantic Web Conference (ISWC)/Asian Semantic Web Conference* (ASWC), 694-707.

Pertanika J. Sci. & Technol. 21 (1): 205 - 216 (2013)

SCIENCE & TECHNOLOGY

Journal homepage: http://www.pertanika.upm.edu.my/

Modified Multi-Class Classification using Association Rule Mining

Yuhanis Yusof* and Mohammed Hayel Refai

School of Computing, UUM College of Arts and Sciences, Universiti Utara Malaysia, 06010 Sintok, Kedah, Malaysia

ABSTRACT

As the amount of document increases, automation of classification that aids the analysis and management of documents receive focal attention. Classification, based on association rules that are generated from a collection of documents, is a recent data mining approach that integrates association rule mining and classification. The existing approaches produces either high accuracy with large number of rules or a small number of association rules that generate low accuracy. This work presents an association rule mining that employs a new item production algorithm that generates a small number of rules and produces an acceptable accuracy rate. The proposed method is evaluated on UCI datasets and measured based on prediction accuracy and the number of generated association rules. Comparison is later made against an existing classifier, Multi-class Classification based on Association Rule (MCAR). From the undertaken experiments, it is learned that the proposed method produces similar accuracy rate as MCAR but yet uses lesser number of rules.

Keywords: Classification, association rule, rule mining, rule production, data mining

INTRODUCTION

The availability of high performance computers, data collection tools and huge memory capacities has made gathering and saving huge quantities of data possible. For example, the number of sales transactions executed during one year in a large retail supermarket such as Carrefour is numerous and the amount of data on the World Wide Web (WWW) is extremely massive as well. This vast growth of stored databases provides an opportunity for new automated intelligent data analysis methods that summarizes information from these databases. The process of generating this useful knowledge is accomplished using data mining techniques. Liu *et al*. (1998) define data mining as one of the primary steps in Knowledge Discovery from Databases (KDD), which finds and generates useful

Article history:
Received: 31 March 2012
Accepted: 31 August 2012

E-mail addresses:
yuhanis@uum.edu.my (Yuhanis Yusof),
mohammdrefai@yahoo.com (Mohammed Hayel Refai)
*Corresponding Author

ISSN: 0128-7680 © 2013 Universiti Putra Malaysia Press.

hidden knowledge from large databases.

Classification using Association (CuA), which is also known as associative classification, is a research field in data mining that integrates association rule discovery and classification. CuA utilises association rule to discover knowledge and to select a subset of which to build the classifier (Thabtah *et al*., 2010a). The main goal for CuA is to construct a classifier based on the identified knowledge from labelled input. This model is later used to predict the class attribute for a test data case (Baralis *et al*., 2008).

In the last few years, several CuA algorithms have been developed such as CPAR (Yin & Han, 2003), Live and Let Live (L^3G) (Baralis *et al*., 2004), MCAR (Thabtah *et al*., 2005), CACA (Tang & Liao, 1998), BCAR (Yoon & Lee, 2008) and others. These research studies have shown that the approach produces better classifiers (in terms of accuracy) compared to traditional classification data mining approaches like probabilistic (Meretakis & Wuthrich, 1999) and decision tree (Quinlan, 1998). Nevertheless, the CuA algorithm suffers from exponential growth of rules, i.e. they derive large numbers of rules which make the resulting classifiers being outsized and consequently limit their uses since decision makers face difficulty in understanding and maintaining a large set of rules.

In this work, an algorithm named "Modified Multi-class Classification using Association Rule Mining" (MMCAR) is proposed to reduce the number of rules produced by association rule based algorithms. The proposed MMCAR is developed based on the existing approaches of CuA. Nevertheless, MMCAR employs a new rule production algorithm which results in only relevant rules being used to predict test cases. The training method of MMCAR scans training data sets only once (Thabtah *et al*., 2005) and the class assignment (prediction) method makes a group of rule prediction instead of utilising only a single rule.

Different datasets from the UCI repository (Merz & Murphy, 1996) have been utilised to evaluate the proposed learning algorithm and to compare it with other traditional data mining classification techniques, including decision tree (C4.5) (Quinlan, 1993), greedy classification (RIPPER) (Cohen, 1995), and MCAR (Thabtah, 2005). The measures used in the experiments for comparison are the prediction accuracy and the number of rules derived.

The paper is structured as follows: The problem of CuA and its related works are presented in CLASSIFICATION USING ASSOCIATION. The proposed algorithm is discussed in MATERIAL AND METHODS. Datasets and the experiments of using different classification algorithms are demonstrated in RESULTS AND DISCUSSION, while conclusions and suggestions for further research work are given in CONCLUSIONS.

CLASSIFICATION USING ASSOCIATION

CuA is a case of association rule discovery, in which the rule on the right hand side (consequent) is the class label, and the rule on the left hand side (antecedent) is attribute values. Thus, for the rule *R*: $X \Rightarrow Y$, (X) is a conjunction of attribute values, and (Y) is the class attribute. The ultimate goal of CuA is to extract a complete set of rules which is normally called class association rules (CARs) from the training dataset.

The Problem

In the definition of the CuA problem, we employ by Thabtah (2005). Let T be the input training dataset with k different attributes $A_1, A_2, \ldots, A_k$ and L is a set of class labels. A specific attribute value for A_i is represented by a_i, and the class labels of L are represented l_j.

Definition 1: An AttributeValue (A_i, a_i) is combination of between 1 and k different attributes values, e.g. $< (A_1, a_1)>$, $< (A_1, a_1), (A_2, a_2)>$, $(A_1, a_1), (A_2, a_2), (A_3, a_3)>$, …, etc.

Definition 2: A class association rule (CAR) is given in the following format: $(A_{i1}, a_{i1}) \wedge (A_{i2}, a_{i2}) \wedge \ldots \wedge (A_{1k}, a_i k) \rightarrow l_i$, where the antecedent is a conjunction of AttributeValues and the consequent is a class.

Definition 3: The frequency (*freq*) of a CAR in T is the number of cases in T that matches r's antecedent.

Definition 4: The support count (*suppcount*) of a CAR is the number of cases in T that matches r's antecedent and belongs to a class l_i for r.

Definition 5: A CAR (r) passes the *minsupp* if for r, $suppcount(r)/ |T| \geq minsupp$, where $|T|$ is the number of cases in T.

Definition 6: A CAR (r) passes *minconf* if $suppcount(r) /freq(r) \geq minconf$.

CuA Main Steps

Fig.1 depicts the main steps used in CuA. The first step involves the discovery of frequent item set. This requires methods that find complete set of the frequent items by separating those that are potentially frequent and determine their frequencies in the training dataset (step 1). A rule will be produced if an item set exceeds the *Minconf* threshold value. The rule will be in the form of $X \rightarrow l$, where l is the largest frequency class associated with X in the training dataset (Step 2). In step 3, a selection of an effective subset of rules ordering is performed using various procedures, while the quality of the selected subset is measured on an independent (test) data set in step 4.

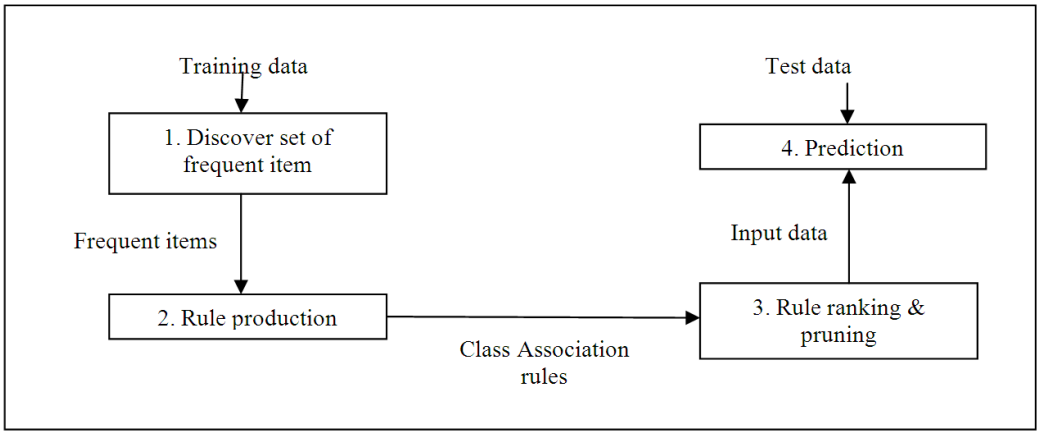

Fig.1: Main Steps in CuA (adopted from Thabtah, 2005)

To explain the CuA discovery of rules and classifier development, consider data shown in Table 1. The table consists of two attributes, A_1 (a_1, b_1, c_1) and A_2 (a_2, b_2, c_2), and two class labels (l_1, l_2). Assume that *Minsupp* = 30% and *Minconf* = 80%, the frequent one, and two items for data depicted in Table 1 are shown in Table 2, along with the associated support and confidence values. The frequent items (in bold) in Table 2 denote those that pass the confidence and support thresholds, which are later converted into rules. Finally, the classifier is constructed using a subset of these rules.

The support threshold is the key to success in CuA. However, for certain applications, rules with large confidence value are ignored because they do not have enough support. Traditional CuA algorithms such as CBA (Liu *et al*., 1998) and MCAR (Thabtah & Cowling, 2007) use one support threshold to control the number of rules derived and may be unable to capture high confidence rules that have low support. In order to explore a large search space and to capture as many high confidence rules as possible, such algorithms commonly tend to set a very low support threshold, which may lead to problems such as generating low statistically support rules and a large number of candidate rules which require high computational time and storage.

In response to these issues, one approach that suspends the support and uses only the confidence threshold to rule generation has been proposed by Wang *et al*. (2001). This confidence-based approach aims to extract all the rules in a dataset that passes the *Minconf* threshold. Other approaches are to extend some of the existing algorithms such as CBA and CMAR. These extensions resulted in a new approach called multiple supports (Baralis *et al*., 2008) that considers class distribution frequencies in a dataset and also assigns a different support threshold to each class. This assignment is done by distributing the global support

TABLE 1: Training Dataset

RowNo	$Attribute_1$	$Attribute_2$	class
1	a_1	a_2	l_1
2	a_1	a_2	l_2
3	a_1	b_2	l_1
4	a_1	b_2	l_2
5	b_1	b_2	l_2
6	b_1	a_2	l_1
7	a_1	b_2	l_1
8	a_1	a_2	l_1
9	c_1	c_2	l_2
10	a_1	a_2	l_1

TABLE 2: Potential Classifier for Data in Table 1

Frequent Items			
Rule Condition	Rule class	Supp	Conf
$<a_2>$	**l_1**	**4/10**	**4/5**
$<a_1>$	l_1	5/10	5/7

threshold to each class corresponding to its number of frequencies in the training dataset, and thus, considers the generation of rules for the class labels with low frequencies in the training data.

An approach called MCAR (Thabtah, 2005) that employs vertical mining was proposed, in which during the first training data scan, the frequent items of size one are determined and their appearances in the training data (rowIds) are stored inside an array in a vertical format. Any item that fails to pass the support threshold is discarded. The rowIds hold useful information that can be used laterally during the training step in order to compute the support threshold by intersecting the rowIds of any disjoint items of the same size. It should be noted that the proposed algorithm of MMCAR also utilises vertical mining in discovering and generating the rules. Next section describes the proposed algorithm based on an example.

MATERIAL AND METHODS

MMCAR goes through three main phases: Training, Construction of classifier, and Forecasting of new cases as shown in Fig.1. During the first phase, it scans the input data set to find frequent items in the form <AttributeValue, class> of size 1. These items are called one-item. The algorithm repeatedly joins them to produce frequent two-items, and so forth. It should be noted that any item that appears in the input dataset less than the *MinSupp* threshold will be discarded. Once all the frequent items of all sizes are discovered, the algorithm will check for the items confidence values. Only if the confidence value is larger than the *MinConf* threshold, it will then become a CAR. Otherwise, the item gets deleted. The next step is to sort the rules according to certain measures and to choose a subset of the complete set of CARs to form the classifier. Details on the proposed MMCAR are given in the next subsections.

CARs Discovery and Production

MMCAR uses an intersection method based on the so-called Tid-list to compute the support and confidence values of the item values. The Tid-list of an item represents the number of rows in the training dataset in which an item has occurred. Thus, by intersecting the Tid-lists of two disjoint items, the resulting set denotes the number of rows, in which the new resulting item has appeared in the training dataset, and the cardinality of the resulting set represents the new item support value.

The proposed algorithm goes over the training dataset only once to count the frequencies of one-items, from which it discovers those that pass the *MinSupp*. During the scan, the frequent one-items are determined, and their appearances in the input data (Tid-lists) are stored inside a data structure in a vertical format. Meanwhile, any item that does not pass the *MinSupp* will be removed. Then, the Tid-lists of the frequent one-item are used to produce the candidate two-item by simply intersecting the Tid-lists of any two disjoint one-items. Consider for instance, the frequent attribute values (size 1) ($<a_1>$, l_1) and ($<a_2>$, l_1) that are shown in Table 2 can be utilised to produce the frequent item (size 2) ($<a_1, a_2>$, l_1) by intersecting their Tid-lists, i.e. (1,3,7,8,10) and (1,6,8,10) within the training dataset (Table 1). The result of the above intersection is the set (1,8,10) in which its cardinality equals 3, and denotes the support value of the new attribute value ($<a_1, a_2>$, l_1). Now, since this attribute value support is larger than

or equivalent to the *MinSupp* threshold (i.e. 30%), this 2-item will become frequent.

The above discussion describes the training approach which is called vertical mining that has been successfully used in association rule discovery (Zaki & Gouda, 2003) and in classification (Thabtah, 2005). This approach transforms the training dataset into items table that contains the locations (Tid-lists) of each item in the training dataset, employs simple intersections among these locations to discover frequent values and produces the rules. Once all the items of all sizes have been discovered, MMCAR will then check for their values and generate those which pass both the *MinSupp* and *MinConf* thresholds as items to be used in the classification association rule(s). The proposed item production algorithm is shown in Fig.2, while Fig.3 illustrates the algorithm utilized by MCAR (Thabtah, 2005).

Building the Classifier

One primary limitation of CuA approach in data mining is the exponential growth of rule (Li *et al*., 2006; Thabtah *et al*., 2006). Thus, a primary motivation of this work is to cut down the number of generated CARs. Prior to pruning redundant rules and to build the classifier, rules

Input: A set of items S
Output: set of S' produced items

$S' \leftarrow 0$
Do
  For each pair of disjoint items I_1, I_2 in S Do
    If ($<I_1 \cup I_2>, c$) passes the *minsupp* threshold
      If ($<I_1 \cup I_2>, c$) passes the *minconf* threshold
      $S' \leftarrow S' \cup (< I_1 \cup I_2 >, c)$
      end if
    end if
  end
end
Return S'

Fig.2: MMCAR Item Production Algorithm

Input: A set of items S
Output: set of S' produced items

scan D for the set S of frequent single items
Do
  For each pair of disjoint items I_1, I_2 in S
    If $<I_1 \cup I_2>$ passes the *MinSupp* threshold
    $S \leftarrow S \cup <I_1 \cup I_2>$
until no items which pass *MinSupp* are found

Fig.3: MCAR Item Production Algorithm

must be sorted in order to prioritize quality rule to be chosen as a part of the classifier. In this work, the rules are sorted according to the following guidelines:

1. The rule with higher confidence is placed in a higher rank.
2. If the confidence values of two or more rules are the same, the rule with higher support will then get a higher rank.
3. If the confidence and the support values of two or more rules are the same, the rule with lesser number of attribute values in the antecedent gets a higher rank
4. If all the above criteria are similar for two or more rules, the rule which was produced first will get a higher rank.

For each sorted rule (CAR), MMCAR applies it on the training dataset, and the rule gets inserted into the classifier if it covers at least one case regardless of the rule class that is similar to that of the training case. Now, once a rule gets inserted into the classifier, all the training cases associated with it are discarded. In situations where a rule fails to cover any training case, it will then be removed. The same process is repeated until no more case remains in the training dataset or all CARs are tested.

In predicting test data case, the prediction method of MMCAR divides all the rules which match the test case into groups; one for each class label to calculate the average confidence and support values. It assigns the test case with the class of the group with the largest average confidence. In cases where there are two or more groups with similar average, the prediction method is considered for the largest average support group. Unlike other current CuA methods like MCAR (Thabtah, 2005) and CBA (Liu, 1998) which employ only the highest confidence rule for predicting the test case, our algorithm makes the prediction decision based on multiple rules (Li *et al*., 2006; Thabtah *et al*., 2006). Finally, in cases when no rules in the classifier are applicable to the test case, the default class (the majority class in the training dataset) will be assigned to that case.

RESULTS AND DISCUSSION

In this section, a recent classification using association algorithm, which is the MCAR (Thabtah, 2005), is compared against MMCAR with reference to classification accuracy and the number of rules produced by the classifier. A total of fourteen (14) UCI datasets (Merz & Murphy, 1996) have been utilized in the experiments. Cross validation which divides training dataset into (n+1) folds arbitrary was employed and learning was performed on the n folds of each iteration. Later, evaluation is undertaken on the remaining holdout fold. The process is repeated n+1 times and the results are obtained by taking the average values. In the experiments, the number of folds in cross validation is set at 10, as employed by Thabtah *et al.* (2005). On the other hand, the main parameters of MMCAR and MCAR, namely, *MinSupp* and *MinConf,* were set to 3% and 50%, respectively, in the experiments. This is since 3% of support usually balances between the number of rules discovered and processing time. All of the experiments were performed on Pentium IV machine with 2.0 GB RAM and 2.6 GH processors.

A.

Results and Analysis

Table 3 contains the results of the classification accuracy, while data in Table 4 depicts the number of association rules produced by MCAR and MMCAR. Data in Table 4 show similar consistency in the classification accuracies of both MMCAR and MCAR. The accuracy values obtained by both MCAR and MMCAR for six data sets (Austra, Balance-scale, Labor, Lymph, Mushroom and Wine) are at the same level; they only differ at the decimal point. For example, using Austra dataset, both classifiers generate 86% accuracy. On the other hand, MMCAR outperformed the accuracy obtained by MCAR in five data sets. Such a scenario is illustrated in Fig.4, where it shows the difference of accuracy values between MMCAR and MCAR. For example, the difference is as high as 2.85% for the Glass dataset, while there is no difference for the Labour dataset.

TABLE 3: Prediction Accuracy

Data set	**MCAR**	**MMCAR**
Austra	86.14	86.26
Balance-scale	76.96	76.17
Breast	94.99	93.83
Cleve	81.84	78.77
Glass	71.35	74.2
Heart-s	81.15	80.51
Iris	92.93	94.26
Labor	83.5	83.5
Led7	71.83	73
Lymph	78.1	78.05
Mushroom	99.6	99.67
Pima	77.12	74.44
Vote	88.2	86.39
Wine	95.73	95.73

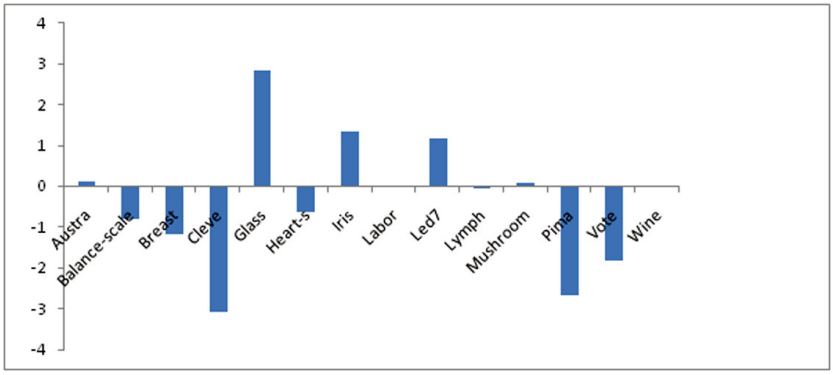

Fig.4: The Difference in Prediction Accuracy

On the other hand, the results of the generated number of rules are depicted in Table 5. Data in the table indicate that the proposed algorithm (i.e. MMCAR) produces less number of rules than MCAR. MMCAR has derived on average 63 rules for the fourteen datasets as compared to MCAR that produced an average of 76 rules. The difference of the generated rules is also illustrated in Fig.5. It is noted that MMCAR produces less number of rules for eight datasets, whereby the highest difference can be seen in the Led7 dataset.

TABLE 4: The Number of Association Rules

Dataset	**MCAR**	**MMCAR**
Austra	193	185
Balance-scale	77	81
Breast	79	80
Cleve	98	93
Glass	43	34
Heart-s	39	29
Iris	16	11
Labor	15	15
Led7	214	87
Lymph	54	54
Mushroom	42	48
Pima	107	80
Vote	83	75
Wine	11	11

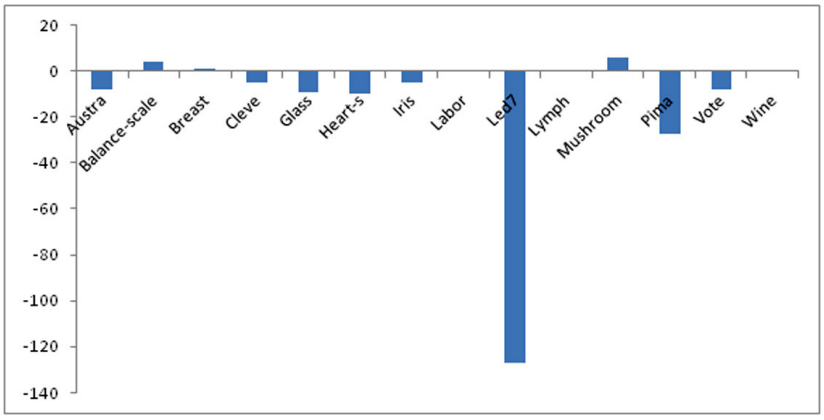

Fig.5: The Difference in the Number of Association Rules

CONCLUSION

In this paper, a modified Multi-class classification based on association rule mining is presented. The so-called MMCAR algorithm includes a new item production algorithm in generating relevant association rules. A more restricted condition is included in the item production so that MMCAR only selects the best related items in producing association rules of the classifier. Hence, a moderate size of association rules will then be obtained. Such a result will aid users in interpreting and understanding the nature of data in the context of study. The proposed MMCAR is proven to be at par with MCAR in prediction accuracy but outperforms the benchmark method in producing lesser number of association rules.

REFERENCES

Baralis, E., Chiusano, S., & Garza, P. (2004). On support thresholds in associative classification. *Proceedings of the 2004 ACM Symposium on Applied Computing*, Nicosia, Cyprus, pp. 553-558.

Baralis, E., Chiusano, S., & Garza, P. (2008). A lazy approach to associative classification. *IEEE Transactions on Knowledge and Data Engineering*, *20*, 156-171.

Cohen, W. W. (1995). Fast effective rule induction. In *Proceedings of the Twelfth International Conference on Machine Learning*, pp. 115-123.

Li, W., Han, L., & Pei, J. (2001). CMAR: Accurate and efficient classification based on multiple class-association rules. In *Proceedings of the ICDM'01* San Jose, CA, p. 369.

Lim, T. S., Loh, W. Y., & Shih, Y. S. (2000). A comparison of prediction accuracy, complexity, and training time of thirty-three old and new classification algorithms. *Machine learning, 40*, 203-228.

Liu, B., Hsu, W., & Ma, Y. (1998). Integrating classification and association rule mining. *Knowledge discovery and data mining,* 80–86.

Meretakis, D., & Wüthrich, B. (1999). Extending naïve Bayes classifiers using long item sets. In *Proceedings of the fifth ACM SIGKDD International Conference on Knowledge Discovery and Data Mining*, San Diego, California, pp. 165-174.

Merz, C., & Murphy, P. (1996). UCI repository of machine learning databases. Retrieved from FTP of ics. uci.edu in the directory pub/machine-learning-databases.

Tang, Z., & Liao, Q. (1998). A new class based associative classification algorithm. *IAENG International Journal of Applied Mathematics, 36*(2), 136-141.

Thabtah, F., Cowling, P., & Peng, Y. (2005). MCAR: multi-class classification based on association rule. In *Proceeding of the 3rd IEEE International Conference on Computer Systems and Applications*, p. 33.

Thabtah, F., Crowling, P., & Hammoud, S. (2006). Improving rule sorting, predictive accuracy and training time in associative classification. *Expert Systems with Applications*, *31*, 414-426.

Thabtah, F. A., & Cowling, P. I. (2007). A greedy classification algorithm based on association rule. *Applied Soft Computing*, *7*, 1102-1111.

Thabtah F., Mahmood Q., McCluskey L., & Abdel-jaber H. (2010). A new Classification based on Association Algorithm. *Journal of Information and Knowledge Management*, *9*(1), 55-64.

Quinlan, J. R. (1993). *C4.5: Programs For Machine Learning*. Morgan Kaufmann.

Quinlan, J. R. (1998). Data mining tools See5 and C5.0. *Technical Report, RuleQuest Research*.

Wang, K., He, Y., & Cheung, D. W. (2001). Mining confident rules without support requirement. In *Proceedings of the Tenth International Conference on Information and Knowledge Management*. Atlanta, Georgia, pp. 89-96.

WEKA (2000). *Data Mining Software in Java*. Retrieved from http://www.cs.waikato.ac.nz/ml/weka.

Yin, X., & Han, J. (2003). *CPAR: Classification based on predictive association rules.* Paper presented at the 2003 SIAM International Conference on Data Mining, Cathedral Hill Hotel, San Francisco, CA, May 1-3, 2003. pp. 331.

Yoon, Y., & Lee, G. G. (2008). *Text Categorization Based on Boosting Association Rules*. Paper presented at the the 2008 IEEE International Conference on Semantic Computing. pp.136-143.

Zaki, M. J., & Gouda, K. (2003). *Fast vertical mining using diffsets*. Paper presented at the 9th ACM SIGKDD International Conference on Knowledge Discovery and Data Mining. Washington, D.C., pp. 326-335.

Pertanika J. Sci. & Technol. 21 (1): 217 - 226 (2013)

SCIENCE & TECHNOLOGY

Journal homepage: http://www.pertanika.upm.edu.my/

Multi-Format Information Fusion through Integrated Metadata Using Hybrid Ontology for Disaster Management

Che Mustapha Yusuf, J.[1,3] *, Mohd Su'ud, M.[2], Boursier, P.[3] and Muhammad, A.[1]

[1]*UniKL-Malaysian Institute of Information Technology, Kuala Lumpur, Malaysia*

[2]*UniKL-Malaysia France Institute, Bangi, Selangor, Malaysia*

[3]*Laboratoire L3i Université de La Rochelle, La Rochelle, France*

ABSTRACT

Finding relevant disaster data from a huge metadata overhead often results in frustrating search experiences caused by unclear access points, ambiguous search methods, unsuitable metadata, and long response times. More frequently, semantic relation between the retrieved objects is neglected. This paper presents a system architecture that makes use of ontologies in order to enable semantic metadata descriptions for gathering and integrating multi-format documents in the context of disaster management. After a brief discussion on the challenges of the integration process, the Multi-format Information Retrieval, Integration and Presentation (MIRIP) architecture is presented. A specific approach for ontology development and mapping process is introduced in order to semantically associate user's query and documents metadata. An ontology model approach was designed to follow inspirational and collaborative approaches with top-down to bottom-up implementation. A prototype of the integrated disaster management information system is currently under development, based on the architecture that is presented in this paper.

Keywords: Ontology Engineering, hybrid ontology, multi-format document, metadata integration, disaster management

INTRODUCTION

In managing disasters at all stages, a large amount of information within multiple media documents is produced and collected. The information contained in spatial and non-spatial documents, which were collected before and after disasters, is composed of collections of features, coverage and high-resolution imageries, snap photos, text report, video and audio clips. Even though

Article history:
Received: 31 March 2012
Accepted: 31 August 2012

E-mail addresses:
jawahir@miit.unikl.edu.my (Che Mustapha Yusuf, J.),
mazliham@unikl.edu.my (Mohd Su'ud, M.),
patrice.boursier@univ-lr.fr (Boursier, P.),
muhammad.unikl@gmail.com (Muhammad, A.)
*Corresponding Author

ISSN: 0128-7680 © 2013 Universiti Putra Malaysia Press.

the documents can be in multiple different formats, multiple characteristics and are available from different sources, their contents may tell an equivalent semantic of objects, the calamity story, share the space-time extension, and may be closely related to each other (see Fig.1).

As the description outside the packaging describes information about such product, metadata also describes the context and elementary contents of a document. With metadata, access to information at the first level to get the document of information can be found by searching. However, extracting relevant information from a massive number of available metadata still remains a challenge. Users often get frustrating search experiences caused by unclear access points, ambiguous search methods, unsuitable metadata, and long response times (Larson *et al*., 2006), especially when metadata is used in various forms to describe different document formats such as spatial and non-spatial metadata (e.g. multimedia metadata). Hence, understanding the semantics of metadata is a good way to combine different sources of information while ensuring effective integration and access to information. Current research into semantic metadata integration still lacks of focus to combine between spatial and non-spatial metadata which hold descriptions of both document types. Most of the works consider only a single format type or a single context type (e.g. texts, images, spatial) as in Gagliardi *et al*. (2005), Hurtienne *et al*. (2008) and Olteanu *et al*. (2008), when implementing schema and/or instance matching to align terminology between different metadata and user's query terms. Such effort is insufficient to solve matching problem within the environment with high structural and semantic heterogeneity.

In the presented context, there is a need to establish and combine users' and metadata conceptualization, as well as to provide machine automatism to semantic metadata integration.

For this purpose, this paper presents a system architecture using ontology to enable semantic metadata descriptions to gather and integrate multi-format documents. An approach for semantic metadata integration using ontology modelling of the available resources is currently being studied in the context management of national disaster and relief in Malaysia.

Challenges to Information Integration: Malaysian Disaster Management

Malaysia has a good mechanism in managing disasters through Malaysian public agencies, particularly amongst the local authorities, police, fire brigades, and medical agencies. The committee is established at Federal-level, State-level and District-level, under the administrative

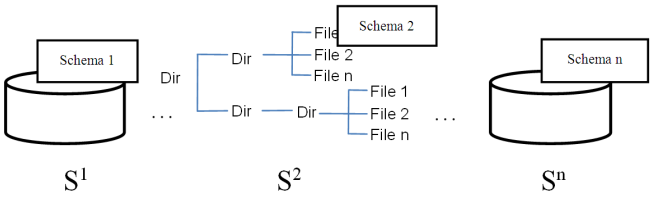

Fig.1: Different document formats that are closely related to each other

control of the National Security Division Secretariat to coordinate all the activities related to disaster. This mechanism is well stated in "Policy and Mechanism in the Management of National Disaster and Relief in Malaysia" or "National Security Council (NSC) Directive No. 20" (Umar, 2011). These agencies perform their own daily work routines and maintain their own information, either manually or in digitized form (e.g., file-systems and Geographic Information System (GIS) and/or non-GIS databases).

During disaster events, a vast amount of information is acquired from different sources to be disseminated amongst them. Various challenges emerge to enforce knowledge sharing, which makes the information integration more difficult. The required datasets are not only difficult to obtain from the system network but also lack automated data coordination at operational level such as during counter-disaster, rescue and relief activities. The major challenge is in the system, structural/schematic and syntactic differences. A diverse distributed storage system is used to store the information that ranges from databases and file-systems. For example, collection of images is stored as Binary Large Object (BLOb) at data provider 1, but as a file-system at data provider 2. The differences in software platform, file formatting and data models certainly add the challenges to interoperability. Furthermore, some data providers provide metadata database to manage data about data they have but some are not. Obviously, the current environment has no composition and consumption of metadata. In order for documents to be identifiable, the metadata should be produced and stored in a format that allows its efficient management. Another challenge arises if metadata system is utilised. Each agency may use different terminologies to refer to similar data, and also different document formats to store spatially and semantically related information.

It is important to note that semantic integration to group and combine data (metadata) from different sources of various agencies involved in a disaster management is necessary. For this purposed, semantic integration has to ensure that only data related to the same real-world entity are merged. Ontology is the current best practice to resolve semantic conflicts in these diverse information sources. Gruber (2007) states that ontology is an enabling technology (a layer of the enabling infrastructure) to enforce knowledge sharing and manipulation. The authors strongly believe that an appropriate ontology development approach should depend on the current organisational environment of Malaysian management of disasters. Majority of the current systems and metadata standards hold less explicit semantics of information (Fig.2), and this makes data fusion tasks difficult (Halevy *et al*., 2006; Haslhofer & Klas, 2010; Haas, 2007). Modern information system is encouraged to embed more semantics in their systems so as to allow a better information integration and this can be achieved by using ontology. This research opens up significant opportunities to achieve more flexible and adaptable ways to start employing ontology within disaster management agencies.

A System Architecture for Multi-format Information Fusion through Metadata Integration Using Hybrid Ontology

The advent of Semantic Web technologies and ontology engineering facilitates the idea to enable semantic metadata integration within various metadata sources. For this purpose, an ontology-based architecture for information retrieval, integration and presentation is formed. The

designed system aims at providing users with data input, discovery and access to multiple media documents via rich ontology-based metadata describing them. The architecture comprehends the semantic matchmaking between user's query and metadata of multi-format information using ontologies. This system architecture is called MIRIP (Multi-format Information Retrieval, Integration and Presentation), conformant to Service Oriented Architecture (SOA) standards (Sprott & Wilkes, 2011). A conceptual notion of the system is depicted in Fig.4. There are three sections involved in the overall process model, namely, provider, mediator and client sections. Details pertaining to the processing components in the architecture are as Fig.2.

Provider section. This section comprises distributed data repositories, which are administered by different data owners. The data repository can be in the type of file-systems and special purpose databases (administration, GIS and multimedia). Information is stored as a set of files containing multiple media types such as GIS vector files, high-resolution aerial photographs and satellite images, snap photo images, audio-video clips and text documents. Metadata exist for managing the various media formats. To provide the semantic descriptions of each metadata, local (source) ontology is constructed according to bottom-up ontology principle. Concurrently, the local ontology is aligned with the upper-ontologies representing the common concepts and its relations.

Mediator section. This section provides a searchable repository of data service descriptions, thus enabling data providers to publish their data and data requestors to search for these data. Semantic metadata-base permits the storage of metadata from various sources. Ontology component provides a common vocabulary to define the relationships between object classes once new metadata are (automatically) registered to the system. The ontology facilitates the retrieval system to identify the relevant media information through metadata, which are semantically annotated and matched to the terms specified in the query.

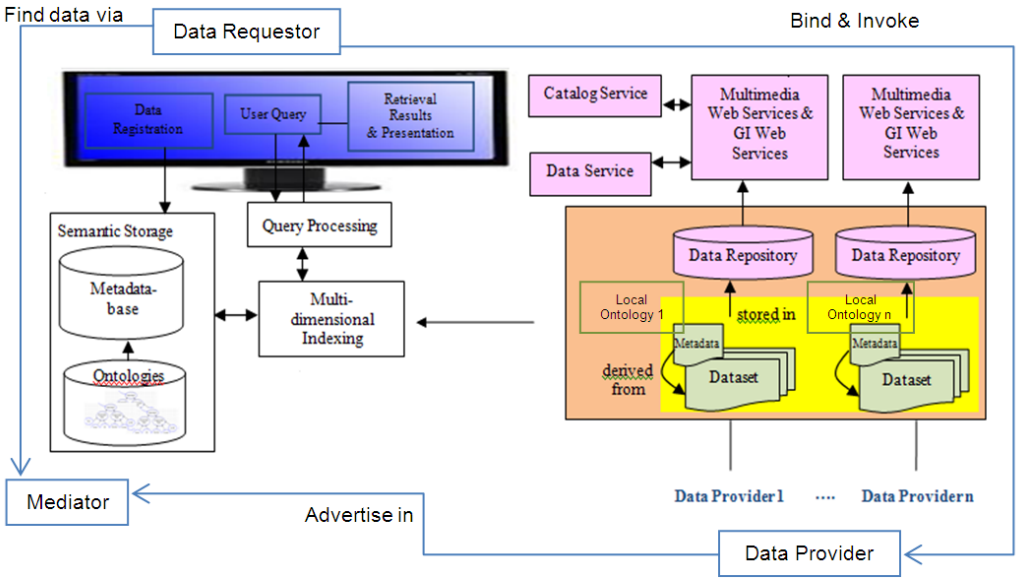

Fig. 2: The MIRIP (Multi-format Information Retrieval, Integration and Presentation) architecture

Client section. This section enables human-machine interaction at registering data services, querying, navigating and accessing the information. By using the *data registration* interface (dRI), data providers can register their available metadata (push) to the catalogue service as data sources. The metadata catalogue is useful to facilitate data requestors to locate and evaluate the data services before it automatically makes a request to access the data. Once data services registration is made, service description is maintained by the mediator. *The user query interface* allows users to provide input to the query to automatically search the required information service. When the request method is posted, a user's request will be sent to the mediator to search for matching values. If a data provider is found, the connection will be bonded between the data provider and the data requestor. *The retrieval results and presentation interface* allow search results from metadata catalogue to be presented in a ranked-list. These search results are delivered to the user through a combination of graphical and textual (e.g. descriptions) elements.

Ontology Modelling for Semantic Integration

In this work, ontology development takes advantages of the hybrid ontology with the implementation of top-down and bottom-up ontology designs (see Fig.4). The upper-ontology used in the hybrid ontology approach transfers the burden of information correlation and filters the query processing system (Mena *et al*., 2000). Following up the top-down design, the set of top-level ontology is firstly provided. Common terms are specified at a very abstract extent, so that a new source ontology can be easily mapped to the upper-ontology. If the new source contains a local concept that is not described in upper-ontology, the common concept that matches with the local concept will be established in the upper shared-vocabulary. Secondly, the source ontologies that contain more specific terms are extended from the primitive terms in the set of top-level ontology. Terms at both levels are comparable easily because the source ontologies only use the vocabulary of top-level ontology. Based on the bottom-up ontology design, the existing source schema and its instances are extracted to generate the source ontologies which contain more high level data descriptions. Then, the source ontologies of all disparate sources are mapped to the abstract concepts of top-level ontology which has been constructed earlier.

In developing the ontology for the current environment and to enable bottom-up ontology mapping, each source must have at least one common concept. Some uncommon concepts that are considered important for query purpose will be declared as sharable in global ontology to avoid data loss. For instance, Source 1 holds concept 'channels' that describe the number of channels represented in the waveform data, such as 1 for mono or 2 for stereo. The concept, however, is not common to another source. Thus, the concept along with its possible sub-concepts will be added in the shared vocabulary. The participating data sources in the integration process have no pre-existing ontologies. Thus, local ontology for each data source will be created with reference to shared-vocabulary. The body of the local ontology is extended to list more specific entities and properties. With no pre-existence of ontology, data sources still have the autonomy to maintain its own name concepts.

The shared-ontologies (vocabularies) include top-level ontology to describe the primitive concepts and domain-specific disaster management ontology. At domain-specific level,

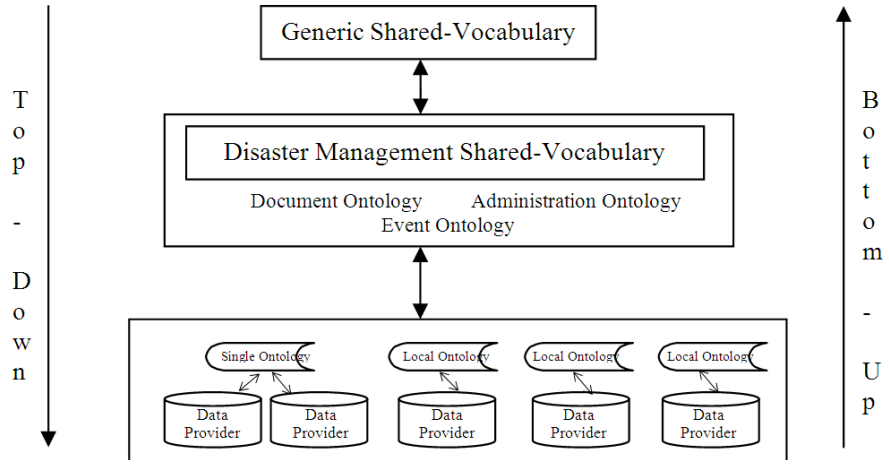

Fig. 3: Ontology model for disaster management domain

document ontology along with administration ontology that is presented by Xu and Zlatanova (2007) are generated to represent the concepts associated with the documents dataset and the providers. The top-level ontology contains common concepts that are associated with space, time and theme. The domain-specific ontology is created to capture spatial and non-spatial concepts related to disaster management. A specific case study of landslide disaster in Malaysia is drawn to demonstrate the applicability of the proposed ontology. So, the ontology also captures details of the landslide concepts which are described as the sub-concepts of natural disaster in the event ontology.

Ontology building methodology, proposed by Uschold and King (1995) and Uschold and Gruniger (1996), is used as basis steps to build the ontology components. The following steps are adhered to properly design the ontologies under provision; 1) Identification of ontology purposes & scopes, 2) Ontology conceptualization, semi-formal specification and formalization, 3) Ontology evaluation and 4) Ontology documentation. The sets of ontology that are still at the development stage play a key role to semantically associate user's query and the document metadata. Consequently, the ontology components here support the classification of resources and retrieval to the resources. Semantic Web ontology languages such as Resource Description Framework Schema-RDFS (Antoniou & Harmelen, 2008) and Web Ontology Language-OWL (W3C, 2009) are utilized along with the Protégé and the Jena API (Protégé, 2011) as an automatic development tool in this work.

Ontology Mapping Methodology

In the modelling ontology, each class and property is assigned with *primary identifier* as in Parts LIBrary (PLIB) ontology (Pierra, 2004) to map between concepts. The *primary identifier* is used to indicate the similarity or different concepts between participating data sources and it upper-vocabularies. Fig.5 depicts the top-down to bottom-up mapping implementation with the use of *primary identifier*. An example of the text document concepts is presented. In the , local

ontology is defined based on the schema of the local data. Data owners will decide their own definition of the local ontology concepts. The concepts that are rational to be disclosed will be pulled out to domain-shared list. Meanwhile, concealed concepts (shaded in Fig.5) will not be shared but can be accessed locally or may be shared (right away or later) in a different domain.

Generic and domain shared-vocabulary are the list of shared concepts for all participating data sources. In this approach, the design of shared-vocabulary begins with inspirational approach (Holsapple & Joshi, 2002). At the initial stage, the specification of generic and domain shared-vocabulary, that are substantially potential to be shared with the group of the data owners, are initiated. Concerned with the importance of information sharing, the data owners may collaboratively (Holsapple & Joshi, 2002) use the existing shared-vocabulary as the anchor and supportively extend it if necessary. However, the data source owners will not be attentive to each other's data. This is important for most of the intelligence systems that are confidentiality-related.

MIRIP PROTOTYPICAL IMPLEMENTATION

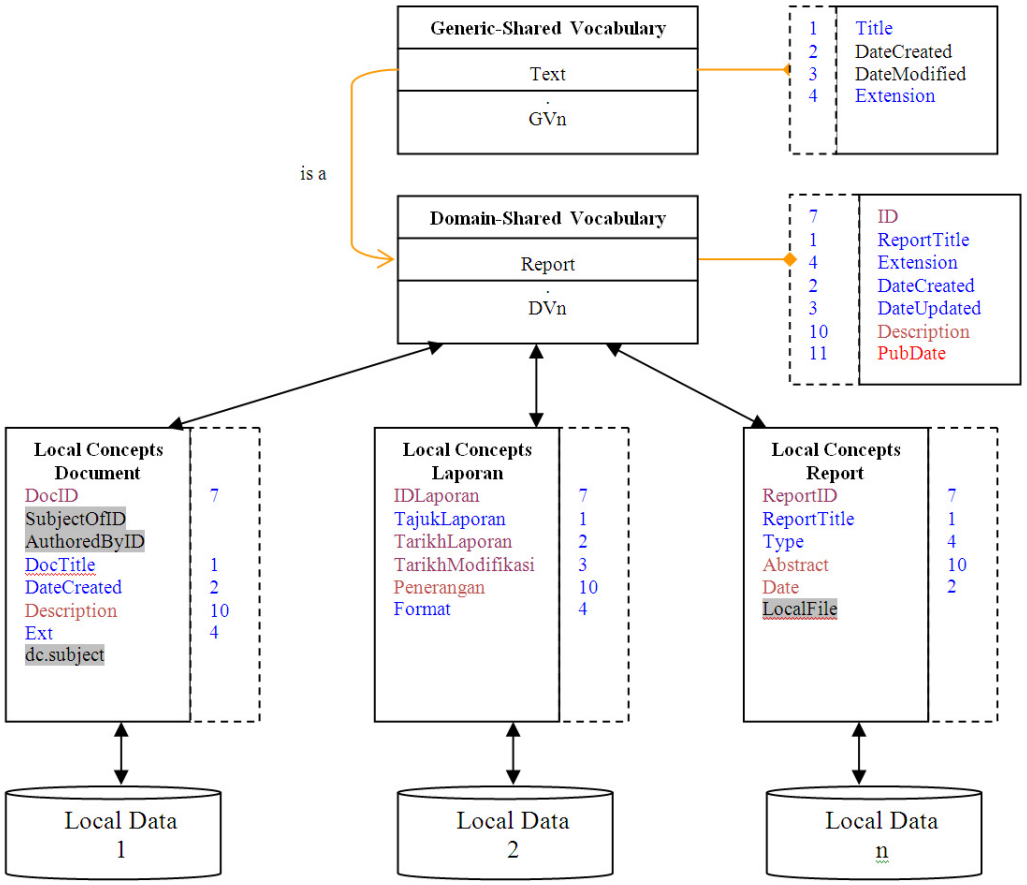

Fig. 4: Top -down to bottom-up ontology mapping

An implementation plan to demonstrate the interaction (data services registration and discovery) within MIRIP is illustrated in disaster management domain. In MIRIP, data providers are from different mapping agencies and institutions involved in disaster management. They present a collection of data services while mediator is employed with a set of data registry services, and client (data requestor) is equipped with a set of client applications.

Data services registration involves data listing process in catalogue services. Data providers can use the MIRIP dRI not only for submitting their new data (metadata), but they can take out data from the catalogue and update some specific data. The following case shows how the data service registration works. Let's assume that the Public Work Department of Malaysia (PWD) is cooperatively giving out a landslide investigation report (in MIRIP geo-portal). Thus, PWD must use the concepts enumerated in ontologies to generate the data service descriptions. With the help of the dRI to access the relevant concepts from ontologies, PWD will perform multiple steps to select an appropriate disaster event (in this case, landslide). In the proposed event ontology shown in Fig.6, 'landslide' is enumerated as a sub-concept of geological natural hazard. After the landslide concept has been chosen, PWD is navigated to stipulate an important attributes (i.e. format, reference date, abstract etc.) for the published data. In the case of publishing spatial dataset, more detail spatial representation properties are required. Once the new metadata registration is submitted, it is stored in the metadata-base (enriched with ontology descriptions).

Data services discovery always concerns with the identification of service descriptions that match a data service requested by the client. From the previous case, if PWD registers multiple datasets, PWD has provided a service description that defines an important metadata which entirely describes the characteristics of services that are deployed on MIRIP geo-portal. This metadata provides an abstract definition of the information that is essential to deploy and interact with a service. Suppose that Malaysian Public Works Institute (Ikram) is about to request datasets about specific landslide resources. Analogous to registration step, Ikram will perform the request (via query interface with catalogue service) by specifying the properties such as the event type, location, date, etc. Since the information about landslide has been

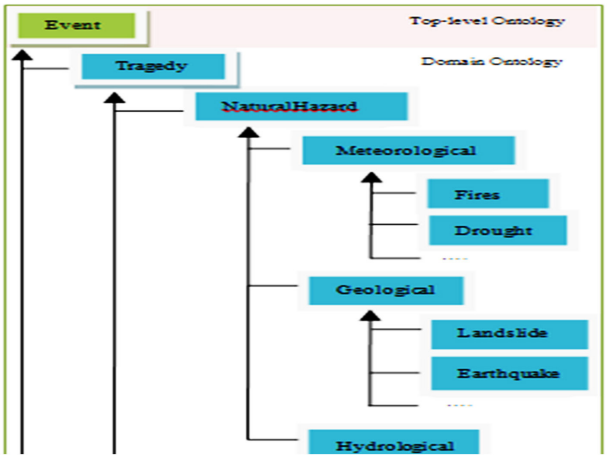

Fig. 5: Snippet of class event and its membership

registered and classified under a specific category and aligned with the ontologies, the query is foreseen to return the relevant result list and ready to be browsed for further discovery (i.e. reiterate search, display and download).

OUTLOOK

This specific system was designed to increase the efficiency in document query and integration, particularly for disaster management domain. The presented ontology-based architecture for a semantic integration of documents via metadata approach was currently developed. Validation upon the designated ontology would be attained with the professional members involved in Malaysian disaster management, particularly with personnel involved with data acquisition and risk analysis. The recent research is still in focus to scrutinize the ontology formation as well as the complex ontology matchmaking process highlighted in this paper to produce ideal mapping between upper and low level ontology. The approach using ontology is foreseeable to help achieve the goal of automatic data search and integration to response a specific query.

REFERENCES

Antoniou, G., & Harmelen, F. V. (2008). *A semantic web primer* (2nd Edition). Cambridge, MA: The MIT Press.

Gagliardi, H., Haemmerlé, O., Pernelle, N., & Saïs, F. (2005). An automatic ontology-based approach to enrich tables semantically. *1st International Workshop on Context and Ontologies: Theory, Practice and Applications*. Pittsburgh, Pennsylvania, pp. 64–71.

Gruber, T. (2007). Ontology of folksonomy: a mash-up of apples and oranges. *International Journal on Semantic Web and Information Systems (IJSWIS), 3*(1), pp. 1-11.

Haas, L. M. (2007). Beauty and the beast: the theory and practice of information integration. *International Conference on Database Theory*, pp. 28-43.

Halevy, A., Rajaraman, A., & Ordille, J. (2006). Data integration: the teenage years. 32nd International Conference on Very Large Databases, September 12-15, Seoul, Korea.

Haslhofer, B., & Klas, W. (2010) A survey of techniques for achieving metadata interoperability. *ACM Computing Surveys (CSUR), 42*(2), 1-37.

Holsapple, C. W., & Joshi, K. D. (2002). A collaborative approach to ontology design. *Communications of the ACM, 45*(2), 42-47.

Hurtienne, J., Weber, K., & Blessing, L. (2008). Prior experience and intuitive use: image schemas in user centred design. *Designing Inclusive Futures*, 107–116.

Larson, J., Olmos Siliceo, M. A., Pereira dos Santos Silva, M., Klien, E., & Schade, S. (2006). *Are geospatial catalogues reaching their goals?* Paper presented at the 9th Agile Conference on Geographical Information Science, Visegrád, Hungary.

Mena, E., Illarramendi, A., Kashyap, V., & Sheth, A. P. (2000). OBSERVER: An approach for query processing in global information systems based on interoperation across pre-existing ontologies. *Distributed and Parallel Databases, 8*(2), 223-271.

Pierra, G. (2004). *The PLIB ontology-based approach to data integration*. Paper presented at the18th IFIP World Computer Congress (WCC'2004), Toulouse, France.

Protégé-Stanford Center for Biomedical Informatics Research. (2011). *Integration of jena in protégé-owl*. Retrieved on June 29, 2011 from http://protege.stanford.edu/plugins/owl/jena-integration.html.

Sprott, D., & Wilkes, L. (2011). *Understanding service-oriented architecture*. Retrieved on August 6, 2011 from msdn.microdsoft.com/en-us/library/ aa480021.aspx.

Olteanu, A., Mustière, S., & Ruas, A. (2008). *Matching imperfect spatial data*. Paper presented at the 7th International Symposium on Spatial Accuracy Assessment in Natural Resources and Environmental Sciences.

Umar, C. M. (2011). *Policy and mechanism on national disaster and relief management*. Retrieved on July 23, 2003 from http://spm.um.edu.my/news/disastermanagement 23072008/ talk02.pdf.

Uschold, M., & King, M. (1995). *Towards a methodology for building ontologies*. Paper presented at the Workshop on Basic Ontological Issues in Knowledge Sharing. Montreal, Canada, pp. 1-13.

Uschold, M., & Gruninger, M. (1996). Ontologies: principles, methods and applications. *Knowledge Engineering Review*, *11*, 93-136.

W3C OWL Working Group (2009). *OWL 2 web ontology language document overview. W3C Recommendation*. Retrieved on July 15, 2011 from http://www.w3.org/TR/ 2009/REC-owl2-overview-20091027/.

Xu, W., & Zlatanova, S. (2007). Ontologies for disaster management response. *Geomatics Solutions for Disaster Management*, 185-200.

Pertanika J. Sci. & Technol. 21 (1): 227 - 238 (2013)

SCIENCE & TECHNOLOGY

Journal homepage: http://www.pertanika.upm.edu.my/

Context Modelling for Just-In-Time Mobile Information Retrieval (JIT-MobIR)

Az Azrinudin Alidin[1]* and Fabio Crestani[2]

[1]*Faculty of Information Technology and Computer Science, Universiti Putra Malaysia, 43400 Serdang, Selangor, Malaysia*

[2]*Faculty of Informatics, Universita' della Svizzera italiana, Via Giuseppe Buffi 13, CH-6904 Lugano, Switzerland*

ABSTRACT

Mobile users have the capability of accessing information anywhere at any time with the introduction of mobile browsers and mobile web search. However, the current mobile browsers are implemented without considering the characteristics of mobile searches. As a result, mobile users need to devote time and effort in order to retrieve relevant information from the web in mobile devices. On the other hand, mobile users often request information related to their surroundings, which is also known as context. This recognizes the importance of including context in information retrieval. Besides, the availability of the embedded sensors in mobile devices has supported the recognition of context. In this study, the context acquisition and utilization for mobile information retrieval are proposed. The "just-in-time" approach is exploited in which the information that is relevant to a user is retrieved without the user requesting it. This will reduce the mobile user's effort, time and interaction when retrieving information in mobile devices. In this paper, the context dimensions and context model are presented. Simple experiments are shown where user context is predicted using the context model.

Keywords: Context recognition, mobile information retrieval, just-in-time information access

INTRODUCTION

It is common now for people to address their information needs by using the web search in mobile devices. Since mobile users are connected to the Internet almost every minute, accessing information has become much faster than years before mobile Internet was introduced. However, performing information retrieval (IR) on mobile devices is rather complex because mobile browsers are implemented without considering the characteristics of

Article history:
Received: 31 March 2012
Accepted: 31 August 2012

E-mail addresses:
azri@fsktm.upm.edu.my (Az Azrinudin Alidin),
fabio.crestani@usi.ch (Fabio Crestani)
*Corresponding Author

ISSN: 0128-7680 © 2013 Universiti Putra Malaysia Press.

mobile information retrieval (mobile IR). Besides, the characteristics of mobile IR are quite different from the traditional IR frameworks.

One notable characteristic of mobile IR is the physical limitations of mobile devices. Mobile devices are built physically small for ease of portability. This makes it challenging for mobile users to operate with the mobile device when they are on the move. Besides, adopting desktop browser to fit the size of a mobile devices screen forces them to spend more time selecting and reading the right information in small font and crowded text (Church *et al.,* 2002). Mobile users also need to put extra attention when using mobile devices because they can easily get distracted by other things going on around them (Sohn *et al.,* 2008). On the other hand, the evolving smart-phone technologies have enabled researchers and developers to exploit the embedded sensors in smartphones to sense users' surrounding information (Lane *et al.,* 2010). The user's surrounding information is also known as context. Context, in general, can be used to overcome the problem of IR systems retrieving too much information that may not be relevant in the user's current situation and also to minimize their involvement in interaction particularly on a mobile device. The embedded sensors on the smartphones make them ideal devices to capture users' context because these users always carry the devices.

The inclusion of context in the IR frameworks has become increasingly important particularly for the implementation of mobile IR. The problem with the current IR systems is that these systems retrieve all relevant information in response to a query without considering the representation of the query. These systems do not have any knowledge about user's preferences, or why the user submits a particular query or what is the user's intention when submitting that particular query. As a result, the relevant information retrieved by the IR systems is too generic and is not within the right user's context, and the user needs to spend time finding the desired information. In order to improve the retrieval results, the implementation of context in the IR frameworks is employed in one of the following retrieval phases: (a) query reformulation, (b) document re-ranking, and (c) document retrieval (Tamine-Lechani *et al.,* 2010). However, in mobile IR, apart from improving the retrieval results, minimizing the user interaction is also a key to increase the user's experience when using the mobile IR. Smartphones can react and adapt to the context to minimize user's interaction and use context as information trigger to pro-actively present information to the user. This is also known as Just-In-Time Information Access system (Leake *et al.,* 1999). For this research, the system is named as Just-In-Time Mobile Information Retrieval (JIT-MobIR). JIT-MobIR works by monitoring context, predicting user's information needs in any given context and proactively providing the user with relevant information with the aim to reduce user's interaction. Thus, the effectiveness of JIT-MobIR is measured both in the capability of the system to understand the context and in the ability of the system to retrieve information that satisfies user's information needs in that particular context.

The motivation of this research is to construct, understand and apply context for developing JIT-MobIR. However, very little work has been done on utilizing context in mobile IR because of the complexity of constructing and generalizing context. Context, by nature, is always changing particularly when a user is on the move. This makes context extremely complex to be identified (Schmidt *et al.,* 1999). How context can be identified and captured by using a smartphone is explained in this paper. In specific, the paper is organized as follows: In the next section, work related to the current study is presented. The context modelling in JIT-MobIR is

introduced subsequently. Then, the implementation of JIT-MobIR is described in detail, with a discussion on the results, followed by conclusion and future work.

DEFINITION OF CONTEXT

According to the Free Online Dictionary of Computing (FOLDOC), context is defined as "*that which surrounds, and gives meaning to, something else*". However, the definition of FOLDOC is too broad and vague, and for this reason, many researchers defined the context according to their own understanding that is influenced by their research observations (Dey & Abowd, 2000; Schilit *et al.,* 1994; Schmidt *et al.,* 1999). Schilit *et al.* (1994) proposed the definition of context based on location awareness. However, Schmidt *et al.* (1999) disagree when context is treated merely as a location as past researchers always do. They describe that context has many aspects in three dimensions: Environment, Self and Activity. Nevertheless, Dey and Abowd (2000) argue that those two definitions of context are experimental oriented and difficult to be applied. They also argue that one aspect of context is not important from others since these aspects will change from one situation to another. Thus, context according to Dey and Abowd (2000) emphasizes that any information will be considered as context when this information helps a user to interact with an application. However, if the information is no longer relevant to the user's interaction, then it is no longer a part of the context. This definition does not restrict where the context is coming from as long as that context helps the user's interaction. Dey and Abowd's (2000) definition of context is "*any information that can be used to characterize the situation of an entity. An entity is a person, place, or object that is considered relevant to the interaction between a user and an application, including the user and applications themselves*". This definition is widely recognized as a formal definition of context by current researchers. The definition also emphasizes that context has several dimensions which can clarify the situation of an entity.

DIMENSIONS OF CONTEXT

Previous works on context awareness usually used location as an approximation of context. Although location is one of the dimensions of context, relying solely on it does not explain the entire context of a user. Schilit *et al.* (1994) explained that context should exploit the changing aspects of the environment. They further summarized the environments as: (a) *Computing environment*, such as network connectivity, communication costs, and nearby resources such as printers and workstations; (b) *User environment*, such as location and user's profile; and (c) *Physical environment*, such as lighting and noise level. However, according to Schmidt *et al.* (1999), the computer environment and the physical environment overlap with each other. They proposed a hierarchical context model where context is divided into general categories of *human environment* and *physical environment*. Beyond these general categories, each of them is further divided into three sub-categories where a set of relevant features is identified. The value of these features will determine the overall user's context. Based on those two works, researchers began to propose their own dimensions of context by expanding, reducing the dimensions or proposing new general models of context according to their own works (Bierig & Göker, 2006; Brown & Jones, 2002; Korpipaa *et al.,* 2003; Raento *et al.,* 2005; Razzaque *et*

al., 2006). However, some researchers often incorporate too many dimensions of context which make the context models too complex to be implemented in smartphones. On the other hand, a few dimensions of context make context models unable to understand the whole context.

CONTEXT AND INFORMATION RETRIEVAL

IR system is dependent upon how efficient a user formulates his information needs into a form of a query to retrieve relevant information. Mizzaro (1998) discusses how the user's actual needs are inadequately represented by the queries. Besides, the retrieval process in the current IR frameworks does not consider any external information other than the queries. This external information is also known as a context. The role of context in the IR frameworks has been discussed by many researchers (see for example, Brown & Jones, 2001; Fuhr, 2005; Jones & Brown, 2004) and also cited as one of the long-term challenges in IR (Allan *et al.,* 2004). According to Fuhr (2005), the definition of IR generic task does suggest the need of IR systems to be user specific and to have the necessary knowledge about the user. This indirectly indicates the importance of including context to the IR frameworks. Meanwhile, Brown and Jones (2001) proposed that a query could be constructed by user's current context on behalf of user in context-aware retrieval framework. The query would be specific to a user and understand that user's situation and information problem. In order to simplify mobile user interaction, Jones and Brown (2004) also suggested the IR system to behave autonomously and pro-actively in retrieving and presenting information to a user with the implementation of context. This would make mobile IR, in some sense, intelligent because information is retrieved and presented to a user without much effort from the user.

CONTEXT MODELING IN JIT-MobIR

Contextual retrieval by definition is application specific (Fuhr, 2005). Since context plays an important role in this research, we need to acquire a complete interpretation of user context. Thus, we proposed our own dimensions of context. These dimensions were created by studying the dimensions proposed by different researchers and mapping it with the embedded sensors in Apple iPhone. Details of our dimensions of the context are described below:

- **User's Profile** – this dimension stores any information about the user. Information such as who the user is and habits are saved in this dimension.
- **Time** – this dimension stores timestamp of every change to other context dimensions. This dimension contains the date, the days, the hours, and the minutes of change dimensions.
- **Location** – this dimension stores the information about where the user is.
- **Sounds** – this dimension identifies the surrounding sounds where the user currently is.
- **Activity** – this dimension identifies and stores user's activity.
- **Agenda** – this dimension contains user's driven data on user's future activities.
- **Speed** – this dimension indicates any change in speed if the user is on the move.
- **Heading** – this dimension updates user's heading in order to recognize if the user has the possibility of visiting previous location in his context.

• **Network** – this dimension indicates if the user is connected to the Internet.

• **Preferences** – this dimension refers to user's interest in some particular topics.

The information on this part will be updated over time since it can be influenced by many factors. These dimensions use only the sensors that are embedded in iPhone in order to identify and capture user's context. The work by Lane *et al.* (2010) discusses in detail the lists of Apple iPhone sensors. However, the extracted sensors data do not represent the whole information of user's context. For example, GPS sensor only specifies user's current location but it does not indicate why the user is at that location. Thus, the sensor data need to be interpreted to understand user's context. Consequently, we developed our own context interpretation model to translate sensors data into the description of user's context. This model consists of four different levels of context interpretation, as depicted in Fig.1.

The levels on this context model are:

• **User's scenario**: situations encountered by a particular user.

• **High-level** context: a description of user's current context. User's current context is characterized by interpreting multiple context dimensions.

• **Context dimensions or low-level context**: a characterization of multiple sensors data into meaningful information. It is recognized that one dimension of a context is a subset of high-level context.

• **Sensors data:** any information collected from embedded sensors in the smart- phone and information from user's interaction with the mobile applications.

In this model, context dimension is regarded as low-level context whereby it interprets and describes information collected from sensors data. The context dimension addresses the basic questions like who the user is, where the user is, what the user does, and many more.

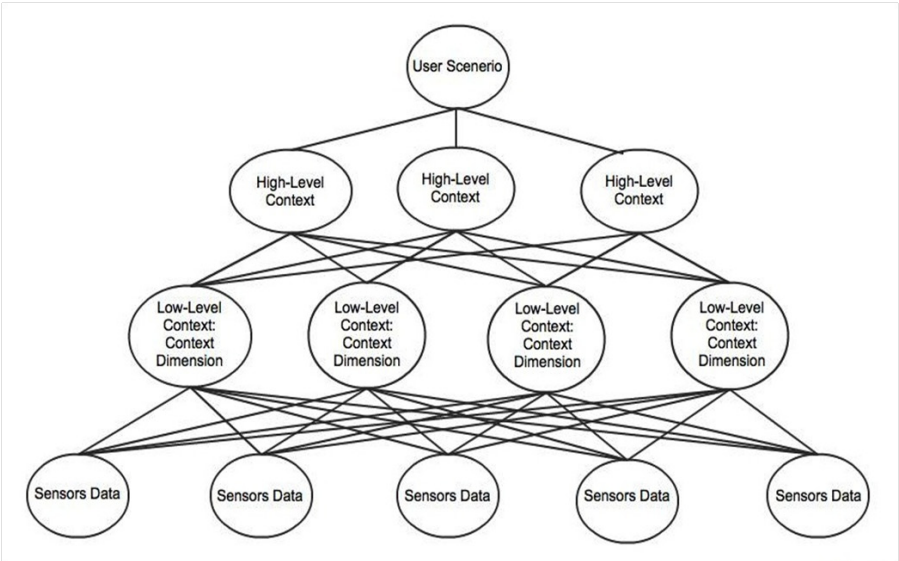

Fig.1: Four levels interpretation of context model

Each context dimension in this model is treated as a subset of high-level context, which is more abstract and difficult to characterize. Besides, the high-level context deals with the semantic relationships between the low-level contexts.

IMPLEMENTATION OF JIT-MobIR

The context model in the previous section is implemented by using the Apple iPhone. The aim of this study was to recognize user's context by using the data from iPhone embedded sensors. The implementation relies solely on iPhone embedded sensors and any external sensor that is not included in the process of acquiring user's context. The conceptual architecture of JIT-MobIR is depicted in Fig.2. In the JIT-MobIR conceptual architecture, the system has two important functions. The first function of the system is to recognize user's context and to infer the user's information needs. The second function is the retrieval system, where it provides two different approaches (pro-active retrieval and query-based retrieval). The pro-active retrieval uses user's information need in context to retrieve relevant information to the user and present it without a request from the user himself. For query-based retrieval, the query submitted by the user is re-formulated by enhancing it with context before it is used to retrieve relevant information. The user's information needs in context and query re-formulation are processed in the server where the contexts are saved. In this architecture, the retrieval process will use a common IR framework and the mechanism will remain unchanged.

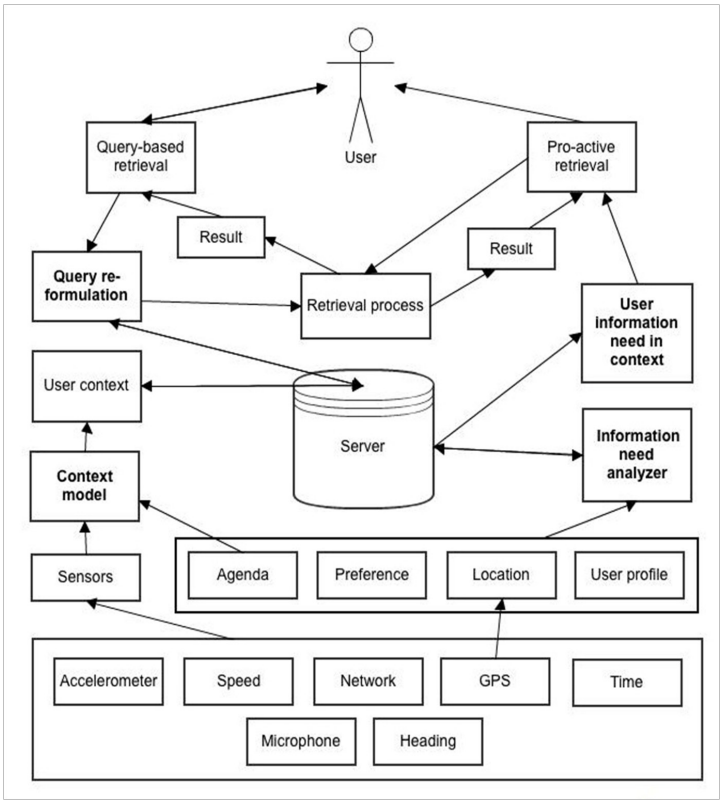

Fig.2: JIT-MobIR conceptual architecture

In order to recognize user context, context model obtains sample data from the embedded sensors. These sample data are classified into low-level context and combined in order to identify high-level context. User's agenda is also extracted in order to recognize if user's context is influenced by the agenda. The system also needs to recognize if the user's current context is a repetition of the user's previous context. If the new user's context is not a repetition of user previous context, the agenda will be examined to determine if it affects the new user's context. Conversely, simple description of the user's context is provided if there is no indication that the context is not a repetition of the user's previous context or the context is affected by agenda. Next, the system infers user's information need in context based on the user's current context and the information need analyzer. However, user's information need in context may fail to infer user's information need. If this happens, the system could predict user's information need through: (a) acquiring the context from different users that are closely similar to the current user's context, or (b) arranging information related to the user's location, preference, and context. The information retrieved based on these approaches may not be required by the user but by presenting the information to the user, the system can update user's preference based on the information selected by the user.

RESULTS

The initial result of recognizing user's context is presented in this section. Since the sensors can be interpreted in various ways, the sensors interpretation in this study is restricted to information that is required by JIR-MobIR, as presented in Fig.3. The sensors data are assigned to the proper dimension with several interpretations. Some of the interpretations are rather straightforward. However, some of the dimensions require a prior pattern in order to distinguish the dimensions value. For example, a prior walking pattern of accelerometer data is required before the context model can recognize it. Thus, initial experiments are conducted to collect these prior patterns where the application captures several users' activities and sounds. The collections of these prior patterns are analyzed and used to automatically interpret the

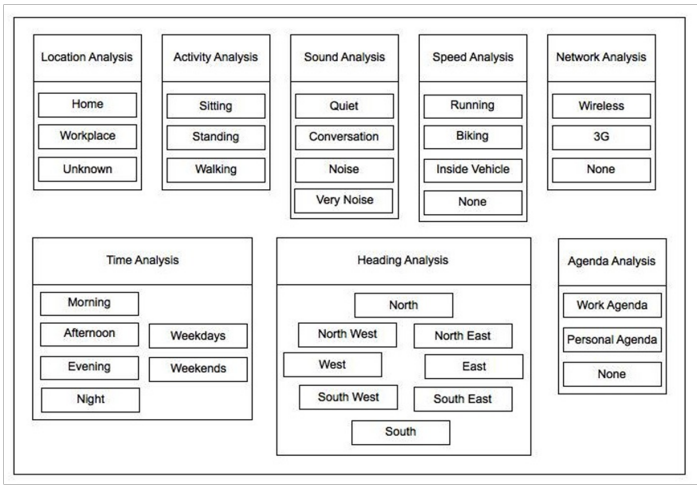

Fig.3: General sensors analysis for the context dimensions

particular dimension. Besides, these patterns need to be general and consistent in interpreting the dimension when implemented in a later stage.

Fig.4 shows the accelerometer axes. The axes are influenced by gravitation force. By examining this force, the orientation of the iPhone can be detected. Then, by collecting the force value over time, the user's activities can be recognized by analyzing the iPhone orientation. For this experiment, iPhone accelerometer and microphone data are collected and analyzed to collect a prior pattern that recognizes the user's activities and the surrounding sounds.

The initial results of recognizing the user's activities are presented in Fig.5, Fig.6 and Fig.7, and the result of analyzing the surrounding sounds is depicted in Fig.8. In this experiment, the iPhone is always placed inside the front pocket of the user's trousers because most of the users often place their smartphones inside the trouser front pocket. The accelerometer data are collected when the user is doing simple activities like sitting, standing and walking. These accelerometer patterns will be used as a reference to automatically recognize the context dimensions of the user's activity in this research.

Fig.5 shows the pattern for recognizing the sitting activities. The x, y, z axes of the accelerometer indicated the orientation of the iPhone. If z axis is equivalent to -1, the screen of the iPhone is facing up and if z axis is equivalent to 1, the screen of the iPhone is facing down. Since the user is sitting, the values of the x and y axes indicate that the user is practically not making any movement.

Fig.6 indicates the pattern when the user is standing. The graph indicates when the user is standing and the user will somehow move a little bit, as indicated by the x and z axes. The orientation of the iPhone is in portrait orientation when y axis is equivalent to -1 or portrait upside down when the y axis equal to 1.

On the other hand, a pattern of accelerometer data when the user is walking is shown in Fig.7. The accelerometer axes are greatly fluctuating and unstable compared to the graphs when the user is sitting and standing. When the user is walking, the user's steps cause the accelerometer to record greater gravitation force as shown in the y axis. Besides, the user's steps when walking also cause the iPhone to receive a vibration, as suggested by the values from the x axis. Hence, the system can automatically distinguish these activities by recognizing the fluctuating pattern of the accelerometer axes. This process will not require too much processing power, which can be implemented inside the iPhone without draining its battery life.

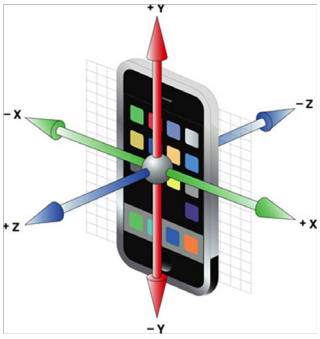

Fig.4: The iPhone accelerometer axes

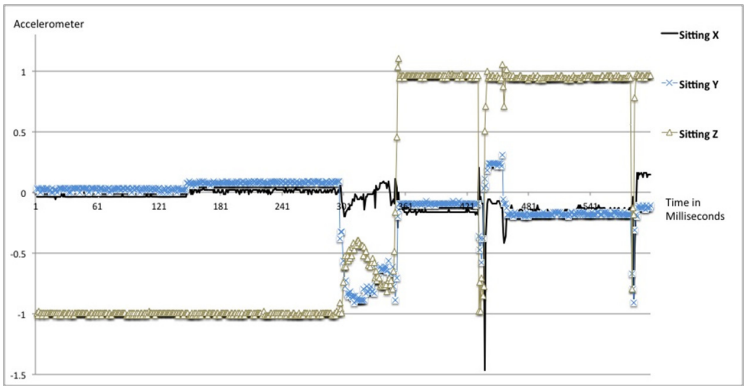

Fig.5: Accelerometer pattern for the sitting activity

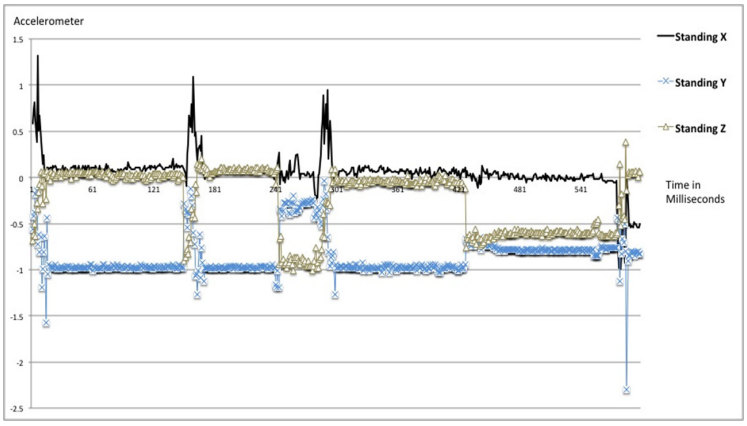

Fig.6: Accelerometer pattern for the standing activity

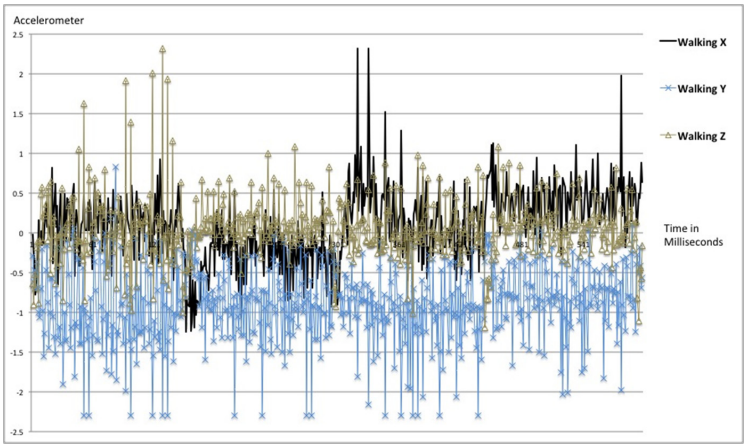

Fig.7: Accelerometer pattern for the walking activity

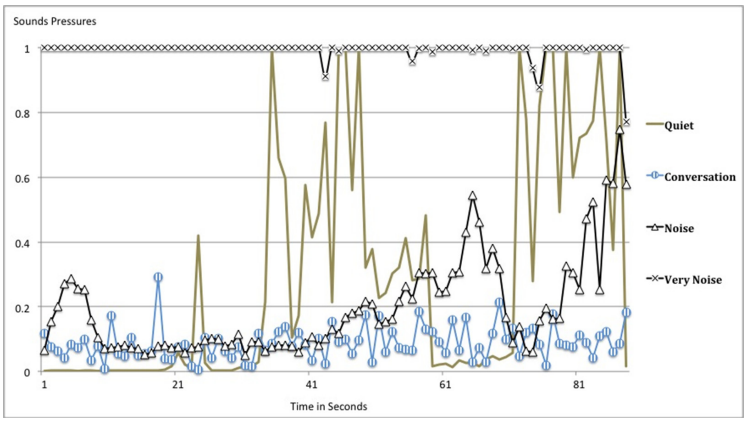

Fig.8: Sound patterns

Fig.8 indicates the patterns of different sound categories. These patterns captured the sound pressure power or decibel from the microphone instead of using sound recognition. There are four sound patterns captured in this experiment, which are: "quiet", "conversation", "noisy" and "very noisy". The "quiet" pattern is probably difficult to capture because the consistently quiet surrounding sound is not easy to obtain. The "conversation" pattern shows that the lowest decibel almost reaches zero decibel because while people are conversing, there are moments when people are silent for brief seconds. The "very noisy" and "noisy" patterns can be differentiated by identifying the lowest and the highest decibels.

CONCLUSION AND FUTURE WORK

The results presented in this paper have shown how context could be identified and captured by using embedded sensors in smartphone. The results collected in this paper will be used as prior patterns to automatically recognize context in a later development without using complex recognition algorithm. This could ensure that smartphone can be used to identify context without draining its battery life.

The next development in this research focuses on context interpretation, context utilization in JIT-MobIR and user's verification of the JIT-MobIR. The current implementation in this study emphasizes on identifying and capturing user's context based on the analysis of the embedded sensors. In order to develop a feasible JIT-MobIR system, three different studies are outlined, and these are:

1. Generating context interpretation, where user's context is automatically interpreted by using the patterns collected in this paper.
2. User's validation, where the system is employed in real situation and the user's validation of his context is collected.
3. Relationship between context and queries, where the system needs to understand how queries can be substituted by context.

ACKNOWLEDGMENTS

The authors gratefully acknowledged the Ministry of Higher Education, Malaysia for the inancial support provided for this study.

REFERENCES

Allan, J. Aslam, J., Belkin, N., Buckley, C., Callan, J., Croft, B., Dumais, S., Fuhr, N., Harman, D., & Harper, D. (2004). Challenges in information retrieval and language modelling. Report of a Workshop held at the Centre for Intelligent Information Retrieval. University of Massachusetts Amherst, September 2002. *Computing Reviews, 45*(7), 437.

Bierig, R., & Göker, A. (2006). *Time, location and interest: an empirical and user-centred study*. Paper presented at the 1st international conference on Information interaction in context, IIiX, pp.79–87.

Brown, P., & Jones, G. (2001). Context-aware retrieval: exploring a new environment for information retrieval and information filtering. *Personal and Ubiquitous Computing*, *5*(4), 253–263.

Brown, P. J., & Jones, G. J. F. (2002). *Exploiting contextual change in context-aware retrieval.* Paper presented at the ACM Symp. on Applied computing, SAC ’02. pp.650–656.

Church, K., Smyth, B., & Keane, M. T. (2006). *Evaluating interfaces for intelligent mobile search*. Paper presented at the International cross-disciplinary workshop on Web accessibility (W4A): Building the mobile web: rediscovering accessibility? W4A’06. pp.69–78.

Dey, A., & Abowd, G. (2000). *Towards a Better Understanding of Context and Context-Awareness*. Paper presented at the CHI’2000 Workshop on The What, Who, Where, When, and How of Context-Awareness. pp.304–307.

Fuhr, N. (2005). Information Retrieval-From Information Access to Contextual Retrieval. *Designing Information Systems. Festschrift für Jürgen Krause,* 47.

Jones, G., & Brown, P. (2004). *The role of context in information retrieval*. Paper presented at the SIGIR 2004 Information Retrieval in Context. pp.20–22.

Korpipaa, P., Mantyjarvi, J., Kela, J., Keranen, H., & Malm, E. (2003). Managing context information in mobile devices. *IEEE Pervasive Computing, 2*(3), 42–51.

Lane, N., Miluzzo, E., Lu, H., Peebles, D., Choudhury, T., & Campbell, A. (2010). A survey of mobile phone sensing. *Communications Magazine, IEEE, 48*(9), 140 –150.

Leake, D. B., Scherle, R., Budzik, J., & Hammond, K. (1999). *Selecting task-relevant sources for just-in-time retrieval.* Paper presented at the AAAI-99 Workshop on Intelligent Information Systems, Menlo Park, CA.

Mizzaro, S. (1998). How many relevances in information retrieval? *Interacting with Computers, 10*(3), 303 – 320.

Raento, M., Oulasvirta, A., Petit, R., & Toivonen, H. (2005). Contextphone: A prototyping platform for context-aware mobile applications. *IEEE Pervasive Computing, 4*(2), 51–59.

Razzaque, M. A., Dobson, S., & Nixon, P. (2006). *Categorization and modelling of quality in context information.* Paper presented at the IJCAI 2005 Workshop on AI and Autonomic Communications.

Schilit, B., Adams, N., & Want, R. (1994). *Context-aware computing applications*. Paper presented at the Workshop on Mobile Computing Systems and Applications. pp.85–90.

Schmidt, A., Aidoo, K., Takaluoma, A., Tuomela, U., Van Laerhoven, K., & Van de Velde, W. (1999). Advanced interaction in context. In H.-W. Gellersen (Ed.)*, Handheld and Ubiquitous Computing* (pp. 89–101). Springer Berlin/ Heidelberg.

Schmidt, A., Beigl, M., & Gellersen, H. (1999). There is more to context than location. *Computers & Graphics, 23*(6), 893 – 901.

Sohn, T., Li, K. A., Griswold, W. G., & Hollan, J. D. (2008). *A diary study of mobile information needs*. Paper presented at the twenty-sixth annual SIGCHI conference on Human Factors in Computing Systems, *CHI'08,* 433–442.

Tamine-Lechani, L., Boughanem, M., & Daoud, M. (2010). Evaluation of contextual information retrieval effectiveness: overview of issues and research. *Knowledge and Information Systems, 24*(1), 1–34.

Pertanika J. Sci. & Technol. 21 (1): 239 - 246 (2013)

PERTANIKA JOURNALS

SCIENCE & TECHNOLOGY

Journal homepage: http://www.pertanika.upm.edu.my/

Using SVMs for Classification of Cross-Document Relationships

Yogan Jaya Kumar[1,2]*, Naomie Salim[2], Ahmed Hamza Osman[2] and Albaraa Abuobieda[2]

[1]Faculty of Information and Communication Technology, Universiti Teknikal Malaysia Melaka, 76100 Durian Tunggal, Melaka, Malaysia

[2]Faculty of Computer Science and Information Systems, Universiti Teknologi Malaysia, 81310 Skudai, Johor, Malaysia

ABSTRACT

Cross-document Structure Theory (CST) has recently been proposed to facilitate tasks related to multi-document analysis. Classifying and identifying the CST relationships between sentences across topically related documents have since been proven as necessary. However, there have not been sufficient studies presented in literature to automatically identify these CST relationships. In this study, a supervised machine learning technique, i.e. Support Vector Machines (SVMs), was applied to identify four types of CST relationships, namely "Identity", "Overlap", "Subsumption", and "Description" on the datasets obtained from CSTBank corpus. The performance of the SVMs classification was measured using Precision, Recall and F-measure. In addition, the results obtained using SVMs were also compared with those from the previous literature using boosting classification algorithm. It was found that SVMs yielded better results in classifying the four CST relationships.

Keywords: CST relation, multi-document, rhetorical relation, SVMs

INTRODUCTION

Discourse analysis in texts has nowadays become very prominent, especially when it involves multiple texts such as documents. The idea of cross-document structural relationship is to investigate the existence of inter-document rhetorical relationships. These rhetorical relations are based on the CST model (Cross-document Structure Theory) (Radev, 2000). Documents which are related to the same topic usually contain semantically related textual units. These textual units can be words, phrases, sentences, or the documents itself. The general schema of CST is shown in Fig.1. In the current work, only the semantic relations between sentences were taken into consideration. Some examples of such semantic connections are "Identity",

Article history:
Received: 31 March 2012
Accepted: 31 August 2012

E-mail addresses:
yogan@utem.edu.my (Yogan Jaya Kumar),
naomie@utm.my (Naomie Salim),
ahmedagraa@hotmail.com (Ahmed Hamza Osman),
albarraa@hotmail.com (Albaraa Abuobieda)
*Corresponding Author

ISSN: 0128-7680 © 2013 Universiti Putra Malaysia Press.

"Contradiction", "Description", and "Historical background". Table 1 shows some examples of the sentence pairs that hold CST relationship. Full descriptions of the CST relations are given in Radev (2000).

The work on CST can be put in line with Rhetorical Structure Theory (RST) (Taboada & Mann, 2006). The difference between these two theories is that RST aims to capture the rhetorical relation between span of adjacent text units, while CST goes across topically related documents to describe its rhetorical relation. In topically related documents, especially news articles, the information contents are closely connected even though the news story comes from various sources. By referring to the description of CST relations shown in Table 1, it can be seen that these types of relations are essential for the analysis of redundancy, complementarity and contradiction among different information sources. Thus, the ability to automatically identify the types of CST relationship will definitely be handy for tasks related to multi-document analysis. A number of research works have addressed the benefits of CST for summarization task (see for instance, Zhang *et al*., 2002; Jorge *et al*., 2010). Nonetheless, a major limitation of these works is that the CST relationships need to be manually annotated by human expert. Human annotation is not only expensive, but it also consumes a lot of time.

There have been efforts put to learn the CST relationships in texts. Zhang *et al*. (2003) used boosting, i.e. a classification algorithm, to identify the presence of CST relationships between sentences. It is an adaptive algorithm which works by iteratively learning previous weak classifiers and adding them to a final strong classifier. The authors experimented with CST annotated article cluster that built the CSTBank corpus. Hence, lexical, syntactic and semantic features were used for data representation. Their classifier was able to identify sentence pairs with no relationship very well, but showed a rather poor performance in classifying the other types of CST relationship.

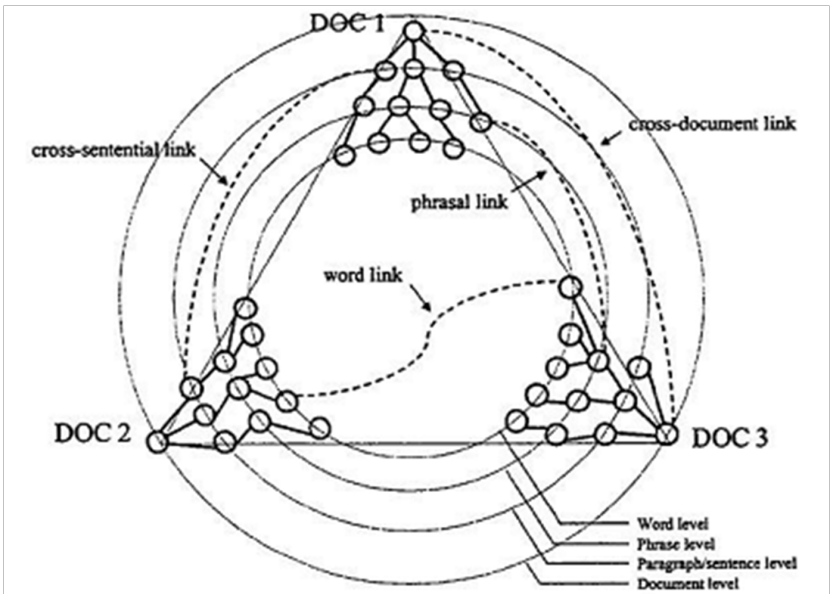

Fig.1: CST general schema (Radev, 2000)

TABLE 1: Some examples of the CST relationship between sentences (source: Zhang *et al*., 2002)

Relationship	Description	Text span 1 (S1)	Text span 2 (S2)
Identity	The same text appears in more than one location	Tony Blair was elected for a second term today.	Tony Blair was elected for a second term today.
Equivalence	Two text spans have the same information content	Derek Bell is experiencing resurgen0ce in his career.	Derek Bell is having a "comeback year."
Translation	The same information content in different languages	Shouts of "Viva la revolucion!" echoed through the night.	The rebels could be heard shouting, "Long live the revolution".
Subsumption	S1 contains all information in S2, plus additional information not in S2	With 3 wins this year, Green Bay has the best record in the NFL.	Green Bay has 3 wins this year.
Contradiction	Conflicting information	There were 122 people on the downed plane.	126 people were aboard the plane.
Historical Background	S1 gives historical context to information in S2	This was the fourth time a member of the Royal Family has gotten divorced.	The Duke of Windsor was divorced from the Duchess of Windsor yesterday.

In another related work, Miyabe *et al*. (2008) investigated on the identification of CST relationship types by using cluster-wise classification with SVM classifier. They used a Japanese cross-document relation corpus annotated with CST relationships. The authors proposed using the detected "Equivalence" relations to address the task of "Transition" identification. In particular, similarity through the variable noun phrases was used for transition identification. They obtained F-measure of 75.50% for equivalence and 45.64% for transition. However, their approach is only limited to the two aforementioned relations.

Closely related to our work is the approach by Zahri and Fukumoto (2011). The authors determined five types of CST relation between sentences using SVMs. The authors computed the lexical features between sentence pairs using the dataset from the CSTBank corpus. Then, they used the identified CST relations to determine the directionality between the sentences for PageRank (Erkan & Radev, 2004) computation. However there were no experimental results specifically shown on the performance of their CST relationship classification. This is essential because the performance of the classification has direct implication on the final results of the system.

METHODS

Relying on manually annotated text for CST relationship identification consumes a lot of time and resources. Thus, it is favourable to have a system which can automatically identify the existence of the CST relations between pairs of sentences. However, at this point of time, we are only considering four types of CST relations, namely "Identity", "Overlap", "Subsumption", and "Description". More details of these relations are given in Table 2. Meanwhile, further details with examples can be found in Zhang *et al*. (2002).

TABLE 2: The CST relations used in this work

Relationship	Description
Identity	The same text appears in more than one location
Subsumption	S1 contains all information in S2, plus additional information not in S2
Description	S1 describes an entity mentioned in S2
Overlap (partial equivalence)	S1 provides facts X and Y while S2 provides facts X and Z; X, Y, and Z should all be non-trivial

In this study, the publically available CSTBank corpus was exploited (Radev *et al*., 2003) – , i.e. a corpus consisting clusters of English news articles annotated with the CST relationships. Using the datasets from CSTBank, we were able to obtain our training and testing data. Then, the training set comprising of the features between sentence pairs with its corresponding CST relationship was prepared. Each of these sentence pairs was represented using four lexical features which could be useful to differentiate the CST relationships between the sentences. After that 100 pairs of sentences that posed no CST relations were manually selected for the training and test data. The lexical features that were computed for each sentences pair are described in the following.

Cosine similarity – cosine similarity is used to measure how similar two sentences are. Here, the sentences are represented as word vectors having words with tf-idf as the element *value:*

$$\cos(S_1, S_2) = \frac{\sum S_{1,i} \cdot S_{2,i}}{\sqrt{\sum (S_{1,i})^2} \cdot \sqrt{\sum (S_{2,i})^2}} \quad (1)$$

Word overlap – this feature represents the measure on the numbers of words overlapping in the two sentences (after stemming process). This measure is not sensitive to the word order in the sentences:

$$overlap(S_1, S_2) = \frac{\#words(S_1 \cap S_2)}{\#words(S_1 \cup S_2)} \quad (2)$$

Length difference – length difference gives the measure of difference between the lengths of two sentences. It shows how long or how short a sentence is compared to the other:

$$lengdiff(S_1, S_2) = length(S_1) - length(S_2) \quad (3)$$

Length type of S_1 – this feature gives the length type of the first sentence when the lengths of two sentences are compared:

$$lengtype(S_1) = \begin{array}{rl} 1 & \text{if } length(S_1) > length(S_2), \\ -1 & \text{if } length(S_1) < length(S_2), \\ 0 & \text{if } length(S_1) = length(S_2) \end{array} \quad (4)$$

Support Vector Machines (SVMs) (Vapnik, 1995), a supervised machine learning technique commonly used for classification and regression analysis, was employed in this work. SVMs are feature-based classifiers, where each instance from the datasets is usually represented as a feature vector which is then used as an input for machine learning. An excellent introduction to SVMs can be found in Cristianini and Taylor (2000). SVMs are basically two-class classifiers. A support vector machine builds a hyperplane that separates the instances of the two classes. Since ours is a multi-class problem, SVMs built a set of one-versus-one classifiers, and chose the class that is selected by most classifiers. The general flow of the classification process is shown in Fig.2.

Based on the dataset from CSTBank, a total of 477 sentence pairs were selected for the training and 205 sentence pairs were used for the testing. These included the sample of 100 sentence pairs with no CST relationship. First of all, the texts were preprocessed by stop-word filtering and word stemming. After computing each of the feature values for every sentence pair from the training set, they were used as inputs for the training of SVMs. The training data were then trained using the LibSVM tool (Chang & Lin, 2011) on MATLAB. The SVMs model best parameters were chosen after applying 5-folds cross validation. Once the training was completed, the resulting classifier model was tested by using the test data to measure its performance. The performance of SVMs classification was evaluated using Precision, Recall and F-measure.

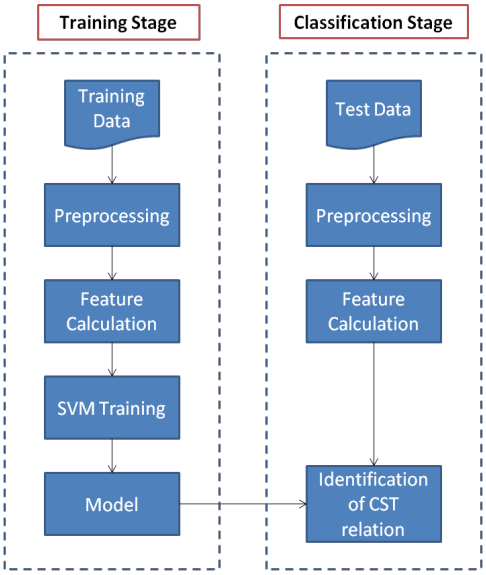

Fig.2: The training and classification processes

RESULTS AND DISCUSSION

Fig.3 shows the results of the classification in the present study. It can be observed that the SVM achieved a high precision and recall in determining the relation "Identity" as compared to the rest of the CST relationships. To detect "No relation" sentence pairs, the precision score was good but its recall was below average. The rest of the relations obtained average results. One possible reason for getting imbalance classification results was probably the features chosen for the SVM training. Since the features used in this work are only of lexical type, SVM might not well differentiate most of the relation types. Thus, it can be assumed that the performance of the classifier can be further improved by selecting better features for training.

With the motivation to observe the general performance of the SVM classification in identifying the CST relationship between sentences, the initial results retrieved were also compared with those obtained by Zhang *et al*. (2003) who had applied boosting classification algorithm (BCA). Table 3 gives the precision, recall and F-measure, while Fig.4 shows the F-measure comparison between the two methods. It was observed that BCA performed well in differentiating non-CST related sentence pairs. However, SVM was found to outperform BCA in classifying the other types of CST relationships.

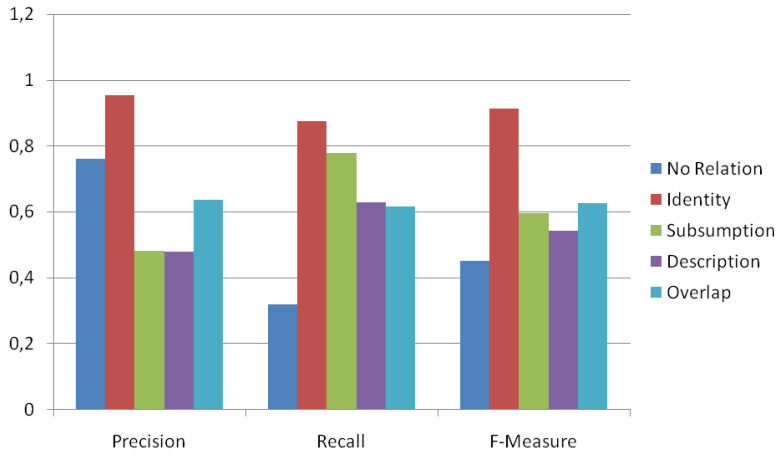

Fig.3: The classification by SVM

TABLE 3: A comparison of the results

Relationship	Precision		Recall		F-Measure	
	BCA	SVM	BCA	SVM	BCA	SVM
No relation	0.89	0.76	0.94	0.32	0.91	0.45
Identity	-	0.95	-	0.87	-	0.91
Subsumption	0.06	0.48	0.04	0.77	0.05	0.59
Description	0.26	0.47	0.21	0.62	0.23	0.54
Overlap	0.55	0.63	0.35	0.61	0.43	0.62

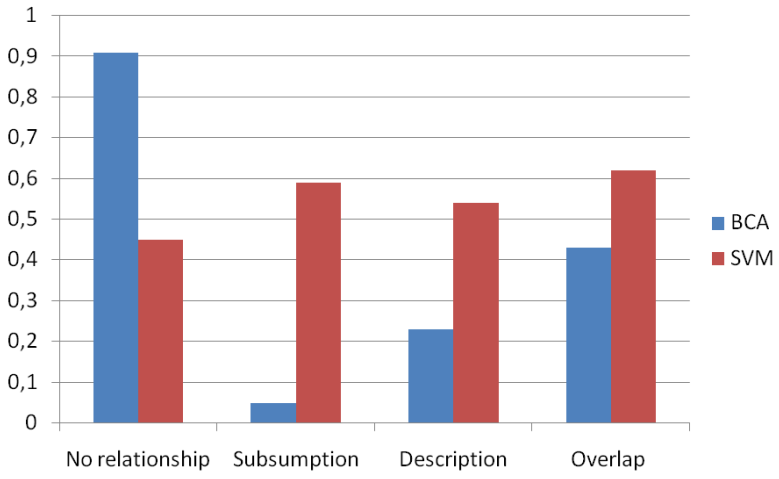

Fig.4: A comparison of the F-measures between BCA and SVM

CONCLUSION

The feasibility to identify the CST relationships between the sentences across topically related documents is a noteworthy advancement for multi-document analysis. However, there have not been sufficient studies presented in the literature to automatically identify these CST relationships. In this paper, an attempt to investigate the performance of SVMs classification technique for identifying four types of CST relations (namely, "Identity", "Overlap", "Subsumption", and "Description") was carried out. In order to achieve this, the publically available CSTBank corpus (i.e. the corpus with human annotated CST relationships) was exploited so as to obtain the required training and testing data. Each instance of these datasets was represented using the lexical features.

The performance of the SVMs classification was evaluated using Precision, Recall and F-measure. The experimental results showed that we were able to detect "Identity" relation very well and also produced average results for the other types of relations. Moreover, the results obtained using SVMs were also compared with those retrieved from the previous literature using boosting classification algorithm. It was observed that overall, the SVMs classification yields better results. Currently, the authors are investigating further into improving the performance of the classifier by proposing additional semantic features such as noun phrases, verb phrases, etc. for feature vector representation. By being able to produce better classification accuracy, it can be stated that many applications related to multi document analysis will gain benefit out of it.

ACKNOWLEDGEMENTS

The research was sponsored by IDF and the Ministry of Science Technology and Innovation, under the University's research grant vote number 01H74, Universiti Teknologi Malaysia.

REFERENCES

Chang, C. C., & Lin C. J. (2011). LIBSVM: a library for support vector machines. *ACM Transactions on Intelligent Systems and Technology, 2*27(1-27), 27.

Cristianini, N., & Shawe-Taylor, J. (2000). *An Introduction to Support Vector Machines and Other Kernel-Based Learning Methods*. Cambridge: Cambridge University Press.

Erkan, G., & Radev D. R. (2004). LexPageRank: Prestige in multi-document text summarization. *In Proceedings of the Conference on Empirical Methods in Natural Language Processing*, 365-371.

Jorge, M. L. C., & Pardo, T. S. (2010). Experiments with CST-based Multidocument Summarization. *Workshop on Graph-based Methods for Natural Language Processing, ACL*, 74–82.

Miyabe, Y., Takamura, H., & Okumura, M. (2008). Identifying cross-document relations between sentences. *In Proceedings of the 3rd International Joint Conference on Natural Language Processing*, 141–148.

Radev, D. R. (2000). *A Common Theory of Information Fusion from Multiple Text Sources Step One: Cross-Document Structure.* Paper presented at the 1st ACL SIGDIAL Workshop on Discourse and Dialogue, 10, pp.74-83.

Radev, D. R., & Otterbacher, J. (2003). *CSTBank Phase I*. Retrieved at http://tangra.si.umich.edu/clair/CSTBank/phase1.htm

Taboada, M., & Mann, W. C. (2006). Rhetorical Structure Theory: Looking Back and Moving Ahead. *Discourse Studies, 8*, 423-459.

Vapnik, V. (1995). *The Nature of Statistical Learning Theory*. New York: Springer Verlag.

Zahri, N. A. H .B., & Fukumoto, F. (2011). *Multi-document Summarization Using Link Analysis Based on Rhetorical Relations between Sentences.* Paper presented at the 12th International Conference on Computational Linguistics and Intelligent Text Processing, 2, pp.328-338.

Zhang, Z., Blair-Goldensohn, S., & Radev, D. R. (2002). *Towards CST-Enhanced Summarization*. Paper presented at the 18th National Conference on Artificial Intelligence, pp.439-446.

Zhang, Z., Otterbacher, J., & Radev, D. R. (2003). *Learning cross-document structural relationships using boosting.* Paper presented at the 12th International Conference on Information and Knowledge Management, pp.124-130.

Pertanika J. Sci. & Technol. 21 (1): 247 - 260 (2013)

PERTANIKA JOURNALS

SCIENCE & TECHNOLOGY

Journal homepage: http://www.pertanika.upm.edu.my/

Usability of Educational Computer Game (UsaECG): A Quantitative Approach

Hasiah Mohamed@Omar[1]*, Azizah Jaafar[2] and Rohana Yusoff[1]

[1]*Faculty of Computer & Mathematical Sciences, Universiti Teknologi MARA, 23000 Dungun, Terengganu, Malaysia*

[2]*Institute of Visual Informatics, Universiti Kebangsaan Malaysia , 43600 Bangi, Selangor, Malaysia*

ABSTRACT

Heuristic Evaluation (HE) is used as a basis in developing a new technique to evaluate usability or educational computer games known as Playability Heuristic Evaluation for Educational Computer Game (PHEG). PHEG was developed to identify usability problems that accommodate five heuristics, namely, interface, educational elements, content, playability and multimedia. In HE process, usability problems are rated based on severity score and this is followed by presentation of a mean value. The mean value is used to determine the level of usability problems; however, in some cases, this value may not accurate because it will ignore the most critical problems found in a specific part. In developing PHEG, a new quantitative approach was proposed in analyzing usability problems data. Numbers of sub-heuristics for each heuristic involved were taken into account in calculating percentage for each heuristic. Functions to calculate critical problems were also introduced. Evaluation for one educational game that was still in development process was conducted and the results showed that most of the critical problems were found in educational elements and content heuristics (57.14%), while the least usability problems were found in playability heuristic. In particular, the mean value in this analysis can be used as an indicator in identifying critical problems for educational computer games.

Keywords: Usability of educational computer game, tool, interface, playability, multimedia

INTRODUCTION

In application development process, evaluation plays an important and integral part. This evaluation can be carried out either during the development (formative) or once the development is completed (summative). Expert evaluators may involve in any stage either formative or summative and real (potential) users are normally involved during summative evaluation. Meanwhile, selection

Article history:
Received: 31 March 2012
Accepted: 31 August 2012

E-mail addresses:
hasia980@tganu.uitm.edu.my (Hasiah Mohamed@Omar),
aj@ftsm.ukm.my (Azizah Jaafar),
rohanayu@tganu.uitm.edu.my (Rohana Yusoff)
*Corresponding Author

ISSN: 0128-7680 © 2013 Universiti Putra Malaysia Press.

of the evaluators depends on the types of application, evaluation techniques and tools. One of the many popular applications nowadays is computer games. The popularity of computer games leads to the increment of computer game development that integrates educational elements in it. There are a lot of researches conducted on the integrations of computer games and educational elements in the perspective of impact, implication and effects (Yee Leng *et al*., 2010). The terms used for these applications are known as game based learning, computer games, educational computer games and digital game based learning (Kato, 2010; Papastergiou, 2009; Robertson & Howells, 2008).

The integration of fun to be played by the users and also the ability to contribute to the teaching and learning processes have become vital elements in any educational games development process. In order to merge these elements, comprehensive evaluation technique is needed during the development process. One of the evaluation techniques that is normally used by expert evaluators is Heuristic Evaluation (HE). In particular, HE is used by expert evaluators to examine the interface of any applications during interactive design process. The experts' involvement in the evaluation process is able to help developers to detect usability problem before the game can be released (Hasiah & Azizah, 2011b). The ability and the characteristics of HE have been used as a basis in developing specific heuristic technique to evaluate educational computer games (ECG). This technique is known as Playability Heuristic Evaluation for Educational Computer Game (PHEG), which consists of five heuristics, namely, interface (IN), educational element (ED), content (CN), playability (PL) and multimedia (MM) (Hasiah & Azizah, 2010). The experts who are involved in the evaluation process are from various backgrounds based on the heuristics provided, such as interface expert (for IN), educational technologies (for ED), subject matter experts (for CN), multimedia experts (for MM) and game developers (for PL).

The experts' involvement in the evaluation process shows a significant impact in identifying usability problems based on their knowledge and experiences. On the other hand, gathering experts in one place to conduct an evaluation is not an easy task since experts' work commitments need to be taken into consideration. In order to overcome this problem, an evaluation system known as AHP_HeGES was developed to assist the evaluation process. This online system can be used by the experts to conduct the evaluation and it is capable of handling the experts from various backgrounds at one time (Hasiah & Azizah, 2011b). A pilot study was conducted to test the system with the involvement of an expert for each heuristic. All the experts were able to accomplish the evaluation process accordingly, as well as to identify and list down usability problems based on the sub-heuristics involved and rate severity scale.

In analyzing the HE data or known as usability problems, severity rating plays important roles in helping developers to predict the level of usability problems in any application that is being evaluated. The experts normally identified all usability problems after inspecting the interface of the applications and rating the severity rating score based on the severity that was introduced by Nielsen (1995). Most of the papers have reported that the presentations of severity rating were calculated based on the mean of the severity rating (Nielsen, 1995; Pinelle *et al*., 2009; Ssemugabi & Villiers, 2007; Tan, Liu & Bishu, 2009).

The aim of this study was to propose potential quantitative analysis approach for usability of ECG based on the usability problems (results) presented in Hasiah and Azizah (2011b).

This paper reports the potential quantitative analysis for PHEG data in order to estimate the usability level of ECG. This research is important to facilitate game developers to get evaluators' feedback and usability problems of the ECG that is still in the development process.

HEURISTIC EVALUATION

Heuristics evaluation (HE) is a design guideline which serves as a useful evaluation tool for both product designers and usability professional (Nielsen & Molich, 1990). HE is an inspection evaluation technique that is normally used by an expert to find any usability problem in any product or system (Mureen *et al*.,2007; Nielsen & Molich, 1990). In particular, HE is commonly used for formative evaluation where the product or system is still in a development process. HE involves a small number of evaluators (expert in specific field) who have been assigned to inspect a system according to heuristics or guidelines that are relevant and focused on the interface of the system. HE is a light-weight process that can be cheap, fast, and easy to apply in an evaluation process (Nielsen, 1994). It can be used both in the design and evaluation phases of development and can even be applied to paper-based designs before the first working prototype is created (Nielsen & Molich, 1990). Studies on HCI have shown that using five evaluators may be enough to find most usability problems, while adding more will reduce the benefit to the cost ratio, and hence, suggesting that three may suffice (Nielsen & Molich, 1990). It can be used both in design and evaluation phases of development and can even can be applied to paper-based designs before the first working prototype is created. The HE technique has emerged from an evaluation of software (system and products) to one of the most popular applications nowadays, that is, games (Hasiah & Azizah, 2010).

In HE, there is a list of heuristics attributes that cover common criteria for any system that focuses on user's interface and interaction elements. These elements cover all the perspective of the system in general but in terms of educational computer game (ECG), to the best of our knowledge, there are no specific heuristics which accommodate all the elements in ECG, such as educational design and contents. Therefore, another set of heuristics that focuses on ECG is required. The argument for the requirement is the usability in ECG should deal with several elements of education if they are to be applied in teaching and learning officially. Hence, the elements of education, such as content and educational design, should be taken into consideration in the evaluation. A specific evaluation technique that is dealing with all the important criteria of educational computer games is known as Heuristic Evaluation for Educational Computer Game (PHEG) (Hasiah & Azizah, 2011a). In particular, PHEG accommodates five heuristics in evaluating the usability of educational computer games (UsaECG), interface, educational element, content, playability and multimedia.

EVALUATION PROCESS IN HE

Heuristic evaluation is a discount usability engineering method for quick, cheap, and easy evaluation of a user interface design (Kirmani, 2008). The goal of the evaluation process in HE is to find the usability problems in the design so that they can be attended to as parts of an iterative design process (Kirmani, 2008). The HE, developed by Nielsen and Molich in 1990 (Nielsen & Molich, 1990), is a technique used to evaluate the usability, with the inspection

being carried out mainly by evaluators, normally referred to as expert evaluators. The studies by Nielsen (1995) have shown that a number between 3 and 5 evaluators is enough. "It detects approximately 42% of serious design problems and 32% of minor problems, depending on the number of evaluators who reviewed the site" (Nielsen, 1995). In order to make a HE efficient and to provide quality results, the phases below should be taken into consideration:

1. Prior training: The evaluator must become familiar with the interface for a few minutes to learn the website and to be able to carry out the HE agilely.
2. Evaluations: The evaluator follows the set of heuristics to find deficiencies or to catalogue the website as usable. He can write comments.
3. Rate severity: The evaluator should determine the severity of each of the problems encountered. It is therefore appropriate that the priority of the problems is rated. He suggests three parameters: Frequency of problems occurs (are the users affected by the occurrence of the problem, and persistence of the problem). Is it a one-time problem and can the users overcome once they know about it or will the users repeatedly be bothered by the problem? (Nielsen & Molich, 1990). The problems in each parameter can score on a scale of 0 (not a usability problem) to 4 (catastrophe: it is obligatory to fix it) (Nielsen & Molich, 1990).
4. Review: In order to analyze each of the evaluations made to present a report with all the problems and possible resolutions by taking into account the qualitative analysis obtained (Nielsen & Molich, 1990).

Presentation of the usability problems have been made more meaningful based on rating scale (Nielsen, 1995). Rating scale is used to rate the severity of usability problems that have been identified during the evaluation process. The rating scale are based on the number with specific meaning, namely; 4 (Usability catastrophe: imperative to fix this before product can be released), 3 (Major usability problem: important to fix, so should be given high priority), 2 (Minor usability problem: fixing this should be given low priority), 1 (Cosmetic problem only: need not be fixed unless extra time is available on project) and 0 (I don't agree that this is a usability problem at all) (Nielsen, 1995).

CALCULATION OF THE USABILITY PROBLEM FOUND IN HE

A comparative evaluation study that investigated the extent to which HE identifies usability problems in a web-based learning application and compares the results with those of the survey evaluations among end-users (learners) was conducted (Ssemugabi & Villiers, 2007). Four evaluators (experts) in different expertise (user interface design, instructional/educational design and teaching) were invited and they agreed to participate in the evaluation process. There were a total of 58 problems identified by the experts and the severity rating was used to categorize the problems found. All the usability problem found were then divided into 2 categories, namely, major problem for severity scores 4 and 5 and minor for severity scores 1 and 2. Data were presented based on the numbers of problem founds and the mean of severity rating.

Network Game Heuristic (NGH) was developed by Pinelle *et al*. (2009), who later conducted an evaluation process with ten participations who had previous experiences with

usability evaluation and experience with multiplayer networked games (double experts). The participants evaluated and rated the usability problem using the Nielsen's severity rating (Nielsen, 1995). The results are shown in a form of table that summarizes the heuristic, total problem and mean severity. The evaluation results showed that the new heuristics were effective at specializing the evaluation process for multiplayer network games. The argument here was the way the results are being presented in term of severity rating. By having the mean value for the severity rating, it is debatable that it will not show the real level of the usability problems in the network game that is being evaluated.

Web evaluation using Heuristic Evaluation and user testing was also conducted (Tan *et al*., 2009). For HE, nine expert evaluators were recruited and defined as who had graduated level coursework in human computer interaction and in human factors of web design. The evaluators independently examined the interfaces and judged their compliance with a set of heuristics. After the evaluation process had been completed, all the findings (usability problems) were compiled and reported. The problems were classified on the basis of severity. A set of severity criteria was established to rate the severity of the problems. The three different severity ratings included were severe, medium and mild problems. Severe problems included catastrophic usability problems, where users were unable to do their work and major problems where users had difficulty, but were still able to find workarounds. Hence, fixing the problems is a mandatory. Medium problems included medium usability problems where users stumbled over the problem, but could quickly adapt to it. Fixing the problems should be given medium priority. Mild problems included minor usability problems, where users could easily work around the problem. Fixing the problems should be given low priority. Meanwhile, usability problem found was presented based on the numbers and the type of severity (namely, severe, medium and mild).

Quantitative analysis for a heuristic evaluation was adapted from González *et al*. (2009). To the best of our knowledge, this is one of the few studies that has attempted to quantitatively analyze heuristic evaluation data (usability problems). Research conducted by González *et al*. (2009) was based on UsabAIPO project that had initiated new experiment to obtain quantitative result after a heuristic evaluation process. Function of UsabAIPO was introduced and this gave the estimation of the degree or the level of usability of the website. The number of heuristics and sub-heuristics involved play an important role in developing the functions and overall calculation. The results are presented in the form of percentage of the overall usability. Usability level can be considered as good when its value is higher than 80% and 100%. This also means that all the sub-heuristics are satisfied or fulfilled (González *et al*., 2009).

PLAYABILITY HEURISTIC EVALUATION FOR EDUCATIONAL GAMES (PHEG)

Heuristic Evaluation (HE) is used as a basis in developing specific heuristic technique to evaluate educational computer games known as Playability Heuristic Evaluation for Educational Computer Game (PHEG) consisting of five heuristics, namely, interface (IN), educational element (ED), content (CN), playability (PL) and multimedia (MM) (Hasiah & Azizah, 2011a). The experts who are involved in the evaluation process came from various backgrounds,

and in this case, interface expert (for IN), educational technologies (for ED), subject matter experts (for CN), multimedia experts (for MM) and game developers (for PL). The criteria for usability evaluation of educational computer games (UsaECG) consist of 5 heuristics and 37 sub-heuristics. Table 1 below shows the PHEG.

TABLE 1: Playability Heuristic for Educational Computer Games (PHEG)
(Source: Hasiah & Azizah, 2011a)

Heuristic and Sub heuristics	
Interface (IN)	
IN1	Visibility of system status.
IN2	Match between system and the real world.
IN3	User control and freedom.
IN4	Consistency and standards.
IN5	Error prevention.
IN6	Recognition rather than recall.
IN7	Flexibility and efficiency of use.
IN8	Aesthetic and minimalist design.
IN9	Help users recognize, diagnose, and recover from errors.
IN10	Help and documentation.
Educational Element (ED)	
ED1	Clear learning objectives.
ED2	Suitable for learning process.
ED3	Functions as self directed learning tools.
ED4	Considers the individual learning level differences.
ED5	Provide feedback about the knowledge being constructed.
ED6	Offers the ability to select the level of difficulty in games.
Content (CN)	
CN1	Reliable and proven content with correct syllabus flow.
CN2	Clear structure of content.
CN3	Screen navigation is precise.
CN4	Supporting learning materials is relevant.
CN5	Content materials are engaging.
CN6	The content is chunk based on topic and subtopic.
Playability (PL)	
PL1	Provide enough information to get started to play.
PL2	Control keys follow standard conventions.
PL3	Users should always be able to identify their score in the game.
PL4	Users able to save games in different states.
PL5	Successful users in completing all the activities in a module are rewarded.
PL6	Challenges provided are positive game experiences.
PL7	The game is enjoyable to replay.

TABLE 1: (Continued)

Heuristic and Sub heuristics	
Multimedia (MM)	
MM1	Each multimedia element used serves a clear purpose.
MM2	Usage of multimedia elements is suitable with the content.
MM3	Combinations of multimedia elements are adequate.
MM4	The presentation of multimedia elements is well managed.
MM5	Numbers of multimedia elements for each screen is not more than 2 elements.
MM6	The use of multimedia elements support meaningfully the information provided.
MM7	The quality of multimedia elements used is good.
MM8	The use of multimedia elements enhances the content presentation.

RESEARCH METHODOLOGY

This study was carried out based on the previous set of heuristic and sub-heuristics that were developed to evaluate UsaECG (Hasiah & Azizah, 2011a) known as Playability Heuristic for Educational Computer Games (PHEG). PHEG consists of 5 heuristics such as (Interface (IN), Educational Element (ED), Content (CN), Playability (PL) and Multimedia (MM)). Heuristic for Interface consists of 10 sub-heuristics, and this is followed by heuristic for Educational Element (6 sub-heuristics), heuristic for Content (6 sub-heuristic), heuristic for Playability (7 sub-heuristics) and heuristic for Multimedia (8 sub-heuristics). Each heuristic was weighted according to its sub-heuristics, represented in the form of percentage of the sub-heuristic weight corresponding to the heuristic, as shown in Table 2.

Table 2 shows the heuristics, the number of sub-heuristics for each heuristic and its weighting used to calculate the total percentage of the educational computer games usability. The formula, called UsaECG(x), is as follows:

$$\text{UsaECG}(x) = ((\text{IN}/0.2073) + (\text{ED}/0.1622) + (\text{CN}/0.1622) + (\text{PL}/0.1892) + (\text{MM}/0.2162))/5 \quad (1)$$

where, IN represents the score of Interface heuristic, ED is Educational Element heuristic, CN is Content heuristic, PL is Playability heuristic and MM is Multimedia heuristic. UsaECG refers to as the weighted mean and it can refer to an indicator for the overall usability of ECG. Each of these variables (IN, ED, CN, PL and MM) obtains the corresponding value when applying the next formula:

$$F(x) = (\sum H / \sum Ht) \times P \quad (2)$$

where, $\sum H$ is the summation of the severity scores for each sub-heuristic group, P is the percentage for the current group, and $\sum Ht$ represents the summation of the sub-heuristic group in the worst case (in the event that all severity ratings are 4).

TABLE 2: Percentage assigned for each sub-heuristic in UsaECG

Heuristic	Total Sub heuristic	Weight each sub heuristic	Weight each sub heuristic (%)
Interface (IN)	10	0.2703	27.03
Educational Element (ED)	6	0.1622	16.2
Content (CN)	6	0.1622	16.2
Playability (PL)	7	0.1892	18.92
Multimedia (MM)	8	0.2162	21.62
Total	37	1	100

The usability of educational computer games [usaECG(x)] gives an estimation of the degree or the level of critical usability problem found, namely, the value of the overall critical usability problem found of the educational computer games. In Table 2, function (1) and function (2) are derived from González *et al*. (2009), which we found as one of the promising attempt to quantitatively analyze the results of a usability evaluation based on the HE method. Function (2) was then modified in order to simplify the calculation.

EVALUATION PROCESS

There are six steps involved in the evaluation process. First, the experts were identified and contacted through email. The experts who agreed to join the evaluation process replied and they were provided with the URL of the evaluation system (AHP_HeGES). Then, the experts performed the evaluation based on the provided PHEG with the explanation on how to conduct the process. The experts identified usability problem and rated severity scale. Once the evaluation was completed, the admin was able to view the usability problems found (data) and then performed the analysis. Fig.1 below shows the flow of the said evaluation process.

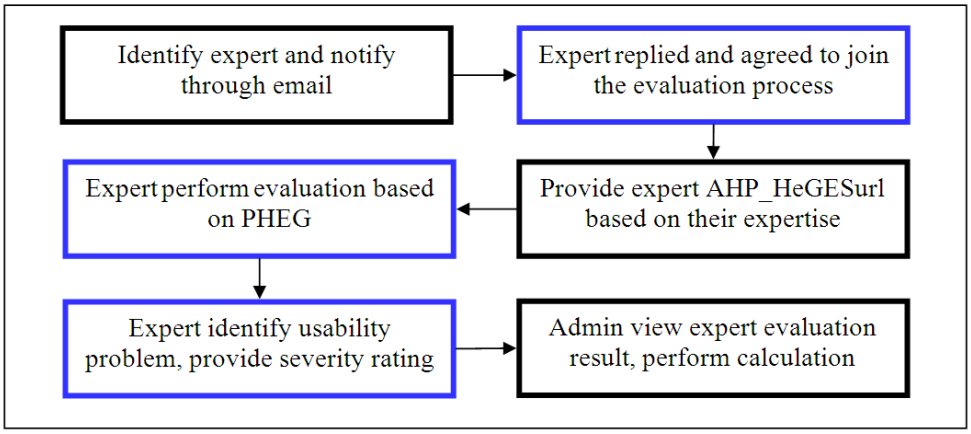

Fig.1: Evaluation flow (Source: Hasiah & Azizah, 2011b)

There were five expert evaluators involved in the process which consisted of a HCI expert, an educational element expert, a content expert, a playability expert (game developer) and a multimedia expert. The educational game used for the evaluation process was DatabaseFun game. Table 3 shows the profile of the experts involved and Table 4 presents the number of usability problems found by all the experts.

TABLE 3: Profile of Expert Evaluators

Expert Evaluators	Highest Qualification	Professional Role	Duties/course taught (relevant to this study)
IN	MSc	Senior lecturer in Science System	Experience in teaching HCI for the past 5 years
ED	MSc	Senior lecturer in Education faculty	Teaches Instructional Design and Technology
CN	MSc	Senior lecturer in System Science	Teaches Database for 3 years
PL	Bsc	Game developer	Has been involved in developing game for the past 3 years
MM	MSc	Senior lecturer in IT	Teaches multimedia for 4 years

TABLE 4: Usability Problems and Rating Found by Experts (Source: Hasiah & Azizah, 2011b)

Expert	Usability Problems	Severity Rating				
		4	3	2	1	0
IN	10	2	4	3	1	0
ED	8	3	2	1	1	1
CN	9	1	3	3	2	0
PL	8	3	2	2	0	1
MM	9	3	2	2	2	0

Extracting Result Analysis

Based on the results of usability problem found in Table 3, the calculation for ∑H, P and ∑Ht was conducted. Table 4 shows the calculation of ∑H, P and ∑Ht based on the usability problem found for each heuristic. ∑H is the summation of the severity scores for each sub-heuristic group, P is the percentage for the current group, and ∑Ht represents the summation of the whole group in the worst case (in the event that all ratings were 4). The usability problem found for the calculation purposes focused on the criticality of usability problem found, i.e. where severity score was 4. An example of the calculation on how the value of ∑H for expert IN is as follows:

$$\sum H = (4*2) + (3*4) + (2*3) + (1*1)$$
$$= 8 + 12 + 6 + 1$$
$$= 27$$

The example of the calculation on how the value of ∑Ht for expert IN is as follows:

$$\sum Ht = 4*2$$
$$= 8$$

The results in Table 4 represent the value for each heuristics; for example, F(IN) = (8/27) * 27.03 is F(IN) = 8.0089. The value of 29.63% represents the critical usability problem found in the interface for the ECG evaluated. In term of usability level, it was about 70%, which meant that it still could not be considered good, as mentioned by González *et al*. (2009), whereby the usability level could be considered as good when its value higher is than 80% and 100% or when all the sub-heuristics are fulfilled.

TABLE 5: Calculation for Each Heuristic

Expert	Usability Problems Found	Example of Calculation				
		∑H	∑Ht	P	F(x)	F(x)%
IN	10	27	8	27.03	8.0089	29.63
ED	8	21	12	16.2	9.2571	57.14
CN	9	21	12	16.2	9.2571	57.14
PL	8	22	4	18.92	3.4400	18.18
MM	9	24	12	21.62	10.8100	50.00
Mean (indicator)						42.42

Evaluation Results

The function for UsaECG (x) was used to calculate the overall critical usability problem found in the ECG evaluated.

$$UsaECG(x) = ((IN/0.2073) + (ED/0.1622) + (CN/0.1622) + (PL/0.1892) + (MM/0.2162)) / 5$$

Based on the function, UsaECG(x), the critical problem for each heuristic was calculated and presented in the form of a bar graph, as shown in Fig.2. Here, UsaECG(x) refers to weighted mean and it is an indicator for the overall usability of ECG.

$$UsaECG(x) = ((8.0089/0.2073) + (9.2571/0.1622) + (9.2571/0.1622) + 3.4400/0.1892) + (10.8100/0.2162)) / 5$$
$$UsaECG(x) = (29.63 + 54.14 + 57.14 + 18.18 + 50.00) / 5$$
$$UsaECG(x) = 42.42$$

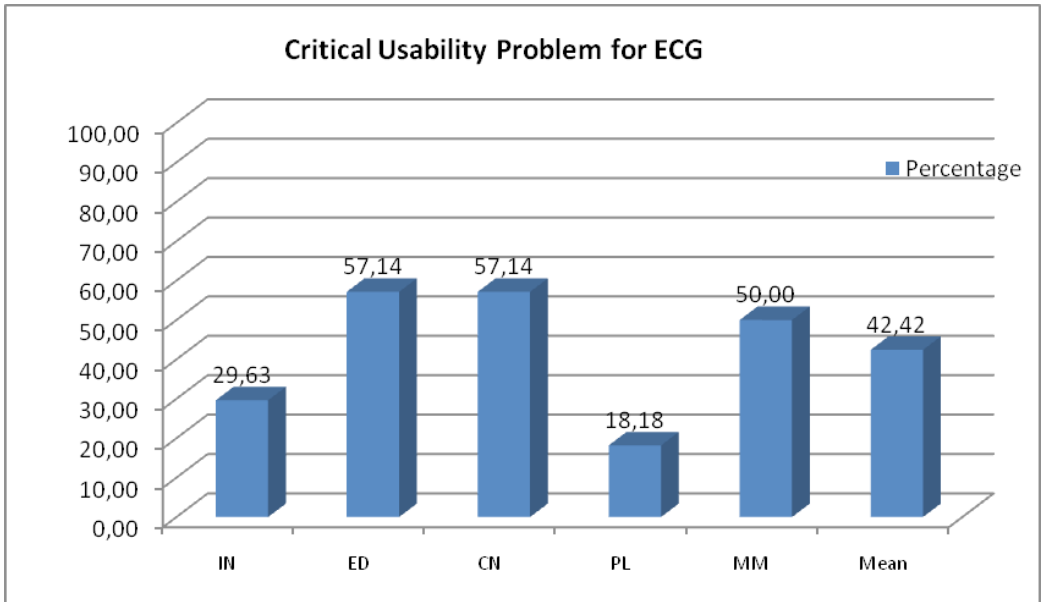

Fig.2: The Percentage of Critical Usability Problem for ECG

Fig.2 shows the percentage of the critical problem found for each heuristic. The most critical problem was found in Educational Element and Content heuristics, whereby there was 57.14% critical problems found for each heuristic. The least critical problem found was in Playability heuristic, whereby the value was 18.18%, indicating that in term of usability level for Playability, it is considered as good (González *et al*., 2009) because the value is 81.82%. Even though the usability level for Playability can be considered as good, there is a need to look in details for each usability problem found in order to help developers to improve ECG.

The mean value (42.42%) for the overall critical problem found in ECG represents an indicator for the overall usability level of ECG. Meanwhile, the overall result shown in Fig.3 should be able to help developers to grasp the idea on the part that needs to be improved accordingly. The Educational Element and Content heuristics need to be given priority in term of improvement, followed by Multimedia, Interface and Playability.

DISCUSSION

Usability problems found in most of the heuristic evaluation processes presented are based on severity rating. Several studies have presented severity rating based on the mean of severity scale, i.e. the value represents the score level of usability problems. In some cases, the mean value may not be accurate to represent the usability problems found. This is because the mean value will ignore the most critical problems found in specific part. One of the possible solutions to overcome this problem is by analyzing the numbers of severity rating for the critical problems found. The quantitative analysis for HE (González *et al*., 2009) was adapted as a basis of this analysis. Some modifications were done in order to simplify the analysis process. The function for UsaECG(x) and F(x) was used to help in the analysis of the data.

The number of the sub-heuristics for each heuristic was used in order to calculate the percentage for each heuristic. Based on the percentage presented, further calculation and function were developed. The values (%) for each critical problem found were extracted from the developed functions. This value should be able to help developers to simply get the results of the evaluation for the ECG that is still in the development process. The presentation of the results in the form of percentage is one of the distinctive results from this process. This will help game developers to shorten the process of analyzing the usability problem found.

CONCLUSION

Evaluating educational computer games using Playability Heuristic Evaluation for Educational Computer Games (PHEG) technique shows the ability of the new technique in identifying usability problems. Meanwhile, the involvement of expert evaluators demonstrates the numbers of usability problems found and the score of the usability problems. The new approach in analyzing critical usability problems found was introduced in order to fabricate more presentable results. The functions to calculate critical problems, based on the number of sub-heuristics, were created. The presentation of the critical usability problems should be able to help ECG developers to easily grab the most critical part that needs to be improved. This particular approach contributes to the body of knowledge in quantitatively analysing usability problems. The outcome of the analysis can be used to indicate the overall critical usability problems of educational computer games. Thus, a future study is suggested to be carried out on the evaluation processes involving expert evaluators (3 to 5) for each heuristic to detect more usability problems. The analysis process needs to take into consideration the number of problems found in term of its uniqueness. Based on the uniqueness of the problems, the overall critical problems can be calculated accurately.

REFERENCES

Allen, Mureen, Currie, Leanne M., Bakken, Suzanne, Patel, Vimla L., & Cimino, J. J. (2006). Heuristic evaluation of paper-based Web pages: A simplified inspection usability methodology. *Journal of Biomedical Informatics, 39*(4), 412-423.

González, M., Masip, L., Granollers, A., & Marta, O. (2009). Quantitative analysis in a heuristic evaluation experiment. *Advances in Engineering Software, 40*(12), 1271-1278.

Hasiah M.O. and Azizah J. (2010). *Challenges in the evaluation of educational computer games.* Paper presented at the International Symposium on Information Technology (ITSim), Kuala Lumpur, Malaysia.

Hasiah M. O., & Azizah J. (2011a). *Methodology to evaluate interface of educational computer game* Paper presented at the Pattern Analysis and Intelligent Robotics (ICPAIR), Kuala Lumpur, Malaysia.

Hasiah M. O., & Azizah J. (2011b). *Tools to Evaluate Usability of Educational Computer Game (UsaECG).* Paper presented at the 2nd International Conference on User Science and Engineering (i-USEr 2011), Kuala Lumpur, Malaysia.

Hvannberg, E. T., Law, E. L. -C., & Lárusdóttir, M. K. (2007). Heuristic evaluation: Comparing ways of finding and reporting usability problems. *Interacting with Computers, 19*(2), 225-240.

Kato, P. M. (2010). Video games in health care: Closing the gap. *Review of General Psychology, 14*(2), 113-121.

Kirmani, S. (2008). Heuristic Evaluation Quality Score (HEQS): Defining Heuristic Expertise. *Journal of Usability Studies, 4*(1), 49-59.

Nielsen, J. (1995). Severity ratings for usability problems Retrieved 15 February, 2012 from http://www.useit.com/papers/heuristic/severityrating.html.

Nielsen, J., & Molich, R. (1990). *Heuristic evaluation of user interfaces*. Paper presented at the Proceedings of the SIGCHI conference on Human factors in computing systems: Empowering people, Seattle, Washington, United States.

Papastergiou, M. (2009). Digital Game-Based Learning in high school Computer Science education: Impact on educational effectiveness and student motivation. *Computers & Education, 52*(1), 1-12.

Pinelle, D., Wong, N., Stach, T., & Gutwin, C. (2009). *Usability heuristics for networked multiplayer games*. Paper presented at the Proceedings of the ACM 2009 international conference on Supporting group work, Sanibel Island, Florida, USA.

Robertson, J., & Howells, C. (2008). Computer game design: Opportunities for successful learning. *Computers & Education, 50*(2), 559-578.

Ssemugabi, S., & Villiers, R. D. (2007). *A comparative study of two usability evaluation methods using a web-based e-learning application*. Paper presented at the Annual Research Conference of the South African institute of Computer Scientists and Information Technologists on IT Research in Developing Countries (SAICSIT), Port Elizabeth, South Africa.

Tan, W. -S, Liu, D., & Bishu, R. (2009). Web evaluation: Heuristic evaluation vs. user testing. *International Journal of Industrial Ergonomics, 39*(4), 621-627.

Yee L. E., Zah bte Wan Ali, Wan bt. Mahmud, Rosnaini, & Baki Roselan. (2010). Computer games development experience and appreciative learning approach for creative process enhancement. *Computers & Education, 55*(3), 1131-1144.

Pertanika J. Sci. & Technol. 21 (1): 261 - 272 (2013)

SCIENCE & TECHNOLOGY

Journal homepage: http://www.pertanika.upm.edu.my/

The Role of Similarity Measurement in an Agent-Based Supplier Selection Framework

Alireza Jahani*, Masrah Azrifah Azmi Murad, Md. Nasir Sulaiman and Hasan Selamat

Faculty of Computer Science and Information Technology, Universiti Putra Malaysia, 43400 Serdang, Selangor, Malaysia

ABSTRACT

Similarity measurement is a critical component in any case-based reasoning (CBR) system. CBR is a superior technique for solving new problems based on previous experiences. Main assumption in CBR relies on the hypothesis that states similar problems should have similar solutions. This paper describes a comparative analysis on several commonly used similarity measures (Canberra, Clark, and Normalized Euclidean distance) in retrieving phase of the case-based reasoning approach to facilitate supplier selection. In addition, the proposed agent-based supplier selection framework was designed to use customer's defined weights to evaluate the price, volume, quality grade, and delivery date of supply materials, and also provide them with alternative products which are closest to their first order if it was out of stock. Finally, based on the proposed framework, a numerical example of the used approach is illustrated.

Keywords: Supplier selection, intelligent agent, customer knowledge management, case based reasoning, similarity measures

INTRODUCTION

In general, knowledge management has been of interest to companies because they realize that it can contribute to their competitive advantage. Therefore, in emphasizing on knowledge as a key competitive factor in the global economy, these companies may be overlooking a major element, i.e. customer knowledge. This means the knowledge that a customer has about the issues that are related to the products or services that he is interested in buying. Since the firm has a better understanding of the customer's expectations and needs, it will be able to improve customer service and thus

Article history:
Received: 31 March 2012
Accepted: 1 September 2012

E-mail addresses:
jahani@fsktm.upm.edu.my (Alireza Jahani),
masrah@fsktm.upm.edu.my (Masrah Azrifah Azmi Murad),
nasir@fsktm.upm.edu.my (Md. Nasir Sulaiman),
hasan@fsktm.upm.edu.my (Hasan Selamat)
*Corresponding Author

ISSN: 0128-7680 © 2013 Universiti Putra Malaysia Press.

achieve customers' satisfaction and retention. Better relationships with the customer can lead to increased sales and then new customers (García-Murillo & Annabi, 2002).

A supply chain is a network of organizations and their associated activities like procurement, manufacturing and distribution that work together to produce value for customers (Wang *et al*., 2008). Competitive advantage in tomorrow's environment will go to those enterprises that can consistently anticipate and implement customer-winning supply chain competencies (Ross, 2003). On the other hand, selecting the suitable suppliers has influence on the short- and long-term profits or losses of companies which spend a significant amount of their time and money on purchasing parts. Various selection criteria, weighting methods, and intelligent models have been used to support the supplier selection of organizations (Chang-Joo & Chung-Hsing, 2011). However, the failure of coordination between manufacturers and suppliers results in excessive delays and ultimately leads to poor customer services (Lee *et al*., 2001). Then, there is a need for an automated and integrated system framework. This paper aims to present such a framework for cooperation and information exchange that can receive orders and preferences from customers, generate production plans and material requirement specifications, check the inventory, make a build or buy decision, call suppliers for proposals, as well as receive and evaluate material offers, select the best suppliers, negotiate with them, and satisfy the requirements of the negotiating parties. These can be useful for all the stakeholders, especially customers who are more crucial for any company's survival.

RELATED WORK

The benefits of adopting agent technology in SCM (Supply Chain Management) systems have been recognized in an increasingly wide variety of applications. The agent technology facilitates the integration of the entire supply chain as a networked system of independent echelons (Gjerdrum *et al*., 2001). Agents are also capable of solving the problem of matching supply to demand and carrying out information exchange, uncertainty resolution, and preferences revision (Blecker & Graf, 2003). Due to the large amount of data collected and it is hard to remember every customer's preferences, agents can play a key role to collect and analyze this information, and then customers could be recognized later and presented by a series of alternatives that suit their preferences (García-Murillo & Annabi, 2002).

A number of researchers have attempted to apply agent technology to manufacturing integration, supply sourcing, supply chain management, negotiation, information transfer and knowledge sharing within a supply chain. Among other, Saad *et al*. (1995) proposed a Production Reservation approach by using a bidding mechanism based on the Contract Net protocol to generate production plan and schedule. Meanwhile, Barbuceanu and Fox (1997) proposed organizing supply chain as a network of cooperating agents, each performing one or more supply chain functions and coordinating their actions with other agents (Barbuceanu and Fox, 1997). Maturana *et al*. (1999) developed a hybrid agent-based mediator-centric Framework, called MetaMorph, to integrate partners, suppliers and customers dynamically with the main enterprise via the Internet and Intranets (Maturana *et al*., 1999). Min and Bjornsson (2000) presented a conceptual model of agent-based supply chain automation, in which a project agent gathers actual construction progress information and sends them to subcontractor

agents and supplier agents, respectively, over the Internet (Min and Bjornsson, 2000). Jiao *et al*. applied multi-agent paradigm to collaborative multi-contract negotiation in a global manufacturing supply chain (Jiao *et al*., 2006). Wentao designed an agent-based negotiation model for the sourcing of construction supplies based on a new parallel bargaining protocol and Bayesian learning model (Wentao, 2008).

Typically, supplier selection is a multi-criteria decision problem (Weber *et al*., 1991; Ghodsypour & O'Brien, 1998). The suggested methods in the related literature can be classified into two categories, namely, mathematical programming models and weighting models. The mathematical programming model has a problem in dealing with qualitative criteria that are very important in decision making (Ghodsypour & O'Brien, 1998). Chang and Chung (2011) developed a multi-criteria decision making (MCDM) model for a manufacturing company to select suppliers based on customer order dependent weighting method to determine the weights of the supplier selection criteria. This was achieved by modelling the relationship between the customer order factors and supplier selection criteria, using a knowledge base with if-then rules (Chang-Joo & Chung-Hsing, 2011).

However, most of the above works have not applied the case based on reasoning method with customers' defined weights in the supplier selection and find alternative supplies due to the stock out. Failure to account for that may either lead to unsatisfied customer demand and loss of market share. Therefore, in order to keep customers and the multi-criteria decision making nature of supplier selection, first, this paper aims to present an agent-based supply chain framework in support of selecting the best suppliers by means of the proposed case-based reasoning approach. CBR is in the subset of weighting models. This framework is going to evaluate material offers, negotiate with suppliers and customers on the price and terms of quotation in the negotiation process and make successful agreements with the final supplier. In addition, this framework also wants to take into consideration customers' knowledge and provide them with alternative supplies, which are closest to their first order, if the manufacturer is unable to supply it. Then, the performance of the supplier's selection process will be improved to reach a real "win-win" situation and the mentioned problems like unsatisfied customers and then losing them can be reduced.

AN AGENT-BASED SUPPLY SELECTION FRAMEWORK

The proposed agent-based supply chain framework can generate a flexible, reconfigurable and coordinated approach for supplier selection process, both across enterprises and within an enterprise. In this framework, there is a FIPA-compliant (The Foundation for Intelligent Physical Agents) multi-agent system composed of a seller agent, a design agent, a procurement agent, a buyer agent, and a case-base for keeping suppliers records. Each agent performs one or more supply chain functions independently and coordinates its actions with other agents. This framework is illustrated in Fig.1 and the major components of the proposed framework are described below. Besides in this section, the order management and the supplier selection mechanism, along with Case-Based Reasoning (CBR) approach, will be defined later.

Seller agent provides an intelligent interface for the customers to place their personal orders. It is responsible for acquiring orders and preferences' weights from customers, handling order

modification or cancellation. *Design agent* is responsible to gather all the incoming orders from the seller agent and eliciting relevant information regarding customer's preferences. Another task of this agent is product planning and placing Material Requirement Specification (MRS) into case structures and also sending them to *Procurement agent* and receives offers from it. *The Procurement agent* decomposes MRS into specific categories to generate and advertise Call For Proposals (CFP) through the *Buyer agent* as an intelligent interface to all the potential suppliers. Buyer agent is responsible for the general negotiation process that is divided into three consecutive phases: inviting, bidding and awarding. Whenever an order comes to a buyer agent, it invites potential suppliers to bid by sending a CFP to seller agents of suppliers. Then, it will collect and evaluate all the bids based on *Suppliers' Case-Base* and choose the one with maximal utility as a winner, and thus the winner supplier is awarded the contract. A few rounds of conversation may take place, where several proposals and counter-proposals are exchanged. The negotiation will end when one party accepts or rejects the other party's proposal, or when any party terminates the negotiation process on its own (Jiao *et al*., 2006). *Suppliers' Case-Base* keeps supplier information files as cases and gathers information on the past and new suppliers in order to identify alternative suppliers. This information includes the name of each supplier, a list of the available materials and their attributes, the supplier's delivery history, the supplier's quality records, the supplier's overall desirability, and general information about the supplier's plant and management.

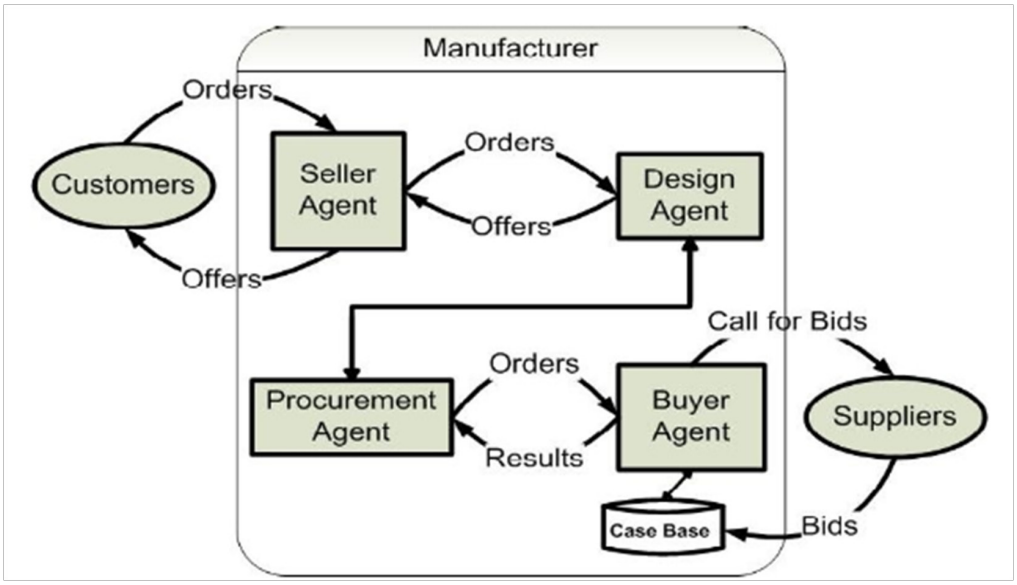

Fig.1: Multi-agent based supply chain framework

Order Management and the Supplier Selection Mechanism

Here, the major activities of the proposed framework are briefly described for a better understanding:

1. The customer places an order through the seller agent to the design agent.
2. The design agent will formulate the MRS and make a case structure of CBR approach for the ordered product and then send it to the procurement agent.
3. The Procurement agent checks the inventory regarding stocked finished products and raw materials based on the MRS structure. If the stock has enough resources, then there is no need for supplying.
4. Otherwise, the procurement agent must manage supplying sufficient raw materials from the suppliers.
5. The procurement agent advertises its outgoing orders with CFPs through the buyer agent for all the potential suppliers.
6. After receiving the CFPs, the potential suppliers make the decision of bidding and then bid on the case base of buyer agent.
7. After receiving all the bids, the buyer agent will evaluate the suppliers in consideration of price, due date, quality grade, volume, and so on, and then choose the most suitable suppliers.
8. If some or all supply materials of the customer's first order are found during the supplying process, the procurement agent will try to generate alternative product recommendations based on the received bids and offer them to the customers.
9. If the customer accepts the new offer, the buyer agent will then choose the suppliers who bid the alternative product's materials.
10. The buyer agent proclaims the award of bid and gives necessary replies to the un-chosen suppliers.
11. The supplier who has won the bid carries out manufacturing to fulfil the incoming orders.
12. The supplier delivers its finished products to the manufacturer.

Case-Based Reasoning (CBR) Approach

One of the most important contributions of this paper is that it shows how buyer agents can check orders with received bids from its associated case-based and responds to requests from the procurement agent. After receiving all the bids and storing them in the case base, the buyer agent retrieves from the case base cases that are identical or at least most similar due to the features of the new order's case. According to Maturana *et al*. (1999), the process of CBR strategy includes four steps (retrieve, reuse, revise and retain), which constitute the CBR cycle but the revised and retrained steps are not inculded in the scope of this paper. However, before the cycle can be run, another step, case description, should also be performed for both case base construction and application of case knowledge. Here are the explanations for each step that starts with Case Description:

1) Case Description: The CBR mechanism starts with the description of a new order which corresponds to a new case. Case description concerns with deciding what contents

are to be stored in a case. It is important for the new case to be adequately described so that the retrieval of appropriate previous or newcomer's cases from the case base is possible. By considering order constraints which contain MRSs for ordered products, this research adopts the case structure as shown in Table 1 to describe each case. Product ID numbers, a certain product for its own and required materials; Product name indicates the name of the product; Price indicates the offered price to customers or suggested by customers in an incoming order; Volume shows the requested quantity of ordered products from customers or bidding quantity from suppliers; Quality Grade specifies the requested quality for each material; Delivery Time is the requested time by customer for each order. For suppliers, it indicates the possible delivery time for their bids.

TABLE 1: Case structure and content

Case Attribute	Attribute Value
Product ID	Integer, from 01 to n
Product name	text
Price	Integer, from 1 to n
Volume	Integer, from 1 to n
Quality Grade	Integer, from 1 to 5
Delivery Time	Integer, number of days

2) Case Retrieval: Case retrieval is finding the most similar case from the case base according to the features of a new case. A CBR method seriously depends on this step to find the order's matches of incoming bids from suppliers. There are numerous similarity measures in use today. While different similarity measure employs different algorithms, they have basically the same in functionality, and these are to take two objects as input and output as a measure of their similarity. The existence of many similarity measures does not always give a clear choice of an appropriate measure for a particular application domain. Hence, it is often convenient to be able to experiment with different measures before a final version is decided upon (Long *et al.*, 2004).

In this paper, three similarity measures (namely, Canberra, Clark, and Normalized Euclidean distance) were used as similarity functions in the nearest neighbour algorithm, one of the widely used methods to identify the similarity between cases employed here to perform the retrieval task. For the nearest neighbour algorithm, the similarity of two cases was calculated according to (1), as follows:

$$similarity(O,S) = \frac{\sum_{i=1}^{n} w_i \times sim(O_i, S_i)}{\sum_{i=1}^{n} w_i} \quad (1)$$

In (1), *O* is the new order, *S* is the incoming bid from the suppliers, O_i and S_i are the features *i* of *O* and *S,* respectively, w_i is the weight of feature *i*, and $sim(O_i, S_i)$ is the similarity function of the feature *i*. The value of $sim(O_i, S_i)$ is calculated in three different ways; the normalized absolute difference of the individual level is called Canberra in the equation (3), the squared root of half of the divergence is called Clark in the equation (3), and Normalized Euclidean distance in the equation (4):

Canberra:

$$sim(O_i, S_i) = 1 - \frac{\left|O_{i_k} - S_{i_k}\right|}{\left|O_{i_k} + S_{i_k}\right|} \tag{2}$$

Clark:

$$sim(O_i, S_i) = 1 - \frac{\left|O_{i_k} - S_{i_k}\right|^2}{\left|O_{i_k} + S_{i_k}\right|^2} \tag{3}$$

Normalized Euclidean:

$$sim(O_i, S_i) = 1 - \sqrt{\sum_{k=1}^{m} \frac{\left(O_{i_k} - S_{i_k}\right)^2}{\sigma^2}} \tag{4}$$

The weights of the features, which have been obtained from the customers, are applied to select the closest suppliers' bid to the customer's order. The role of the supplier selection mechanism is to calculate the similarity of each feature of the bids during the supplier selection and also to rank the alternative suppliers.

3) Case Reuse: Once the same case or the most similar case to the incoming order is selected from the received bids, it will then be offered to the customer. For the same cases, the suggested case can be reused by direct copy. However, for most situations that have different values in their attributes, the seller agent can offer the retrieved case as an alternative to the customer who can either accept or reject it.

CASE STUDY

In order to illustrate the proposed method of this paper, the case study of Moxober, a leading mobile phone manufacturing company in Finland (which has also been used by Jiao *et al*., 2006) was also used for the current work. Fig.2 shows Moxober's product structure at three levels: component arts, subassemblies and the final product. Nearly all the components parts

were produced by Moxober, but with the development of global economy and booming telecommunication market, it has changed to a global manufacturing strategy focusing on key technologies and its core competency while outsourcing major component manufacturing activities, such as the manufacturing of peripherals like batteries and chargers, memory chips and LCD panels.

In Moxober's supply chain network, customers and suppliers are spread worldwide. The mobile phone company plays the role of the manufacturer. Its direct suppliers, which are labelled as Supplier I, provide resources like software, PCB (Printed Circuit Board), LCD (Liquid Crystal Display), cover and peripheral. Its suppliers' suppliers (which are labelled as Supplier II) provided sub-resources like chip, board, interface, charger, and battery to the corresponding Supplier I. The next issue is to determine a specific configuration of the global manufacturing supply chain network for each individual customer order of a particular product model.

In this paper, the operation of this specific supply chain network is analysed by means of an agent-based supply chain framework and giving a numerical example for using CBR in the supplier selection process. In fact, actual employment of a supplier should be consistent with the product fulfilment process of a specific customer's order to achieve customers' satisfaction.

Now, suppose a customer's order is from Wenzhou China. This customer places his order through the seller agent of the mobile phone company. Through interaction, the customer can configure various ordering parameters such as product features like quality grade, quantity, price, and delivery date. The order information then goes to the design agent for product planning and determining a set of MRSs for each order along with the defined constraints. Then, the MRSs will be organized into three case structures for LCD, Cover and Peripheral, and then forwarded to the procurement Agent.

In order to accelerate the delivery, the procurement agent decides to allocate the final assembly of this order to the Xiamen plant in China - a process which involves the requirement specification of three material types, namely, LCD, Charger and Battery. The software design and PCB assembly operations are still held in Finland. The buyer agent will broadcast the material requirements to the potential suppliers who will bid on the platform of this agent to win the supplier selection procedure.

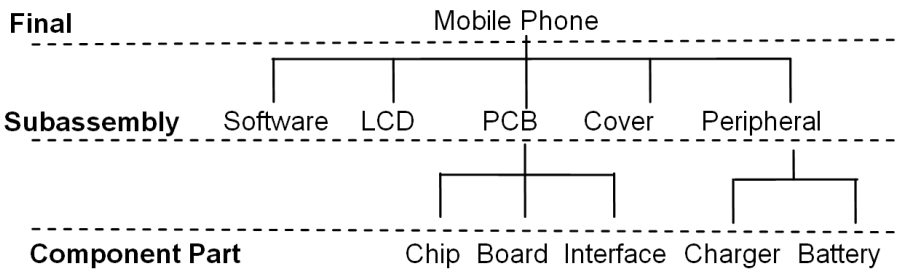

Fig.2: The BOM structures of Moxober mobile phones (Jiao *et al*., 2006)

Since that customer defines the range for his order, the best values which are the highest for attributes like volume and quality and the lowest for attributes like price and delivery date were used to find more suitable alternative products. For example, the best values of the price, volume, quality, and delivery date for MRS1 are:

$$\text{Order}_{\text{high}} = (01;013;\text{Charger};20;\&800;5;20)$$

Table 2 shows the case structure of an incoming order (ID=#13) related to MRSs, in addition to the defined weight by the customer for each attribute.

TABLE 2: Case structure values

Case Attribute	MRS1	MRS2	MRS3	W
Product ID	O1;013	02;013	03;013	-
Product name	Charger	Battery	LCD	-
Price	20-30	50-80	100-120	2
Volume	600-800	1200-1600	1000	4
Quality Grade	3-5	2-4	4-5	5
Delivery Date	20	15	12	4

Table 3 shows all the incoming bids received from the suppliers and the offered values for each attribute, including price, volume, quality, and delivery date.

TABLE 3: Incoming Bids

MRS	Bid	Volume	Price	Due Date	Quality Grade
MRS 1 Charger	Bid11:Supplier01	800	20	20	5
	Bid12:Supplier02	1000	25	18	4
	Bid13:Supplier03	800	20	18	3
MRS 2 Battery	Bid21:Supplier04	1000	65	22	4
	Bid22:Supplier05	1400	70	10	4
	Bid23:Supplier06	2000	45	18	3
MRS 3 LCD	Bid31:Supplier07	1000	120	11	5
	Bid32:Supplier08	1200	100	10	4
	Bid33:Supplier09	900	90	15	3

Now, for the nearest neighbour algorithm, which is used to find the most similar bid, and the similarity of highest values of orders with each bid are calculated as follows. For example, the similarity of order 1 and supplier 1's bid for MRS1 are:

$$sim_{price}(O_{1_{High}}, S_1) = 1 - \left|\frac{20-30}{|20|+|30|}\right| = 0.8 \qquad sim_{volume}(O_{1_{High}}, S_1) = 1 - \left|\frac{800-800}{|800|+|800|}\right| = 1,$$

$$sim_{quality}(O_{1_{High}}, S_1) = 1 - \left|\frac{5-5}{|5|+|5|}\right| = 1 \qquad sim_{delivery-date}(O_{1_{High}}, S_1) = 1 - \left|\frac{20-20}{|20|+|20|}\right| = 1,$$

$$Similarity(O_{1_{High}}, S_1) = \frac{(0.8\times 2)+(1\times 4)+(1\times 5)+(1\times 4)}{2+4+5+4} = 0.973$$

Table 4 shows all the results of similarity function calculations for the highest values of the received orders and suppliers' bids for each MRS. The weight of each attribute is assumed to be both equal to 1 and with various weights from 1 to 5 for each attribute.

TABLE 4: The overall similarity function results

MRS	Bids	Utility (Jiao *et al*., 2006)	W=1			W=1-5		
			Canberra	Clark	Euclidean	Canberra	Clark	Euclidean
MRS 1 Charger	Bid01	0.68	0.922	0.986	-1	0.943	0.991	0.434
	Bid02	0.73	0.936	0.993	-1.499	0.936	0.993	0.037
	Bid03	0.75	0.846	0.970	-1.828	0.846	0.969	-0.414
MRS 2 Battery	Bid04	0.65	0.868	0.974	-1.499	0.872	0.974	0.058
	Bid05	0.72	0.916	0.987	-1.499	0.919	0.987	0.058
	Bid06	0.69	0.843	0.969	-1.828	0.843	0.976	-0.414
MRS 3 LCD	Bid07	0.77	0.989	0.999	-0.414	0.988	0.999	0.623
	Bid08	0.71	0.903	0.990	-1.828	0.902	0.989	-0.414
	Bid09	0.69	0.873	0.975	-1.828	0.870	0.971	-0.414

The results show that the weighted attributes do not play an important role in the awarding process of three similarity measures and the satisfaction of the MRS constraints. For instance, if w=1, the bid of supplier 2 with the highest similarity for MRS1 would be selected in both the Canberra and Clark measures and supplier 1 is selected in Normalized Euclidean distance measure. The only exception in the awarding process is for Canberra similarity measure when different weights are applied. Table 5 lists the winners of the awarding process in comparison to (Jiao *et al*., 2006) the utility values for each MRS. In Jiao *et al*. (2006) for MRS, S1 was selected; however in this paper, S2 is selected due to the proposed mechanism and considering the different weights for different attributes.

TABLE 5: Winners

MRS	Utility (Jiao *et al*., 2006)	W=1			W=1-5		
		Canberra	Clark	Euclidean	Canberra	Clark	Euclidean
MRS 1 Charger	S3	S2	S2	S1	S1	S2	S1
MRS 2 Battery	S5	S5	S5	S4, S5	S5	S5	S4, S5
MRS 3 LCD	S7	S7	S7	S7	S7	S7	S7

CONCLUSION

This paper presents an agent-based Supply Chain framework for supplier selection by considering the influence of different similarity measures in case-based reasoning process. The process involved selecting the best suppliers using the CBR method to match incoming orders with those of the received bids from the suppliers. In the proposed framework, customer orders have various weights in the CBR approach. Sometimes, the manufacturer is unable to supply and to provide their customers' first order. Therefore, the main contribution of this research is to take the customers' preferences into consideration and to provide them with alternatives which are most similar to their first order from various suppliers. The second contribution is to use the CBR approach in finding the most similar alternatives by using three different similarity measures, namely, Canberra, Clark, and Normalized Euclidean distance. During the ordering process, customers can define the features' importance of their orders by weight. Hence, in the case retrieval level, these weights can help to find the most similar bids and offer alternative products to the customers based on their desires. The results of the numerical example show that the proposed approach is robust enough to find the closest bid to the received order and rewards the winner supplier. The improvement and development of the prototype of the proposed framework should be submitted to further studies.

REFERENCES

Barbuceanu, M., & Fox, M. S. (1997). *Integrating communicative action, conversations and decision theory to coordinate agents*. Paper presented in AAMAS-97, 1997 Marina del Rey (pp. 49 - 58). California, United States. 267667: ACM.

Blecker, T., & Graf, G. (2003). Multi agent systems in internet based production environments—an enabling infrastructure for mass customization. In F.T. Piller, R. Reichwald, & M. Tseng (Eds). MCPC 2003, 2003. Munich.

Chang-Joo, Y., & Chung-Hsing, Y. (2011). *Customer order dependent supplier selection*. Paper presented in ICNIT (pp. 57-62), 21-23 June 2011.

Garcia-Murillo, M., & Annabi, H. (2002). Customer Knowledge Management. *The Journal of the Operational Research Society, 53,* 875-884.

Ghodsypour, S. H., & O'Brien, C. (1998). A decision support system for supplier selection using an integrated analytic hierarchy process and linear programming. *International Journal of Production Economics,* 56-57, 199-212.

Gjerdrum, J., Shah, N., & Papageorgiou, L. G. (2001). A combined optimization and agent-based

approach to supply chain modelling and performance assessment. *Production Planning & Control: The Management of Operations, 12***,** 81 - 88.

Jiao, J., You, X., & Kumar, A. (2006). An agent-based framework for collaborative negotiation in the global manufacturing supply chain network. *Robotics and Computer-Integrated Manufacturing, 22***,** 239-255.

Lee, E. -K., Ha, S., & Kim, S. -K. (2001). Supplier selection and management system considering relationships in supply chain management. *Engineering Management, IEEE Transactions, 48***,** 307-318.

Long, J., Stoecklin, S., Schwartz, D. G., & Patel, M. (2004). *Adaptive similarity metrics in case-based reasoning*. Paper presented in the 6th IASTED International Conference on Intelligent Systems and Control, 260-265.

Maturana, F., Shen, W., & Norrie, D. H. (1999). MetaMorph: an adaptive agent-based architecture for intelligent manufacturing. *International Journal of Production Research, 37*, 2159 - 2173.

MIN, J. U., & Bjornsson, H. (2000). *Agent based supply chain management automation*. Paper presented in ICCCBE-VIII (pp. 1001-1006). Stanford University, California, USA.

Ross, D. F. (2003). *Introduction to e-supply chain management: engaging technology to build market-winning business partnerships.* St. Lucie Press.

Saad, A., Kawamura, K., & Biswas, G. (1995). *Performance evaluation of contract net-based heterarchical scheduling for flexible manufacturing systems*. Paper presented in IJCAI-95 (pp. 310-321). Montreal, Canada.

Wand, M., Liu, J., Wang, H., Cheung, W. K., & Xie, X. (2008). On-demand e-supply chain integration: A multi-agent constraint-based approach. *Expert Systems with Applications, 34***,** 2683-2692.

Weber, C. A., Current, J. R., & Benton, W. C. (1991). Vendor selection criteria and methods. *European Journal of Operational Research, 50,* 2-18.

Wentao, L. (2008). *An Agent-Based Negotiation Model for the Sourcing Of the Condtruction Suppliers* (Doctoral thesis dissertation). The University of Hong Kong.

REFEREES FOR THE PERTANIKA
JOURNAL OF SCIENCE AND TECHNOLOGY

VOL. 21(1) JAN. 2013

The Editorial Board of the Journal of Tropical Agricultural Science wishes to thank the following for acting as referees for manuscripts published in this issue of JST.

Abdul Aziz Abdul Rahman
(UM, Malaysia)

Abdul Razak Daud
(UKM, Malaysia)

Adem Kilicman
(UPM, Malaysia)

Aida Mustapha
(UPM, Malaysia)

Alfian Abdul Halin
(UPM, Malaysia)

Anuar Kassim
(UPM, Malaysia)

Azlina Harun@ Kamaruddin
(USM, Malaysia)

Barkawi Sahari
(UPM, Malaysia)

Chukwu Ogbonnaya
(Federal University of Technology, Nigeria)

Evi Indriasari Mansor
(UPM, Malaysia)

Fatimah Khalid
(UPM, Malaysia)

Hailiza Kamarulhaili
(USM, Malaysia)

Hakim S. Sultan Aljibori
(UM, Malaysia)

Hazizan Md Akil
(USM, Malaysia)

Hazura Zulzalil
(UPM, Malaysia)

Ibrahim Abu Talib
(UKM, Malaysia)

Kamaruzzaman Yunus
(IIUM, Malaysia)

Lili Nurliyana Abdullah
(UPM, Malaysia)

Lilly Suriani Affendey
(UPM, Malaysia)

Lim Kean Pah
(UPM, Malaysia)

M. Abdul Maleque
(MMU, Malaysia)

Maisarah Ali
(IIUM, Malaysia)

Mar Yah Said
(UPM, Malaysia)

Mas Rina Mustaffa
(UPM, Malaysia)

Masrah Azrifah Azmi Murad
(UPM, Malaysia)

Mohamad Rushdan Md Said
(UPM, Malaysia)

Mohamed Abd Rahman
(UPM, Malaysia)

Mohamed Ansari M. Nainar
(UNITEN, Malaysia)

Mohd Sapuan Salit
(UPM, Malaysia)

Muhammad Sayuti Fadhil
(Universitas Malikussaleh, Indonesia)

Noraini Che Pa
(UPM, Malaysia)

Norhayati Mohd Ali
(UPM, Malaysia)

Novia Admodisastro
(UPM, Malaysia)

Oon Shea Ming
(UM, Malaysia)

Pathiah Abdul Samat
(UPM, Malaysia)

Puteri Suhaiza Sulaiman
(UPM, Malaysia)

Risby Mohd Sohaimi
(UPNM, Malaysia)

Rodziah Atan
(UPM, Malaysia)

Sa'adah Hassan
(UPM, Malaysia)

Sahari Japar
(UPM, Malaysia)

Salmi Baharom
(UPM, Malaysia)

Shamala Subramaniam
(UPM, Malaysia)

Sharifah Md Yasin
(UPM, Malaysia)

Takaomi Arai
(UPM, Malaysia)

Tey Beng Ti
(UPM, Malaysia)

Wan Ramli Wan Daud
(UKM, Malaysia)

Zulkarnain Zainal
(UPM, Malaysia)

UPM- Universiti Putra Malaysia
UKM- Universiti Kebangsaan Malaysia
USM- Universiti Sains Malaysia
UM- Universiti Malaya

IIUM- International Islamic University of Malaysia
UPNM- Universiti Pertahanan Nasional Malaysia
UNITEN- Universiti Tenaga Nasional
MMU- Multimedia University

Special Acknowledgement

The **JST Editorial Board** gratefully *acknowledges* the assistance of **Doreen Dillah**, who served as the English language editor for this issue.

While every effort has been made to include a complete list of referees for the period stated above, however if any name(s) have been omitted unintentionally or spelt incorrectly, please notify the Executive Editor, *Pertanika* Journals at nayan@upm.my.

Any inclusion or exclusion of name(s) on this page does not commit the *Pertanika* Editorial Office, nor the UPM Press or the University to provide any liability for whatsoever reason.

Pertanika

Our goal is to bring high quality research to the widest possible audience

Journal of Science & Technology

INSTRUCTIONS TO AUTHORS

(Manuscript Preparation & Submission Guidelines)

Revised: July 2012

We aim for excellence, sustained by a responsible and professional approach to journal publishing. We value and support our authors in the research community.

Please read the guidelines and follow these instructions carefully; doing so will ensure that the publication of your manuscript is as rapid and efficient as possible. The Editorial Board reserves the right to return manuscripts that are not prepared in accordance with these guidelines.

About the Journal

Pertanika is an international peer-reviewed journal devoted to the publication of original papers, and it serves as a forum for practical approaches to improving quality in issues pertaining to tropical agriculture and its related fields. *Pertanika* began publication in 1978 as Journal of Tropical Agricultural Science. In 1992, a decision was made to streamline *Pertanika* into three journals to meet the need for specialised journals in areas of study aligned with the interdisciplinary strengths of the university. The revamped Journal of Science and Technology (JST) is now focusing on research in science and engineering, and its related fields. Other *Pertanika* series include Journal of Tropical Agricultural Science (JTAS); and Journal of Social Sciences and Humanities (JSSH).

JST is published in **English** and it is open to authors around the world regardless of the nationality. It is currently published two times a year i.e. in **January** and **July**.

Goal of *Pertanika*

Our goal is to bring the highest quality research to the widest possible audience.

Quality

We aim for excellence, sustained by a responsible and professional approach to journal publishing. Submissions are guaranteed to receive a decision within 12 weeks. The elapsed time from submission to publication for the articles averages 5-6 months.

Indexing of *Pertanika*

Pertanika is now over 33 years old; this accumulated knowledge has resulted in Pertanika journals being indexed in SCOPUS (Elsevier), EBSCO, DOAJ, AGRICOLA, and CABI etc. JST is indexed in SCOPUS, EBSCO, DOAJ, ISC and ERA .

Future vision

We are continuously improving access to our journal archives, content, and research services. We have the drive to realise exciting new horizons that will benefit not only the academic community, but society itself.

We also have views on the future of our journals. The emergence of the online medium as the predominant vehicle for the 'consumption' and distribution of much academic research will be the ultimate instrument in the dissemination of the research news to our scientists and readers.

Aims and Scope

Pertanika Journal of Science and Technology aims to provide a forum for high quality research related to science and engineering research. Areas relevant to the scope of the journal include: *bioinformatics, bioscience, biotechnology and bio-molecular sciences, chemistry, computer science, ecology, engineering, engineering design, environmental control and management, mathematics and statistics, medicine and health sciences, nanotechnology, physics, safety and emergency management*, and related fields of study.

Editorial Statement

Pertanika is the official journal of Universiti Putra Malaysia. The abbreviation for *Pertanika* Journal of Science & Technology is *Pertanika J. Sci. Technol.*

Guidelines for Authors

Publication policies

Pertanika policy prohibits an author from submitting the same manuscript for concurrent consideration by two or more publications. It prohibits as well publication of any manuscript that has already been published either in whole or substantial part elsewhere. It also does not permit publication of manuscript that has been published in full in Proceedings. Please refer to Pertanika's **Code of Ethics** for full details.

Editorial process

Authors are notified on receipt of a manuscript and upon the editorial decision regarding publication.

Manuscript review: Manuscripts deemed suitable for publication are sent to the Editorial Board members and/or other reviewers. We encourage authors to suggest the names of possible reviewers. Notification of the editorial decision is usually provided within to eight to ten weeks from the receipt of manuscript. Publication of solicited manuscripts is not guaranteed. In most cases, manuscripts are accepted conditionally, pending an author's revision of the material.

Author approval: Authors are responsible for all statements in articles, including changes made by editors. The liaison author must be available for consultation with an editor of *The Journal* to answer questions during the editorial process and to approve the edited copy. Authors receive edited typescript (not galley proofs) for final approval. Changes **cannot** be made to the copy after the edited version has been approved.

Manuscript preparation

Pertanika accepts submission of mainly four types of manuscripts. Each manuscript is classified as **regular** or **original** articles, **short communications**, **reviews**, and proposals for **special issues**. Articles must be in **English** and they must be competently written and argued in clear and concise grammatical English. Acceptable English usage and syntax are expected. Do not use slang, jargon, or obscure abbreviations or phrasing. Metric measurement is preferred; equivalent English measurement may be included in parentheses. Always provide the complete form of an acronym/abbreviation the first time it is presented in the text. Contributors are strongly recommended to have the manuscript checked by a colleague with ample experience in writing English manuscripts or an English language editor.

Linguistically hopeless manuscripts will be rejected straightaway (e.g., when the language is so poor that one cannot be sure of what the authors really mean). This process, taken by authors before submission, will greatly facilitate reviewing, and thus publication if the content is acceptable.

The instructions for authors must be followed. Manuscripts not adhering to the instructions will be returned for revision without review. Authors should prepare manuscripts according to the guidelines of *Pertanika*.

1. Regular article

Definition: Full-length original empirical investigations, consisting of introduction, materials and methods, results and discussion, conclusions. Original work must provide references and an explanation on research findings that contain new and significant findings.

Size: Should not exceed 5000 words or 8-10 printed pages (excluding the abstract, references, tables and/or figures). One printed page is roughly equivalent to 3 type-written pages.

2. Short communications

Definition: Significant new information to readers of the Journal in a short but complete form. It is suitable for the publication of technical advance, bioinformatics or insightful findings of plant and animal development and function.

Size: Should not exceed 2000 words or 4 printed pages, is intended for rapid publication. They are not intended for publishing preliminary results or to be a reduced version of Regular Papers or Rapid Papers.

3. Review article

Definition: Critical evaluation of materials about current research that had already been published by organizing, integrating, and evaluating previously published materials. Re-analyses as meta-analysis and systemic reviews are encouraged. Review articles should aim to provide systemic overviews, evaluations and interpretations of research in a given field.

Size: Should not exceed 4000 words or 7-8 printed pages.

4. Special issues

Definition: Usually papers from research presented at a conference, seminar, congress or a symposium.

Size: Should not exceed 5000 words or 8-10 printed pages.

5. Others

Definition: Brief reports, case studies, comments, Letters to the Editor, and replies on previously published articles may be considered.

Size: Should not exceed 2000 words or up to 4 printed pages.

With few exceptions, original manuscripts should not exceed the recommended length of 6 printed pages (about 18 typed pages, double-spaced and in 12-point font, tables and figures included). Printing is expensive, and, for the Journal, postage doubles when an issue exceeds 80 pages. You can understand then that there is little room for flexibility.

Long articles reduce the Journal's possibility to accept other high-quality contributions because of its 80-page restriction. We would like to publish as many good studies as possible, not only a few lengthy ones. (And, who reads overly long articles anyway?) Therefore, in our competition, short and concise manuscripts have a definite advantage.

Format

The paper should be formatted in one column format with at least 4cm margins and 1.5 line spacing throughout. Authors are advised to use Times New Roman 12-point font. Be especially careful when you are inserting special characters, as those inserted in different fonts may be replaced by different characters when converted to PDF files. It is well known that 'μ' will be replaced by other characters when fonts such as 'Symbol' or 'Mincho' are used.

A maximum of eight keywords should be indicated below the abstract to describe the contents of the manuscript. Leave a blank line between each paragraph and between each entry in the list of bibliographic references. Tables should preferably be placed in the same electronic file as the text. Authors should consult a recent issue of the Journal for table layout.

Every page of the manuscript, including the title page, references, tables, etc. should be numbered. However, no reference should be made to page numbers in the text; if necessary, one may refer to sections. Underline words that should be in italics, and do not underline any other words.

We recommend that authors prepare the text as a **Microsoft Word** file.

1. Manuscripts in general should be organised in the following order:

    - **Page 1: Running title.** (Not to exceed 60 characters, counting letters and spaces). This page should **only** contain the running title of your paper. The running title is an abbreviated title used as the running head on every page of the manuscript.

      In addition, the **Subject areas m**ost relevant to the study **must be indicated on this page.** Select the appropriate subject areas from the Scope of the Journals provided in the Manuscript Submission Guide.

      A **list** of n**umber of black and white / colour figures and tables should also be indicated on this page.** Figures submitted in color will be printed in colour. See "*5. Figures & Photographs"* for details.

    - **Page 2: Author(s) and Corresponding author information.** This page should contain the **full title** of your paper with name(s) of all the authors, institutions and corresponding author's name, institution and full address (Street address, telephone number (including extension), hand phone number, fax number and e-mail address) for editorial correspondence. The names of the authors **must** be abbreviated following the international naming convention. e.g. Salleh, A.B., Tan, S.G., or Sapuan, S.M.

      Authors' addresses. Multiple authors with different addresses must indicate their respective addresses separately by superscript numbers:

      George Swan[1] and Nayan Kanwal[2]
      [1]Department of Biology, Faculty of Science, Duke University, Durham, North Carolina, USA.
      [2]Office of the Deputy Vice Chancellor (R&I), Universiti Putra Malaysia, Serdang, Malaysia.

    - **Page 3**: This page should **repeat** the **full title** of your paper with only the **Abstract** (the abstract should be less than 250 words for a Regular Paper and up to 100 words for a Short Communication). **Keywords** must also be provided on this page (Not more than eight keywords in alphabetical order).

    - **Page 4 and subsequent pages**: This page should begin with the **Introduction** of your article and the rest of your paper should follow from page 5 onwards.

    Abbreviations. Define alphabetically, other than abbreviations that can be used without definition. Words or phrases that are abbreviated in the introduction and following text should be written out in full the first time that they appear in the text, with each abbreviated form in parenthesis. Include the common name or scientific name, or both, of animal and plant materials.

    Footnotes. Current addresses of authors if different from heading.

2. **Text.** Regular Papers should be prepared with the headings **Introduction**, **Materials and Methods**, **Results and Discussion, Conclusions** in this order. Short Communications should be prepared according to "*8. Short Communications."* below.

3. **Tables.** All tables should be prepared in a form consistent with recent issues of *Pertanika* and should be numbered consecutively with Arabic numerals. Explanatory material should be given in the table legends and footnotes. Each

table should be prepared on a separate page. (Note that when a manuscript is accepted for publication, tables must be submitted as data - .doc, .rtf, Excel or PowerPoint file- because tables submitted as image data cannot be edited for publication.)

4. **Equations and Formulae.** These must be set up clearly and should be typed triple spaced. Numbers identifying equations should be in square brackets and placed on the right margin of the text.

5. **Figures & Photographs.** Submit an original figure or photograph. Line drawings must be clear, with high black and white contrast. Each figure or photograph should be prepared on a separate sheet and numbered consecutively with Arabic numerals. Appropriate sized numbers, letters and symbols should be used, no smaller than 2 mm in size after reduction to single column width (85 mm), 1.5-column width (120 mm) or full 2-column width (175 mm).

6. Failure to comply with these specifications will require new figures and delay in publication. For electronic figures, create your figures using applications that are capable of preparing high resolution TIFF files acceptable for publication. In general, we require **300 dpi or higher resolution for coloured and half-tone artwork** and **1200 dpi or higher for line drawings**. For review, you may attach low-resolution figures, which are still clear enough for reviewing, to keep the file of the manuscript under 5 MB. Illustrations may be produced at extra cost in colour at the discretion of the Publisher; the author could be charged Malaysian Ringgit 50 for each colour page.

7. **References.** Literature citations in the text should be made by name(s) of author(s) and year. For references with more than two authors, the name of the first author followed by *'et al*.' should be used.

   Swan and Kanwal (2007) reported that …
   The results have been interpreted (Kanwal *et al.* 2009).

   - References should be listed in alphabetical order, by the authors' last names. For the same author, or for the same set of authors, references should be arranged chronologically. If there is more than one publication in the same year for the same author(s), the letters 'a', 'b', etc., should be added to the year.

   - When the authors are more than 11, list 5 authors and then et al.

   - Do not use indentations in typing References. Use one line of space to separate each reference. The name of the journal should be written in full. For example:

     Jalaludin, S. (1997a). Metabolizable energy of some local feeding stuff. *Tumbuh, 1,* 21-24.

     Jalaludin, S. (1997b). The use of different vegetable oil in chicken ration. *Malayan Agriculturist, 11,* 29-31.

     Tan, S.G., Omar, M.Y., Mahani, K.W., Rahani, M., & Selvaraj, O.S. (1994). Biochemical genetic studies on wild populations of three species of green leafhoppers *Nephotettix* from Peninsular Malaysia. *Biochemical Genetics*, *32,* 415 - 422.

   - In case of citing an author(s) who has published more than one paper in the same year, the papers should be distinguished by addition of a small letter as shown above, e.g. Jalaludin (1997a); Jalaludin (1997b).

   - Unpublished data and personal communications should not be cited as literature citations, but given in the text in parentheses. 'In press' articles that have been accepted for publication may be cited in References. Include in the citation the journal in which the 'in press' article will appear and the publication date, if a date is available.

8. **Examples of other reference citations**:

   Monographs: Turner, H.N., & Yong, S.S.Y. (2006). *Quantitative Genetics in Sheep Breeding*. Ithaca: Cornell University Press.

   Chapter in Book: Kanwal, N.D.S. (1992). Role of plantation crops in Papua New Guinea economy. In Angela R. McLean (Ed.), *Introduction of livestock in the Enga province PNG* (p. 221-250). United Kingdom: Oxford Press.

   Proceedings: Kanwal, N.D.S. (2001). Assessing the visual impact of degraded land management with landscape design software. In Kanwal, N.D.S., & Lecoustre, P. (Eds.), *International forum for Urban Landscape Technologies* (p. 117-127). Lullier, Geneva, Switzerland: CIRAD Press.

9. **Short Communications** should include **Introduction, Materials and Methods, Results and Discussion, Conclusions** in this order. Headings should only be inserted for Materials and Methods. The abstract should be up to 100 words, as stated above. Short Communications must be 5 printed pages or less, including all references, figures and tables. References should be less than 30. A 5 page paper is usually approximately 3000 words plus four figures or tables (if each figure or table is less than 1/4 page).

   *Authors should state the total number of words (including the Abstract) in the cover letter. Manuscripts that do not fulfill these criteria will be rejected as Short Communications without review.

STYLE OF THE MANUSCRIPT

Manuscripts should follow the style of the latest version of the Publication Manual of the American Psychological Association (APA). The journal uses American or British spelling and authors may follow the latest edition of the Oxford Advanced Learner's Dictionary for British spellings.

SUBMISSION OF MANUSCRIPTS

All articles should be submitted electronically using the ScholarOne web-based system. ScholarOne, a Thomson Reuters product provides comprehensive workflow management systems for scholarly journals. For more information, go to our web page and click "**Online Submission**".

Alternatively, you may submit the electronic files (cover letter, manuscript, and the **Manuscript Submission Kit** comprising *Declaration* and *Referral* forms) via email directly to the Executive Editor. If the files are too large to email, mail a CD containing the files. The **Manuscript Submission Guide** and **Submission Kit** are available from the *Pertanika*'s home page at http://www.pertanika.upm.edu.my/ or from the Executive Editor's office upon request.

All articles submitted to the journal **must comply** with these instructions. Failure to do so will result in return of the manuscript and possible delay in publication.

Please do **not** submit manuscripts to the editor-in-chief or to any other office directly. All manuscripts must be **submitted through the executive editor's office** to be properly acknowledged and rapidly processed at the address below:

Dr. Nayan KANWAL
The Executive Editor
Pertanika Journals, UPM Press
Office of the Deputy Vice Chancellor (R&I)
IDEA Tower II, UPM-MTDC Technology Centre
Universiti Putra Malaysia
43400 UPM, Serdang, Selangor
Malaysia

E-mail: executive_editor.pertanika@upm.my; tel: + 603-8947 1622.
or visit our website at http://www.pertanika.upm.edu.my/home.php for further information.

Authors should retain copies of submitted manuscripts and correspondence, as materials can not be returned. Authors are required to inform the Executive Editor of any change of address which occurs whilst their papers are in the process of publication.

Cover letter

All submissions must be accompanied by a cover letter detailing what you are submitting. Papers are accepted for publication in the journal on the understanding that the article is original and the content has not been published or submitted for publication elsewhere. This must be stated in the cover letter.

The cover letter must also contain an acknowledgement that all authors have contributed significantly, and that all authors are in agreement with the content of the manuscript.

The cover letter of the paper should contain (i) the title; (ii) the full names of the authors; (iii) the addresses of the institutions at which the work was carried out together with (iv) the full postal and email address, plus facsimile and telephone numbers of the author to whom correspondence about the manuscript should be sent. The present address of any author, if different from that where the work was carried out, should be supplied in a footnote.

As articles are double-blind reviewed, material that might identify authorship of the paper should be placed on a cover sheet.

Peer review

Pertanika follows a **double-blind peer-review** process. Peer reviewers are experts chosen by journal editors to provide written assessment of the **strengths** and **weaknesses** of written research, with the aim of improving the reporting of research and identifying the most appropriate and highest quality material for the journal.

In the peer-review process, three referees independently evaluate the scientific quality of the submitted manuscripts. Authors are encouraged to indicate in the **Referral form** using the **Manuscript Submission Kit** the names of three potential reviewers, but the editors will make the final choice. The editors are not, however, bound by these suggestions.

Manuscripts should be written so that they are intelligible to the professional reader who is not a specialist in the particular field. They should be written in a clear, concise, direct style. Where contributions are judged as acceptable for publication on the basis of content, the Editor reserves the right to modify the typescripts to eliminate ambiguity and repetition and improve communication between author and reader. If extensive alterations are required, the manuscript will be returned to the author for revision.

The Journal's review process

What happens to a manuscript once it is submitted to *Pertanika*? Typically, there are seven steps to the editorial review process:

1. The executive editor and the editorial board examine the paper to determine whether it is appropriate for the journal and should be reviewed. If not appropriate, the manuscript is rejected outright and the author is informed.

2. The executive editor sends the article-identifying information having been removed, to three reviewers. Typically, one of these is from the Journal's editorial board. Others are specialists in the subject matter represented by the article. The executive editor asks them to complete the review in three weeks and encloses two forms: (a) referral form B and (b) reviewer's comment form along with reviewer's guidelines. Comments to authors are about the appropriateness and adequacy of the theoretical or conceptual framework, literature review, method, results and discussion, and conclusions. Reviewers often include suggestions for strengthening of the manuscript. Comments to the editor are in the nature of the significance of the work and its potential contribution to the literature.

3. The executive editor, in consultation with the editor-in-chief, examines the reviews and decides whether to reject the manuscript, invite the author(s) to revise and resubmit the manuscript, or seek additional reviews. Final acceptance or rejection rests with the Editorial Board, who reserves the right to refuse any material for publication. In rare instances, the manuscript is accepted with almost no revision. Almost without exception, reviewers' comments (to the author) are forwarded to the author. If a revision is indicated, the editor provides guidelines for attending to the reviewers' suggestions and perhaps additional advice about revising the manuscript.

4. The authors decide whether and how to address the reviewers' comments and criticisms and the editor's concerns. The authors submit a revised version of the paper to the executive editor along with specific information describing how they have answered' the concerns of the reviewers and the editor.

5. The executive editor sends the revised paper out for review. Typically, at least one of the original reviewers will be asked to examine the article.

6. When the reviewers have completed their work, the executive editor in consultation with the editorial board and the editor-in-chief examine their comments and decide whether the paper is ready to be published, needs another round of revisions, or should be rejected.

7. If the decision is to accept, the paper is sent to that Press and the article should appear in print in approximately three months. The Publisher ensures that the paper adheres to the correct style (in-text citations, the reference list, and tables are typical areas of concern, clarity, and grammar). The authors are asked to respond to any queries by the Publisher. Following these corrections, page proofs are mailed to the corresponding authors for their final approval. At this point, only essential changes are accepted. Finally, the article appears in the pages of the Journal and is posted on-line.

English language editing

Pertanika **emphasizes** on the linguistic accuracy of every manuscript published. Thus all authors are required to get their manuscripts edited by **professional English language editors**. Author(s) **must provide a certificate** confirming that their manuscripts have been adequately edited. A proof from a recognised editing service should be submitted together with the cover letter at the time of submitting a manuscript to Pertanika**. All costs will be borne by the author(s)**.

This step, taken by authors before submission, will greatly facilitate reviewing, and thus publication if the content is acceptable.

Author material archive policy

Authors who require the return of any submitted material that is rejected for publication in the journal should indicate on the cover letter. If no indication is given, that author's material should be returned, the Editorial Office will dispose of all hardcopy and electronic material.

Copyright

Authors publishing the Journal will be asked to sign a declaration form. In signing the form, it is assumed that authors have obtained permission to use any copyrighted or previously published material. All authors must read and agree to the conditions outlined in the form, and must sign the form or agree that the corresponding author can sign on their behalf. Articles cannot be published until a signed form has been received.

Lag time

A decision on acceptance or rejection of a manuscript is reached in 3 to 4 months (average 14 weeks). The elapsed time from submission to publication for the articles averages 5-6 months.

Hardcopies of the Journals and off prints

Under the Journal's open access initiative, authors can choose to download free material (via PDF link) from any of the journal issues from Pertanika's website. Under "Browse Journals" you will see a link entitled "Current Issues" or "Archives". Here you will get access to all back-issues from 1978 onwards.

The **corresponding author** for all articles will receive one complimentary hardcopy of the journal in which his/her articles is published. In addition, 20 off prints of the full text of their article will also be provided. Additional copies of the journals may be purchased by writing to the executive editor.

Pertanika

Our goal is to bring high quality research to the widest possible audience

Pertanika is an international peer-reviewed leading journal in Malaysia which began publication in 1978. The journal publishes in three different areas — Journal of Tropical Agricultural Science (JTAS); Journal of Science and Technology (JST); and Journal of Social Sciences and Humanities (JSSH).

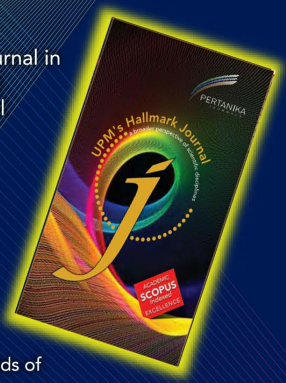

JTAS is devoted to the publication of original papers that serves as a forum for practical approaches to improving quality in issues pertaining to tropical agricultural research or related fields of study. It is published four times a year in **February**, **May**, **August** and **November**.

JST caters for science and engineering research or related fields of study. It is published twice a year in **January** and **July**.

JSSH deals in research or theories in social sciences and humanities research with a focus on emerging issues pertaining to the social and behavioural sciences as well as the humanities, particularly in the Asia Pacific region. It is published four times a year in **March**, **June**, **September** and **December**.

Why should you publish in *Pertanika* Journals?

Benefits to Authors

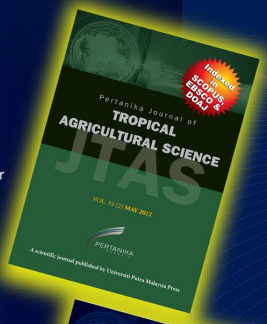

PROFILE: Our journals are circulated in large numbers all over Malaysia, and beyond in Southeast Asia. Recently, we have widened our circulation to other overseas countries as well. We will ensure that your work reaches the widest possible audience in print and online, through our wide publicity campaigns held frequently, and through our constantly developing electronic initiatives via *Pertanika* online submission system backed by Thomson Reuters.

QUALITY: Our journals' reputation for quality is unsurpassed ensuring that the originality, authority and accuracy of your work will be fully recognised. Each manuscript submitted to Pertanika undergoesa rigid **originality check**. Our double-blind peer refereeing procedures are **fair and open, and we aim to help authors** develop and improve their work. Pertanika JTAS is now over 33 years old; this accumulated knowledge has resulted in Pertanika being indexed in **SCOPUS** (Elsevier), **Thomson** (Biosis), **EBSCO**, **CABI**, **AGRICOLA**, **Google Scholar**, **MyAIS**, **ISC** and **ERA**.

AUTHOR SERVICES: We provide a rapid response service to all our authors, with dedicated support staff for each journal, and a point of contact throughout the refereeing and production processes. Our aim is to ensure that the production process is as smooth as possible, is borne out by the high number of authors who publish with us again and again.

LAG TIME: Submissions are guaranteed to receive a decision within **14 weeks**. The elapsed time from submission to publication for the articles averages 5-6 months. A decision of acceptance of a manuscript is reached in 3 to 4 months (average 14 weeks).

Call for Papers

Pertanika invites you to explore frontiers from all fields of science and technology to social sciences and humanities. You may contribute your scientific work for publishing in UPM's hallmark journals either as a regular article, short communication, or a review article in our forthcoming issues. Papers submitted to this journal must contain original results and must not be submitted elsewhere while being evaluated for the *Pertanika* Journals.

Submissions in English should be accompanied by an abstract not exceeding 300 words. Your manuscript should be no more than 6,000 words or 10-12 printed pages, including notes and abstract. Submissions should conform to the *Pertanika* style, which is available at www.pertanika.upm.edu.my or by mail or email upon request.

Papers should be double-spaced 12 point type (Times New Roman fonts preferred). The first page should include the title of the article but no author information. Page 2 should repeat the title of the article together with the names and contact information of the corresponding author as well as all the other authors. Page 3 should contain the title of the paper and abstract only. Page 4 and subsequent pages to have the text - Acknowledgments - References - Tables - Legends to figures – Figures, etc.

Questions regarding submissions should only be directed to the Executive Editor, *Pertanika* Journals.

Remember, *Pertanika* is the resource to support you in strengthening research and research management capacity.

An Award Winning International- Malaysian Journal

FEB. 2008

Mail your submissions to:

The Executive Editor
Pertanika Journals, UPM Press
Office of the DVC (R&I)
IDEA Tower II, UPM-MTDC Technology Centre
Universiti Putra Malaysia
43400 UPM, Serdang, Selangor
Malaysia

Tel: **+6 03 8947 1622**

nayan@upm.my
www.pertanika.upm.edu.my

Pertanika **is Indexed in SCOPUS, EBSCO, DOAJ & ISC**

Selected Articles from UPM-Malaysian Nuclear Agency Symposium 2011
Guest Editor: Mohd Sapuan Salit
Guest Editorial Board: Mansor Ahmad, Syams Zainudin, Hawa Ze Jaafar, Fathinul Fikri Ahmad Saad, Kamarudin Hashim and Mohamad Azwar Hashim

Selected Articles from The International Conference on Information Retrieval and Knowledge Management, CAMP'12
Guest Editors: Shyamala Doraisamy and Ramlan Mahmod
Guest Editorial Board: Lili Nurliyana Abdullah, Rusli Abdullah, Masrah Azmi Murad, Rodziah Atan and Rabiah Abdul Kadir

Pertanika Journal of Science & Technology
Vol. 21 (1) Jan. 2013

Contents

Pertanika Editorial Office
Office of the Deputy Vice Chancellor (R&I),
1st Floor, IDEA Tower II,
UPM-MTDC Technology Centre
Universiti Putra Malaysia
43400 UPM Serdang
Selangor Darul Ehsan
Malaysia

http://www.pertanika.upm.edu.my/
E-mail: executive_editor.pertanika@upm.my
Tel: +603 8947 1622/1620

UPM Press
Universiti Putra Malaysia
43400 UPM Serdang
Selangor Darul Ehsan
Malaysia

http://penerbit.upm.edu.my
E-mail : penerbit@putra.upm.edu.my
Tel : +603 8946 8855/8854
Fax : +603 8941 6172

ISSN 0128-7680
01 >
9 770128 768083